ENDOTHELIAL JAM-A FACILITATES REOVIRUS BLOODSTREAM SPREAD

By

Caroline Ming-Hwei Lai

Dissertation

Submitted to the Faculty of the

Graduate School of Vanderbilt University

in partial fulfillment of the requirements

for the degree of

DOCTOR OF PHILOSOPHY

in

Microbiology and Immunology

December, 2013

Nashville, Tennessee

Approved:

Christopher R. Aiken, Ph.D.

Terence S. Dermody, M.D.

Ambra Pozzi, Ph.D.

Luc Van Kaer, Ph.D.

John V. Williams, M.D.

To my parents,

who love and support me unconditionally

To my brother,

who taught me strength and perseverance

ACKNOWLEDGEMENTS

I am grateful for the financial support I have received throughout the duration of my thesis work. Support was provided by the Medical Scientist Training Program (Public Health Service award T32 GM07347), the Molecular Basis of Reovirus Pathogenesis Grant (Public Health Service award R37 A138296), and the Blood Brain Barrier Penetration by Neurotropic Reovirus Grant (Public Health Service award F31 NS074596). Additional support was provided by the Vanderbilt-Ingram Cancer Center (Public Health Service award P60 DK20593), the Vanderbilt Institute for Clinical and Translational Research (Public Health Service award UL1 RR024975), and the Elizabeth B. Lamb Center for Pediatric Research.

I would like to thank Terry Dermody for being an incredible mentor. Terry is one of the hardest working people I know and his work ethic and drive remind me of the importance of our work. Terry has an unwavering commitment to mentoring, and his feedback and guidance has helped me to be a more effective scientist and person. He has always been a great listener, and never hesitated to share invaluable advice on scientific, career, and life problems. I am grateful for the countless hours that he has spent on my behalf to help me succeed.

I can not thank the Dermody lab and alumni enough for friendships and guidance. I would like to especially thank Bernardo Mainou for teaching me to pay attention to details and work as hard as I can every day and Jenn Konopka for being a mentor not only in science but also for life. Life on the seventh floor was always fun and full of life. You both kept me grounded and provided laughs during the rough times. I'd like to thank

Karl Boehme for being a great mentor and friend. I thank the entire Dermody lab, past and present, for fun times and tremendous support. Each member of the Dermody lab has made the last four years some of the most memorable I will ever have.

I would like to thank all of my scientific colleagues who contributed to this work. Bernardo Mainou obtained the beautiful confocal images of endothelial cells and Alison Ashbrook provided assistance with intravenous inoculations. Dr. Charles Parkos provided JAM-A flox/flox animals used to generate mouse strains essential for the studies to determine *in vivo* determinants of reovirus spread. Dr. Kwang-Sik Kim provided the endothelial cell line that was essential for studies of reovirus infection. Various research cores at Vanderbilt University provided valuable assistance with various aspects of this work. The Transgenic Mouse/Embryonic Stem Cell Shared Resource, especially Jennifer Skelton, generated transgenic mice that were used in mouse studies. The Flow Cytometry Shared Resource, especially Dave Flaherty, assisted in optimizing studies of reovirus infectivity using flow cytometry. The Cell Imaging Shared Resource provided the instruments to capture confocal micrographs. The Antibody and Protein Resource assisted in purification of JAM-A-specific antibody. I would like to thank the lab teams and staff that make up the Division of Pediatric Infectious Diseases and the Elizabeth B. Lamb Center for Pediatric Research for scientific discussions and friendly conversations. I would like also to thank the staff, faculty, and students of the Department of Pathology, Microbiology, and Immunology for unwavering support, constructive mentoring, and friendship.

I thank the members of my thesis committee for their helpful suggestions and insightful guidance during my graduate training. I thank Chris Aiken, my committee

chair, for helpful discussions and excellent organization of the meetings. I thank Ambra Pozzi for providing a fresh perspective and helpful advice. I thank John Williams for contributing expertise in viral pathogenesis and guidance with difficult experiments. I thank Luc Van Kaer for his expertise in mouse genetics and advice at critical times.

I would like to thank my previous mentors for contributing to my development as an individual and scientist. Ed Roy has a passion for science and knowledge that inspired me to begin my journey in science. Eve Gallman provided essential guidance during my undergraduate years. Erik Barton spent numerous hours mentoring me and provided helpful advice at critical times. Debbie Lenschow and Skip Virgin took a chance on me and provided me with invaluable guidance and experience in lab research and in the hospital. I am grateful for these individuals and their passion for science and commitment to mentoring, qualities that have inspired me and helped to guide me to where I am today.

I would not be where I am without my family. My mom and dad provided me with limitless opportunities, supported, and encouraged me to follow my dreams. My parents taught me to live life to the fullest and to work hard. My brother taught me strength and perseverance. I have not met someone who has worked harder to overcome hardship. I am so proud of him and am thankful for his love and support for me always. My sister-in-law Ruby has become close friend in whom I can confide. I would finally like to thank my best friend and strongest supporter, Barry Kang. He is an excellent listener and has shared in all my ups and downs with patience and love. He has spent a countless number of hours supporting me and I could not ask for a better partner in life. Thank you for always sticking by me and encouraging me.

TABLE OF CONTENTS

LIST OF TABLES

LIST OF FIGURES

LIST OF ABBREVIATIONS

BBB	blood brain barrier
BODIPY	boron-dipyrromethene
BTV	bluetongue virus
CAR	coxsackievirus and adenovirus receptor
CHO	Chinese hamster ovary cells
CNS	central nervous system
Cre	Cre recombinase
DAPI	4',6-diamidino-2-phenylindole
DENV	dengue virus
ds	double-stranded
EBV	Epstein-Barr virus
EDTA	ethylenediaminetetraacetic acid
EM	electron microscopy
ESCRT	endosomal sorting complexes required for transport
FAE	follicle-associated epithelium
GALT	gut-associated lymphoid tissue
HIV-1	human immunodeficiency virus 1
HBMEC	human brain microvascular endothelial cell
Ig	immunoglobulin
ISVP	infectious subvirion particles
JAM-A	junctional adhesion molecule A
KO	knock-out
M cell	microfold cell
MEF	murine embryonic fibroblasts
MEL	murine erythroleukemia cells

MFI	mean fluorescence intensity
MLN	mesenteric lymph node
MOI	multiplicity of infection
PDZ	post-synaptic density protein (PSD95), Drosophila disc large tumor suppressor (Dig1), zona occludens 1 (ZO-1)
PFU	plaque forming units
PPRSV	porcine reproductive and respiratory syndrome virus
RNA	ribonucleic acid
SA	sialic acid
siRNA	small-interfering RNA
T1L	reovirus strain type 1 Lang
T2J	reovirus strain type 2 Jones
T3D	reovirus strain type 3 Dearing
TEER	transendothelial electrical resistance
TUNEL	terminal deoxynucleotidyl transferase dUTP nick-end labeling
TJ	tight junction

CHAPTER I

INTRODUCTION

An essential step in the pathogenesis of many viruses is systemic dissemination to target organs where secondary replication can occur. Viral replication at targeted sites of secondary replication is often manifested as the clinical symptoms associated with viral infection. The bloodstream is a common route used by many viral pathogens to ensure widespread dissemination in infected hosts. Although viremia is a well-established prerequisite to spread of the virus to sites of secondary replication, mechanisms used by viruses to gain entry into or exit from the bloodstream are not well understood.

Mammalian orthoreoviruses (reoviruses) are nonenveloped, double-stranded (ds) RNA viruses that are transmitted primarily by the fecal-oral route. Systemic dissemination of reoviruses occurs via bloodstream and neural routes, and the patterns of spread and pathogenesis differ based on viral serotype. While reoviruses infect virtually all mammals, disease manifestations of reovirus infection are seen only in the very young. Reovirus infection of newborn mice results in various disease phenotypes including biliary atresia, myocarditis, hydrocephalus, and encephalitis. A robust neonatal mouse model and a facile reverse genetics system has allowed for the use of reovirus to be used as a model to dissect mechanisms of viral hematogenous dissemination.

When this work was initiated, a proteinaceous receptor for reovirus, junctional adhesion molecule A (JAM-A), had been found to mediate hematogenous dissemination of reovirus *in vivo.* However, the precise mechanism by which JAM-A promotes

bloodstream spread was unknown. I hypothesized that expression of JAM-A in endothelial cells is required for reovirus entry into and egress from the bloodstream and subsequent dissemination to targeted sites of secondary replication. In Chapter II, I report that endothelial but not hematopoietic JAM-A is required for bloodstream dissemination using mice with tissue-specific alterations in JAM-A expression. In Chapter III, I present data demonstrating the requirement of sialic acid and JAM-A in reovirus infection of polarized endothelial cells in culture. In Chapter IV, I show that reovirus egress from polarized endothelial cells is directional and occurs noncytolytically. Together, these findings indicate that the endothelium is an essential mediator of reovirus pathogenesis. Furthermore, my work demonstrates that the precise expression of a viral receptor is critical for bloodstream dissemination.

Reoviruses

Viruses of the *Reoviridae* family infect a wide range of host organisms, including mammals, birds, insects, and plants (1). The *Reoviridae* includes rotaviruses, the most common diarrheal pathogen among children (2), orbiviruses, which are economically important pathogens of sheep, cattle, and horses (3), and reoviruses. Three reovirus serotypes (T1, T2, and T3) currently circulate in humans and other mammals. The serotypes are distinguished on the basis of antibody-mediated neutralization of infectivity and inhibition of hemagglutination. Each serotype is represented by a prototype strain isolated from a human host: type 1 Lang (T1L), type 2 Jones (T2J), and type 3 Dearing (T3D). These strains differ dramatically in host cell tropism, mechanisms of cell killing,

modes of dissemination, and central nervous system (CNS) disease. In particular, studies of T1 and T3 reoviruses have generated foundational knowledge about strategies used by viruses to replicate and cause neural injury. Development of a plasmid-based reverse genetics system allows introduction of mutations into the viral genome to test specific hypotheses about the structure and function of viral proteins and RNAs (4, 5). In concert with an experimentally facile mouse model of infection (6, 7), reovirus is an ideal experimental platform for studies of virus-host interactions.

Reoviruses are nonenveloped, icosahedral viruses that contain a genome consisting of 10 segments of dsRNA (Figure I-1) (1). There are three large (L1, L2, L3), three medium (M1, M2, M3), and four small (S1, S2, S3, S4) dsRNA segments that are packaged in an equimolar stoichiometric relationship with one copy of each per virion. With the exception of the M3 and S1 gene segments, each of the reovirus gene segments is monocistronic. Reovirus virions are composed of two concentric protein shells, the outer capsid and core (Figure I-1) (8). The outer capsid consists of heterohexameric complexes of the μ1 (encoded by M2) and σ3 (encoded by S4) proteins. At each of the icosahedral five-fold symmetry axes, the attachment protein σ1 (encoded by S1) extends from turret-like structures formed by pentamers of λ2 (encoded by L2) protein. The inner core shell is formed by parallel asymmetric dimers of λ1 (encoded by L3) protein that are stabilized by σ2 (encoded by S2) protein. The λ3 (encoded by L1) and μ2 (encoded by M1) proteins are anchored to the inner surface of the core via interactions with λ1. Lastly, the M3 gene segment encodes nonstructural proteins μNS and μNSC, the S3 gene segment encodes nonstructural protein σNS, and the S1 gene segment encodes nonstructural protein σ1s.

A

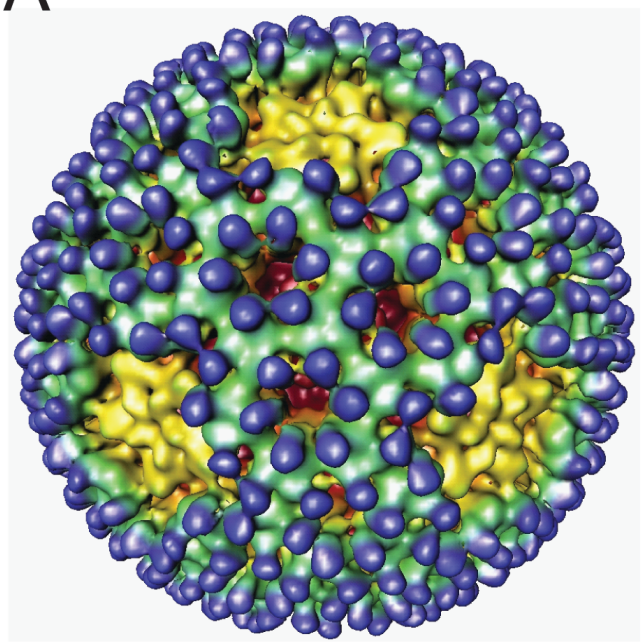

B

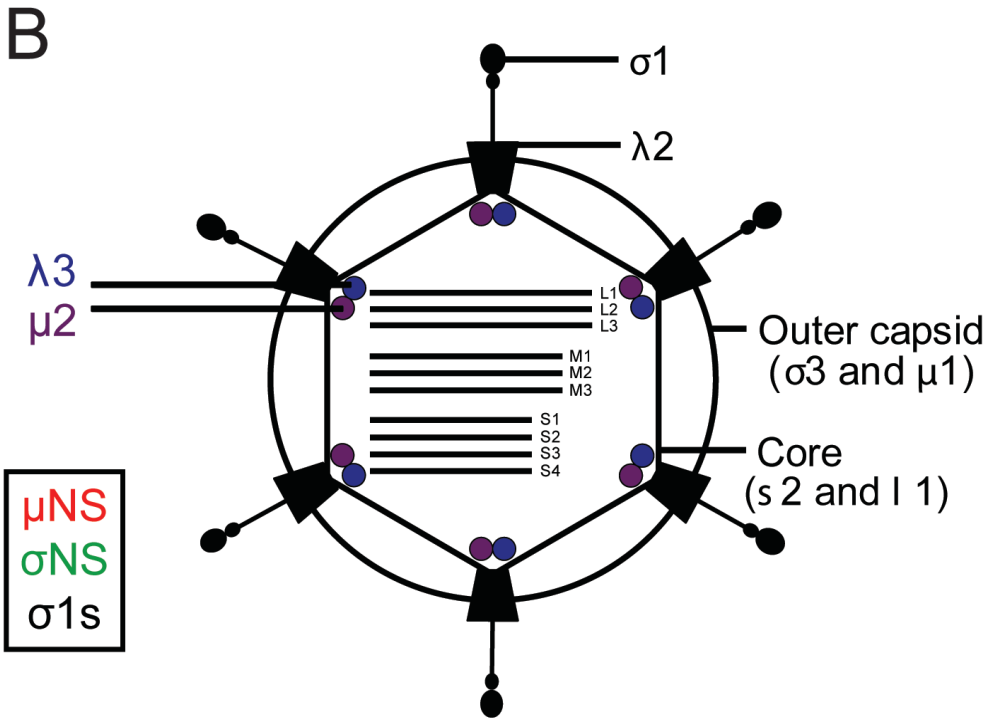
σ1
λ2
λ3
μ2
L1
L2
L3
M1
M2
M3
S1
S2
S3
S4
Outer capsid
(σ3 and μ1)
Core
(s 2 and I 1)
μNS
σNS
σ1s

Figure I-1. The reovirus virion. (A) Cryo-electron micrograph image reconstruction of a reovirus virion. Outer-capsid protein σ3 (blue), is the initial target for virion disassembly in infected cells. Pentameric λ2 protein (yellow) forms an insertion pedestal for σ1, which is the viral attachment protein. From Nason et al. (2001). (B) Schematic of a reovirus virion. Reovirus particles are formed from two concentric protein shells, the outer capsid and core. The core contains the viral genome, which consists of ten dsRNA segments. Reovirus also encodes nonstructural proteins, σNS, μNS, μNSC, and σ1s.

Reovirus Attachment and Entry

Viral attachment protein σ1 is a long filamentous molecule with head-and-tail morphology (Figure I-2A) (9-12). The σ1 protein is comprised of three distinct structural domains: an N-terminal α-helical coiled-coil tail, a central β-spiral body, and a C-terminal globular head (9, 11). Short regions of undefined structure separate each domain and are hypothesized to permit molecular flexibility required to engage cellular receptors during viral entry (Figure I-2A) (9-11, 13). Attachment of the σ1 protein to cell-surface receptors initiates reovirus infection of susceptible host cells (14, 15). The σ1 protein targets two different receptors, α-linked sialic acid (SA) (16-21) and JAM-A (22-24). Residues in the T1 σ1 head domain (21) and T3 σ1 β-spiral body domain bind SA (11, 25); sequences in the head domain of both T1 and T3 σ1 engage JAM-A (22, 26).

Residues in the T3 σ1 protein that interact with SA have been identified using structure-guided point-mutant viruses. The T3 σ1 residues Asn198, Arg202, Leu203, Pro204, and Gly205 are required for hemagglutination and infection of murine erythroleukemia (MEL) cells, which are dependent on SA engagement for productive T3 reovirus infection (Figure I-3) (11). Residues in the T1 σ1 protein that engage SA also have been identified using studies of structure-guided point mutant viruses. The T1 σ1 residues Val354, Ser370, and Gln371 are required for hemagglutination and infection of murine embryonic fibroblasts (MEFs), which are dependent on SA engagement for T1 reovirus infection (21). A glycan array was performed and identified ganglioside GM2 as the glycan engaged by T1 reovirus (21).

JAM-A is used as a receptor by all reovirus serotypes (23, 24). Each σ1 trimer is capable of binding three independent JAM-A monomers (24). Structural and biochemical studies identified residues in the D-E loop of the σ1 head that mediate interactions with JAM-A. Residues Thr380, Gly381, and Asp 382 engage JAM-A via polar interactions (Figure I-4) (26). Mutations of these residues in the reovirus σ1 protein diminishes JAM-A engagement (26).

After receptor binding, reovirus virions are internalized into endosomes via a process dependent on β1 integrin (27) and distributed to organelles marked by Rab7 and Rab9 where viral disassembly takes place (28). During viral disassembly, outer-capsid protein σ3 is degraded by cathepsin proteases, attachment protein σ1 undergoes a conformational change, and outer-capsid protein μ1 is cleaved to form infectious subvirion particles (ISVPs) (29). The μ1 cleavage fragments undergo conformational rearrangement to facilitate endosome penetration and delivery of transcriptionally active core particles into the cytoplasm (30, 31). Primary transcription occurs within the viral core, and nascent RNAs are translated or encapsidated into new viral cores, where they serve as templates for negative-strand synthesis. Within new viral cores, secondary rounds of transcription occur. Outer-capsid proteins are added to nascent cores, which silences viral transcription and yields progeny viral particles.

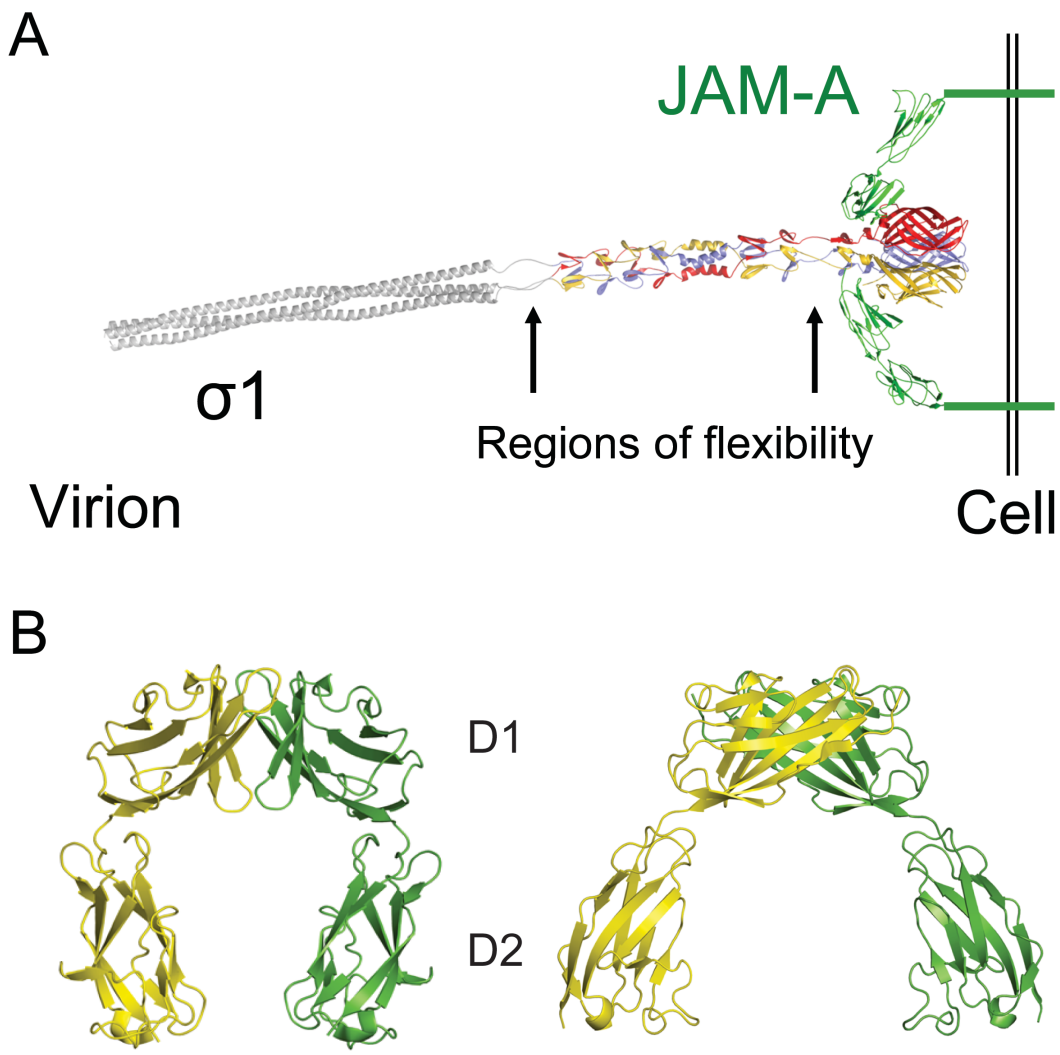

Figure I-2. Structure of σ1 and JAM-A. (A) Full-length model of attachment protein σ1 bound to JAM-A. A model of full-length σ1 extending from the virion is shown as a ribbon drawing, with the known structure of the C-terminus in tricolor and the predicted structure of the N-terminus in grey. Arrows indicate predicted regions of flexibility. A model of full-length JAM-A is shown in green as a ribbon drawing of the known structure of the extracellular domain and a schematic representation of the transmembrane and intracellular domains. For clarity, only two JAM-A monomers are shown bound to σ1. Adapted from Kirchner et al. (2008). (B) Structure of human JAM-A D1 and D2 domains. Ribbon drawings of a JAM-A homodimer, with one monomer shown in yellow and the other in green. Two orthogonal views are displayed. Adapted from Prota et al. (2003).

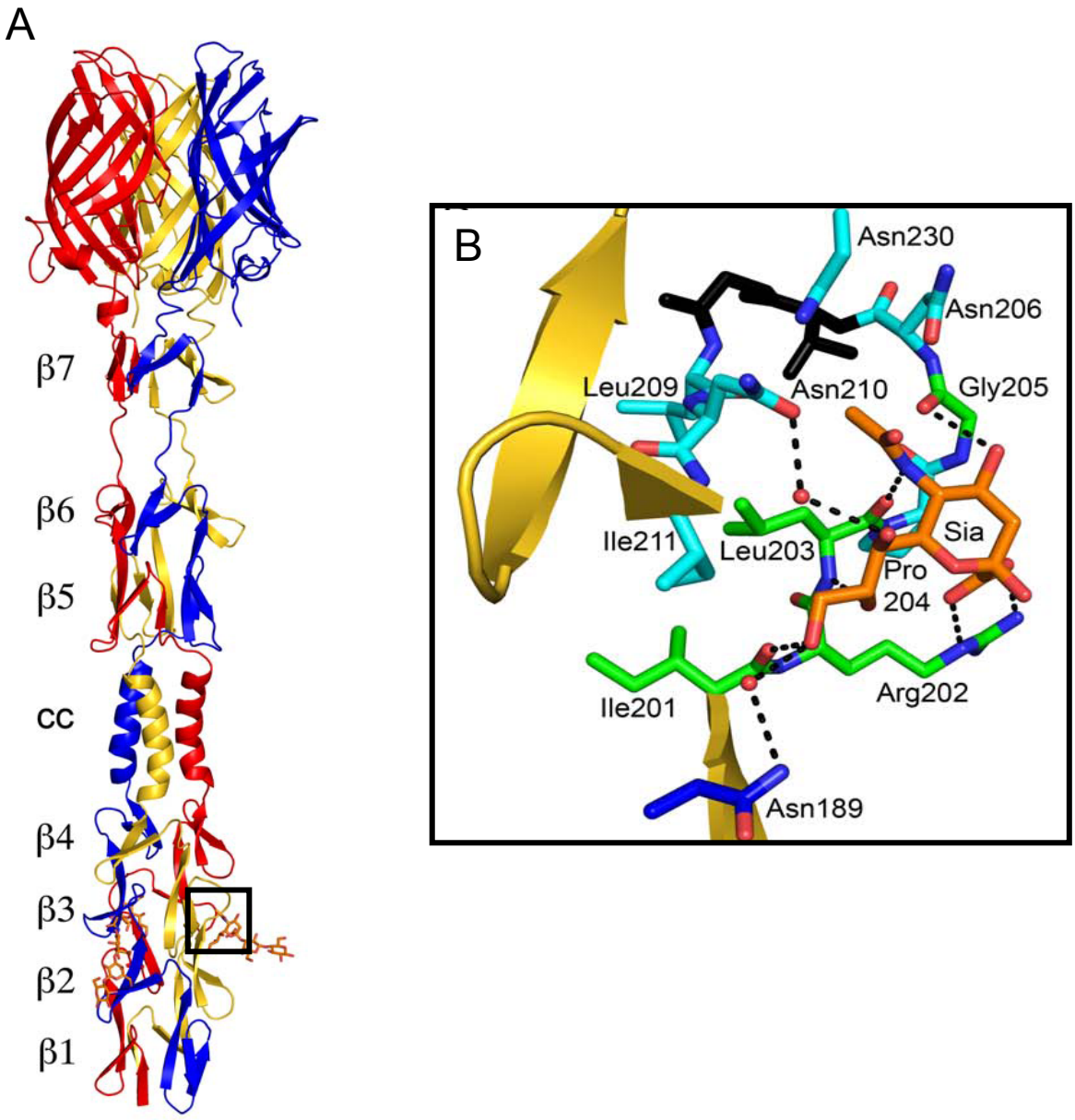
A
β7
β6
β5
cc
β4
β3
β2
β1
B
Asn230
Asn206
Leu209
Asn210
Gly205
Ile211
Leu203
Sia
Pro
204
Ile201
Arg202
Asn189

Figure I-3. Critical contacts of T3D σ1 and SA. (A) Ribbon drawing of the T3D σ1 body and head domains in complex with α-2,3-sialyllactose. The σ1 monomers are shown in red, blue, and yellow. The body domain consists of seven triple β-spiral repeats (β1–β7) and an α-helical coiled-coil domain (cc) that is inserted between β-spiral repeats β4 and β5. The bound α-2,3-sialyllactose is shown in stick representation and colored in orange. The black box indicates the enlarged region depicted in (B). (B) Detailed interactions between σ1 and the terminal SA of α-2,3-sialyllactose. Residues in the binding region are drawn in ball and stick representation, while the rest of the protein is shown as a ribbon drawing. The σ1 residues forming hydrogen bonds or salt bridges with the ligand are shown in green, and residues forming van der Waals contacts are shown in cyan. The side chain of Asn189 (colored dark blue) is contributed by a neighboring σ1 monomer. SA is shown in ball-and-stick representation, with carbons colored orange, oxygens colored red, and nitrogens colored blue. Bridging waters are shown as orange spheres. Hydrogen bonds and salt bridges are represented with broken lines. Adapted from Reiter et al. (2011).

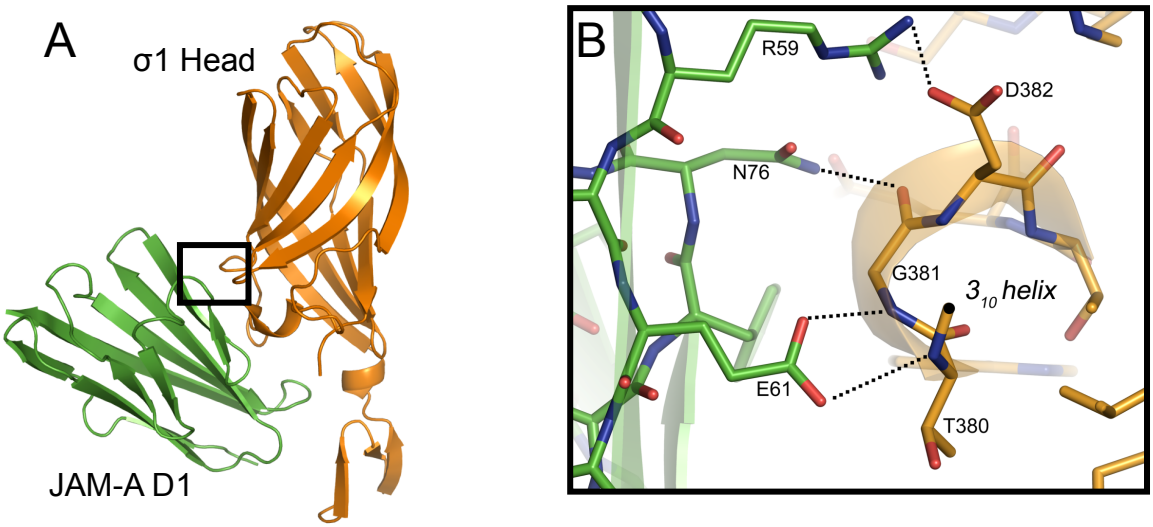

Figure I-4. Critical contacts at the σ1 head-JAM-A D1 interface. (A) Overview displaying the location of residues in the σ1 head-JAM-A D1 complex shown in (B). D1 and σ1 head are colored green and orange, respectively. The black box indicates the enlarged region depicted in (B). (B) Carbon atoms are shown in green (D1) or orange (σ1H), oxygen atoms in red, and nitrogen atoms in blue. Dotted lines represent hydrogen bonds and salt bridges. For clarity, only interacting residues are shown. Amino acids are labeled in single-letter code. (B) Interactions between D1 and residues in the 3_{10} helix in the D–E loop of σ1H. The 3_{10} helix is depicted transparently so that the main chain interactions are visible. Adapted from Kirchner et al. (2008).

Reovirus Assembly and Egress

Assembly of reovirus particles is thought to occur in cytoplasmic viral inclusions, which contain viral proteins, double-stranded RNA, and virion particles at various stages of maturation. Empty cores and fully-assembled particles are evident in electron micrographs of viral inclusions (32). The synthesis of genomic dsRNA and viral core assembly likely occur simultaneously, and assembly of the outer capsid occurs subsequent to formation of the complete core particle (1). The addition of reovirus attachment protein σ1 to the outer capsid requires host chaperone proteins Hsc70 and Hsp90 (33, 34). Reovirus release from host cells is hypothesized to occur via a lytic mechanism, but the egress pathway is not understood (1). Reovirus induces apoptosis (35-38), which may contribute to viral release from some cell types.

JAM-A

JAM-A is the only known proteinaceous receptor for reovirus. It mediates entry of prototype and field-isolate strains of all three reovirus serotypes (22, 23). JAM-A is a member of the immunoglobulin (Ig) superfamily of proteins that functions in cell-cell adhesion (39). It is expressed on the surface of endothelial and epithelial cells as a component of tight junctions (TJs) that maintain the integrity of barriers formed between polarized cells (40, 41). JAM-A also is expressed on hematopoietic cells, where it mediates leukocyte extravasation (42, 43), and on platelets, where it functions in platelet activation during blood clot formation (39, 44). JAM-A contains three distinct structural

domains: an N-terminal ectodomain, a single-span transmembrane anchor, and a C-terminal cytoplasmic tail (Figure I-2) (24). The ectodomain consists of two Ig-like domains, a membrane-distal D1 domain and a membrane-proximal D2 domain (Figure I-2B). The cytoplasmic tail terminates in a post-synaptic density protein (PSD95), Drosophila disc large tumor suppressor (Dig1), zona occludens 1 (ZO-1) (PDZ)-binding domain that interacts with intracellular TJ components (45, 46). JAM-A participates in homotypic interactions between D1 domains on opposing monomers (24). An interaction between two JAM-A monomers on adjacent cells promotes cell adhesion (47-49).

The σ1 protein interacts with the JAM-A D1 domain to adhere reovirus virions to the surface of target cells (26). JAM-A residues Ar59, Glu61, Lys63, Leu72, Tyr75, and Asn76 are required for σ1 binding and reovirus infectivity (50). Interestingly, the σ1-JAM-A interaction is substantially stronger (approximately 1000-fold) than the interaction between JAM-A monomers (26). Consequently, σ1 binding to JAM-A likely disrupts JAM-A homodimers. Studies using JAM-A knock-out (KO) mice indicate that JAM-A is required for the establishment of viremia, which is essential for dissemination and disease in newborn mice following peroral inoculation of reovirus (51). JAM-A is not required for reovirus replication in the murine CNS or development of encephalitis (51). These findings suggest that reovirus utilizes other cell-surface receptors to mediate entry into specific cell types.

JAM-A is localized to the apical junctional complex that link epithelial and endothelial cells together. Endothelial cells are specialized cells that line blood vessels, and are responsible for separating the vascular compartment from surrounding tissue. Endothelial cells are linked together via the interactions of several cell-surface proteins

(52). Tight junctions are comprised of occludins, claudins, coxsackie and adenovirus receptor (CAR), JAM-A, and endothelial cell-selective adhesion molecule (ESAM), and nectin (52). Adherens junctions include vascular endothelial cadherin (VE-cadherin) and vascular endothelial protein tyrosine phosphatase (VE-PTP) (52). Adjacent endothelial cells also are linked by platelet endothelial cell adhesion molecule (PECAM) and neural cadherin (N-cadherin) (52). Several TJ proteins act as viral receptors or facilitators of viral entry. Occludin is used by coxsackie B virus for internalization (53) and along with claudin-1 is required for hepatitis C virus infection of liver cells (54). CAR is used by both adenovirus and coxsackievirus infection (55) and JAM-A also serves as a receptor for feline calicivirus (56). The pathogenesis of these viruses requires traversal of polarized epithelial cell barriers, making TJ proteins logical targets for viral entry. In addition, *Helicobacter pylori* interacts with JAM-A to induce epithelial barrier dysfunction (57). Understanding how JAM-A facilitates infection of polarized cells may shed light on how other viruses and pathogens utilize TJ proteins as receptors or entry mediators.

Reovirus Pathogenesis

Reoviruses have been isolated from the stools of healthy (58, 59) and ill (60) children as well as a variety of animals (60). These findings suggest that reovirus is ingested into and shed from the gastrointestinal tract. The dynamics of reovirus infection *in vivo* have largely been elucidated using experimental mouse and rat model systems. Following entry into the gastrointestinal tract, intestinal proteases rapidly convert

reovirus virions to ISVPs, suggesting that the form of the reovirus particle that initiates infection in the intestine is the ISVP (61-63). In newborn mice, cells at the tips of microvilli are readily infected (Figure I-5), whereas cells in the intestinal crypts are spared (51, 64). In contrast, intestinal crypt cells are infected in adult mice, and cells at the villus tips are uninfected (65). Infectious reovirus can be recovered following peroral inoculation from the duodenum, jejunum, ileum, and colon (65, 66). However, the vast majority of virus is produced in the ileum. This differential production of virus may be due to the capacity of reovirus to infect Peyer patches. Reoviruses are thought to penetrate the intestinal barrier via transport across microfold (M) cells (Figure I-5), which are specialized cells of the follicle-associated epithelium (FAE) that overlay the Peyer patches (67-70). M cells transfer antigens from the intestinal lumen to lymphoid cells of the gut-associated lymphoid tissue (GALT) (71) and serve to monitor luminal contents by exposing Peyer patch lymphoid cells to food antigens, the intestinal microbiota, and intestinal microbial pathogens. This process is essential for induction of oral tolerance and activation of immune responses to pathogenic microorganisms (71). The preferential targeting of crypt cells observed in adult mice is hypothesized to result from transcytosis of virus across M cells and subsequent infection of crypt cells via the basolateral surface (72). However, M cells also take up reovirus in neonatal mice (51, 64, 67), suggesting that viral transcytosis across M cells is unlikely to explain the difference in intestinal cell tropism observed in adult and newborn mice. It is possible that the proliferative status of stem cells in the crypts of adult mice may recapitulate the cellular environment of neonatal intestinal cells, thereby facilitating reovirus infection of intestinal crypt cells.

Systemic reovirus infection is thought to originate from infected lymphoid cells in the Peyer patch (Figure I-5). From the Peyer patch, reovirus transits intestinal lymphatics to the mesenteric lymph node (MLN) and ultimately enters the bloodstream via the thoracic duct (51, 64, 67). Many pathogens that cause systemic disease, including poliovirus (73, 74) and *Salmonella* (75-77), initiate extraintestinal infection and access the bloodstream via this route. It is possible that in addition to this route reovirus also contacts endothelial cells within the intestine that allow entry into the bloodstream to allow for systemic dissemination.

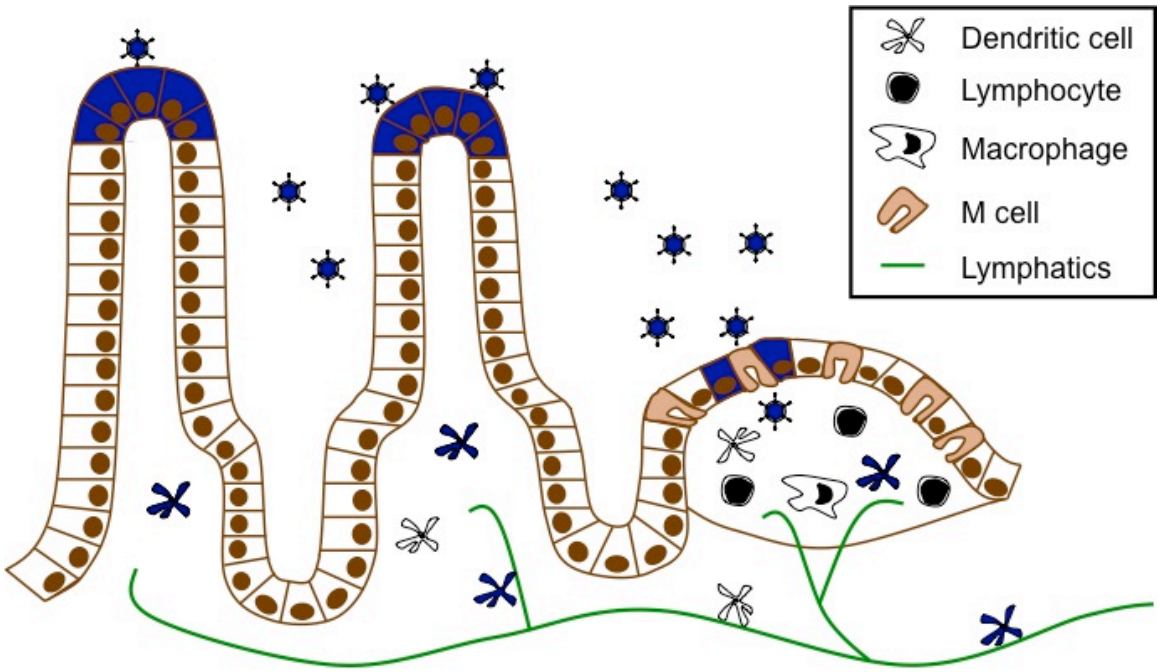

Figure I-5. Model of reovirus dissemination from the intestine. A schematic depicting where reovirus antigen is detected in the intestine following peroral infection. Reovirus antigen is detectable in the tips of microvilli, M cells, and FAE. Infected dendritic cells traffic reovirus out of the intestine via the lymphatic system.

Reovirus reaches the Peyer patches early after infection; viral antigen is detected in Peyer patches within 24 hours after peroral inoculation (51, 64, 67, 69, 70, 78). However, the mechanism by which reovirus infects Peyer patch cells is not known. It is possible that dendritic cells in the Peyer patches take up reovirus virions immediately following viral transcytosis across M cells. This is the most direct route from the intestinal lumen to the Peyer patch and the primary pathway used for processing of intestinal antigens for immune surveillance. A second possibility is that progeny virions released from the basolateral surface of infected FAE cells are taken up by lymphoid cells in Peyer patches. Both viral structural and nonstructural proteins are detected in FAE cells (79), indicating that active viral replication occurs in these cells. However, it is not known whether FAE cells produce virus. A third possibility is that dendritic cells in Peyer patches take up apoptotic fragments from infected FAE cells, which undergo apoptosis following reovirus infection (79). Dendritic cells in the underlying Peyer patches immediately adjacent to apoptotic FAE cells contain both active caspase-3 and reovirus structural proteins (79). These observations suggest that Peyer patch dendritic cells take up apoptotic bodies from infected FAE cells. Additionally, apoptosis induction in the FAE may signal Peyer patch cells to phagocytose the apoptotic remnants, along with reovirus particles.

Regardless of the mechanism by which reovirus accesses Peyer patches, reovirus antigen is detected in the MLN 24 hours after peroral inoculation. Little is known about the cell types that support reovirus growth within the intestine and dissemination to the MLN. In adult mice, $CD11c^+$ dendritic cells harbor reovirus antigen, but these cells are not thought to be actively infected (79). Viral nonstructural proteins are not present in

these cells (79), suggesting that active replication does not occur. $CD11c^+$ dendritic cells are present in neonatal animals (80), but it is not known whether these cells internalize reovirus following peroral inoculation of newborn mice.

From Peyer patches, reovirus is hypothesized to traffic via afferent lymphatics to the MLN, then through efferent lymphatics to the blood. It is possible that infected lymphoid cells or lymphoid cells harboring virus mediate transport from the Peyer patches to the bloodstream. However, migrating dendritic cells rarely exit lymph nodes once they enter and present antigen to B and T cells (81). Thus, the cells responsible for transport of reovirus from the Peyer patch are likely retained in the MLN. Reovirus titers in the MLN increase rapidly after peroral inoculation (51, 64), suggesting that active viral replication occurs in the MLN. However, it also is possible that the increase in viral load in the MLN represents migration of infected lymphoid cells from the Peyer patches. Dissemination from the MLN to the bloodstream may occur as free virus or within another lymphoid cell subset.

An alternative mechanism for accessing the blood is direct uptake of viral particles from the gut. $CD18^+$ phagocytes extend cellular processes between enterocytes to directly sample luminal contents. Dendritic cells also extend processes through the epithelial monolayer while maintaining barrier integrity to sample gut pathogens (82). A number of pathogens, including *Salmonella* (83) and *Yersinia* (84), use macrophages or dendritic cells to invade the bloodstream and cause extraintestinal infection. Following uptake of luminal pathogens, $CD18^+$ phagocytes traffic across the lamina propria and directly into the blood allowing for rapid entry of the pathogen into the bloodstream.

Reoviruses are highly virulent in newborn mice and cause injury to a variety of host organs, including the CNS, heart, and liver (1). T1 and T3 reovirus strains invade the CNS but use different routes and produce distinct pathologic consequences following peroral or intramuscular inoculation. T1 reoviruses spread by hematogenous routes and infect ependymal cells, causing nonlethal hydrocephalus (85-87). T3 reoviruses spread to the CNS by both hematogenous and neural routes and infect neurons (51, 87, 88). In the brain, T3 reoviruses induce neuronal apoptosis, which results in fatal encephalitis (85-87, 89). Studies using T1L × T3D reassortant viruses mapped the major determinant of CNS pathology to the viral S1 gene (90, 91), which encodes attachment protein σ1 and nonstructural protein σ1s (14, 92). Because of its role in viral attachment and entry, these serotype-specific differences in dissemination and disease have largely been ascribed to the σ1 protein. However, σ1s plays a critical role in promoting reovirus spread by the bloodstream (64, 88).

Reovirus Viremia

Reovirus viremia serves to spread virions to sites of secondary replication that are distant from the initial portal of entry. Other *Reoviridae* family members, including bluetongue virus (BTV) and Colorado tick fever virus, produce cell-associated viremia during infection. BTV infects and replicates in mononuclear cells, lymphocytes, and endothelial cells (93-97). Colorado tick fever virus is detected in mature erythrocytes (98). However, arthropod vectors transmit BTV and Colorado tick fever virus, making viremia a necessary part of the viral infectious cycle in nature. Mammalian reoviruses are not

transmitted by arthropod vectors and may produce a distinctly different type of viremia. Studies in which oncolytic reovirus was delivered intravenously to persons with cancer revealed that virus is largely found in hematopoietic cells, specifically mononuclear cells, granulocytes, and platelets (99). Each of these cell types express JAM-A (40, 100, 101), suggesting that reovirus associates with or infects blood cells to disseminate through the blood to target organs. However, in these studies, virus was delivered directly into the bloodstream by intravenous inoculation. It is not known how reovirus spreads systemically following infection from a natural portal, such as the intestine or lung.

Role of Reovirus Receptors in Pathogenesis

Interactions between viral attachment proteins and host cell receptors play a pivotal role in viral pathogenesis. Receptor engagement is a primary mechanism by which viruses target specific cell types. Therefore, patterns of receptor expression are a key determinant of viral disease. Reoviruses engage two types of cellular receptors: cell-surface carbohydrate (16) and JAM-A (16, 22, 23). Both T1 and T3 reoviruses bind cell-surface SA (16-20). However, the domains of σ1 that engage glycans differ between the serotypes (19, 21), as do the specific glycans bound (21).

SA engagement enhances reovirus infection through an adhesion-strengthening mechanism in which viral particles are tethered to the cell surface via a low-affinity interaction with the carbohydrate (102). This interaction maintains the virus on the cell surface and increases the opportunity to engage JAM-A. SA-binding reovirus strains have an increased capacity to infect cells compared with non-SA-binding viruses; pre-

treatment of cells with neuraminidase to remove cell-surface SA eliminates this advantage (102). SA engagement also enhances reovirus tropism for bile duct epithelial cells in mice following peroral inoculation (103). The resulting disease closely mimics biliary atresia in human infants (103), an illness epidemiologically associated with reovirus (104, 105).

Reovirus strains circulating in nature vary in the capacity to bind SA (19, 106). This finding suggests that SA binding comes with a fitness cost. Accordingly, SA binding appears to inhibit the capacity of reovirus to establish infection at mucosal portals of entry. Non-SA-binding viruses infect primary human airway epithelial cells substantially more efficiently than SA-binding strains (107). Moreover, infection of primary human airway epithelial cells by SA-binding viruses is enhanced by removal of cell-surface SA with neuraminidase. Mucosal surfaces are covered with a glycocalyx consisting of polysaccharides and glycoproteins that are rich in SA (107). SA-binding viruses may be trapped by SA within the glycocalyx and incapable of reaching the underlying epithelium (107). However, once infection is established, SA binding may enhance the capacity of reovirus to cause disease. In addition to the capacity to target bile duct epithelium, SA-binding strains are more neurovirulent than non-SA-binding viruses following intracranial inoculation (103). This increase in virulence is likely due to more efficient infection of neurons, which results in neuronal apoptosis and encephalitis. The function of SA binding in reovirus hematogenous spread remains to be determined.

Although all reoviruses bind JAM-A, T1 and T3 reoviruses infect distinct cells and cause serotype-specific patterns of pathologic injury within the CNS. These observations suggest that JAM-A binding does not influence serotype-specific

differences in reovirus neural tropism and CNS disease. Following peroral inoculation, reovirus produces similar titers in the intestine of wild-type and JAM-AKO mice (Figure I-6) (51), suggesting that JAM-A is not required for reovirus replication in the mouse gastrointestinal tract. In sharp contrast, viral titers at all sites of secondary replication are significantly lower in JAM-AKO animals compared with wild-type controls (Figure I-6) (51). Viral loads are comparable within the brains of wild-type and JAM-AKO animals after intracranial inoculation, suggesting that JAM-A is not required for viral replication at this site of secondary replication (51). These results suggest that JAM-A is required for dissemination of the virus from the intestine to replication sites in target organs.

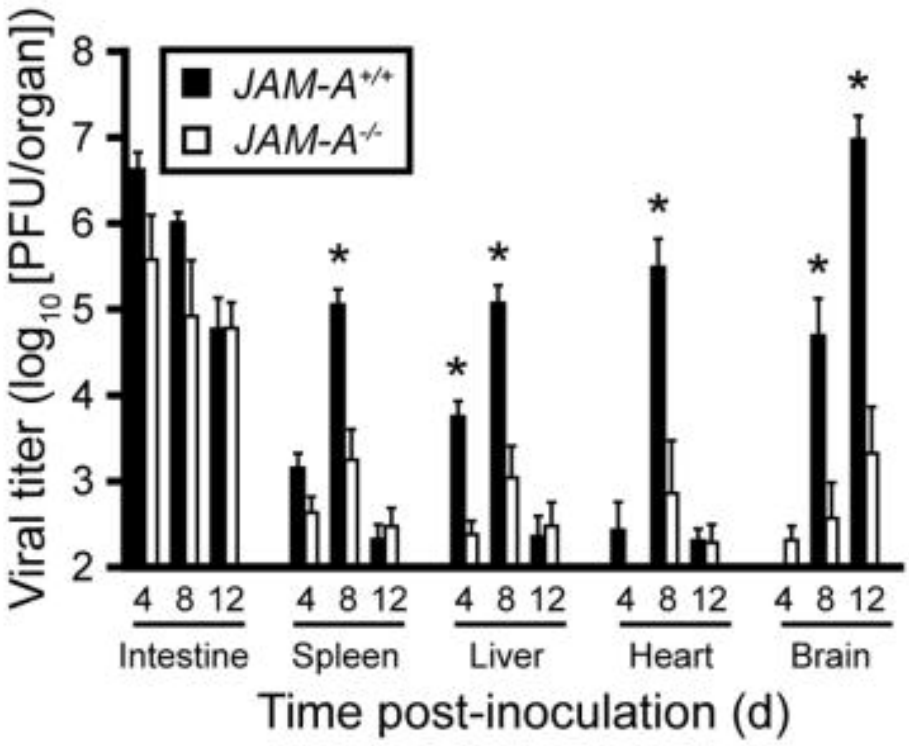

Figure I-6. Reovirus T3SA- is attenuated following peroral inoculation of JAM-A KO mice. Newborn *JAM-A*$^{+/+}$ and *JAM-A*$^{-/-}$ mice were inoculated perorally with 10^4 PFU T3SA-. At days 4, 8, and 12 after inoculation, mice were euthanized, organs were resected, and viral titers were determined by plaque assay. Results are expressed as mean viral titers for 6–13 animals for each time point. Error bars indicate SD. *, $P < 0.05$ by Student's *t* test. Adapted from Antar et al. (2009).

Reovirus Neural Spread

In addition to bloodborne spread, T3 reoviruses use neural circuits to disseminate to the CNS (87, 88). Spread via neural routes is a fundamental mechanism of reovirus pathogenesis that is essential for development of reovirus-induced encephalitis (87, 88). Direct infection of neurons at peripheral sites provides the virus with access to the spinal cord and serves as a conduit to the brain. Although the importance of neural spread to reovirus pathogenesis is well-appreciated, the cellular and molecular mechanisms that underlie neuronal reovirus trafficking are not well understood.

In contrast to hematogenous spread, JAM-A is dispensable for neural dissemination. Although JAM-A is expressed in the brain, the cell types on which it is present have not been defined. JAM-A is found on NG2-glia cells, which are a subset of stem cells that give rise to oligodendrocytes (108). It is unclear whether JAM-A is expressed on peripheral or CNS neurons. Viral titers in the brains of wild-type and JAM-AKO mice are comparable after intracranial inoculation (51). Viral tropism in the brain for hippocampal, thalamic, and cortical regions also does not differ between wild-type and JAM-AKO mice. Concordantly, primary cortical neurons isolated from wild-type and JAM-AKO mice are equally susceptible to reovirus infection and produce equivalent yields of viral progeny (51). Together, these data indicate JAM-A is not required for reovirus infection of neural tissue and suggest that JAM-A is dispensable for reovirus spread by neural routes. These findings further suggest that a cellular receptor distinct from JAM-A mediates reovirus infection of neurons.

Some evidence exists about the means by which reovirus traverses neural circuits. Treatment of animals with colchicine to inhibit fast axonal transport impairs reovirus spread to the spinal cord following hindlimb inoculation (87, 109). However, treatment with β-β′-iminodipropronitrile to inhibit slow axonal transport does not affect reovirus dissemination to the spinal cord (87, 110). These findings suggest that reovirus traffics in neurons along fast axonal transport pathways. However, these inhibitors may act non-specifically to impair other aspects of viral replication. Much work is required to fully elucidate how reoviruses replicate and traffic in neurons.

Reovirus Oncolytics

Reoviruses are superb candidates for oncolytic therapeutics due to their preference for transformed cells and capacity to induce apoptosis (1). It is not well understood why reoviruses preferentially infect transformed cells. Cells with expression of epidermal growth factor receptor and activated Ras signaling pathways have increased susceptibility to reovirus infection (111, 112). In addition, transformed cells often do not have normal interferon responses, have increased receptor availability, more effective infectious particle generation, and increased virus release (1). Currently, reovirus strain T3D is being administered to a variety of cancer patients in Phase I-III clinical trials intravenously due to its poor infectivity within the intestine (1). Spread of reovirus by the bloodstream route enables the virus to target even the smallest foci of tumor cells (99, 113).

Significance of the Research

Viremia is often a key step in viral pathogenesis. The circulatory system ensures systemic spread throughout an infected host. Although this critical process is prerequisite to seeding virus to targeted sites of secondary replication, little is known about how viruses gain access to, replicate within, and egress from the bloodstream. It is possible that pathways into and out of the bloodstream may be conserved amongst viruses that establish viremia during an infectious cycle.

The overarching goal of this dissertation was to determine mechanisms by which reovirus disseminates hematogenously. The central hypothesis was that JAM-A expression on endothelial cells facilitates bloodstream spread of reovirus. In the work presented here, I demonstrate that endothelial JAM-A facilitates reovirus bloodstream entry, viremia, and egress from the circulation using *in vivo* and *in vitro* studies. Future studies will focus on examining the means of reovirus bloodstream transport, egress of reovirus from infected endothelial cells, and reovirus exit from the circulatory system. Understanding mechanisms that govern the spread of reovirus by the bloodstream may shed light on how to inhibit this critical process during viral pathogenesis and also allow manipulation of reovirus to be a more effective oncolytic.

CHAPTER II

ENDOTHELIAL JAM-A FACILITATES REOVIRUS VIREMIA AND BLOODSTREAM SPREAD

Clinical manifestations of viral infection are often dictated by tropism of the virus for a particular cell type or organ. In the case of neurotropic viruses, infection of neurons can lead to encephalitis or other neurologic impairment. However, for many viruses to cause disease, they must first reach target tissues from a site of entry into the host and commonly use lymphatic, hematogenous, or neural pathways to traffic systemically. Infection of cells that facilitate access to these pathways can influence whether viral infection results in symptomatic disease. For example, a neurotropic virus may infect endothelial cells to promote viral entry into the bloodstream and delivery to the CNS. Knowledge gained from studies to determine precisely how viruses disseminate can be used to block this key step in viral pathogenesis and improve vector targeting for clinical purposes.

To determine whether endothelial or hematopoietic JAM-A facilitates reovirus bloodstream dissemination, mice with decreased endothelial cell-specific expression of JAM-A (EndoJAM-AKD) were generated and infected by peroral and intravascular routes. Because EndoJAM-AKD mice also lack JAM-A expression in hematopoietic cells, mice lacking or expressing JAM-A solely in the hematopoietic cell compartment (HematoJAM-AKO and HematoJAM-A, respectively) also were generated to determine whether hematopoietic JAM-A facilitates reovirus bloodstream spread. Viral titers in

blood and at sites of secondary replication were lower in EndoJAM-AKD mice than those in wild-type mice following either peroral or intravascular reovirus inoculation. In contrast, viral titers in blood and at sites of secondary replication in HematoJAM-AKO mice were similar to those in wild-type mice following both peroral and intravascular inoculation. Levels of viremia and viral replication at sites of secondary replication in HematoJAM-A mice were lower than those in wild-type mice following both peroral and intravascular inoculation. Together, these data suggest that endothelial and not hematopoietic JAM-A is required for bloodstream dissemination of reovirus.

Characterization of mice with targeted disruption of JAM-A expression. To determine the role of endothelial JAM-A in reovirus infection, I generated mice lacking JAM-A exclusively in the endothelial cell compartment (Figure II-1). Genotypes of the different mouse strains were confirmed by PCR using primers specific for the Tek-Cre (Cre recombinase) transgene and floxed JAM-A (Table 1, Figure II-1). I assessed cell-surface expression of JAM-A on hematopoietic and endothelial cells of EndoJAM-AKD mice. Surprisingly, I found that cell-surface JAM-A was decreased on endothelial cells and absent on hematopoietic cells in EndoJAM-AKD mice (Figures II-2, II-6, II-7). Compared to JAM-A expression on endothelial cells in wild-type mice, JAM-A expression on endothelial cells in EndoJAM-AKD mice was diminished approximately two-fold as determined by the mean fluorescence intensity (MFI) (Figure II-3).

To determine the role of hematopoietic JAM-A in reovirus infection, I generated mice that either lack or express JAM-A solely in the hematopoietic compartment (Figure II-4). Genotypes of the different mouse strains were confirmed by PCR using primers

specific for the Vav-cre transgene and floxed JAM-A (for HematoJAM-AKO mice) or Vav-JAM transgene and JAM-AKO allele (for HematoJAM-A mice) (Table 1, Figure II-4). I assessed cell-surface JAM-A expression on endothelial and hematopoietic cells of HematoJAM-AKO and HematoJAM-A mice. As expected, JAM-A expression on lung endothelial cells of HematoJAM-AKO mice mirrored that seen in lung endothelial cells of wild-type mice (Figure II-5). In contrast, lung endothelial cells from HematoJAM-A mice, which lack all native JAM-A but express a hematopoietic-specific JAM-A transgene (Figure II-4), had levels of JAM-A expression similar to JAM-AKO mouse lung endothelial cells (Figure II-5). Levels of JAM-A expression on hematopoietic cells collected from HematoJAM-AKO mice were undetectable, but hematopoietic JAM-A expression in HematoJAM-A mice was identical to that seen in wild-type mice (Figures II-5, II-6, II-7). The JAM-A expression phenotypes of the mouse strains used in this study are shown in Table 2.

TABLE 1. Primer sequences used to genotype mice with altered JAM-A expression.

Mouse	Region	Forward Primer	Reverse Primer
JAM-A f/f (WT)	JAM-A Exon 1	TCT TTT CAC CAA TCG GAA CG	AAA AAC TCT AGG AAC TCA CCC AGG A
JAM-AKO (KO)	JAM-A Exon 1	TCT TCT TCA GAC GCC GAA CCT	CCT CTC TTT TCA CCA ATC GGA
Tek-Cre (EKO)	Tek P to Cre	CCC TGT GCT CAG ACA GAA ATG AGA	CGC ATA ACC AGT GAA ACA GCA TTG C
Vav-Cre (HKO)	Vav P to Cre	GAA GGA ACG AGG GTG CAC	TGC CTG TCC CTG AAC ATG TC
Vav-Cre (HKO)	Cre to Vav E	ATG CAG GCT GGT GGC TGG	GGC TCG CGA GGT TTT ACT TGC
Vav-JAM (HJ)	Vav P to JAM-A	GAA GGA ACG AGG GTG CAC	GTG CAG GTC AAT TTG ATG GAC TCG
Vav-JAM (HJ)	JAM-A to Vav E	CAG CTG TCC TGG TAA CAC TGA TTC	GGC TCG CGA GGT TTT ACT TGC

[a]In cases in which two sets of primers for a particular mouse strain are shown, only one was used at any time to determine the genotype.

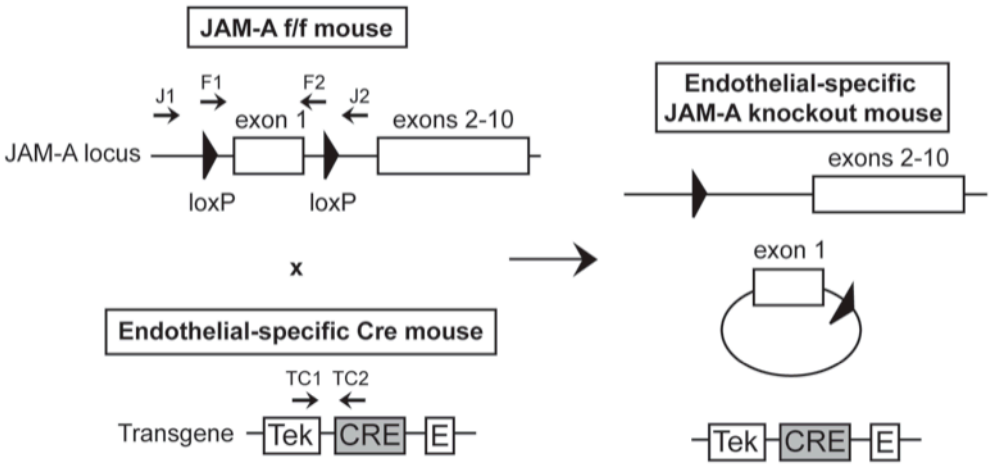

Figure II-1. Generation of EndoJAM-AKD mice. A schematic depicting the generation of EndoJAM-AKD mice used in infection experiments. Exon 1 of JAM-A is flanked by loxP sites in JAM-A f/f mice. Cre recombinase expression in endothelial-specific Cre tg mice is driven by Tek promoter and enhancer sequences from an inserted transgene. Crosses between JAM-A f/f and tissue-specific Cre mice generate mice in which exon 1 of JAM-A is excised in tissues where Cre is expressed. Arrows indicate primer binding sites for JAM-A primers (J1, J2), JAM-A f/f primers (F1, F2), and Tek-Cre primers (TC1, TC2). Tek = Tek promoter, CRE = Cre recombinase, E = Tek enhancer.

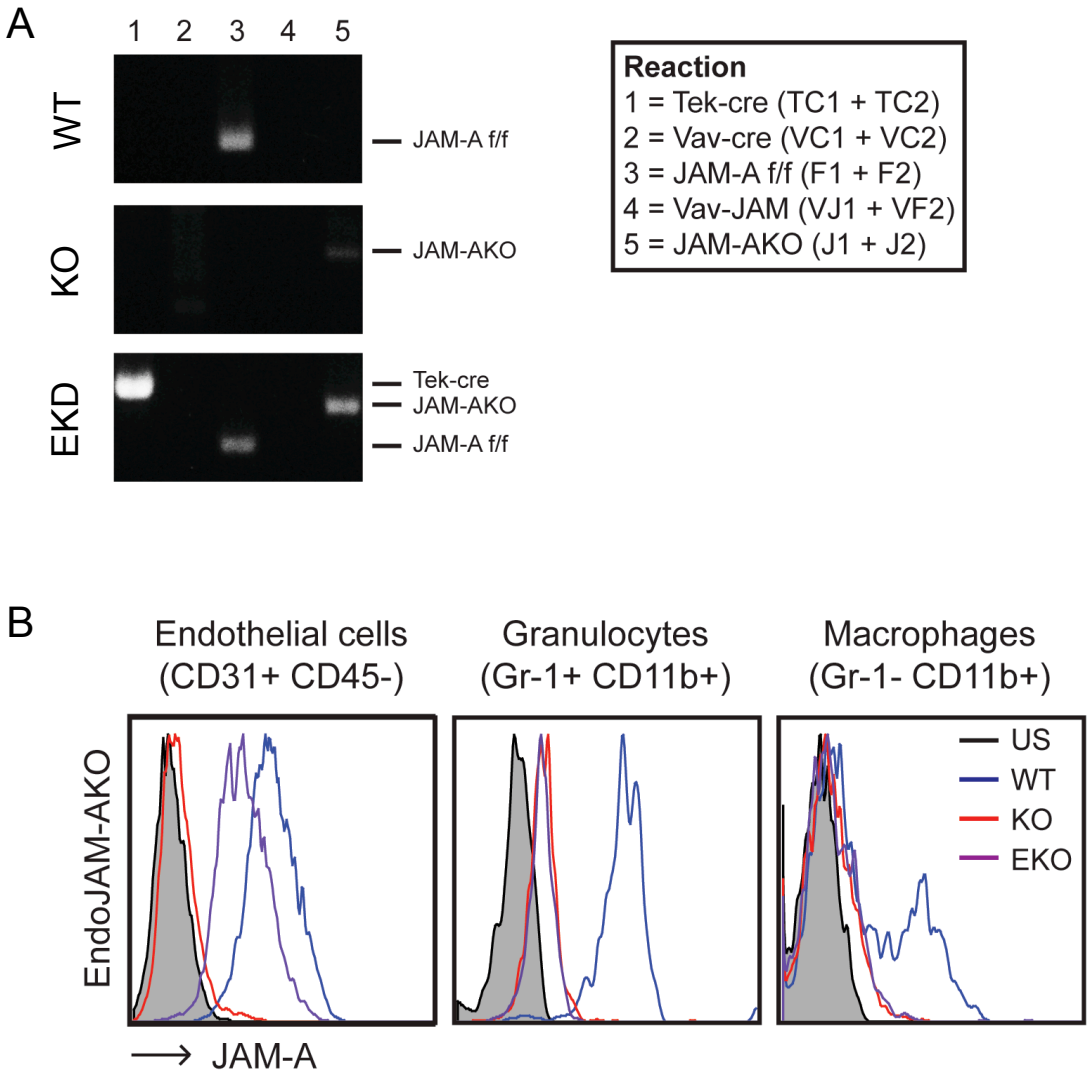

Figure II-2. Characterization of EndoJAM-AKD mice. JAM-A expression was assessed in 6- to 8-week-old mice by genomic DNA PCR and flow cytometry. Hematopoietic cells were collected from blood and spleens, and endothelial cells were cultured from lungs. JAM-A expression was quantified using flow cytometry. (A) Agarose gels displaying bands corresponding to regions of genomic DNA amplified in genotyping PCR reactions. Bands from the following reactions are shown for each mouse strain: JAM-A f/f, Tek-Cre, Vav-Cre, Vav-JAM, JAM-AKO. (B) Flow cytometric profiles of endothelial and hematopoietic cells (peripheral blood granulocytes and macrophages) from each mouse strain. US = Unstained, WT = Wild-type (JAM-A f/f), KO = JAM-AKO, EKD = EndoJAM-AKD.

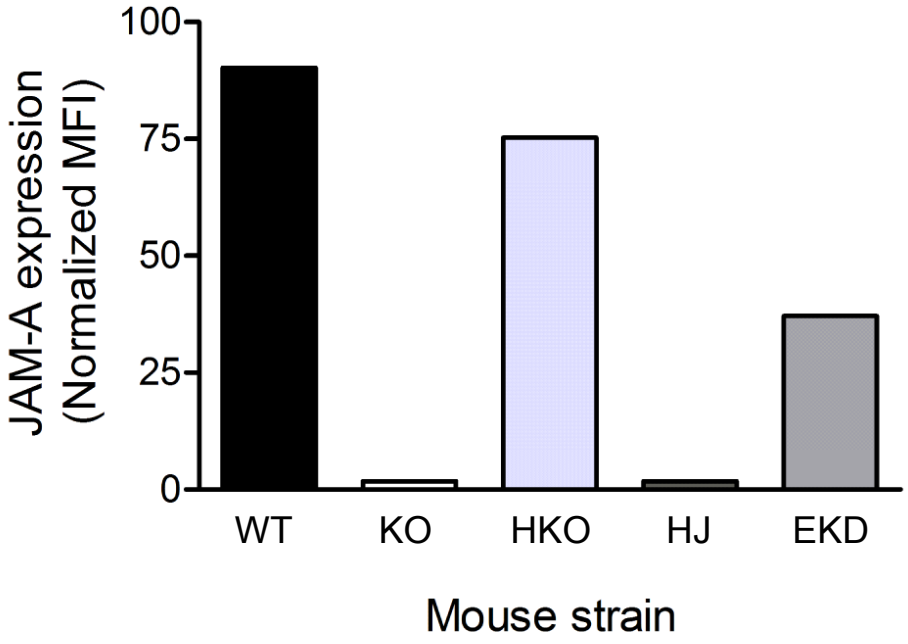

Figure II-3. Quantification of JAM-A expression in primary lung endothelial cells. Endothelial cells were cultured from lungs excised from 6- to 8-week-old mice. Cells were stained with JAM-A-specific antibody and cell-surface JAM-A expression was quantified using flow cytometry. JAM-A expression is displayed as MFI values that were normalized by subtracting MFI of unstained controls. WT = Wild-type (JAM-A f/f), KO = JAM-AKO, EKD = EndoJAM-AKD.

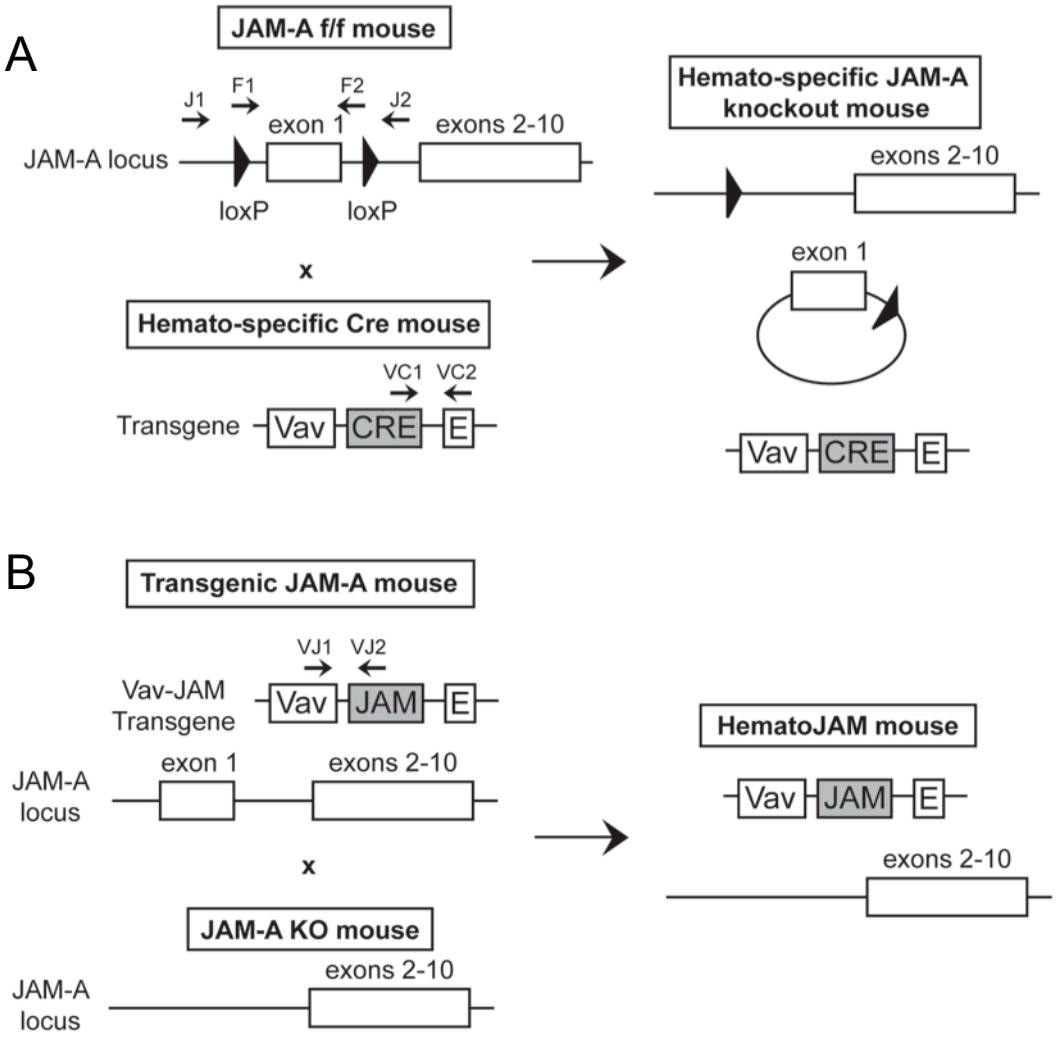

Figure II-4. Generation of HematoJAM-AKO and HematoJAM-A mice. (A) A schematic depicting the generation of HematoJAM-AKO mice used in infection experiments. Cre recombinase expression in hematopoietic-specific Cre tg mice is driven by Vav promoter and enhancer sequences from an inserted transgene. Arrows indicate primer binding sites for JAM-A primers (J1, J2), JAM-A f/f primers (F1, F2), and Vav-cre primers (TC1, TC2). Vav = Vav promoter, CRE = Cre recombinase, E = Vav enhancer. (B) Mice that express JAM-A only within the hematopoietic cell compartment (HematoJAM-A mice) were obtained by generating tg mice expressing a transgene in which JAM-A expression is driven by Vav1 promoter and enhancer sequences. JAM-A expression was abolished by breeding the tg mice with JAM-AKO mice. Arrows indicate primer binding sites for Vav-JAM primers (VJ1, VJ2). Vav = Vav promoter, JAM = JAM-A cDNA, E = Vav enhancer.

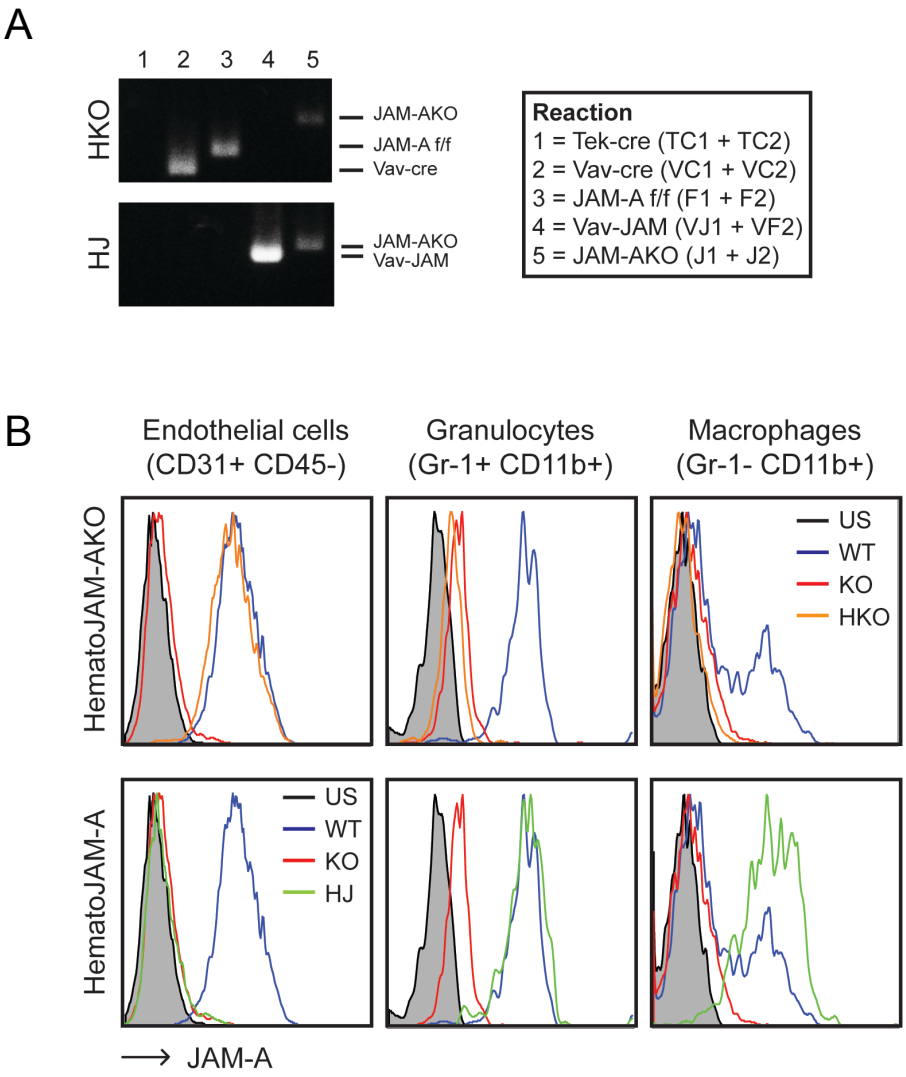

Figure II-5. Characterization of HematoJAM-AKO and HematoJAM-A mice. JAM-A expression was assessed in 6- to 8-week-old mice by genomic DNA PCR and flow cytometry. Hematopoietic cells were collected from blood and spleens, and endothelial cells were cultured from lungs. JAM-A expression was quantified using flow cytometry. (A) Agarose gels displaying bands corresponding to regions of genomic DNA amplified in genotyping PCR reactions. Bands from the following reactions are shown for each mouse strain: JAM-A f/f, Tek-Cre, Vav-Cre, Vav-JAM, JAM-AKO. (B) Flow cytometric profiles of endothelial and hematopoietic cells (granulocytes and macrophages) from each mouse strain. US = Unstained, WT = Wild-type (JAM-A f/f), KO = JAM-AKO, HKO = HematoJAM-AKO, HJ = HematoJAM-A.

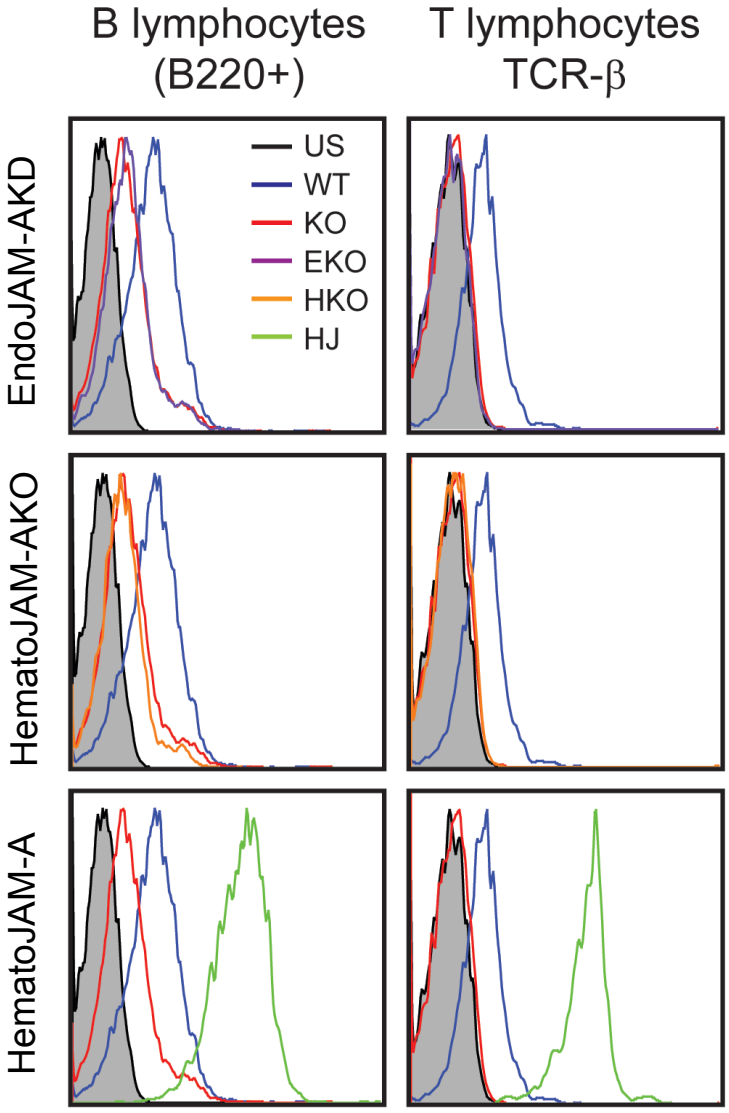

Figure II-6. JAM-A expression in circulating hematopoietic cells. Blood was collected retroorbitally from 6- to 8-week-old mice, and JAM-A expression on leukocytes was quantified using flow cytometry. B and T lymphocytes were defined as the populations that were $B220^{+}$ and TCR-β^{+}, respectively. Each set of histograms includes data from unstained, WT, and JAM-AKO cells along with the indicated genotype. WT = Wild-type (JAM-A f/f), KO = JAM-AKO, EKD = EndoJAM-AKD, HKO = HematoJAM-AKO, HJ = HematoJAM-A.

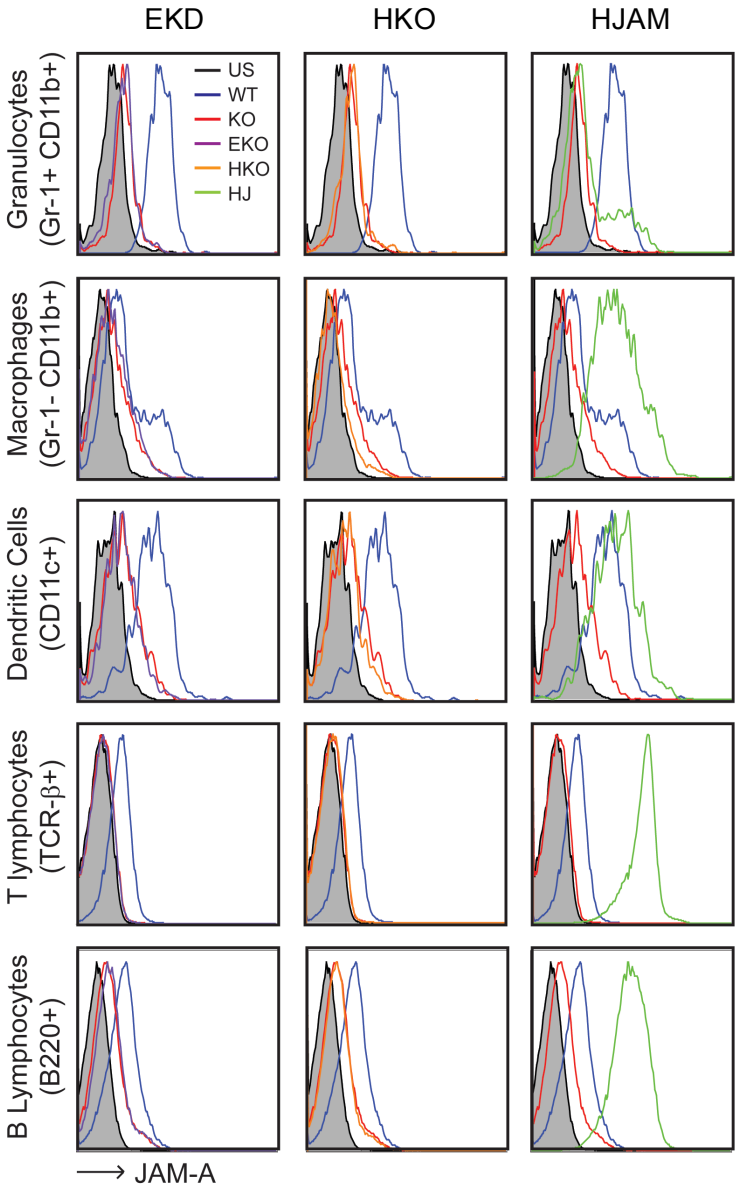

Figure II-7. JAM-A expression in splenocytes. Spleens were excised from 6- to 8-week-old mice, and splenocytes were stained for various hematopoietic cell markers. Granulocytes, macrophages, dendritic cells, B lymphocytes, and T lymphocytes were defined as the populations that were Gr-1$^+$, CD11b$^+$, Cd11c$^+$, B220$^+$, and TCR-β$^+$, respectively. Each set of histograms includes data from unstained, WT, and JAM-AKO cells along with the indicated genotype. WT = Wild-type (JAM-A f/f), KO = JAM-AKO, EKD = EndoJAM-AKD, HKO = HematoJAM-AKO, HJ = HematoJAM-A.

TABLE 2. JAM-A expression in mouse strains used in studies of reovirus bloodstream spread.

Mouse strain	JAM-A Expression	
	Endothelial Cells	Hematopoietic Cells
Wild-type (JAM-A f/f)	+[a]	+
JAM-AKO	-[b]	-
EndoJAM-AKD	↓[c]	-
HematoJAM-AKO	+	-
Hemato-JAM-A	-	+

[a]Wild-type expression; [b]Absent expression;
[c]Expression decreased approximately 50%

Endothelial JAM-A promotes bloodstream dissemination of reovirus. To determine whether endothelial or hematopoietic JAM-A is required for bloodstream spread of reovirus, wild-type, JAM-AKO, EndoJAM-AKD, HematoJAM-AKO, and HematoJAM-A mice were inoculated perorally with reovirus strain T1L. Following peroral inoculation of newborn mice, T1L infects the intestine, disseminates hematogenously, and reaches high titers in most visceral organs (51, 64). Reovirus dissemination was assessed by determining viral titers in organ homogenates and blood of infected mice 4, 8, and 12 d post-inoculation. As anticipated, wild-type, JAM-AKO, and the tissue-specific JAM-A-expressing mice had equivalent viral titers in the intestine (Figure II-8), as replication at this site is not JAM-A-dependent (51). Viral titers were minimally detectable in the brain, heart, and blood of JAM-AKO mice and significantly lower in the spleen and liver compared with those in wild-type animals (Figures II-8, II-9). After peroral reovirus inoculation, HematoJAM-AKO mice, which lack JAM-A only in hematopoietic cells, phenocopied wild-type mice. Viral titers in the heart, spleen, liver, brain, and blood of infected HematoJAM-AKO mice were equivalent to those in infected wild-type mice (Figures II-8, II-9). Viral titers in the brain, heart, spleen, liver, and blood of HematoJAM-A mice, which express JAM-A solely in hematopoietic cells, were similar to those seen in JAM-AKO mice (Figures II-8, II-9). These data suggest that hematopoietic JAM-A is dispensable for reovirus hematogenous dissemination.Viral titers in the spleen, liver, heart, brain, and blood of EndoJAM-AKD mice were significantly lower than those observed in wild-type mice (Figures II-8, II-9). Titers of virus in these animals were similar to those observed in JAM-AKO and HematoJAM-A

mice, suggesting that reovirus hematogenous dissemination is dependent on endothelial but not hematopoietic JAM-A.

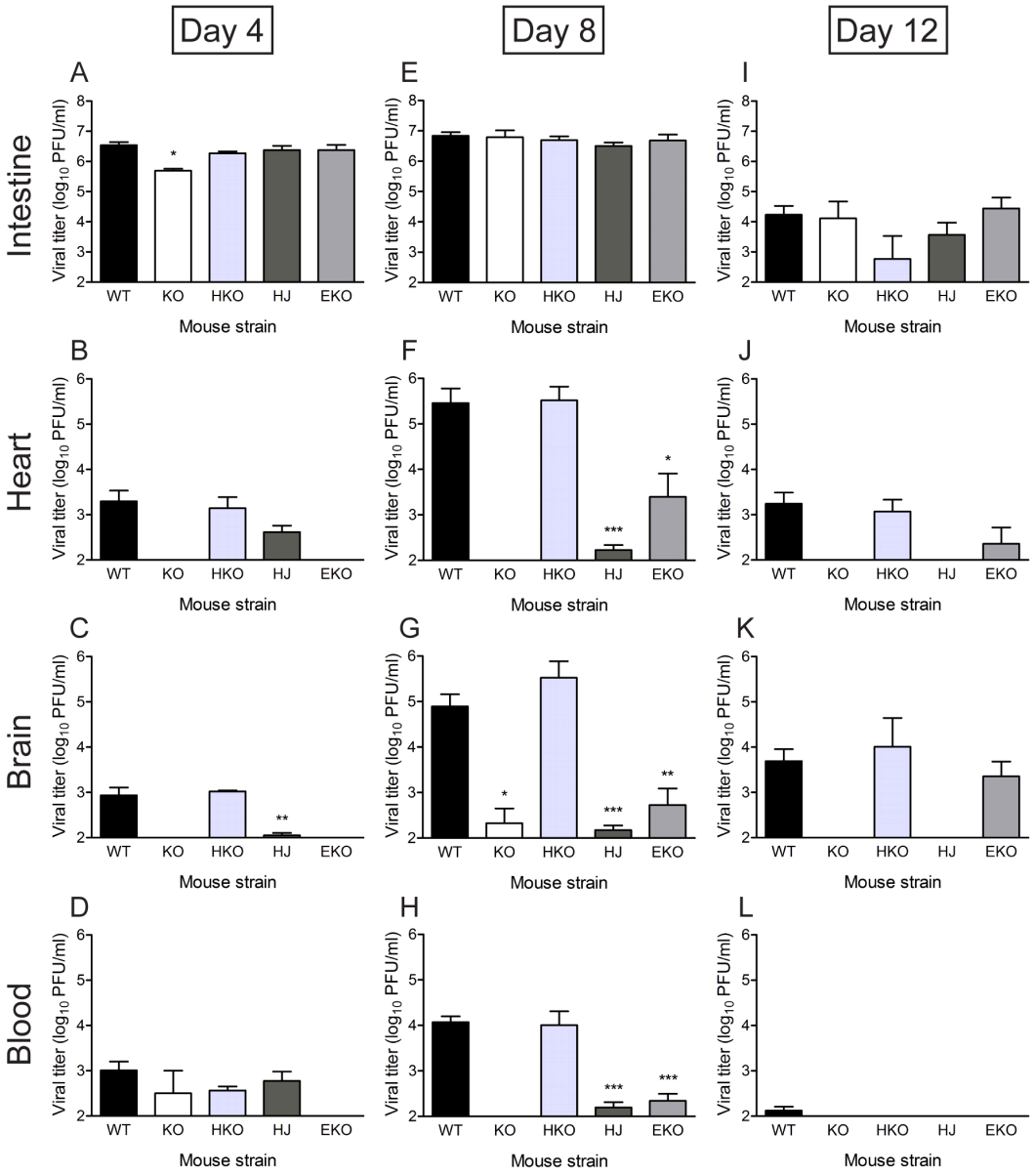

Figure II-8. Endothelial JAM-A is required for reovirus bloodstream spread. Newborn (2-3 d) mice were inoculated perorally with reovirus strain T1L at 1000 plaque forming units (PFU) per mouse. At 4, 8, and 12 d post-inoculation, intestine, heart, and brain were excised and blood was collected into an equal volume of Alsever's solution for determination of viral titer by plaque assay. Results are presented as mean viral titer. Error bars indicate standard deviation. For each time point and mouse strain, two to twenty-two mice were used. WT = Wild-type (JAM-A f/f), KO = JAM-AKO, EKO = EndoJAM-AKO, HKO = HematoJAM-AKO, HJ = HematoJAM-A. *, $P < 0.05$, **, $P < 0.005$, ***, $P < 0.001$ by Student's *t* test.

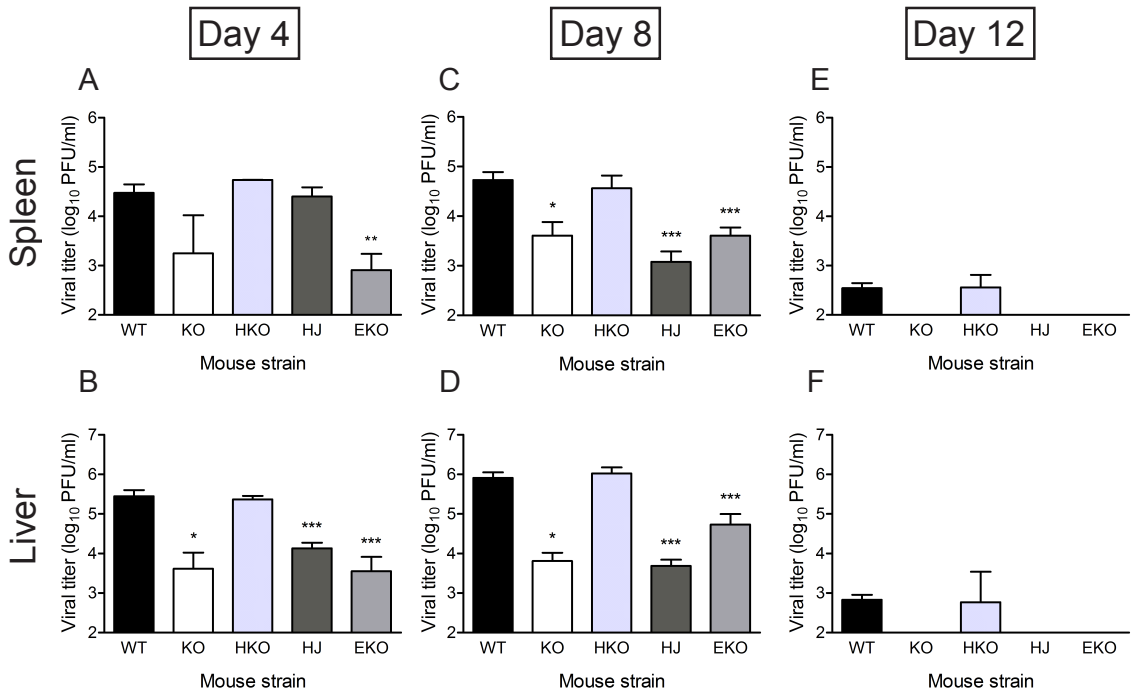

Figure II-9. Reovirus dissemination to the liver and spleen requires endothelial JAM-A. Newborn (2-3 d) mice were inoculated perorally with reovirus strain T1L at 1000 PFU per mouse. At 4, 8, and 12 d post-inoculation, spleen and liver were excised for determination of viral titer by plaque assay. Results are presented as mean viral titer. Error bars indicate standard deviation. For each time point and mouse strain, two to twenty-two mice were used. WT = Wild-type (JAM-A f/f), KO = JAM-AKO, EKO = EndoJAM-AKO, HKO = HematoJAM-AKO, HJ = HematoJAM-A. *, $P < 0.05$, **, $P < 0.005$, ***, $P < 0.001$ by Student's *t* test.

Endothelial JAM-A is required for reovirus egress from the bloodstream. Because the requirement for bloodstream entry may differ from the requirement for bloodstream egress, I used an intravenous inoculation protocol to directly assess the role of JAM-A in reovirus bloodstream egress. Wild-type and JAM-AKO mice were inoculated intravenously with reovirus strain T1L, and viral titers in organ homogenates were determined by plaque assay 8 d post-inoculation (Figure II-10). Viral titers in wild-type mice inoculated intravenously were similar to those in perorally-inoculated wild-type mice (Figures II-8, II-9, II-10). In intravenously-inoculated mice, reovirus disseminated to the intestine, spleen, liver, heart, and brain (Figure II-10). Viral titers in JAM-AKO mice were significantly lower in all organs tested compared with those in wild-type mice, suggesting that reovirus egress from the bloodstream is dependent on JAM-A expression (Figure II-10).

To determine whether endothelial or hematopoietic JAM-A facilitates reovirus egress from the bloodstream, EndoJAM-AKD, HematoJAM-AKO, and HematoJAM-A mice were inoculated intravenously, and viral titers were determined in organ homogenates 8 d post-inoculation. Reovirus titers in HematoJAM-AKO were comparable to those observed in wild-type mice (Figure II-10), suggesting that dissemination to these sites does not require hematopoietic JAM-A. Viral titers in the liver and heart of HematoJAMKO mice were significantly lower than those seen in wild-type mice (Figure II-10). However, the magnitude of this decrease in viral titers is modest. Viral titers in the intestine, spleen, liver, heart, and brain of HematoJAM mice were similar to those observed in JAM-AKO mice, suggesting that hematopoietic JAM-A is not sufficient for reovirus exit from the circulation and infection of these organs (Figure II-10). Viral titers

in EndoJAM-AKD mice were significantly lower in the blood and intestine, spleen, liver, heart, and brain compared with those observed in wild-type mice (Figure II-10). Taken together, these data suggest that reovirus egress from the bloodstream requires endothelial but not hematopoietic JAM-A.

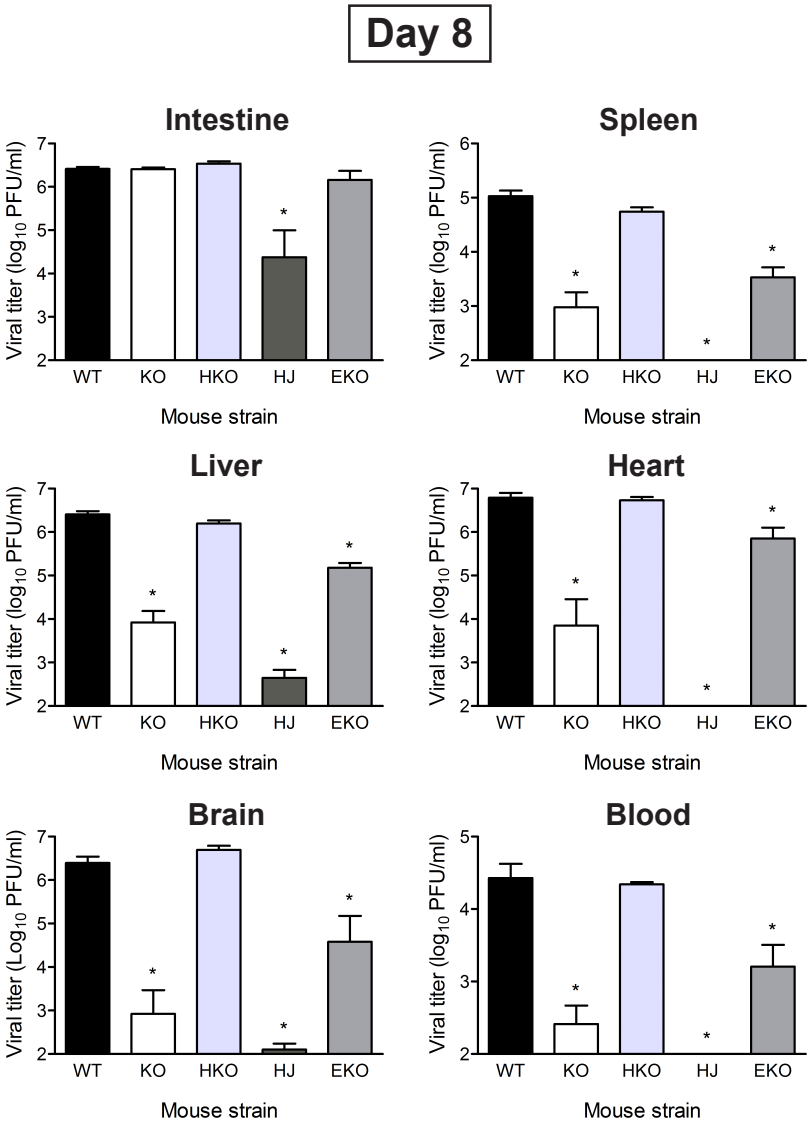

Figure II-10. Reovirus uses endothelial JAM-A to egress from the circulation. Newborn (2-3 d) mice were inoculated perorally with reovirus strain T1L at 1000 PFU per mouse. At 8 d post-inoculation, intestine, spleen, liver, heart, and brain were excised and blood was collected into an equal volume of Alsever's solution for determination of viral titer by plaque assay. Results are presented as the mean viral titer. Error bars indicate standard deviation. For each time point and mouse strain, five to eighteen mice were used. WT = Wild-type (JAM-A f/f), KO = JAM-AKO, EKO = EndoJAM-AKO, HKO = HematoJAM-AKO, HJ = HematoJAM-A. *, $P < 0.05$, **, $P < 0.005$, ***, $P < 0.001$ by Student's *t* test.

Primary endothelial cells are permissive for reovirus infection. Polarized endothelial cells are permissive for reovirus infection *in vitro* (51, 114). Because reovirus spread was limited in EndoJAM-AKD mice, I wondered whether this defect in viral replication is due to a replication defect in the endothelial cell compartment. Primary lung endothelial cells were cultured from lungs excised from wild-type, JAM-AKO, EndoJAM-AKD, HematoJAM-AKO, and HematoJAM-A mice and infected with reovirus strain T1L at a multiplicity of infection (MOI) of 100 PFU per cell. After one replication cycle, cells were collected and stained for reovirus antigen using Alexa Fluor-conjugated reovirus-specific antiserum. The percentage of infected cells for each genotype (Figure II-11) correlated with the level of JAM-A expression in endothelial cells (Figure II-3). These data suggest that reovirus replication in endothelial cells seeds the bloodstream with virus.

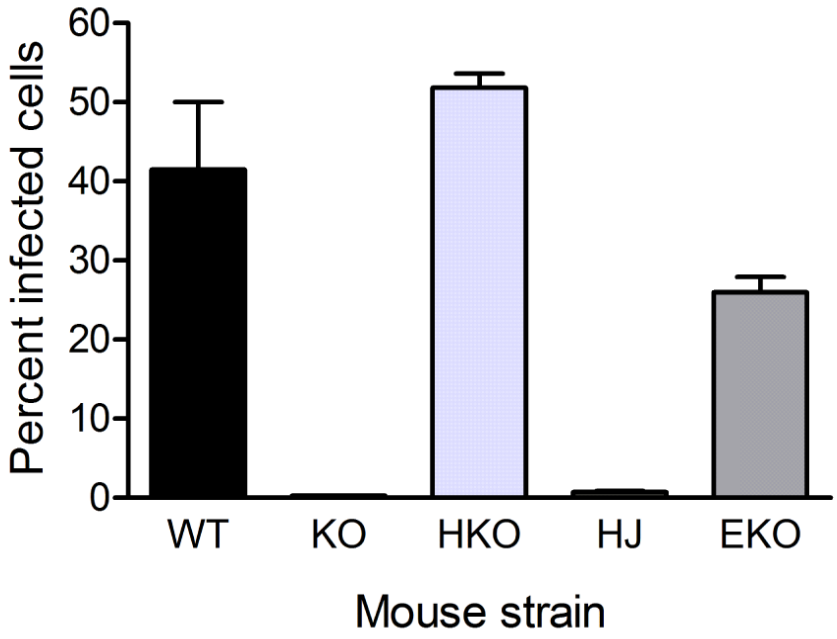

Figure II-11. Reovirus infectivity is diminished in EndoJAM-AKO lung endothelial cells. Endothelial cells were cultured from lungs excised from 6- to 8-week-old mice. Cells were adsorbed with virus strain T1L at an MOI of 100 PFU per cell. After incubation at 37°C for 24 h, cells were harvested and stained for reovirus antigen using Alexa Fluor-conjugated reovirus-specific antiserum. The percentage of infected cells was determined using flow cytometry.

Discussion

Reoviruses are neurotropic viruses that disseminate by hematogenous and neural routes. These viruses are useful experimental models to dissect mechanisms by which viruses gain access to these systemic transport pathways. In this study, I assessed hematogenous reovirus spread in mice with tissue-specific alterations in JAM-A expression. I hypothesized that systemic bloodstream spread of reovirus depends on expression of JAM-A in the endothelium and on hematopoietic cells. The key finding in this chapter is that endothelial but not hematopoietic JAM-A is required for reovirus bloodstream spread.

To generate mice with altered JAM-A expression in the endothelial compartment, I chose to use animals that express Cre driven by the Tek promoter. Tek is a tyrosine kinase that is specific for endothelial cells, but it also is expressed in hematopoietic stem cells (115). Tek-dependent Cre recombinase expression in hematopoietic stem cells likely accounts for the absence of JAM-A expression in all hematopoietic cell types in EndoJAM-AKD mice (Figures II-2B, II-6, II-7). To exclude the possibility that the absence of hematopoietic JAM-A might confound the effects seen in EndoJAM-AKD mice, I generated HematoJAM-AKO and HematoJAM-A mice.

Dissemination by the bloodstream route requires that a virus surmount several physiological obstacles. Reoviruses initially replicate in the small intestine in a JAM-A-independent manner (51), enter into the bloodstream, and target the CNS where replication is again JAM-A-independent (51). Mice lacking JAM-A are protected from reovirus-induced encephalitis because the virus cannot enter the bloodstream (51).

Accordingly, reovirus infection of polarized endothelial cells is dependent on JAM-A (114). When infected from the basolateral (or tissue) surface, polarized endothelial cells route the virus to the luminal (or blood) surface of the polarized monolayer (114). These data suggest that reovirus uses JAM-A to infect endothelial cells to gain access to the bloodstream. EndoJAM-AKD mice, which display diminished JAM-A expression in endothelial cells, have significantly lower levels of viremia after peroral and intravenous inoculation compared with those in wild-type mice (Figures II-8D, H, L and II-10F), suggesting that endothelial JAM-A facilitates reovirus entry into and exit from the bloodstream. Subsequent spread to sites of secondary replication (e.g., brain and heart) after peroral inoculation is significantly diminished in EndoJAM-AKD mice (Figure II-8), suggesting that efficient spread to those sites requires a threshold level of viremia. Although viral titers in organ homogenates prepared from EndoJAMKD mice are significantly lower than those observed in wild-type mice, there is detectable virus at these sites. This finding might be attributable to residual JAM-A expression in the endothelium of EndoJAM-AKD mice or the presence of another host component that facilitates systemic trafficking of reovirus. Nonetheless, my findings provide strong evidence that endothelial JAM-A promotes bloodstream entry during systemic infection.

Many viruses use hematopoietic cells to traffic in an infected host. For example, HIV-1 adheres to dendritic cells prior to contact with their primary target, CD4+ T lymphocytes (116, 117). Because JAM-A is expressed on circulating hematopoietic cells, I hypothesized that reovirus uses leukocytes to traffic within the circulation. Surprisingly, I found that viral titers in the blood and at sites of secondary replication of HematoJAMKO mice, which lack JAM-A in the hematopoietic compartment, are

equivalent to those seen in wild-type mice after peroral and intravenous inoculation (Figures II-8, II-9, II-10). Viral titers in HematoJAM mice, which express JAM-A only in hematopoietic cells, mirrored those seen in JAM-AKO mice (Figures II-8, II-9, II-10), further confirming that hematopoietic JAM-A does not facilitate reovirus spread through the bloodstream. Since reoviruses have been reported to associate with dendritic cells *in vivo* (99), it is possible that reoviruses bind to or infect leukocytes using a molecule distinct from JAM-A. In clinical trials using reovirus strain T3D as an oncolytic agent, the virus was observed to bind human immune cells in the blood (99). Therefore, reovirus strains may differ in the capacity to infect leukocytes *in vivo.*

Development of viremia may occur as a consequence of viral replication in endothelial cells. Flaviviruses like dengue virus (DENV) are capable of infecting endothelial cells and replicate to high titers, lysing the cells to increase viremia (118). In the case of DENV infection, high-titer viremia is required for vectoral transmission of the virus to a naïve host (119). Reovirus viremia is not required for transmission of the virus since reovirus host-to-host spread occurs primarily by the fecal-oral route. Instead, viremia serves to spread reovirus systemically to sites of secondary replication. Viral titers in the blood of JAM-AKO mice are significantly lower than those observed in wild-type mice (Figure II-8D, H, L) (51), suggesting that JAM-A promotes establishment of viremia. Infection of polarized endothelial cells with reovirus requires JAM-A and may serve as a means to amplify reovirus within the bloodstream (114). Apical (or luminal) infection of polarized endothelial cells is efficient, and infected cells release virus noncytolytically from the apical surface (114). Lower viral titers in the blood of EndoJAM-AKD mice and wild-type viral titers in the blood of HematoJAM-AKO mice

after peroral and intravenous inoculation (Figures II-8, II-10) suggest that endothelial and not hematopoietic JAM-A is required for development of viremia.

Reoviruses are superb candidates for oncolytic therapeutics due to their preference for transformed cells and capacity to induce apoptosis (1). Currently, reovirus strain T3D is being administered to a variety of cancer patients in Phase I-III clinical trials intravenously due to its poor infectivity within the intestine (1). Spread of reovirus by the bloodstream route enables the virus to target even the smallest foci of tumor cells (99). By understanding how reovirus interacts with JAM-A on the endothelium, it may be possible to design new reovirus vectors to reach target tumors more efficiently. For example, reoviruses with higher affinity for JAM-A may enter and exit the circulation more readily, allowing for more efficient targeting of tumor cells. On the other hand, generating reoviruses that bind JAM-A with lower affinity may decrease the pathogenicity of the virus by inhibiting viremia. Thus, understanding mechanisms that govern the spread of reovirus by the bloodstream sheds light on how pathogens systemically disseminate and may enhance systemic vector targeting for a host of therapeutic applications.

CHAPTER III

JAM-A FACILITATES REOVIRUS INFECTION OF POLARIZED HUMAN BRAIN MICROVASCULAR ENDOTHELIAL CELLS

Bloodstream dissemination within an infected host is required for the pathogenesis of many viruses. In particular, many neurotropic viruses use the circulation to invade the CNS from a distant site of primary replication. Regardless of the site of entry into the host, viruses that disseminate hematogenously must first traverse an endothelial barrier and egress from the circulation. Although viremia is a well-established dissemination process, precise mechanisms of viral entry into the bloodstream are not well understood.

In this study, I examined reovirus infection of polarized human brain microvascular endothelial cells (HBMECs) to better understand mechanisms of viral entry into the bloodstream. I found that reovirus productively infects polarized endothelial cells from both apical and basolateral routes of adsorption. Regardless of the route of adsorption, reovirus infection of polarized endothelial cells is dependent on engagement of receptors SA and JAM-A. Reovirus infection by the apical route of infection is more efficient than infection by the basolateral route, likely because of increased expression of JAM-A on the apical surface of polarized endothelial cells. These studies provide a new understanding of how viruses infect polarized endothelial cells and identify the endothelium as an important mediator of viral pathogenesis.

Generation of a polarized endothelial cell system for studies of reovirus infection. To investigate how reoviruses might use a polarized endothelium to enter the bloodstream, a polarized endothelial cell system was generated by culturing HBMECs on Transwell inserts. To confirm that the conditions used to cultivate HBMECs on Transwell inserts lead to formation of polarized cultures, transendothelial electrical resistance (TEER) and permeability of the monolayers to diffusion of dextrans was determined. The TEER of HBMECs increased over time in comparison to L929 fibroblast cells, which do not polarize, suggesting the formation of TJs and establishment of polarized cultures (Figure III-1A). The permeability to FITC-labeled dextrans across cultured HBMEC monolayers decreased over time in parallel with increased TEER, with dextran diffusion barely detectable 7 d post-seeding (Figure III-1B). As a control, ethylenediaminetetraacetic acid **(**EDTA) treatment, which chelates divalent cations required for TJ maintenance, enhanced permeability across the HBMEC monolayer (Figure III-1B). Furthermore, TJ protein markers are present in confocal micrographs of HBMECs cultured on Transwells for 7 d (Figure III-1C, white asterisks). These data suggest that HBMECs cultivated on Transwell inserts form TJs and become polarized 7 d post-seeding.

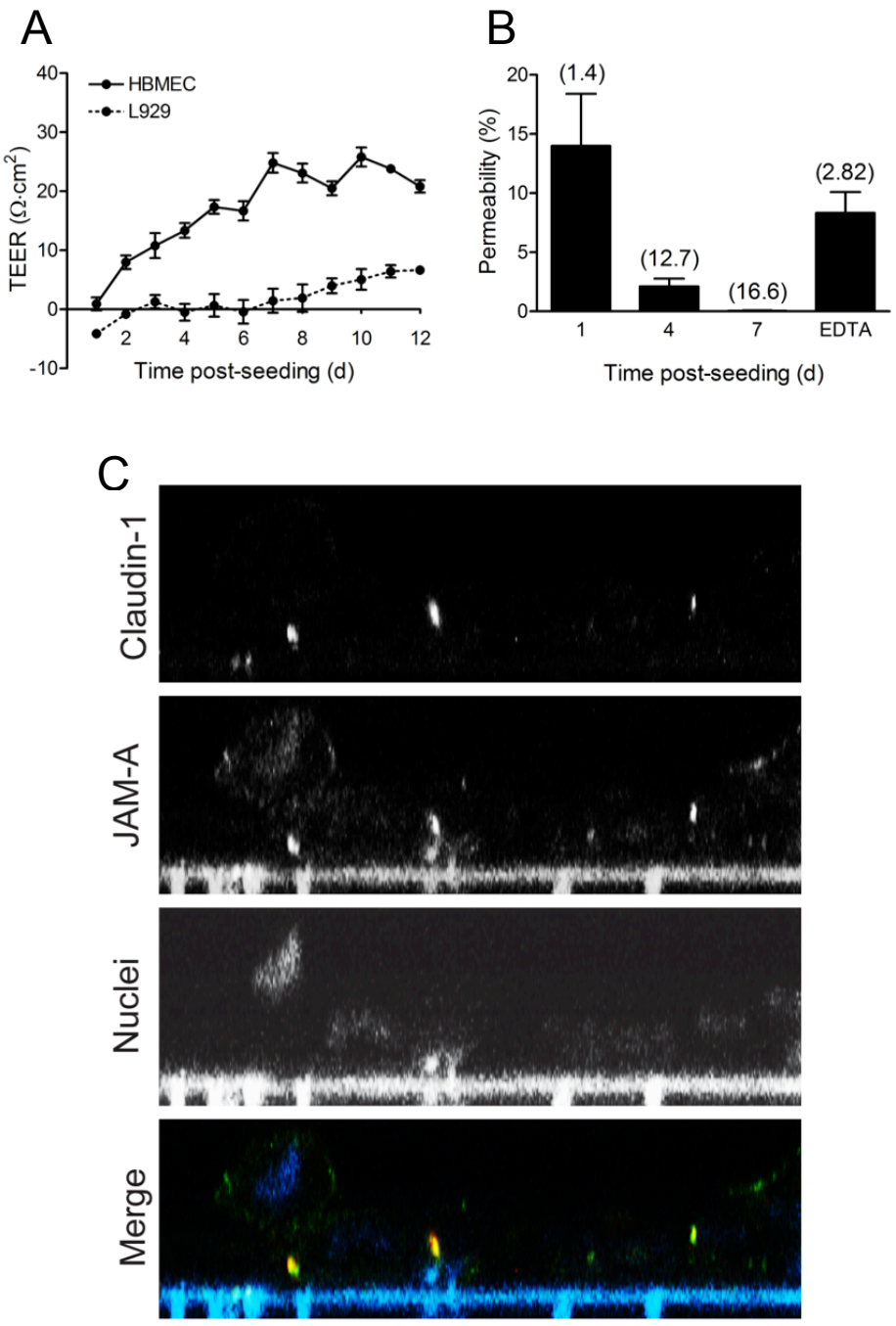
A
HBMEC
L929
TEER (Ω·cm²)
Time post-seeding (d)
B
Permeability (%)
(1.4)
(12.7)
(16.6)
(2.82)
1
4
7
EDTA
Time post-seeding (d)
C
Claudin-1
JAM-A
Nuclei
Merge

Figure III-1. Barrier properties of polarized HBMECs. (A) HBMECs (solid line) and L929 cells (dashed line) cultivated on Transwells were monitored for TEER daily for 12 d. The data are presented as unit area resistance, where normalized TEER is multiplied by the area of the Transwell insert ($\Omega \cdot cm^2$). A representative experiment of two performed is shown, with each experiment conducted in duplicate. Error bars indicate range of data for the duplicates. (B) FITC-labeled dextrans were added to the apical compartment of HBMECs cultivated on Transwell inserts at 1, 4, or 7 d post-seeding. Prior to the addition of dextrans, TEER ($\Omega \cdot cm^2$) was determined and is presented in parentheses above each bar. The percent permeability was determined using the following equation: Permeability (%) = $[\text{FITC-dextran}]^{\text{basolateral}}/([\text{FITC-dextran}]^{\text{basolateral}} + [\text{FITC-dextran}]^{\text{apical}}) \times 100$. On day 7, 2.5 mM EDTA was added to the apical and basolateral compartments as a control to disrupt TJs. A representative experiment of three performed is shown, with each experiment conducted in duplicate. Error bars indicate range of data for the duplicates. (C) HBMECs cultured on Transwells for 7 d were stained for TJ proteins claudin-1 (red) and JAM-A (green) and nuclei (blue). At the bottom of the merged image, blue staining shows the Transwell membrane. Representative images of the cell monolayer in the xz plane are shown. White asterisks indicate colocalization of TJ proteins. Cell images were captured using a Zeiss LSM 510 Meta laser-scanning confocal microscope using a 63×/1.40 Plan-Apochromat objective lens.

Reovirus infection of polarized endothelial cells is more efficient from the apical surface. To determine whether reovirus productively infects polarized endothelial cells, I adsorbed either the apical or basolateral surface of polarized HBMECs with strain T3SA+, a virus that efficiently binds sialic acid and JAM-A (22, 102). Viral titer in cell lysates increased over time regardless of the route of adsorption (Figure III-2A). Following apical adsorption, viral titer peaked at 24 h post- infection, with the yield reaching approximately 1000-fold over input (Figure III-2A). In contrast, following basolateral adsorption, viral replication was delayed with yields of 5-fold at 24 h and 100-fold at 48 h post-infection (Figure III-2A). I observed a similar trend with polarized HBMECs infected with reovirus strain T1L (Figure III-3A). These data indicate that reovirus infection of polarized HBMECs is productive following either apical or basolateral entry routes, but apical adsorption results in more efficient replication and increased viral yields.

Because I observed higher peak titers in polarized HBMECs after apical adsorption, I sought to determine whether initiation of reovirus infection is more efficient when cells are infected apically versus basolaterally. Polarized HBMECs were adsorbed with virus by the apical or basolateral route, and the percentage of reovirus antigen-positive cells was quantified using flow cytometry. Apical adsorption resulted in approximately ten-fold more infected cells compared with that following basolateral adsorption (Figure III-2B). Apical infection of polarized HBMECs by reovirus strain T1L also yielded significantly more infected cells than that observed after basolateral infection (Figure III-3B). As a control, apical or basolateral adsorption of nonpolarized L929

fibroblast cells cultivated on Transwell inserts yielded equivalent numbers of infected cells (Figure III-2B).

To determine whether differences in infectivity are attributable to differences in virus binding, I assessed virus attachment to polarized HBMECs following apical or basolateral adsorption. In concordance with the infectivity data, approximately 10-fold more virus was bound to HBMECs following apical adsorption compared with that following basolateral adsorption (Figure III-2C). As anticipated, virus bound equivalently to L929 fibroblasts following adsorption either apically or basolaterally (Figure III-2C). Together, these data suggest that reovirus binds more efficiently to the apical surface of polarized HBMECs, which results in increased infectivity and replication.

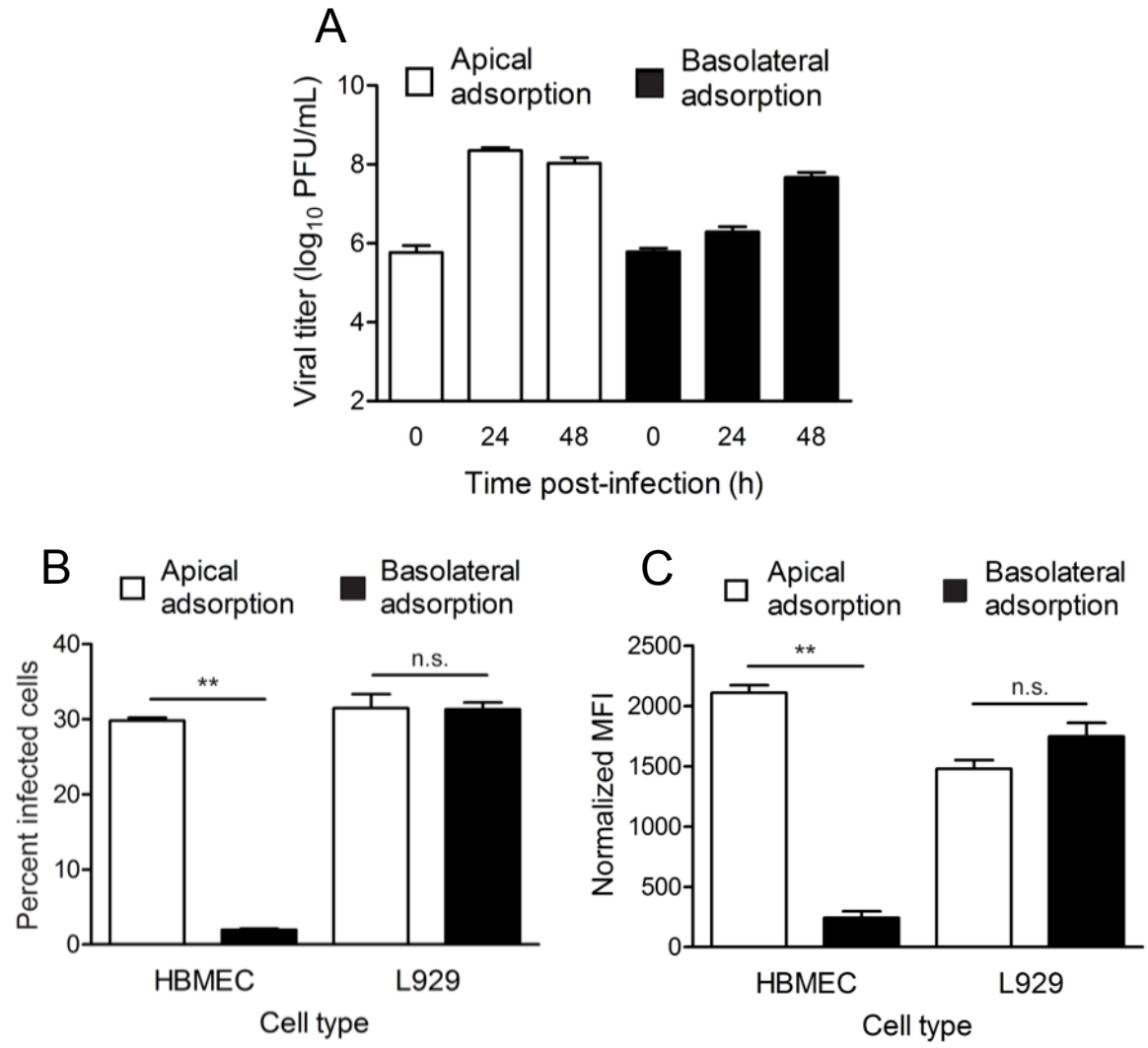
A
Apical adsorption
Basolateral adsorption
Viral titer (log_{10} PFU/mL)
10
8
6
4
2
0
24
48
0
24
48
Time post-infection (h)
B
Apical adsorption
Basolateral adsorption
Percent infected cells
40
30
20
10
0
**
n.s.
HBMEC
L929
Cell type
C
Apical adsorption
Basolateral adsorption
Normalized MFI
2500
2000
1500
1000
500
0
**
n.s.
HBMEC
L929
Cell type

Figure III-2. Reovirus infection of polarized HBMECs is more efficient following adsorption from the apical surface. Polarized HBMECs were adsorbed either apically (white bars) or basolaterally (black bars) with reovirus T3SA+ at an MOI of 10 PFU per cell. (A) Transwell inserts were excised at 0, 24, and 48 h post-infection, and viral titers in cell lysates were determined by plaque assay. A representative experiment of three performed is shown, with each experiment conducted in duplicate. Error bars indicate range of data for the duplicates. (B) HBMECs were incubated for 20-24 h and harvested by trypsinization. Cells were permeabilized and stained with Alexa Fluor-conjugated reovirus-specific antiserum. The percentage of infected cells was determined using flow cytometry. A representative experiment of three performed is shown, with each experiment conducted in duplicate. Error bars indicate range of data for the duplicates. (C) HBMECs were removed immediately after adsorption and stained with Alexa Fluor-conjugated reovirus-specific antiserum. MFI was determined using flow cytometry. A representative experiment of three performed is shown, with each experiment conducted in duplicate. Error bars indicate range of data for the duplicates.**, $P < 0.005$, n.s., not significant.

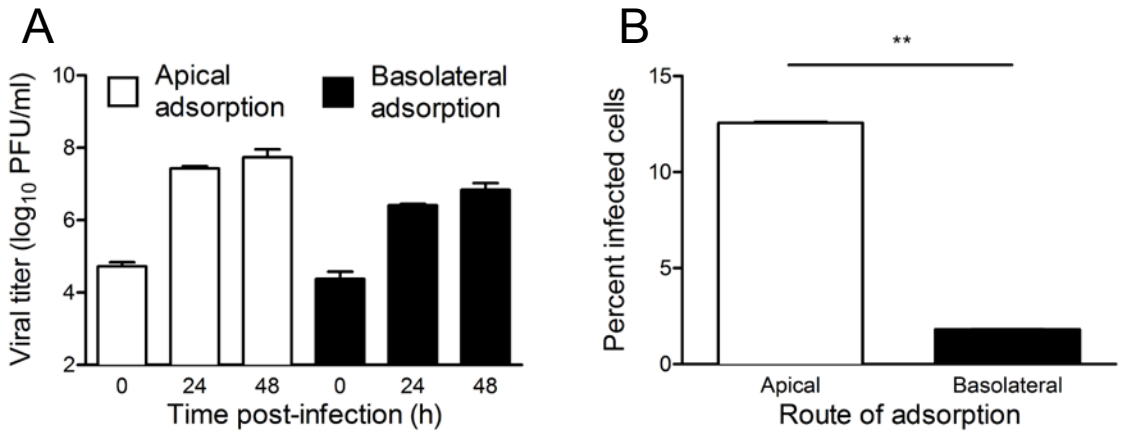

Figure III-3. T1L infection of polarized HBMECs is more efficient by the apical route. Polarized HBMECs were adsorbed either apically or basolaterally with reovirus T1L at an MOI of 10 PFU per cell. After adsorption with virus, cells were incubated for various intervals. (A) Transwell inserts were excised at 0, 24, and 48 h post-infection, and viral titers in cell lysates were determined by plaque assay. A representative experiment of two performed is shown, with each experiment conducted in duplicate. Error bars indicate range of data for the duplicates. (B) HBMECs were incubated for 20-24 h and harvested by trypsinization. Cells were permeabilized, stained with Alexa Fluor-conjugated reovirus-specific antiserum, and the percentage of infected cells was determined using flow cytometry. A representative experiment of two performed is shown, with each experiment conducted in duplicate. Error bars indicate range of data for the duplicates. **, $P < 0.005$.

SA and JAM-A are required for reovirus infection of polarized endothelial cells. To determine whether differences in infectivity of polarized HBMECs after apical or basolateral adsorption are attributable to differences in receptor engagement, I used mutant reovirus strains impaired in the capacity to bind either sialic acid or JAM-A. Single amino acid mutations in the σ1 attachment protein can dramatically diminish binding to these receptors (11, 102). Polarized HBMECs were adsorbed apically or basolaterally with wild-type or mutant reovirus strains, and the percentage of infected cells was quantified 24 h post-infection. There were significantly more infected cells following apical adsorption with wild-type strain type 3 Dearing (rsT3D) compared with mutant strain rsT3D-σ1R202W, which is deficient in SA-binding (11, 120), or mutant strain rsT3D-σ1G381A, which is deficient in JAM-A-binding (Figure III-4A) (26). Treatment of polarized HBMECs with neuraminidase (to remove cell-surface SA) and JAM-A-specific antibody prior to apical virus adsorption significantly decreased infection by rsT3D. Similarly, neuraminidase and JAM-A-specific antibody pretreatment substantially decreased infection of polarized HBMECs by rsT3D-σ1G381A and rsT3D-σ1R202W, respectively (Figure III-4A). Concordantly, rsT3D bound more efficiently to the apical surface of polarized HBMECs compared with the mutant virus strains, and virtually all virus binding was abolished with neuraminidase or JAM-A-specific antibody pretreatment (Figure III-4C). I observed a similar trend after basolateral adsorption in that diminished receptor engagement by mutant viruses or blockade of receptor engagement using inhibitors significantly decreased the percentage of virus-infected and virus-bound cells (Figure III-4B and D). However, the overall percentage of infected cells and levels of virus binding after basolateral adsorption were substantially less than those

following apical adsorption, which diminishes the magnitude of the observed differences (note the different y-axis scales in Figure III-4). Reovirus mutant rsT3D-σ1R202W bound to the basolateral surface of HBMECs equivalently to wild-type rsT3D but infected significantly fewer cells, suggesting that SA engagement may enhance reovirus replication at a post-attachment step following basolateral adsorption of polarized endothelial cells. These data suggest that infection of polarized endothelial cells is dependent on virus binding to sialylated glycans and JAM-A on the apical and basolateral surfaces of polarized endothelial cells, but binding to the apical surface is more efficient.

To determine whether increased binding of reovirus to the apical surface of polarized HBMECs is attributable to enhanced receptor expression, I examined the distribution of JAM-A on polarized HBMECs by confocal microscopy. Polarized HBMEC monolayers were stained using antibodies specific for TJ protein claudin-1 as well as JAM-A (Figure III-5A). Substantially more JAM-A staining was detected at the apical surface of the polarized cell monolayer (Figure III-5B), including non-junction sites that lack detectable claudin-1 staining (Figure III-5A). Confocal micrographs of apical portions of cells showed a stippled pattern of JAM-A expression. In equatorial sections of cells, JAM-A was distributed at the cell periphery, presumably in contact with JAM-A on adjacent cells. In these images, TJ puncta marked by claudin-1 and JAM-A colocalization are clearly visible (Figure III-5A, white asterisks). At the basolateral surface, the JAM-A signal was diminished in intensity and diffusely localized compared with JAM-A staining at the apical surface (Figure III-5). Increased distribution of JAM-A to the apical surface of polarized HBMECs may allow reovirus to bind and infect these cells more efficiently from this route.

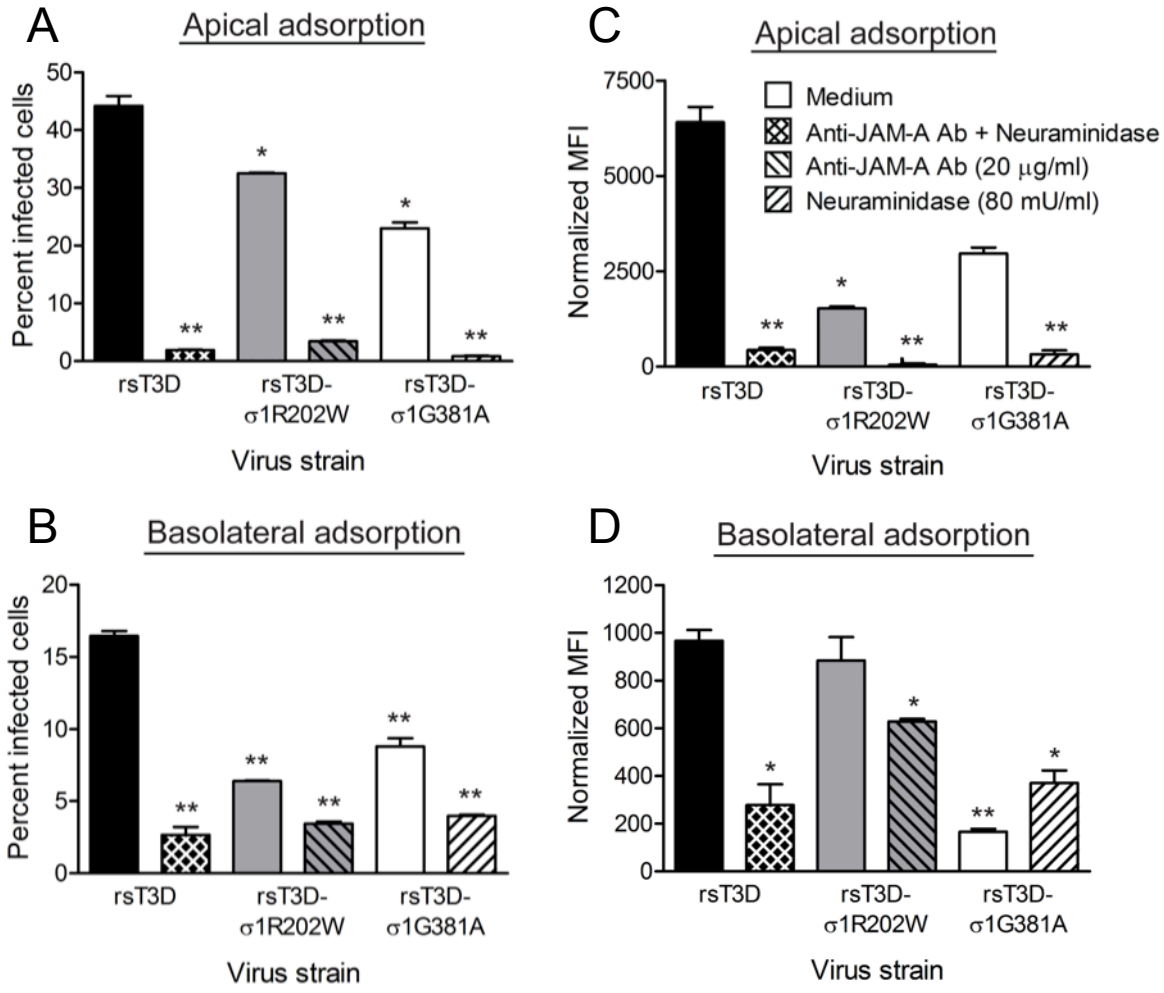

Figure III-4. JAM-A and sialic acid are required for reovirus infection of polarized HBMECs. Polarized HBMECs were adsorbed either apically (A,C) or basolaterally (B,D) at an MOI of 10 PFU per cell with reovirus strains rsT3D, rsT3D-σ1R202W, or rsT3D-σ1G381A in the presence or absence of anti-JAM-A antibody (20 μg/ml) or *A. ureafaciens* neuraminidase (80 mU/ml). (A,B) Cells were incubated for 20-24 h, removed from Transwells using trypsin, permeabilized, and incubated with Alexa Fluor-conjugated reovirus-specific antiserum. The percentage of infected cells was determined using flow cytometry. A representative experiment of two performed is shown, with each experiment conducted in duplicate. Error bars indicate range of data for the duplicates. (C,D) Cells were harvested from Transwells immediately after adsorption and stained with Alexa Fluor-conjugated reovirus-specific antiserum. MFI was quantified using flow cytometry. Note that different y-axis scales are used for apical and basolateral adsorption. A representative experiment of two performed is shown, with each experiment conducted in duplicate. Error bars indicate range of data for the duplicates. *, $P < 0.05$; **, $P < 0.005$

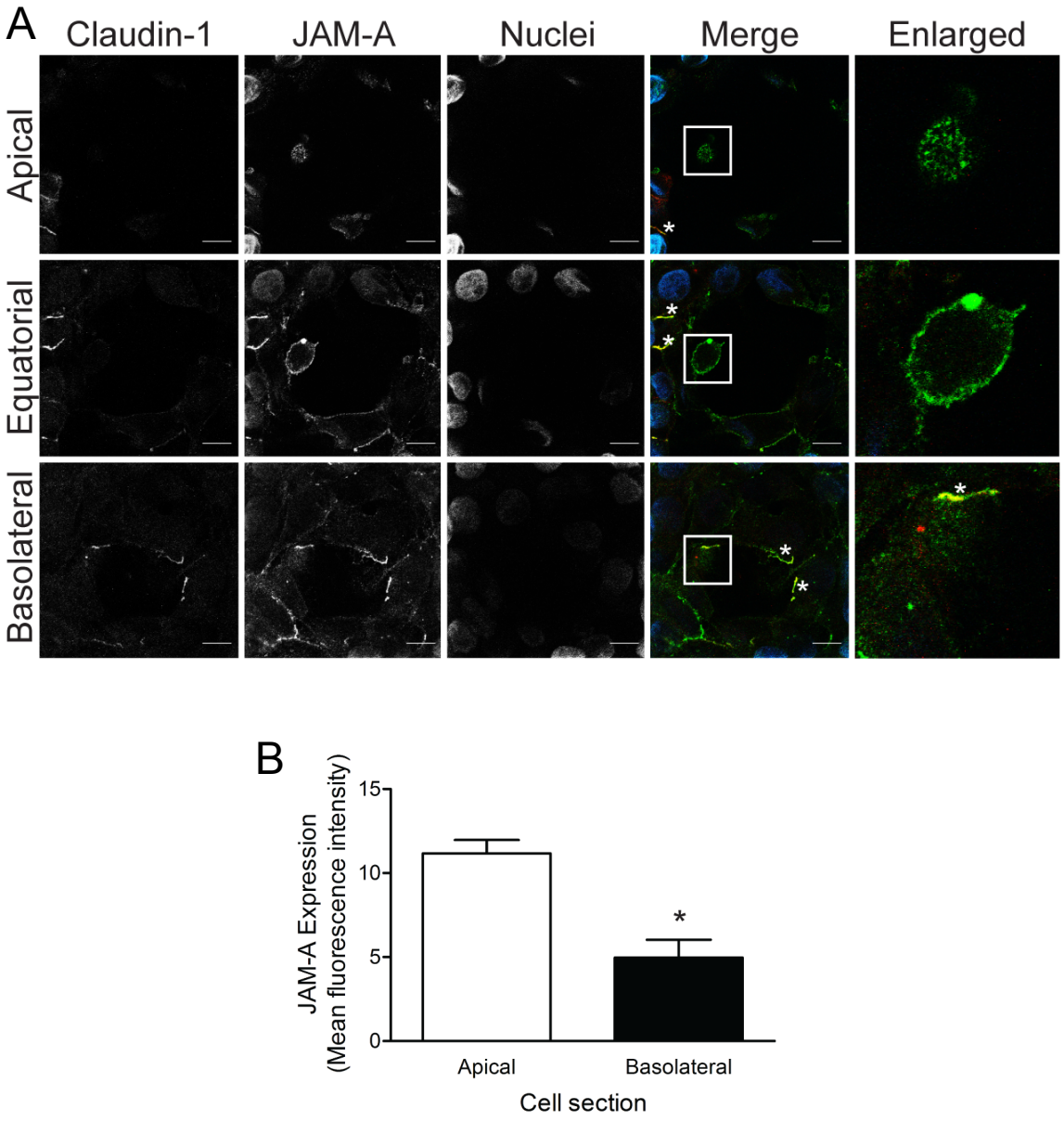

Figure III-5. Polarized HBMECs express JAM-A predominantly at the apical surface. (A) Polarized HBMECs were stained for JAM-A (green), claudin-1 (red), and nuclei (blue) and imaged by confocal microscopy. Shown are images of the apical, equatorial, and basolateral regions of a single, representative z-stack. Colocalization of TJ proteins is indicated by white asterisks. Scale bar indicates 10 μm. Enlarged images of the white boxed areas are shown in the bottom panels. Cell images were captured using a Zeiss LSM 510 Meta laser-scanning confocal microscope using a 63×/1.40 Plan-Apochromat objective lens. (B) JAM-A channel MFI of apical and basolateral sections of individual cells (n = 5) was quantified. Error bars indicate standard deviation. *, $P < 0.05$

Reovirus infection does not alter endothelial cell TJ integrity. To determine whether reovirus infection alters the integrity of TJs in the polarized monolayer, I quantified the TEER at both early and late times post-adsorption. After adsorption with an MOI of 1000 PFU per cell, no significant alteration in TEER was observed in an interval from 0 to 2 h post-infection (Figure III-6). I conclude from these data that reovirus does not alter the function of endothelial TJs at early time points during infection.

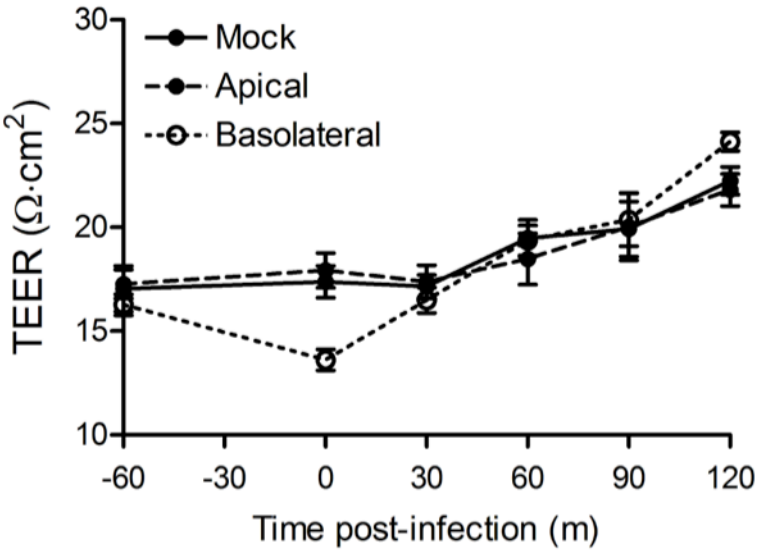

Figure III-6. Reovirus infection of polarized HBMECs does not disrupt TJs at early times post-infection. Polarized HBMECs were mock-infected (closed symbol, solid line) or adsorbed either apically (closed symbol, dashed line) or basolaterally (open symbol, dotted line) with reovirus T3SA+ at an MOI of 1000 PFU per cell. Cells were washed, fresh medium was added to the apical and basolateral compartments, and TEER was determined at the times shown. A representative experiment of two performed is shown, with each experiment conducted in duplicate. Error bars indicate range of data for the duplicates. TEER from the various samples was compared using one-way ANOVA. Student's *t* test was used to evaluate differences between mock- and apical-infected or mock- and basolateral-infected samples. No differences were statistically significant.

Discussion

Disease caused by many viruses in an infected host occurs after bloodstream spread from an initial site of infection to distant target sites. Reoviruses are neurotropic viruses that first replicate within the small intestine and disseminate systemically via the blood, nerves, and lymphatics. Reovirus penetration of the endothelium to invade the bloodstream may occur within the intestine or lymph nodes to allow establishment of primary viremia. To investigate reovirus infection of the endothelium, I cultured HBMECs on Transwell membranes until polarization was achieved (Figure III-1). Although reoviruses use TJ protein JAM-A as a receptor, TEER was not altered immediately following reovirus adsorption (Figure III-6), suggesting that TJ integrity remains intact after infection. Adsorption of polarized endothelial cells either apically or basolaterally with reovirus resulted in productive infection (Figures III-2 and III-3). Interestingly, reovirus strain T3D replicated more efficiently than strain T1L in polarized endothelial cells (compare Figures III-2 and III-3). This difference might be due to differences in cell-surface expression of the sialylated glycans used by the different reovirus serotypes or cell-intrinsic properties of endothelial cells that confer serotype-dependent differences in reovirus susceptibility. Regardless of the serotype, replication was more efficient when reovirus was adsorbed to the endothelial cell apical surface (Figures III-2 and III-3), and significantly more reovirus antigen-positive cells were detected following adsorption by this route (Figures III-2B and III-3B). The observed increase in infectivity and replication after apical adsorption is most likely due to increased virus binding to the apical surface (Figure III-2C). The number of cells bound

by virus was actually higher than the number of cells productively infected. This finding suggests that not all viral particles bound to the cell surface complete an infectious cycle, a phenomenon observed in other cell lines (121-123). Reovirus infection of polarized endothelial cells by either the apical or basolateral route requires engagement of sialylated glycans and JAM-A (Figure III-4). Consistent with these findings, substantially more JAM-A is distributed to the apical than the basolateral surface of polarized HBMECs (Figure III-5). Subconfluent, non-polarized HBMECs are substantially more susceptible to reovirus infection than are polarized HBMECs (Figure III-7), presumably due to higher levels of JAM-A on the cell surface and absence of a restriction of JAM-A expression to TJs.

Although bloodstream spread is an important step in the pathogenesis of many viral diseases, mechanisms used by viruses to gain entry into the blood are not well understood. My work describes how viral infection of endothelial cells may allow access into the circulation. I show that reovirus productively infects polarized endothelial cells by both apical and basolateral routes. Infection after apical adsorption is more efficient compared with basolateral adsorption due to increased utilization of SA and JAM-A at the apical surface. And although reovirus infection of polarized endothelial cells requires engagement of JAM-A, TJ function remains intact at early time points of infection. Since TJ proteins are used as receptors by a diverse array of viruses, including adenovirus (55), feline calicivirus (56), hepatitis C virus (124, 125), and several picornaviruses (55, 126), my findings may provide a more general understanding of how viruses establish viremia for bloodstream spread.

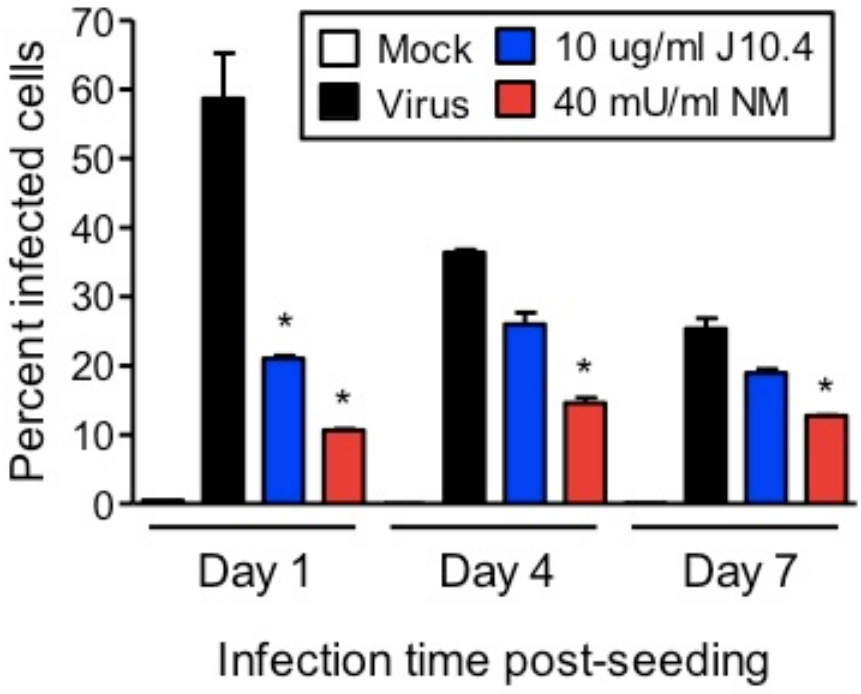

Figure III-7. Subconfluent endothelial cells are more permissive for reovirus infection than confluent endothelial cells. HBMECs were plated at a density of 10^5 cells per well and cultured for 1, 4, or 7 d prior to adsorption with reovirus strain T3SA+. Cells were incubated in OptiMEM alone (mock), OptiMEM containing JAM-A-specific antibody (J10.4), or OptiMEM containing *A. ureafaciens* neuraminidase (NM) for 1 h at room temperature prior to the addition of virus. HBMECs were adsorbed with reovirus at an MOI of 10 PFU per cell for 1 h at room temperature, and the amount of virus was adjusted according to the number of cells on the day of adsorption. After incubation at 37C for 20-24 h, cells were collected, permeabilized, and stained using Alexa Fluor-conjugated reovirus-specific antiserum. The percentage of infected cells was quantified using flow cytometry. Shown is a representative graph of duplicate samples, with the experiment repeated twice. Error bars indicate range of data for the duplicates. **, $P < 0.005$

CHAPTER IV

REOVIRUS IS RELEASED NONCYTOLYTICALLY FROM THE APICAL SURFACE OF POLARIZED HUMAN BRAIN MICROVASCULAR ENDOTHELIAL CELLS

Viral access to the bloodstream requires traversal of the endothelium. Invasion of the bloodstream by viruses can occur by direct inoculation of the virus via an insect vector, dismantling TJs that connect endothelial cells, productive infection of endothelial cells, or hijacking of hematopoietic cells that normally exist within the circulation. Reoviruses invade the bloodstream of a host shortly after inoculation of the gastrointestinal tract and establish viremia, however, mechanisms used by reoviruses to gain access to the bloodstream are not known. In the previous chapter, I showed that reoviruses productively infect polarized endothelial cells in a receptor-dependent manner. If productive infection of endothelial cells serves as a means to direct reovirus into the bloodstream, infected endothelial cells should route virions directionally into the bloodstream or undergo cell lysis to release virus nonspecifically into the circulatory system. Because many viruses disseminate hematogenously, understanding mechanisms used by reovirus to gain entry into the vascular compartment may shed light on how other viruses establish viremia and aid in the development of inhibitors of this key step in viral pathogenesis.

In this study, I determined how reoviruses are released from infected polarized endothelial cells to better understand mechanisms of viral entry into the bloodstream. I

found that regardless of the route of adsorption, reovirus release occurs exclusively from the apical surface of polarized endothelial cells. Interestingly, I found that despite the high titers of reovirus released into the supernatant, infected polarized cells do not undergo cell death. These studies suggest that infection via the tissue (basolateral) side of the endothelium results in release of progeny virions apically into the blood vessel lumen. Furthermore, these findings highlight a new route of reovirus egress from infected cells that is independent of cell lysis.

Reovirus is released apically from infected polarized endothelial cells. To determine whether reovirus release from infected polarized endothelial cells was directional, polarized HBMECs were adsorbed apically or basolaterally with reovirus strain T3SA+, and titers within the apical and basolateral compartments were quantified at various intervals by plaque assay. After apical adsorption, viral titer in the apical compartment increased more than 30-fold at 24 h and more than 3000-fold at 48 h (Figure IV-1A). Interestingly, no virus was detected in the basolateral compartment at any time point tested (Figure IV-1A). After basolateral adsorption, virus was detected in the basolateral compartment at all intervals tested (Figure IV-1B). However, titers did not increase over time, suggesting that infectious virus in this compartment is most likely residual virus from the inoculum. Viral titer in the apical compartment was detected at 24 h post-infection and increased approximately 100,000-fold by 48 h post-infection (Figure IV-1B). I found that reovirus strain T1L exhibited a similar pattern of release from infected polarized endothelial cells (Figure IV-1C, D). TEER of polarized endothelial cells adsorbed either apically or basolaterally did not significantly decrease over the course of

infection, suggesting that endothelial TJs remained intact (Figure IV-2). Therefore, regardless of the route of adsorption, reovirus egress from polarized endothelial cells occurs from the apical surface.

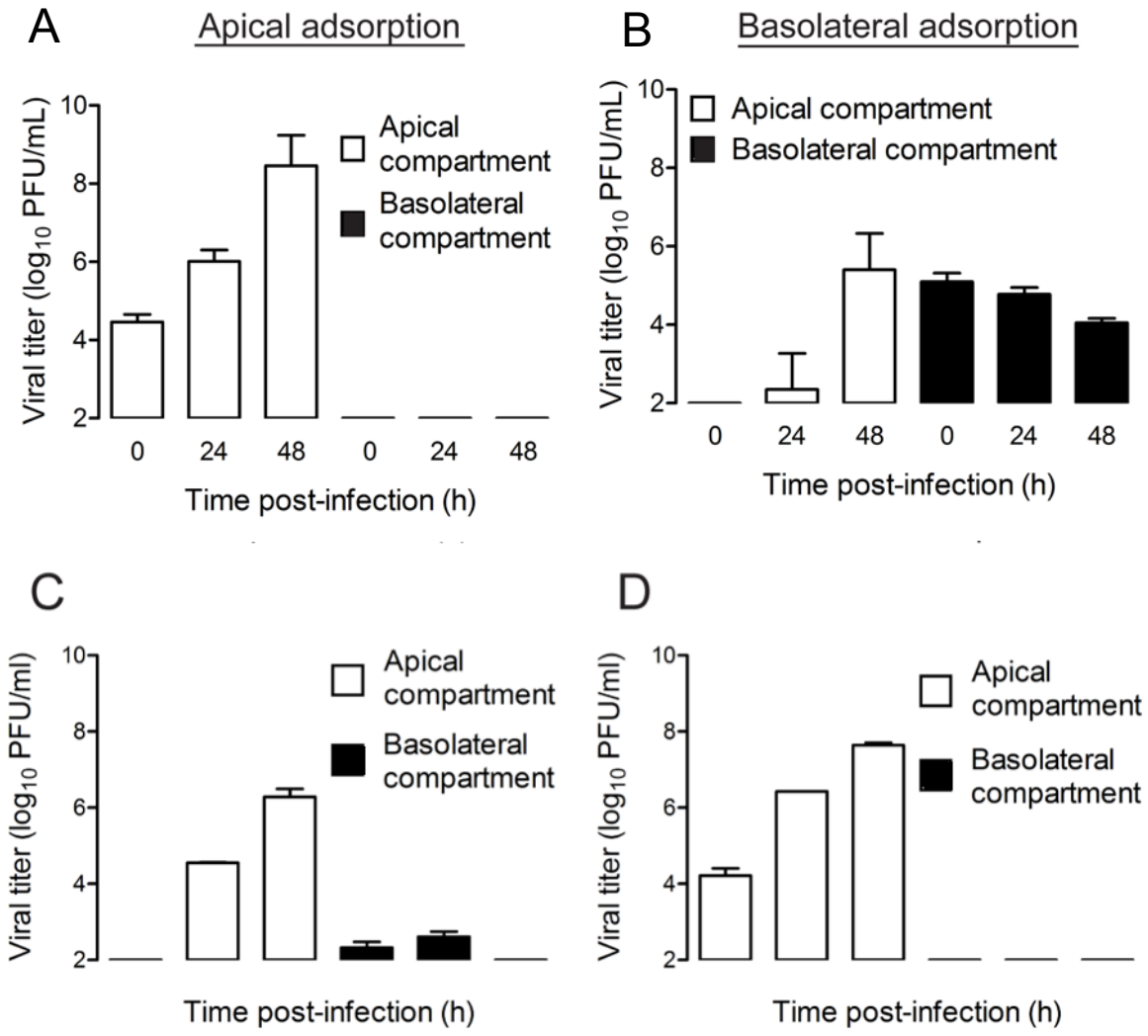

Figure IV-1. Reovirus release from polarized HBMECs occurs from the apical surface. Polarized HBMECs were adsorbed either apically (A,C) or basolaterally (B,D) with reovirus T3SA+ (A,B) or T1L (C,D) at an MOI of 10 PFU per cell. Cells were washed, fresh medium was added to the apical and basolateral compartments, and cells were incubated for the times shown. Viral titers in the medium from the apical (white bars) or basolateral (black bars) compartments were determined by plaque assay. A representative experiment of three performed is shown, with each experiment conducted in duplicate. Error bars indicate range of data for the duplicates.

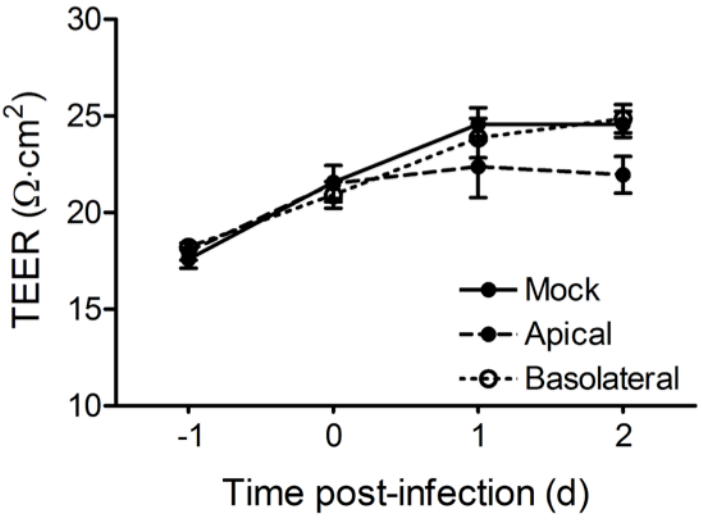

Figure IV-2. Reovirus infection of polarized HBMECs does not disrupt TJs at late times post-infection. Polarized HBMECs were mock-infected (closed symbol, solid line) or adsorbed either apically (closed symbol, dashed line) or basolaterally (open symbol, dotted line) with reovirus T3SA+ at an MOI 10 PFU per cell. Cells were washed, fresh medium was added to the apical and basolateral compartments, and TEER was determined at the times shown. A representative experiment of three performed is shown, with each experiment conducted in duplicate. Error bars indicate range of data for the duplicates. TEER from the various samples was compared using one-way ANOVA. Student's *t* test was used to evaluate differences between mock- and apical-infected or mock- and basolateral-infected samples. No differences were statistically significant.

Reovirus egress from polarized HBMECs occurs noncytolytically. To determine whether reovirus egress from infected polarized HMBECs is associated with cell lysis, I assessed cell viability using trypan blue staining. Polarized HBMECs or confluent L929 cells cultured on Transwells were adsorbed apically or basolaterally at an MOI of 10 PFU per cell, and cell viability was quantified 24 h post-infection. Levels of HBMEC lysis were less than background levels of lysis in mock-treated HBMECs after either apical or basolateral virus adsorption (Figure IV-3). In contrast, more than half the population of infected L929 cells were lysed at 24 h post-infection (Figure IV-3). These data suggest that reovirus infection of polarized HBMECs does not compromise cell viability.

Reovirus is capable of inducing apoptosis in many types of cultured cells (35-38) and in the CNS of infected mice (87, 127-129). Although polarized HBMECs remain intact after reovirus infection, I wondered whether reovirus egress from polarized HBMEC monolayers might occur via apoptosis. To test this hypothesis, polarized HBMECs were adsorbed apically or basolaterally at an MOI of 100 PFU per cell, and levels of apoptosis were quantified at 24 and 48 h post-infection using terminal deoxynucleotidyl transferase dUTP nick-end labeling (TUNEL) staining. At 24 h post-infection, 17.7% of cells were infected after apical adsorption, but apoptosis was detectable in only 0.9% of those cells (Figure IV-4A). At 24 h after basolateral adsorption, 3.0% of cells were infected, but apoptosis was not detected in those cells (Figure IV-4A). At 48 h post-apical adsorption, 29.5% of cells were infected with reovirus, with only 3.0% showing evidence of apoptosis (Figure IV-4A). After basolateral adsorption, 6.6% of cells were infected with reovirus, yet only 1.4% of those cells were apoptotic (Figure IV-4A). As a positive control for apoptosis, treatment of

polarized HBMECs with staurosporine resulted in ~ 50% of cells displaying evidence of apoptosis with a concomitant decrease in TEER (Figure IV-4), suggesting that the low levels of apoptosis in reovirus-infected cells are not attributable to an inherent block to apoptosis in HBMECs. Additionally, levels of apoptosis in reovirus-infected HBMECs were lower than in mock-infected cells using the complementary acridine orange and annexinV staining assays (Figure IV-5). These data suggest that reovirus egress from polarized HBMECs occurs without inducing apoptosis.

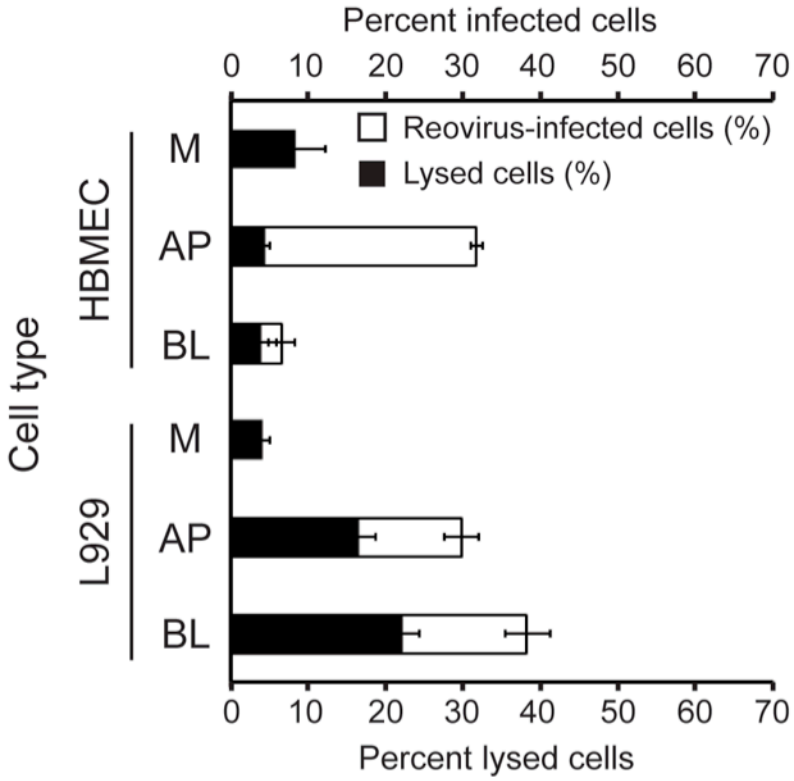

Figure IV-3. Reovirus infection of polarized HBMECs does not induce cell lysis. Polarized HBMECs or confluent L929 cells cultured on Transwells were mock-infected (M) or adsorbed either apically (AP) or basolaterally (BL) with reovirus T3SA+ at an MOI of 10 PFU per cell. Cells were washed, fresh medium was added to the apical and basolateral compartments, and cells were incubated at 37°C for 20-24 h. Cells were harvested and incubated with trypan blue or permeabilized and stained for reovirus antigen using Alexa Fluor-conjugated reovirus-specific antiserum. The percentage of infected cells (white bars) and the percentage of lysed cells (black bars) are shown in a stacked column graph. A representative experiment of two performed is shown, with each experiment conducted in duplicate. Error bars indicate range of data for the duplicates.

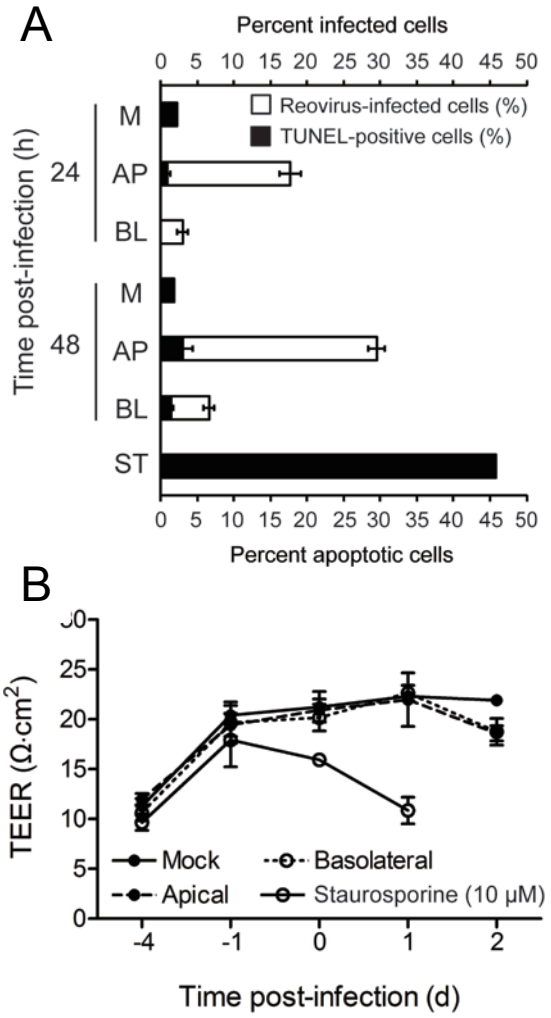

Figure IV-4. Reovirus infection of polarized HBMECs is noncytolytic. Polarized HBMECs were mock-infected (M) or adsorbed either apically (AP) or basolaterally (BL) with reovirus T3SA+ at an MOI of 100 PFU per cell. Cells were incubated at 37°C and harvested at 24 or 48 h post-infection. As a control for apoptosis, staurosporine (ST, 10 μM) was added to the medium in the apical and basolateral compartments of uninfected cells, which were incubated for 18 h. (A) Cells were stained for reovirus antigen using Alexa Fluor-conjugated reovirus-specific antiserum and apoptosis using the TUNEL technique. The percentage of infected cells (white bars) and percentage of TUNEL-positive cells (black bars) within the population of infected cells are shown in a stacked column graph. A representative experiment of three performed is shown, with each experiment conducted in duplicate. Error bars indicate range of data for the duplicates. (B) TEER was recorded for each sample at the time of cell harvest. A representative experiment of three performed is shown, with each experiment conducted in duplicate. Error bars indicate range of data for the duplicates.

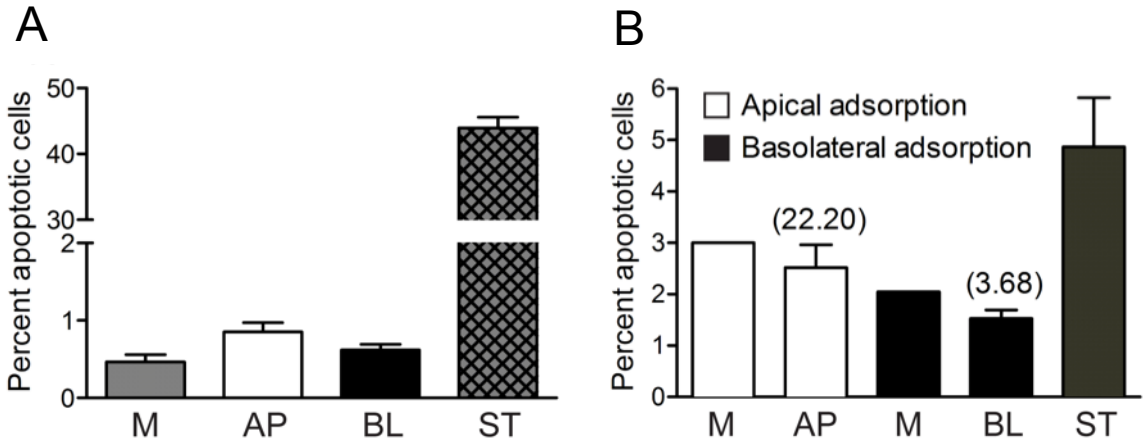

Figure IV-5. Reovirus infection of polarized HBMECs does not induce cell death. Polarized HBMECs were mock-infected (M) or adsorbed either apically (AP) or basolaterally (BL) with reovirus T3SA+ at an MOI of 100 PFU per cell. Cells were incubated at 37ºC and harvested at 24 h post-infection. As a control for apoptosis, staurosporine (ST, 10 μM) was added to the medium in the apical and basolateral compartments of uninfected cells, which were incubated for 18 h. (A) Cells were harvested, washed, and stained with acridine orange dye. The number of apoptotic cells was enumerated under brightfield microscopy. A representative experiment of three performed is shown, with each experiment conducted in duplicate. Error bars indicate range of data for the duplicates. (B) Cells were harvested and stained either for apoptosis using Alexa Fluor-conjugated antibody specific for AnnexinV or reovirus antigen using Alexa Fluor-conjugated reovirus-specific antiserum. The percentage of infected cells (within parentheses above the respective bars) and percentage of AnnexinV-positive cells are shown. A representative experiment of three performed is shown, with each experiment conducted in duplicate. Error bars indicate range of data for the duplicates.

Discussion

Productive infections are characterized by successful viral entry into, replication and assembly within, and exit from a host cell. Because nonenveloped viruses do not require the incorporation of host cell membranes into progeny virions, these viruses are thought to exit infected cells mainly by the induction of apoptosis and cell lysis. Interestingly, hepatitis A virus, a nonenveloped member of the *Picornaviridae*, exits infected cells in exosome-like vesicles as a possible mechanism to evade humoral immunity (130). Until now, reoviruses have not been shown to egress from infected cells in a noncytolytic manner.

Infection of endothelial cells is a possible mechanism for reovirus entry into the bloodstream. In this chapter, I show that reovirus strains T1 and T3 are directionally released apically from infected polarized endothelial cells (Figure IV-1) in a manner that maintains TJ function (Figure IV-2). Furthermore, I found that reovirus release from infected polarized endothelial cells does not induce cell death and lysis (Figures IV-3, 4, and 5).

Regardless of the route of adsorption, reovirus egress from infected polarized HBMECs occurs solely from the apical surface (Figure IV-1). Similarly, reovirus infection of polarized human airway epithelial cells results in apical release of progeny virions (107). Although TEER did not change appreciably over a timecourse of reovirus infection of HBMECs (Figure IV-2), I questioned whether infected cells are extruded from the monolayer in a manner analogous to epithelial cell turnover (131). If so, I would expect TEER to be maintained despite detection of an increased number of nonviable

cells over time. To test this hypothesis, I used trypan blue staining to determine whether polarized HBMECs infected with reovirus are lysed. Compared with infected L929 cells, which display substantial cytopathic effect after reovirus infection (Figure III-2) (38), polarized HBMECs infected with reovirus apically or basolaterally do not undergo cell lysis (Figure IV-3), despite the presence of high viral titers in cells and supernatants (Figures III-1 and IV-1). Apical or basolateral adsorption of polarized HBMECs with reovirus led to an increase in reovirus antigen-positive cells, but the number of apoptotic cells did not increase above those in mock-treated samples (Figure IV-4). I conclude from these data that regardless of the route of entry, reovirus release occurs from the apical surface in a manner that maintains cell viability. Because infection of polarized endothelial cells is noncytolytic, clearance of reovirus from an infected host may require cytotoxic T lymphocyte-mediated immunity in addition to neutralizing antibodies (132-136).

Virus infection of endothelial cells may serve as an additional mechanism to produce and maintain high levels of viremia. For example, DENV infection of endothelial cells leads to high-titer viremia by inducing endothelial cell apoptosis, resulting in endothelial barrier dysfunction and vascular leak (118). Murine cytomegalovirus primarily infects hepatocytes, but virus produced from infected hepatic endothelial cells is responsible for dissemination to other organs (137, 138). Similarly, reovirus may use the endothelium as a means to amplify to high titers in the bloodstream. Reovirus infection from the basolateral route is not efficient (Figures III-2, III-3), but progeny viral particles are efficiently transported to and released from the apical surface of polarized endothelial cells (Figure IV-1). Once released, progeny virions have access

to the apical surface of adjacent endothelial cells and can enter those cells efficiently. This cycle may serve as a mechanism to generate high titers of virus in the bloodstream, which are observed during reovirus infection (51, 64, 120). Sialylated glycans and JAM-A are required for infection of endothelial cells by both apical and basolateral routes, which may account for the absence of viremia in reovirus-infected JAM-AKO mice (51).

How reovirus exits the bloodstream is not clear from my studies. Because JAM-A is present on the surface of hematopoietic cells, it is possible that reovirus-infected hematopoietic cells transport the virus from the bloodstream to sites of secondary replication including the CNS. It also is possible that cells adjacent to blood vessels become infected as a consequence of infection of the endothelium. Epstein-Barr virus (EBV) binding to B cells leads to conjugate formation between B cells and epithelial cells, resulting in EBV entry into epithelial cells (139, 140). Blood vessels in the brain closely appose pericytes and astrocytes, and reovirus infection of endothelial cells may induce modifications of these cells resulting in invasion of the CNS.

My studies of reovirus infection of polarized endothelial cells have identified a new mechanism for reovirus egress. Maintenance of cell viability may ensure that reovirus can replicate to high titers to generate viremia and subsequent targeting of organs where secondary replication can occur. The findings I have made with my *in vivo* and *in vitro* systems to study the role of endothelial JAM-A in reovirus bloodstream spread suggest that infection of the endothelium and apical release of reovirus from these cells serve as a mechanism for reovirus entry into the bloodstream and amplification in the circulation.

CHAPTER V

SUMMARY AND FUTURE DIRECTIONS

Many viruses use the bloodstream as a means to disseminate systemically within the infected host. Because viruses capable of bloodstream spread may share similar mechanisms of dissemination, understanding how reovirus disseminates by this route may aid in the development of therapeutics that target this critical step in viral pathogenesis. Prior to the initiation of my work, JAM-A was known to be a proteinaceous receptor for reoviruses that mediates hematogenous dissemination. The goal of my dissertation work was to determine precisely how JAM-A expression *in vivo* facilitates reovirus bloodstream spread. In this chapter, I will summarize the work I have accomplished, discuss potential implications of the findings, and pose future directions for this research.

Role of receptors in viremia and systemic viral spread

Viremia is an important step in the pathogenesis of many viruses. Seeding of the bloodstream ensures systemic virus spread. For arboviruses, high titers of virus in the blood are required for host-to-host transmission. DENV replicates in endothelial cells to generate high bloodstream titers (118). For other viruses that are not transmitted by an insect vector, dissemination by the blood allows the virus to reach sites of secondary replication. For murine cytomegalovirus, primary viremia allows the virus to infect

hepatocytes (137, 138). However, high titers in the blood occur after infection of endothelial cells to produce secondary viremia (137, 138). Although viremia is a common step in the life cycle of many viruses, little is known about how bloodstream entry and egress occurs. Understanding mechanisms by which viruses traverse the endothelium may allow for the design of broad-spectrum therapeutics that target the systemic dissemination of viruses. Furthermore, elucidating mechanisms by which reovirus disseminates by the blood may allow for the design of oncolytic vectors that spread more effectively.

Interactions with specific receptors initiate the infectious life cycle of viruses. Receptors serve to tether virus particles to the cell surface and initiate viral cell entry. JAM-A is expressed on a variety of cell types in many different tissues (39-41, 42 , 43, 44). JAM-AKO mice are protected from reovirus-induced morbidity and mortality after peroral virus inoculation but succumb to reovirus-induced encephalitis after intracranial virus inoculation (51). This observation suggests that JAM-A is dispensable for reovirus neuropathogenesis. Rather, I found that JAM-A must be expressed in endothelial cells for dissemination to the CNS (Figure II-8). If JAM-A is absent on the endothelium, as in EndoJAM-AKD mice, virus cannot reach sites of secondary replication, and the pathogenesis of reovirus virulence is consequently diminished. I present evidence that JAM-A, although expressed at various sites, facilitates an exquisitely specific step in the reovirus-host encounter by facilitating bloodstream entry into and egress from the circulatory system.

Primary endothelial cells are permissive for reovirus infection (51), which suggests that reovirus infects endothelial cells *in vivo* during systemic spread. Reovirus

infection of endothelial cells may route virions into the circulation, amplify virus within the bloodstream, or a combination of both effects (Figure V-1). When examining infection of polarized endothelial cells *in vitro,* reovirus is capable of infecting cells from both apical and basolateral routes (Figures III-2 and III-3). The basolateral route of adsorption simulates reovirus infection of the endothelium from a tissue (Figure V-1). This route of infection is less efficient than apical infection (Figures III-2 and III-3), which simulates reovirus infection of polarized endothelial cells from within the blood (Figure V-1). Infection by both routes results in replication and efficient release of progeny virions from the apical surface (Figure IV-1). These findings suggest that reovirus amplification occurs in endothelial cells, which serves to establish viremia in an infected host.

Several unanswered questions remain. From my work, endothelial JAM-A is clearly required for efficient bloodstream entry and exit. However, it is not clear how reovirus uses JAM-A to infect endothelial cells. I found that JAM-A is localized to the apical surface and TJs of polarized HBMECs in culture. However, do these cells faithfully simulate the endothelial surface *in vivo*? And if so, does reovirus engage junctional JAM-A or JAM-A localized to the luminal surface? Second, it is not known how reovirus transits within the vascular compartment. I found that hematopoietic JAM-A is dispensable for reovirus bloodstream spread. Do virus particles exist freely in the plasma? Or are viruses associated with hematopoietic cells or platelets in a JAM-A-independent manner? Third, it is unclear how reovirus exits the bloodstream. Mechanisms of reovirus entry into the bloodstream also may be used for viral egress from this compartment. Lastly, I observed noncytolytic reovirus egress from polarized

endothelial cells. This type of viral egress has not been described for reoviruses and suggests that there exist cell type-specific modes of reovirus release.

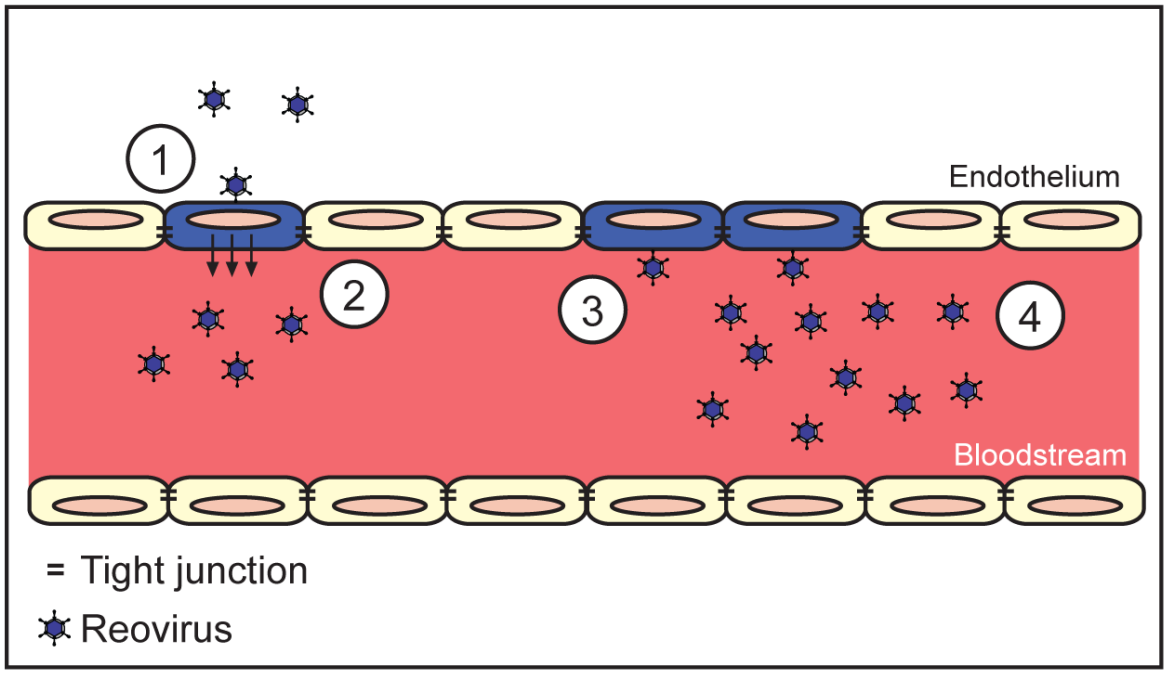

Figure V-1. Model for reovirus infection of the endothelium. A cross-sectional schematic of a blood vessel is shown. The blood vessel is lined with endothelial cells that are linked via TJs (black bars). Following reovirus infection of endothelial cells from the basolateral surface (1), virus is routed apically (or luminally) into the bloodstream (2). Once within the bloodstream, virus is capable of infecting endothelial cells from the apical surface (3). Reovirus binding to JAM-A, found mostly within tight junctions, and sialic acid at the apical surface may account for the increased efficiency of infection. After reovirus infects cells from the apical surface, progeny virions are routed apically into the bloodstream. The efficiency of apical infection may allow for endothelial amplification of reovirus (4), resulting in higher levels of viremia within an infected host. From Boehme et al. (2013).

JAM-A-Dependent Reovirus Infection of Endothelial Cells

Because JAM-A is a TJ protein, the distribution of JAM-A in subconfluent cells may differ from that observed in confluent or polarized cells. I found that subconfluent HBMECs were more susceptible to reovirus infection than confluent HBMECs (Figure III-7). Furthermore, reovirus infection was lessened to a greater extent in subconfluent cells than in confluent cells when a JAM-A-specific antibody was administered prior to virus adsorption (Figure III-7). These data suggest that reovirus infection of subconfluent HBMECs occurs via JAM-A expressed abundantly on the cell surface. In support of this idea, this interaction can be blocked by addition of JAM-A-specific antibody. In confluent cells, antibody may not be able to access junctional JAM-A, and reovirus infection may be inhibited to a lesser extent by JAM-A-specific antibody. Regardless of where reovirus interacts with JAM-A, it is unclear how reovirus-JAM-A interactions progress to productive infection. In epithelial cells, JAM-A localizes to the TJ and is thought to recruit other proteins to the TJ via signaling through its cytoplasmic tail domain (141, 142). Through interactions with Afadin and Rap-1, JAM-A regulates the levels of β1 integrin (143). This function of JAM-A may be important in facilitating reovirus internalization.

In non-polarized Chinese hamster ovary (CHO) cells, reovirus infection can occur in the absence of the cytoplasmic tail of JAM-A (144). However, different requirements for infection may exist in settings where JAM-A functions in TJ maintenance. To determine whether reovirus usurps JAM-A signaling functions to facilitate infection of polarized endothelial cells, reovirus infection can be assessed in brain microvascular or

pulmonary endothelial cells cultured from JAM-AKO mice stably transfected with mutant JAM-A constructs (Figure V-2). A mutant JAM-A construct lacking the cytoplasmic domain (JAM-AΔCT) can be expressed in JAM-AKO endothelial cells to determine whether the cytoplasmic tail is required for reovirus infection. A mutant JAM-A construct with the JAM-A ectodomain fused to a glycosylphosphatidylinositol (GPI) anchor (JAM-AΔTM) can be expressed in JAM-AKO endothelial cells to determine whether the transmembrane domain is required for reovirus infection. If the transmembrane domain or cytoplasmic tail is required for reovirus internalization, contributions of specific cytoplasmic tail residues to reovirus infection could be defined using JAM-A constructs with an altered PDZ-binding motif (JAM-APDZmut) and phosphorylation sites (JAM-A Cluster 1-4) (FigureV-2). The JAM-A cytoplasmic tail incorporates twelve potential phosphoacceptor sites (serines, threonines, or tyrosines). To test the requirement of cytoplasmic tail phosphorylation sites for reovirus infection of polarized endothelial cells, the twelve possible phosphoacceptor residues could be changed to alanine in clusters of three (Figure V-2). The cluster mutants will collectively disrupt all potential phosphorylation sites within the JAM-A cytoplasmic tail. The JAM-A cluster mutants could be stably introduced into JAM-AKO endothelial cells, followed by infection with reovirus.

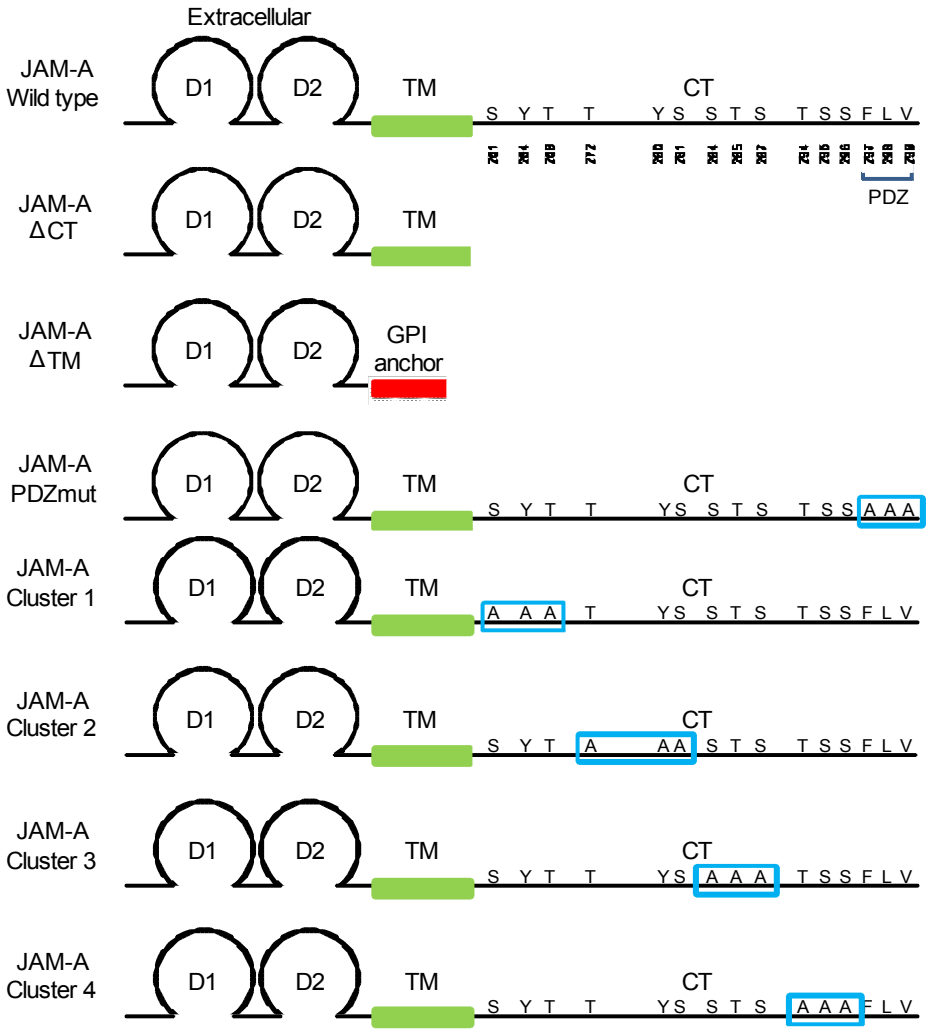

Figure V-2. Mutant JAM-A constructs. Schematic depictions of wild-type and mutant JAM-A constructs are shown. Extracellular D1 and D2 Ig-like domains, a single transmembrane (TM) domain, and the cytoplasmic tail (CT) are shown. The PDZ-binding motif (PDZ) is located within the JAM-A CT and potential phosphorylation residues are indicated with residue number. Residues to be altered in each mutant are boxed in blue.

Reovirus Viremia

Reoviruses are neurotropic viruses that are transmitted primarily by the fecal-oral route(1). Spread within the blood from the gastrointestinal tract to the CNS indicates that reovirus stably exists in body compartments that differ dramatically. For example, the luminal environment within the intestine differs substantially from the sterile environment of the CNS. The blood compartment contains many cellular components, including erythrocytes, leukocytes, and platelets, in addition to serum components. It is not clear whether reoviruses exist within the cellular or serum compartment within the bloodstream. Reovirus binds to erythrocytes by interacting with cell-surface glycophorin, a sialoglycoprotein, in hemagglutination assays (25). In Chapter II, I show that hematopoietic JAM-A does not facilitate reovirus hematogenous spread, but another cell-surface molecule may be used by reovirus for binding interactions with or productive infection of these cells. JAM-A on the surface of platelets facilitates platelet activation and clot formation (44); reovirus may bind to platelets during systemic spread in the circulation. To determine how reovirus exists in the circulation, blood from reovirus-infected mice could be harvested and fractionated into erythrocyte, leukocyte, platelet, and serum fractions. Each blood component could be titered by plaque assay to determine which compartment contains reovirus particles. Determining how reovirus traffics within the blood has implications for generating reovirus oncolytic vectors that exist more stably within the blood.

Reovirus Bloodstream Egress

I provide evidence in Chapters II and III that infection of endothelial cells in a JAM-A-dependent manner facilitates reovirus bloodstream entry and egress. However, it is not understood how reovirus egress from the vascular compartment occurs. Reovirus infection of polarized endothelial cells *in vitro* suggests that endothelial cell infection does not direct virus particles basolaterally into the surrounding tissue. I envision three possibilities for reovirus bloodstream exit. First, reovirus engagement of JAM-A may induce TJ dysfunction, resulting in vascular leak. Vascular permeability studies may determine whether reovirus engagement of endothelial JAM-A dismantles TJs *in vivo.* Methylene blue and sodium fluorescein are tracers that are commonly used in studies of vascular permeability (145-147). These molecules do not normally diffuse through endothelial TJs but can be detected and quantified in tissues where TJ function is compromised. Mouse adenovirus-1 infection of endothelial cells reduces TJ protein expression and decreases barrier function in polarized endothelial cell monolayers (148). Coxsackieviruses engage decay-accelerating factor, an apically distributed protein of polarized epithelial cells, to disrupt TJs (149). In doing so, coxsackieviruses gain access to the basolaterally located CAR (53). HIV-1 gp120 diminishes expression of TJ proteins and increases vascular permeability (150). In Chapters III and IV, I found that reovirus infection of polarized endothelial cells in culture does not reduce the TEER, suggesting that TJs remain intact. However, what happens *in vivo* may be different from what is observed in cell-culture systems, and studies should be performed to determine whether reovirus induces vascular leak.

Second, it is possible that reovirus infection of endothelial cells induces local changes in the endothelium that result in infection of perivascular cells. EBV binding to B cells can result in conjugate formation between B cells and epithelial cells (139, 140). This interaction leads ultimately to infection of the epithelium. Reovirus infection of the endothelium may lead to infection of cells closely apposed to blood vessels. For example, the blood brain barrier (BBB) is composed of endothelial cells and their TJs, pericytes, and astrocyte foot processes. In a pilot experiment to determine whether cells of the BBB also are susceptible to reovirus infection, I adsorbed a confluent monolayer of human brain pericytes with reovirus strains T1L and T3D. I found that these cells are permissive for infection by either reovirus strain (Figure V-3). Infection of astrocytes that are closely associated with the brain microvasculature may be an alternative route of entry into the CNS.

Third, it is possible that reovirus uses hematopoietic cells to exit the circulatory system. Although I provide evidence in Chapter II that hematopoietic JAM-A is dispensable for reovirus dissemination, it is possible that reovirus uses a receptor distinct from JAM-A to either bind to or infect hematopoietic cells. Since reoviruses have evolved to use different receptors for infection and replication within the gastrointestinal tract, bloodstream, and CNS, it is possible that an unknown receptor exists for trafficking of virus out of the bloodstream and into target tissues. Furthermore, reovirus is associated with leukocytes in the blood of cancer patients receiving intravenous reovirus oncolytic therapy (99). To determine whether reovirus binds to or infects hematopoietic cells *in vivo,* splenocytes and peripheral blood leukocytes could be collected from reovirus-infected animals and assessed for reovirus antigen. Flow cytometric profiles of different

hematopoietic cell subsets could be used to identify whether a particular cell type is used by reovirus to traffic systemically.

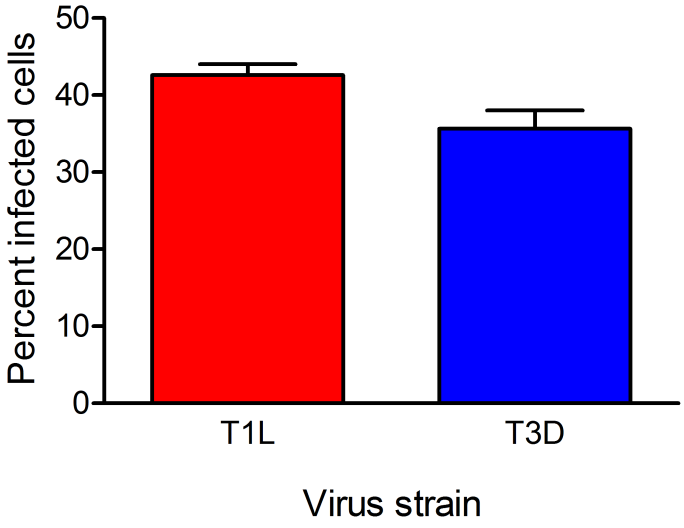

Figure V-3. Human brain pericytes are permissive for infection by reovirus strains T1L and T3D. Confluent monolayers of human brain pericytes were adsorbed with reovirus strains T1L or T3D at an MOI of 100 PFU per cell at room temperature for 1 h. After incubation at 37°C for 24 h, cells were fixed and stained with reovirus-specific antiserum. The percentage of infected cells was determined using indirect immunofluorescence.

Reovirus Noncytolytic Egress

When examining reovirus infection of polarized endothelial cells, I found that release of virus occurs noncytolytically. Mechanisms of reovirus egress are not well understood, but viral release from cells has traditionally been linked to cell lysis (1). I wondered whether viral release independent of cell lysis or cell death only occurred in the context of a polarized cell monolayer. I found that reovirus infection of subconfluent HBMECs induced very little cell death compared to that observed after infection of L929 murine fibroblasts (Figure V-4). These data suggest that reovirus exhibits cell type-specific modes of egress.

To determine possible pathways used by reovirus to exit infected cells in the absence of cell lysis or cell death, I examined electron micrographs of reovirus-infected polarized HBMECs. In these images, I found that reovirus cytoplasmic inclusions in polarized HBMECs appeared to incorporate membranes (Figure V-5). It is possible that reovirus recruits membranes to viral inclusions to enable assembled reovirus particles to exit infected cells via exocytosis. Hepatitis A virus, a nonenveloped virus, is capable of exiting infected cells using exosomes in an endosomal sorting complexes required for transport (ESCRT)-dependent manner (130). Interestingly, in examining infected polarized HBMECs by electron microscopy, I observed viral particles exiting an intact cell (Figure V-6).

Because I observed membrane-like structures in reovirus inclusions, I wondered how membranes might be recruited or generated. Poliovirus interacts with autophagy proteins to egress from cells noncytolytically (151). Porcine reproductive and respiratory

syndrome virus (PPRSV) activates autophagy to replicate efficiently (152). Interestingly, reovirus infection of multiple myeloma cells upregulates autophagy machinery but induces apoptosis in these cells (153). To determine whether autophagy is induced following reovirus infection of HBMECs, I assessed cleavage of LC3, a protein found in autophagosome membranes (154), in infected polarized HBMECs as an indicator of autophagic activity. I found that after apical and basolateral infection there was no significant cleavage of LC3-I to LC3-II (Figure V-7), suggesting that autophagy is not being induced during reovirus infection. However, these data do exclude the possibility that individual proteins in the autophagy pathway are being used independently of the formation of autophagosomes. To determine whether other autophagy proteins are important for reovirus noncytolytic egress, expression of autophagy proteins could be diminished using small-interfering RNA (siRNAs), and virus release could be quantified in these cells.

An alternative possibility for the presence of membranes in reovirus inclusions is that membranes are generated *de novo*. Poliovirus activates fatty acid import and upregulates cellular long chain acyl-CoA synthetase activity resulting in genesis of phospholipids that are incorporated into replication complexes (155). To determine whether reovirus infection increases fatty acid import, infected cells could be labeled with boron-dipyrromethene (BODIPY)-labeled fatty acid. Subsequent experiments would include downregulating expression of enzymes involved in phospholipid synthesis and evaluating viral egress in these cells. These studies would shed light on egress of reovirus in the absence of cell lysis.

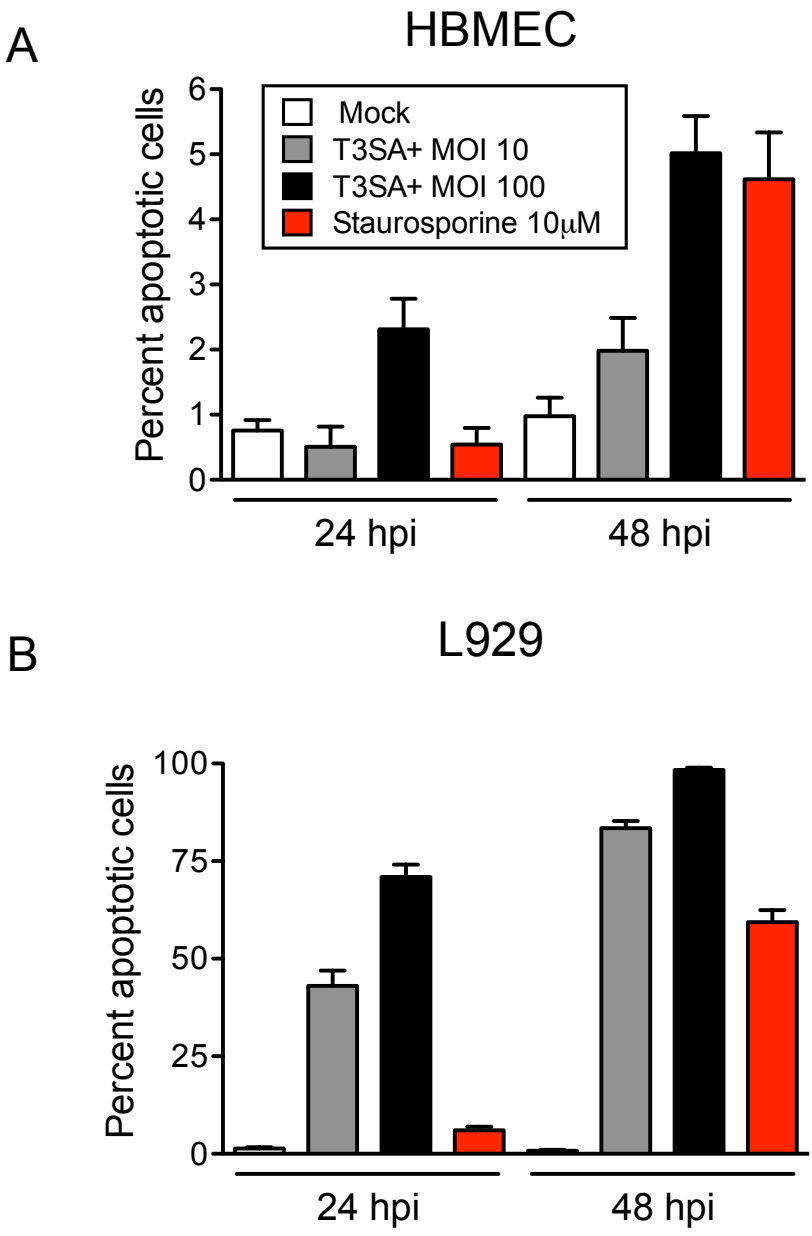

Figure V-4. Reovirus infection does not induce cell death in subconfluent HBMECs. Subconfluent HBMECs (A) or L929 murine fibroblasts (B) were either mock-treated (white bars) or adsorbed with reovirus strain T3SA+ at an MOI of 10 (gray bars) or 100 (black bars) PFU per cell. After incubation at 37°C for 24 or 48 h, cells were trypsinized and stained with acridine orange dye. The percentage of apoptotic cells was determined as the number of apoptotic nuclei divided by the total number of nuclei. Cells were incubated in 10 μM staurosporine as a positive control for cell death.

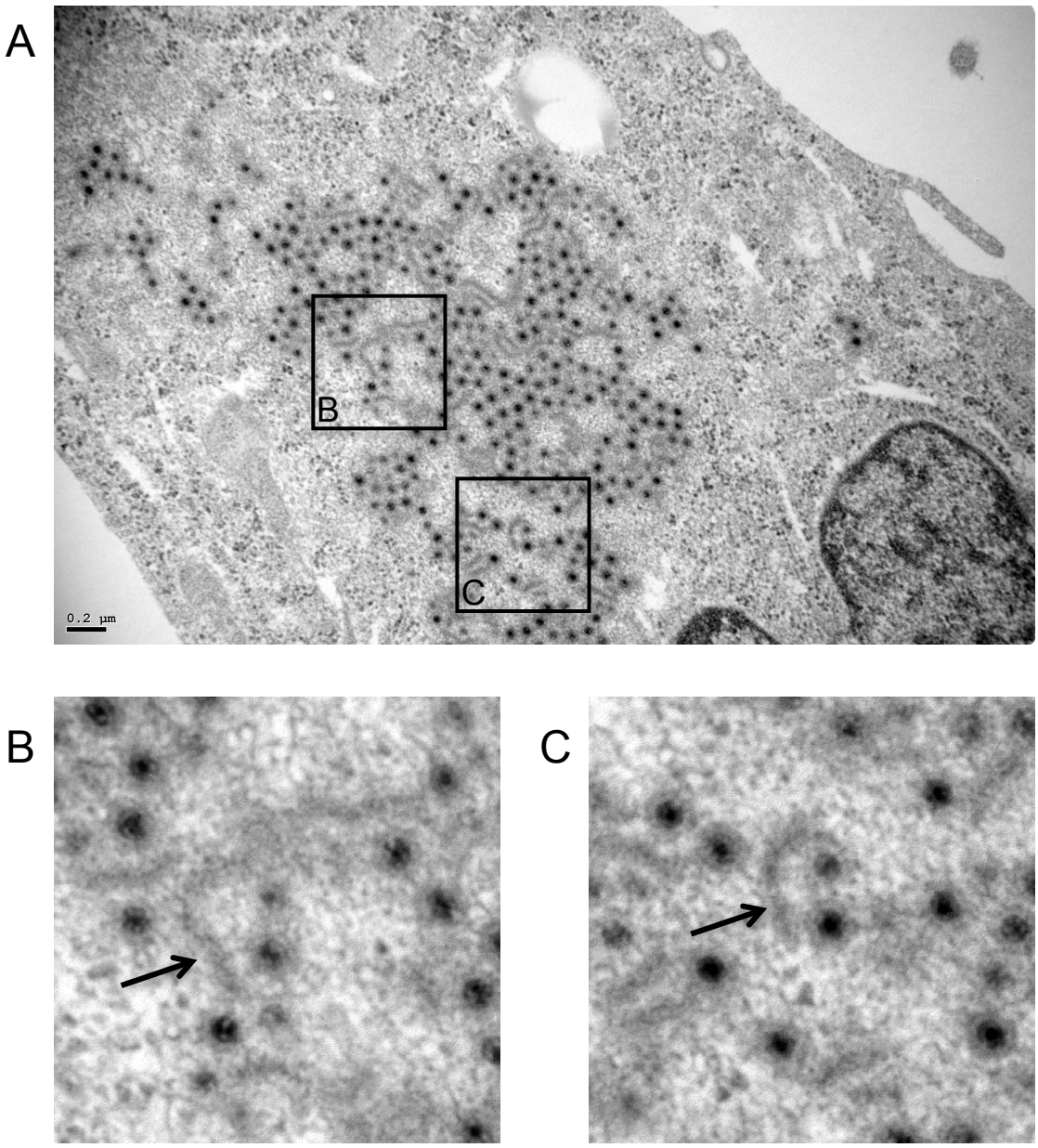

Figure V-5. Reovirus cytoplasmic inclusions contain membrane-like structures. Polarized HBMECs were adsorbed with reovirus strain T3SA+ at an MOI of 10 PFU per cell. After incubation at 37°C for 24 h, cells were fixed in 4% paraformaldehyde and 1% electron microscopy (EM)-grade glutaraldehyde. (A) Image of an infected cell with a cytoplasmic inclusion. Boxed regions are enlarged in (B) and (C). Scale bars: 0.2 µm. (B and C) Enlarged regions of the cytoplasmic inclusion shown in (A). Arrows indicate membrane-like structures.

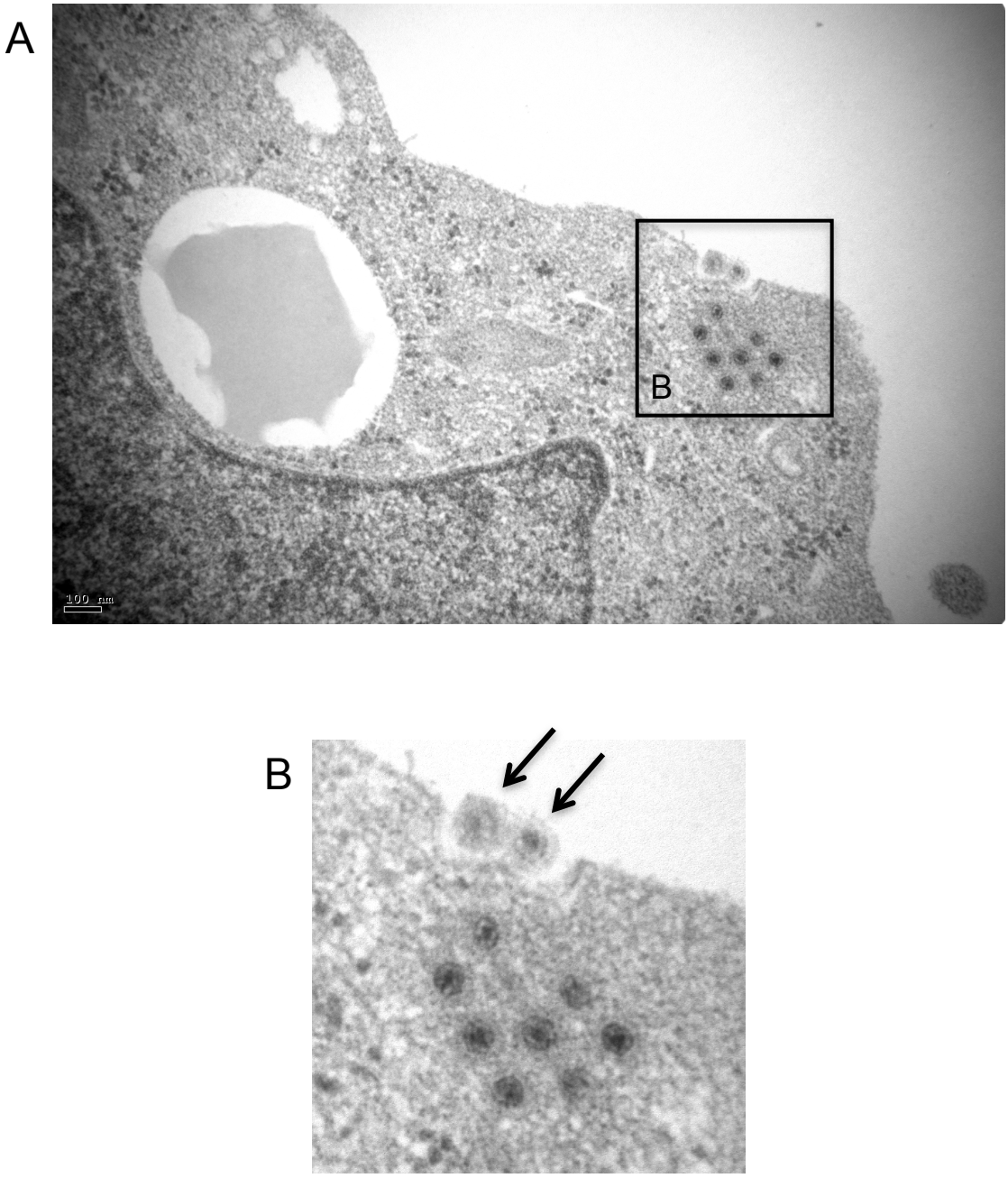

Figure V-6. Reovirus egress from an intact cell. Polarized HBMECs were adsorbed with reovirus strain T3SA+ at an MOI of 10 PFU per cell. After incubation at 37°C for 24 h, cells were fixed in 4% paraformaldehyde and 1% EM-grade glutaraldehyde. (A) Image of an infected cell with a cytoplasmic inclusion. Boxed regions are enlarged in (B). Scale bars: 100 nm. (B) Enlarged region of the boxed region shown in (A). Arrows indicate exiting virus particles.

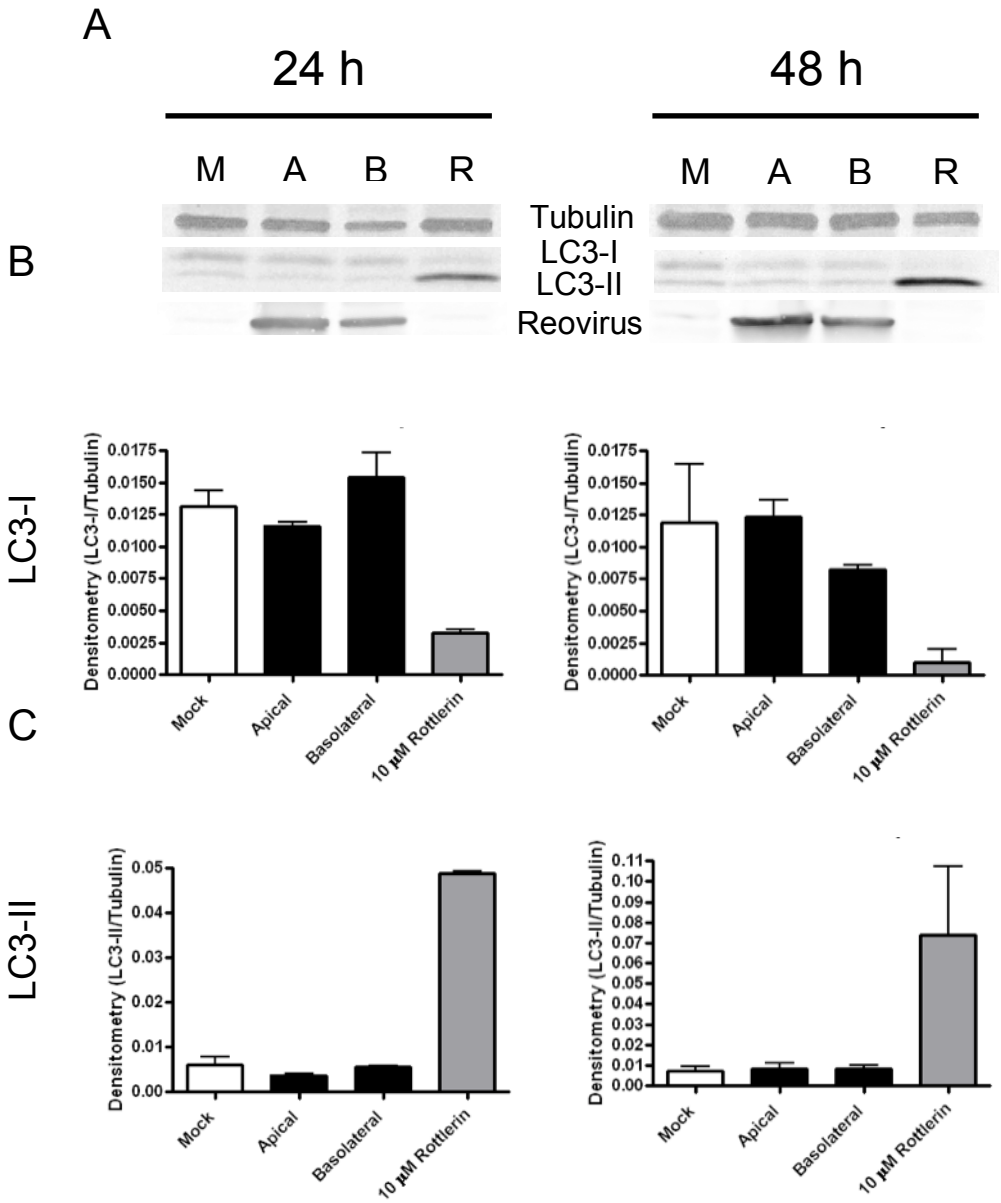
A
24 h
48 h
M
A
B
R
M
A
B
R
B
Tubulin
LC3-I
LC3-II
Reovirus
LC3-I
C
Densitometry (LC3-I/Tubulin)
0.0175
0.0150
0.0125
0.0100
0.0075
0.0050
0.0025
0.0000
Mock
Apical
Basolateral
10 μM Rottlerin
Densitometry (LC3-I/Tubulin)
0.0175
0.0150
0.0125
0.0100
0.0075
0.0050
0.0025
0.0000
Mock
Apical
Basolateral
10 μM Rottlerin
LC3-II
Densitometry (LC3-II/Tubulin)
0.05
0.04
0.03
0.02
0.01
0.00
Mock
Apical
Basolateral
10 μM Rottlerin
Densitometry (LC3-II/Tubulin)
0.11
0.10
0.09
0.08
0.07
0.06
0.05
0.04
0.03
0.02
0.01
0.00
Mock
Apical
Basolateral
10 μM Rottlerin

Figure V-7. Reovirus infection of polarized HBMECs does not induce autophagic activity. Polarized HBMECs were adsorbed either apically (A) or basolaterally (B) with reovirus strain T3SA+ at an MOI of 10 PFU per cell. After incubation at 37°C for 24 or 48 h, cell lysates were prepared from each sample and subjected to SDS-PAGE. (A) Immunoblots of mock-treated (M), apically-adsorbed (A), or basolaterally-adsorbed (B) polarized HBMECs. Rottlerin-treated cells (R) were used as positive controls for autophagy. The left panel shows samples collected 24 h post-adsorption and the right panel shows samples collected 48 h post-adsorption. (B and C) Quantification of the LC3-I (B) and LC3-II (C) densitometry units observed in the immunoblot shown in (A). Densitometry units for each sample were normalized against a tubulin control. The left panel shows samples collected 24 h post-adsorption and the right panel shows samples collected 48 h post-adsorption.

Conclusions

Defining factors that govern reovirus dissemination in the blood is essential for optimum use of reovirus in clinical applications. Reovirus efficiently replicates in and kills cancer cells (99, 156). Phase I-III clinical trials are underway to test the efficacy of reovirus as an adjunct to conventional cancer therapies (99, 156) (157). Following intravenous administration, reovirus must navigate and exit the bloodstream to infect solid organ tumors. Intratumoral injection of reovirus may allow for enhanced replication in tumor cells and subsequent spread through the blood to target metastatic tumor foci. Thus, determining viral and cellular determinants underlying how reoviruses gain access to the blood compartment, spread within the bloodstream, and exit from the circulation may aid in oncolytic design.

Use of the reverse genetics system may allow engineering of reovirus therapeutics with mutations that increase vector potency or safety by manipulating dissemination determinants (4). For example, during intratumoral reovirus administration, mutating the residues in reovirus attachment protein σ1 that interact with JAM-A may decrease bloodstream spread from the tumor and retain higher reovirus titers within the tumor microenvironment. Furthermore, this virus may have fewer adverse effects due to systemic reovirus spread. It is possible that mutating residues important for reovirus interactions with JAM-A will decrease tumor cell infection, however infectivity could be unchanged due to SA engagement (158, 159). The presence of proteases in the tumor microenvironment (160) also may result in the formation of ISVPs, which are more infectious than virion particles (1, 161).

In this dissertation, I present data showing that endothelial JAM-A facilitates reovirus bloodstream spread. Reovirus infection of the endothelium may serve to route virions into and amplify titers in the vascular compartment. Understanding mechanisms of reovirus dissemination will provide broader insight into events at the pathogen-host interface that lead to systemic disease and may aid in the development of therapeutics that target this critical step in viral pathogenesis.

CHAPTER VI

MATERIALS AND METHODS

Cells, Viruses, Enzymes, and Antibodies

Spinner-adapted murine L929 fibroblast cells were grown in either suspension or monolayer cultures as described (28, 64). Human brain microvascular endothelial cells (HBMECs) (162, 163) were grown in RPMI-1640 medium (Mediatech) supplemented to contain 10% FBS, 10% NuSerum (BD Biosciences), nonessential amino acids (Sigma), 1 mM sodium pyruvate, MEM vitamins (Mediatech), 2 mM L-glutamine, 100 U/ml penicillin, 100 μg/ml streptomycin, and 25 ng/ml amphotericin B. HBMECs and L929 cells were cultured on collagen-coated Transwells (6.5 mm diameter, 0.4 μm pores; Costar) for 7 d prior to infection or imaging experiments.

Reovirus strain T1L is a laboratory stock. Strain T3SA+ was generated as described (102). Recombinant viruses rsT3D, rsT3D-σ1R202W, and rsT3D-σ1G381A were generated using plasmid-based reverse genetics (26, 120). Virus was purified as described (164). Viral titers were determined by plaque assay using L929 cells (134).

The immunoglobulin G (IgG) fraction of a rabbit antiserum raised against strains T1L and T3D (122) was purified by protein A-Sepharose as described (102, 103). Reovirus-specific IgG was conjugated to Alexa Fluor-647 or Alexa Fluor-488 using APEX antibody labeling kits (Invitrogen). Human JAM-A-specific monoclonal antibody J10.4 (provided by Charles Parkos, Emory University) and claudin-1-specific antibody (ab15098, Abcam) were used in confocal microscopy imaging experiments in HBMECs.

Murine JAM-A-specific polyclonal antibody (AF1077; R&D Systems) was used to characterize mouse strains. Alexa Fluor-conjugated antibodies (Invitrogen) were used as secondary antibodies.

Generation of mouse strains

EndoJAM-AKD mice, which have decreased endothelial JAM-A and lack hematopoietic JAM-A, or HematoJAM-AKO mice, which lack JAM-A only within the hematopoietic compartment, were generated using cre-lox technology. Female JAM-A flox/flox mice were bred to male Tek-cre transgenic (tg) mice (165) to generate EndoJAM-AKD mice (Figure II-1) or male Vav-cre tg mice (166) to generate HematoJAM-AKO mice (Figure II-4). Litters from these breeding pairs were used for infection experiments. HematoJAM-A mice, which lack native JAM-A but overexpress JAM-A within the hematopoietic compartment, were obtained by first generating Vav-JAM tg mice in which JAM-A expression is driven by the hematopoietic-specific vav promoter (Figure II-4). Vav-JAM tg mice were then bred to JAM-AKO mice to ablate native JAM-A expression (Figure II-4). All strains used for these studies were maintained on a C57BL/6 background. Cell-surface expression of JAM-A in endothelial and hematopoietic cells was assessed in the different mouse strains using flow cytometry. JAM-A expression profiles of the mouse strains are shown in Table 2.

Mouse genotypes were confirmed using PCR. Primer sequences used for genotyping experiments are shown in Table 1. Mouse ear clippings or aliquots of homogenized organ were employed for genomic DNA extraction using the REDExtract-N-Amp Tissue PCR Kit (Sigma).

Mouse infection studies

Two- to three day-old mice were inoculated perorally or intravenously with purified reovirus strain T1L diluted in PBS. Peroral inoculations were performed as described (51, 64). Intravenous inoculations were performed following anesthesia by hypothermia (88, 167). The proper depth of anesthesia was assessed visually by lack of response to external stimuli. Anesthetized mice were positioned on a Wee Sight transilluminator (Phillips) to visualize the superficial temporal vein. A dose of 50 microliters of virus inoculum was administered via a 33-gauge 0.25-inch needle (Cadence) attached to a 1-ml syringe by a T-connector extension set (Braun). Successful inoculation was assessed by blanching of the superficial temporal vein and noting reflux of blood from the injection site upon removal of the needle. Pups were placed on a warming pad until consciousness was regained. At various times post-inoculation, organs were excised, submerged into PBS, subjected to two freeze-thaw cycles, and sonicated until homogenized. Viral titers in organ homogenates were determined by plaque assay (134). Blood was collected into an equal volume of Alsever's solution (Sigma), subjected to two freeze-thaw cycles, sonicated, and processed for viral titer determination by plaque assay (134). Animal husbandry and experimental procedures were performed in accordance with Public Health Service policy and approved by the Vanderbilt University School of Medicine Institutional Animal Care and Use Committee.

Flow cytometry

Hematopoietic cells were harvested from peripheral blood or from spleens of 6- to 8-week-old mice. Erythrocytes were lysed using ACK lysis buffer at room temperature for

5 min. Leukocytes were collected by centrifugation at 1000 *x g* for 5 min, and hematopoietic cell subsets were identified using antibodies specific for granulocytes (Gr-1), B cells (B220), T cells (TCRβ), macrophages (CD11b), and dendritic cells (CD11c). Expression of cell-surface JAM-A was assessed using an antibody specific for JAM-A (AF1077; R&D Systems).

Lung endothelial cells were harvested as described (168). Lungs were excised from euthanized animals and flushed with 10 ml 2.5 mM EDTA, followed by 5 ml 0.25% trypsin in 2.5 mM EDTA. Following incubation at 37°C for 30 min, lungs were minced with a scalpel and washed with 1 ml complete DMEM. Cells were collected by centrifugation at 1000 *x g* for 10 min, resuspended in 1.5 ml EBM-2 medium supplemented to contain EGM-2 MV SingleQuots (hEGF, hydrocortisone, gentamicin, amphotericin B, VEGF, hFGF-B, IGF-1, ascorbic acid, and heparin) (Lonza), and cultivated in 6-well plates coated with 0.2% gelatin. Lung endothelial cells were cultured at 37°C for 5-7 d, washed twice with PBS on day 3, and supplemented with fresh EBM-2 medium. Expression of cell-surface JAM-A was assessed by flow cytometry following staining of cells with antibodies specific for hematopoietic cells (CD45), endothelial cells (CD31), and JAM-A. To determine whether cell-surface expression of JAM-A correlates with reovirus infectivity, lung endothelial cells were infected at a MOI of 100 PFU per cell. After incubation at 37°C for 20-24 h, cells were collected, and stained with Alexa Fluor-conjugated reovirus antiserum. The percentage of infected cells was determined using flow cytometry. All cell staining was quantified using FlowJo software (Tree Star).

Transwell collagen coating

Transwell inserts were incubated with 100 µl rat tail collagen I (50 µg/ml; Sigma) in the presence of ammonium hydroxide at room temperature for 15 min. Transwell inserts were washed three times using Hanks balanced salt solution (Mediatech) and once with sterile water (Invitrogen) and allowed to dry at room temperature for 2 h. HBMECs or L929 cells were cultured on the apical surface of collagen-treated Transwell inserts for 7 d (Figure VI-1), with the apical compartment containing 200 µl medium and the basolateral compartment containing 1 ml medium. Medium within the apical and basolateral compartments was replaced with fresh medium 3 and 6 d post-seeding. TEER was quantified 3 and 6 d post-seeding, on the day of infection, and at various intervals post-infection using an EndOhm-6 Voltohmmeter (Figure VI-1B).

TEER measurements

TEER across polarized HBMEC monolayers was quantified at 3 and 6 d post-seeding, on the day of infection, and at various intervals post-infection using an EVOM Voltohmmeter and EndOhm-6 cup electrode (World Precision Instruments). TEER readings for test samples were normalized by subtracting TEER of blank collagen-coated Transwells. The data are presented as unit area resistance ($\Omega \cdot cm^2$) (169).

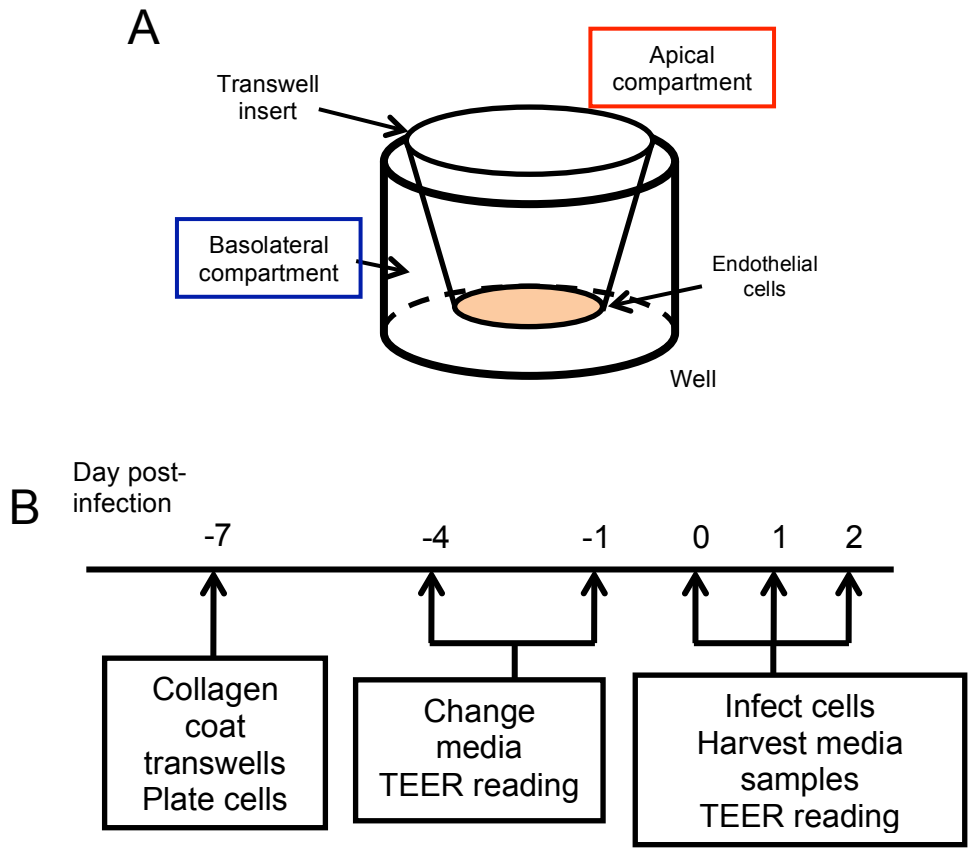

Figure VI-1. Transwell schematic and infection timeline. (A) A schematic of a Transwell insert is shown. Transwell inserts are coated with collagen prior to the addition of endothelial cells. Endothelial cells are plated on the apical surface of the Transwell insert and media is added to the basolateral surface. (B) A schematic depicting a timeline of an infection experiment. Seven days prior to infection, Transwell inserts are coated with collagen and cells are plated. Media is changed 3 and 6 d post-seeding, and TEER measurements are recorded to monitor polarization status of the monolayer. On day 7 post-seeding, the endothelial cell monolayer is polarized and can be used for an infection experiment.

Permeability assay

On 1, 4, and 7 d post-seeding, FITC-labeled 10 kDa dextrans (FITC-dextrans, 25 μg/ml; Sigma) were added to the apical compartment of HBMECs seeded on Transwell membranes in 200 μl incomplete RPMI medium and 1 ml medium was added to the basolateral compartment. Cells were incubated at 37°C for 4 h, and medium from the apical and basolateral compartments was collected. FITC fluorescence in the medium obtained from each compartment was assessed using a Plate Chameleon Multilabel Detection Platform (Hidex) with 485 nm excitation and 535 nm emission filters. Dextran concentration was determined from the FITC fluorescence intensity using a standard curve generated with the FITC-dextrans. The degree of permeability was determined using the following equation: Permeability (%) = $[\text{FITC-dextran}]^{\text{basolateral}}/([\text{FITC-dextran}]^{\text{basolateral}} + [\text{FITC-dextran}]^{\text{apical}}) \times 100$. On day 7, permeability also were assessed for a sample in which 2.5 mM EDTA (Mediatech) was added to the apical and basolateral compartments to disrupt TJs.

Virus assays

Polarized HBMECs cultivated on Transwell inserts were adsorbed with virus apically or basolaterally at a MOI of 10 PFU per cell. For apical adsorption, 30 μl of virus inoculum was added to the apical compartment. For basolateral adsorption, the Transwell insert was inverted in a sterile dish, and 30 μl of virus inoculum was added to the basolateral surface. In some experiments, cells were treated with medium, anti-JAM-A antibody (20 μg/ml), or *Arthrobacter ureafaciens* neuraminidase (80 mU/ml; MP Biomedicals) prior to virus adsorption. After adsorption of virus at room temperature for 1 h, cells were washed

twice with PBS, and 200 µl medium was added to the apical compartment and 1 ml medium was added to the basolateral compartment. For viral release assays, medium from the apical or basolateral compartments was collected at various intervals, and viral titers in medium from each compartment were determined by plaque assay using L929 cells (134). For viral replication assays, Transwell membrane inserts were removed from Transwells using a scalpel, submerged in 500 µl medium, and subjected to two cycles of freezing and thawing. Viral titers in cell lysates were determined by plaque assay using L929 cells (134).

For infectivity studies, cells were incubated at 37°C for 20-24 h, harvested with 0.05% trypsin-EDTA (Invitrogen) at room temperature, and quenched with medium collected from the apical compartment of the respective sample. Cells were stained with Alexa Fluor-conjugated reovirus-specific antiserum as described (28). The percentage of reovirus antigen-positive cells was determined using flow cytometry. For binding studies, cells were detached from the Transwell insert immediately after adsorption with Cellstripper (Mediatech) at 37°C for 5 min and stained using Alexa Fluor-conjugated reovirus-specific antiserum as described (28). The MFI of each sample was determined using flow cytometry. All cell staining was quantified using FlowJo software (Tree Star).

Human brain microvascular pericytes were cultured until confluent. Cells were adsorbed at an MOI of 100 PFU per cell at room temperature for 1 h, washed twice, replaced with fresh medium, and incubated at 37°C for 24 h. Cells were fixed and stained with reovirus-specific antiserum and 4',6-diamidino-2-phenylindole (DAPI). Reovirus infectivity was assessed by indirect immunofluorescence.

Cell imaging

Polarized HBMECs were fixed in 100% methanol at -20°C for 5 min. Cells were blocked in PBS containing 5% bovine serum albumin (BSA) at room temperature for 30 min. Cells were stained with antibodies specific for JAM-A (1:1000) and claudin-1 (1:100) as described (28, 170). After staining, Transwell membranes containing cells were excised using a scalpel. Membranes were placed onto glass slides, and glass coverslips (#1.5; Thermo Scientific) were mounted using Aqua-Poly/Mount mounting medium (Polysciences, Inc.). Cell images were captured using a Zeiss LSM 510 Meta laser-scanning confocal microscope using a 63×/1.40 Plan-Apochromat objective lens. A standard threshold pixel intensity was employed for all images, and the pinhole size used was identical for all fluorophores. Images represent a single or series of sections from within a z-stack and were adjusted for brightness and contrast to the same extent. MFI of pixels from apical and basolateral sections of cells (n = 5) was quantified using ImageJ software (NIH).

Trypan blue exclusion assay

HBMECs and L929 cells were cultured on Transwell inserts until polarized and confluent, respectively. Virus was adsorbed apically or basolaterally at an MOI of 10 PFU per cell, and cells were incubated at 37°C for 20-24 h. After incubation, cells were harvested using trypsin-EDTA, quenched with medium collected from the apical compartment, and washed once with PBS. A small aliquot (20 µl) of cells was removed for analysis of cell lysis. An equal volume of trypan blue (0.4% w/v din PBS; Mediatech) was added to cells, followed by incubation at room temperature for 3 min. Lysed and

intact cells were enumerated using a hemocytometer with brightfield microscopy. The percentage of reovirus-infected cells was quantified from the remainder of each sample using flow cytometry.

TUNEL assay

Polarized HBMECs were adsorbed with virus at an MOI of 100 PFU per cell, washed twice with PBS, and incubated at 37°C for 24 or 48 h. Cells were removed from the Transwell using trypsin-EDTA, quenched with medium collected from the apical compartment, washed once with PBS, and assayed for the percentage of apoptotic cells using the TUNEL technique (APO-BrdU TUNEL assay kit; Invitrogen) according to the manufacturer's instructions. After TUNEL staining, cells were stained with Alexa Fluor-conjugated reovirus-specific antiserum (1:1000) at 4°C for 30 min, washed, and pelleted. The samples were resuspended in 0.5 ml propidium iodide-containing buffer. Stained cells were analyzed for apoptosis and reovirus antigen-positive cells using flow cytometry.

Acridine Orange assay

Polarized HBMECs were adsorbed with virus at an MOI of 100 PFU per cell, washed twice with PBS, and incubated at 37°C for 24 h. Cells were removed from the Transwell using trypsin-EDTA, quenched with medium collected from the apical compartment, washed once with PBS, and resuspended in a volume to obtain a final concentration of 1 x 10^6 cells/mL. Acridine orange dye (50 μl per 1 mL cells; PBS containing 100 μg/ml acridine orange and 100 μg/ml ethidium bromide [Bio-Rad]) was added and the

percentage of apoptotic cells was determined by enumerating the number of acridine orange-stained nuclei versus unstained nuclei under brightfield microscopy.

AnnexinV/Dead Cell Apoptosis assay

Polarized HBMECs were adsorbed with virus at an MOI of 100 PFU per cell, washed twice with PBS, and incubated at 37°C for 24 h. Cells were removed from the Transwell using Cellstripper, quenched with FACS buffer, washed once with PBS, and assayed for the percentage of apoptotic cells using AnnexinV staining (Alexa Fluor 488 annexinV/Dead Cell Apoptosis Kit; Invitrogen) according to the manufacturer's instructions. A portion of each cell sample was stained with Alexa Fluor-conjugated reovirus-specific antiserum. Stained cells were analyzed for apoptosis or reovirus-positive antigen using flow cytometry.

Transmission electron microscopy

Apically-infected and basolaterally-infected HBMEC Transwell samples were fixed in 4% paraformaldehyde and 1% glutaraldehyde. Samples were washed with PBS four times, and incubated in 1% osmium and 0.8% potassium ferricyanide in the dark at 4°C for 1 h. Transwell membranes were washed with PBS four times and incubated in solutions containing increasing concentrations of acetone (50%, 70%, 90%, 100%, in water) on ice for 10 min. After the last incubation in 100% acetone, new 100% acetone was replaced and cells were incubated on ice for 10 min. Samples were then incubated overnight in a solution containing equal volumes of acetone and epoxy resin. Transwell samples were placed in 100% epoxy resin for 10 h, moved to new 100% epoxy resin,

placed in in plastic embedding capsules, and polymerized at 60°C for 48 h. Consecutive, ultrathin (50 nm) sections were collected on parallel-bar copper grids (with 300 mesh) using an Ultramicrotome UC6 (Leica). Copper grids containing samples were stained in a solution containing saturated uranyl acetate in the dark at room temperature for 20 min. After incubation, grids were washed in four drops of distilled water, incubated in lead citrate for 2 min, and washed with four drops of distilled water (170). Grids were dried at room temperature and images were acquired using an electron microscope (JEOL 1011 100 KV).

Immunoblotting

Immunoblot analysis of cell lysates was performed as described (170). Total cell lysates of HBMECs adsorbed apically or basolaterally with reovirus strain T3SA+, or treated with rottlerin (10 μM) were resolved by SDS-PAGE and immunoblotted with primary antibodies specific for tubulin, LC3, or reovirus-specific antiserum. Membranes were scanned using an Odyssey imaging system, and band intensity was quantified using the Odyssey software suite.

Statistical analysis

Experiments were performed in duplicate and repeated at least twice. Representative results of single experiments are shown. Mean values were compared using an unpaired Student's *t* test or one-way ANOVA (GraphPad Prism). Error bars denote the range of data or standard deviation. *P* values of < 0.05 were considered to be statistically significant.

APPENDIX A

DIRECTIONAL RELEASE OF REOVIRUS FROM THE APICAL SURFACE OF POLARIZED ENDOTHELIAL CELLS

Caroline M. Lai, Bernardo A. Mainou, Kwang-Sik Kim, Terence S. Dermody

mBio 4(2):e0049-13; 2013

Directional Release of Reovirus from the Apical Surface of Polarized Endothelial Cells

Caroline M. Lai,[a,b] Bernardo A. Mainou,[b,c] Kwang S. Kim,[d] Terence S. Dermody[a,b,c]

Department of Pathology, Microbiology and Immunology,[a] Elizabeth B. Lamb Center for Pediatric Research,[b] and Department of Pediatrics,[c] Vanderbilt University School of Medicine, Nashville, Tennessee, USA; Department of Pediatrics, Division of Pediatric Infectious Diseases, Johns Hopkins School of Medicine, Baltimore, Maryland, USA[d]

ABSTRACT **Bloodstream spread is a critical step in the pathogenesis of many viruses. However, mechanisms that promote viremia are not well understood. Reoviruses are neurotropic viruses that disseminate hematogenously to the central nervous system. Junctional adhesion molecule A (JAM-A) is a tight junction protein that serves as a receptor for reovirus. JAM-A is required for establishment of viremia in infected newborn mice and viral spread to sites of secondary replication. To determine how viruses gain access to the circulatory system, we examined reovirus infection of polarized human brain microvascular endothelial cells (HBMECs). Reovirus productively infects polarized HBMECs, but infection does not alter tight junction integrity. Apical infection of polarized HBMECs is more efficient than basolateral infection, which is attributable to viral engagement of sialic acid and JAM-A. Viral release occurs exclusively from the apical surface via a mechanism that is not associated with lysis or apoptosis of infected cells. These data suggest that infection of endothelial cells routes reovirus apically into the bloodstream for systemic dissemination in the host. Understanding how viruses invade the bloodstream may aid in the development of therapeutics that block this step in viral pathogenesis.**

IMPORTANCE **Bloodstream spread of viruses within infected hosts is a critical but poorly understood step in viral disease. Reoviruses first enter the host through the oral or respiratory route and infect cells in the central nervous system. Spread of reoviruses to the brain occurs by blood or nerves, which makes reoviruses useful models for studies of systemic viral dissemination. In this study, we examined how reoviruses infect endothelial cells, which form the walls of blood vessels. We found that reovirus infection of endothelial cells allows the virus to enter blood vessels and serves as a means for the virus to reach high titers in the circulation. Understanding how reovirus is routed through endothelial cells may aid in the design of antiviral drugs that target this important step in systemic viral infections.**

Received 20 January 2013 **Accepted** 14 March 2013 **Published** 9 April 2013

Citation Lai CM, Mainou BA, Kim KS, Dermody TS. 2013. Directional release of reovirus from the apical surface of polarized endothelial cells. mBio 4(2):e00049-13. doi:10.1128/mBio.00049-13.

Editor Anne Moscona, Weill Medical College

Address correspondence to Terence S. Dermody, terry.dermody@vanderbilt.edu.

Bloodstream dissemination within an infected host is required for the pathogenesis of many viruses. In particular, many neurotropic viruses use the circulation to invade the central nervous system (CNS) from a distant site of primary replication. Regardless of the site of entry into the host, viruses that disseminate hematogenously must first traverse an endothelial barrier and egress from the circulation. Although viremia is a well-established dissemination process, precise mechanisms of viral entry into or exit from the bloodstream are not well understood.

Mammalian orthoreoviruses (reoviruses) are neurotropic viruses that disseminate hematogenously to the CNS, where they display serotype-specific patterns of tropism for neural cells. Serotype 1 reoviruses spread strictly by the bloodstream and infect ependymal cells within the CNS, causing nonlethal hydrocephalus (1–3). In contrast, serotype 3 reoviruses spread neurally and hematogenously, infect neurons within the CNS, and cause fatal encephalitis (1, 4, 5). These serotype-specific differences in neuropathogenesis segregate with the viral S1 gene (2, 3), which encodes attachment protein σ1 and nonstructural protein σ1s (6–8). Both S1 gene products play key roles in reovirus pathogenesis (4, 5, 9–11), with σ1 targeting reovirus to specific host cells (12–14) and σ1s contributing to lymphatic and bloodstream spread (5, 10).

Reoviruses engage two known cellular receptors, oligosaccharides terminating in sialic acid and junctional adhesion molecule A (JAM-A), via attachment protein σ1 by using an adhesion-strengthening mechanism (15). Virions are first tethered to the cell surface by low-affinity binding to the relatively more abundant sialic acid, followed by high-affinity interactions with JAM-A (15). JAM-A is a member of the immunoglobulin superfamily and is expressed in epithelial and endothelial cells, where it functions in the formation and maintenance of tight junctions (TJs) (16–18). JAM-A also is expressed on the surface of hematopoietic cells and platelets, where it facilitates leukocyte extravasation and platelet activation, respectively (16, 19, 20). In mice, the capacity of reovirus to bind sialic acid enhances neurovirulence (9, 21) and allows infection of bile duct epithelial cells, producing a disease that mimics biliary atresia in human infants (9). In contrast, the capacity of reovirus to bind JAM-A is required for the establishment of viremia and dissemination to sites of secondary replica-

tion through the blood (4). The function of sialic acid and JAM-A in reovirus infection of polarized endothelial cells is not known.

In this study, we examined reovirus infection of polarized endothelial cells to better understand mechanisms of viral entry into and egress from the bloodstream. We found that reovirus productively infects polarized endothelial cells from both apical and basolateral routes of adsorption. Infection was more efficient after adsorption from the apical surface, a property attributable to the binding of sialic acid and JAM-A. Interestingly, reovirus was released exclusively from the apical surface in a noncytolytic manner. These studies provide a new understanding of how viruses infect polarized endothelial cells and identify the endothelium as an important mediator of viral pathogenesis.

RESULTS

Reovirus infection of polarized endothelial cells is more efficient from the apical surface. To determine whether reovirus productively infects polarized endothelial cells (see Fig. S1 in the supplemental material), we adsorbed either the apical or the basolateral surface of polarized human brain microvascular endothelial cells (HBMECs) with strain T3SA+, a virus that efficiently binds sialic acid and JAM-A (15, 22). The viral titer in cell lysates increased over time, regardless of the route of adsorption (Fig. 1A). Following apical adsorption, the viral titer peaked at 24 h postinfection, with the yield reaching approximately 1,000-fold over the input. In contrast, following basolateral adsorption, viral replication was delayed, with yields of 5-fold at 24 h and 100-fold at 48 h postinfection. These data indicate that reovirus infection of polarized HBMECs by either the apical or the basolateral entry route is productive, but apical adsorption results in more efficient replication and increased viral yields.

Because we observed higher peak titers in polarized HBMECs after apical adsorption, we sought to determine whether initiation of reovirus infection is more efficient when cells are infected apically than when they are infected basolaterally. Polarized HBMECs were adsorbed with virus by the apical or basolateral route, and the percentage of reovirus antigen-positive cells was quantified by flow cytometry. Apical adsorption resulted in approximately 10-fold more infected cells than did basolateral adsorption (Fig. 1B). As a control, apical or basolateral adsorption of nonpolarized L929 fibroblast cells cultivated on Transwell inserts yielded equivalent numbers of infected cells (Fig. 1B).

To determine whether differences in infectivity are attributable to differences in virus binding, we assessed virus attachment to polarized HBMECs following apical or basolateral adsorption. In concordance with the infectivity data, approximately 10-fold more virus was bound to HBMECs following apical adsorption than following basolateral adsorption (Fig. 1C). As anticipated, virus bound equivalently to L929 fibroblasts following adsorption either apically or basolaterally (Fig. 1C). Together, these data suggest that reovirus binds more efficiently to the apical surface of polarized HBMECs, which results in increased infectivity and replication.

Sialic acid and JAM-A are required for reovirus infection of polarized endothelial cells. To determine whether differences in the infectivity of polarized HBMECs after apical or basolateral adsorption are attributable to differences in receptor engagement, we used mutant reovirus strains impaired in the capacity to bind either sialic acid or JAM-A. Single amino acid mutations in the σ1 attachment protein can dramatically diminish binding to these

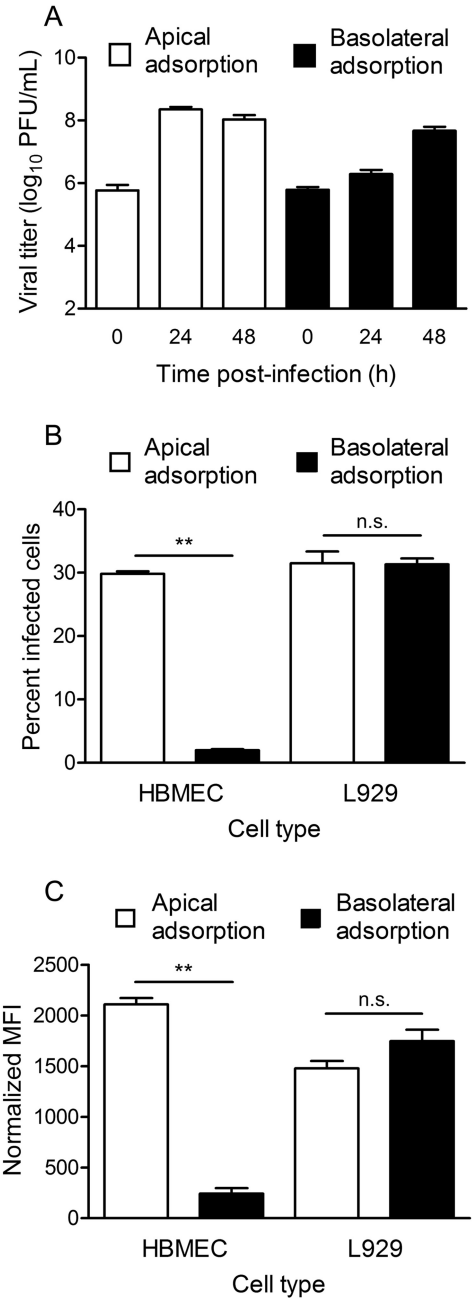

FIG 1 Reovirus infection of polarized HBMECs is more efficient following adsorption from the apical surface. Polarized HBMECs were adsorbed either apically (white bars) or basolaterally (black bars) with reovirus T3SA+ at an MOI of 10 PFU per cell. (A) Transwell inserts were excised at 0, 24, and 48 h postinfection, and viral titers in cell lysates were determined by plaque assay. A representative experiment of three performed, with each experiment conducted in duplicate, is shown. Error bars indicate the range of data for the duplicates. (B) HBMECs were incubated for 20 to 24 h and harvested by trypsinization. Cells were permeabilized and stained with Alexa Fluor-conjugated, reovirus-specific antiserum. The percentage of infected cells was determined by flow cytometry. A representative experiment of three performed, with each experiment conducted in duplicate, is shown. Error bars indicate the range of data for the duplicates. (C) HBMECs were removed immediately after adsorption and stained with Alexa Fluor-conjugated, reovirus-specific antiserum. MFI was determined by flow cytometry. A representative experiment of three performed, with each experiment conducted in duplicate, is shown. Error bars indicate the range of data for the duplicates. **, $P < 0.005$.

receptors (15, 23). Polarized HBMECs were adsorbed apically or basolaterally with wild-type or mutant reovirus strains, and the percentage of infected cells was quantified at 24 h postinfection. There were significantly more infected cells following apical adsorption with wild-type strain type 3 Dearing (rsT3D) than after apical adsorption with mutant strain rsT3D-σ1R202W, which is deficient in sialic acid binding (21, 23), or mutant strain rsT3D-σ1G381A, which is deficient in JAM-A binding (24) (Fig. 2A). Treatment of polarized HBMECs with neuraminidase (to remove cell surface sialic acid) and JAM-A-specific antibody prior to apical virus adsorption significantly decreased infection by rsT3D. Similarly, neuraminidase and JAM-A-specific antibody pretreatment substantially decreased infection of polarized HBMECs by rsT3D-σ1G381A and rsT3D-σ1R202W, respectively (Fig. 2A). Concordantly, rsT3D bound more efficiently to the apical surface of polarized HBMECs than did the mutant virus strains, and virtually all virus binding was abolished by neuraminidase or JAM-A-specific antibody pretreatment (Fig. 2C). We observed a similar trend after basolateral adsorption in that diminished receptor engagement by mutant viruses or blockade of receptor engagement with inhibitors significantly decreased the percentages of virus-infected and virus-bound cells (Fig. 2B and D). However, the overall percentage of infected cells and levels of virus binding after basolateral adsorption were substantially lower than those following apical adsorption, which diminishes the magnitude of the observed differences (note the different *y* axis scales in Fig. 2C and D). Reovirus mutant rsT3D-σ1R202W bound to the basolateral surface of HBMECs equivalently to wild-type rsT3D but infected significantly fewer cells, suggesting that sialic acid engagement may enhance reovirus replication at a postattachment step following basolateral adsorption of polarized endothelial cells. These data suggest that infection of polarized endothelial cells is dependent on virus binding to sialylated glycans and JAM-A on the apical and basolateral surfaces of polarized endothelial cells, but binding to the apical surface is more efficient.

To determine whether increased binding of reovirus to the apical surface of polarized HBMECs is attributable to enhanced receptor expression, we examined the distribution of JAM-A on polarized HBMECs by confocal microscopy. Polarized HBMEC monolayers were stained with antibodies specific for TJ protein claudin-1, as well as JAM-A (Fig. 3A). Substantially more JAM-A staining was detected at the apical surface of the polarized cell monolayer (Fig. 3B), including nonjunction sites that lack detectable claudin-1 staining (Fig. 3A). Confocal micrographs of apical portions of cells showed a stippled pattern of JAM-A expression. In equatorial sections of cells, JAM-A was distributed at the cell periphery, presumably in contact with JAM-A on adjacent cells. In these images, TJ puncta marked by claudin-1 and JAM-A colocalization are clearly visible (Fig. 3A, white asterisks). At the basolateral surface, the JAM-A signal was diminished in intensity and diffusely localized compared with JAM-A staining at the apical surface (Fig. 3A and B). Increased distribution of JAM-A to the apical surface of polarized HBMECs may allow reovirus to bind and infect these cells more efficiently by this route.

Reovirus is released apically from infected polarized endothelial cells. We next determined whether progeny virus is released apically or basolaterally from infected polarized endothelial cells. Polarized HBMECs were adsorbed apically or basolaterally with virus, and titers within the apical and basolateral compartments were quantified at various intervals by plaque assay. After

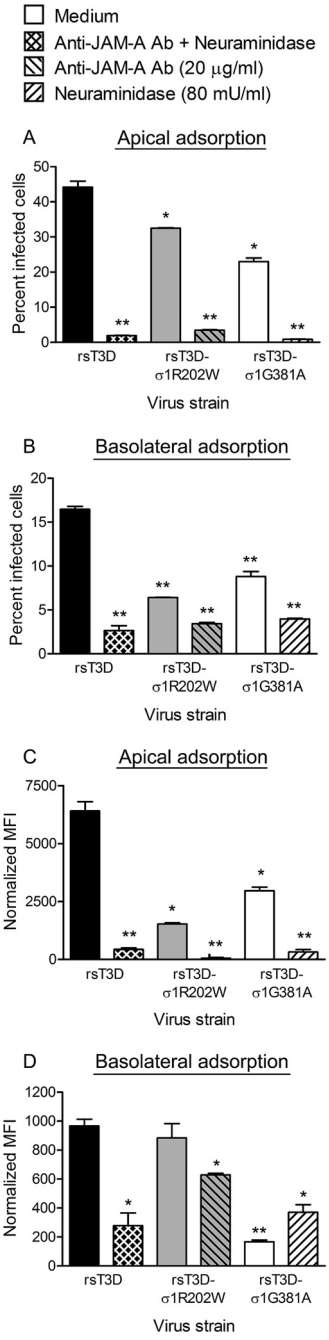

FIG 2 JAM-A and sialic acid are required for reovirus infection of polarized HBMECs. Polarized HBMECs were adsorbed either apically (A, C) or basolaterally (B, D) at an MOI of 10 PFU per cell with reovirus strain rsT3D, rsT3D-σ1R202W, or rsT3D-σ1G381A in the presence or absence of anti-JAM-A antibody (Ab; 20 μg/ml) or *A. ureafaciens* neuraminidase (80 mU/ml). (A, B) Cells were incubated for 20 to 24 h, removed from Transwell inserts with trypsin, permeabilized, and incubated with Alexa Fluor-conjugated, reovirus-specific antiserum. The percentage of infected cells was determined by flow cytometry. A representative experiment of two performed, with each experiment conducted in duplicate, is shown. Error bars indicate the range of data for the duplicates. (C, D) Cells were harvested from Transwell inserts immediately after adsorption and stained with Alexa Fluor-conjugated, reovirus-specific antiserum. MFI was quantified by flow cytometry. Note that different *y* axis scales are used for apical and basolateral adsorption. A representative experiment of two performed, with each experiment conducted in duplicate, is shown. Error bars indicate the range of data for the duplicates. *, $P < 0.05$; **, $P < 0.005$.

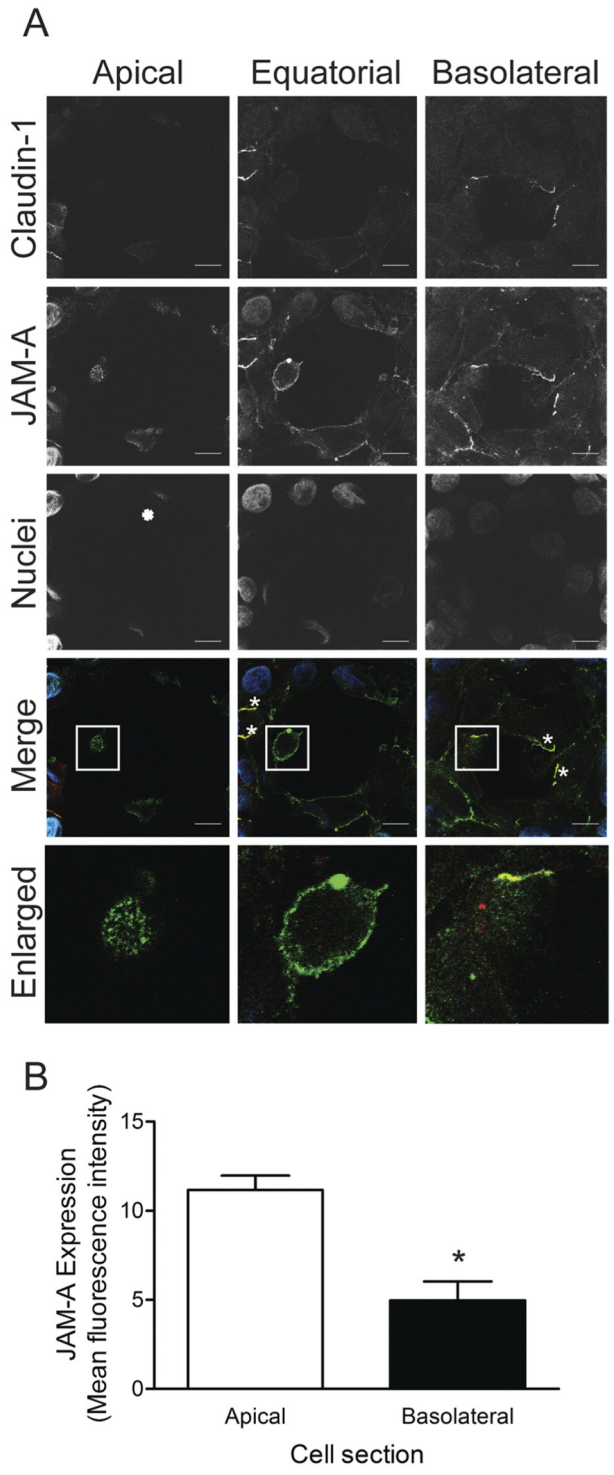

FIG 3 Polarized HBMECs express JAM-A predominantly at the apical surface. (A) Polarized HBMECs were stained for JAM-A (green), claudin-1 (red), and nuclei (blue) and imaged by confocal microscopy. Shown are images of the apical, equatorial, and basolateral regions of a single representative *z* stack. Colocalization of TJ proteins is indicated by white asterisks. The scale bar indicates 10 μm. Enlarged images of the white-boxed areas are shown in the bottom panels. Cell images were captured with a Zeiss LSM 510 Meta laser-scanning confocal microscope with a 63×/1.40 Plan-Apochromat objective lens. (B) JAM-A channel MFI of apical and basolateral sections of individual cells ($n = 5$) was quantified. Error bars indicate standard deviations. *, $P < 0.05$.

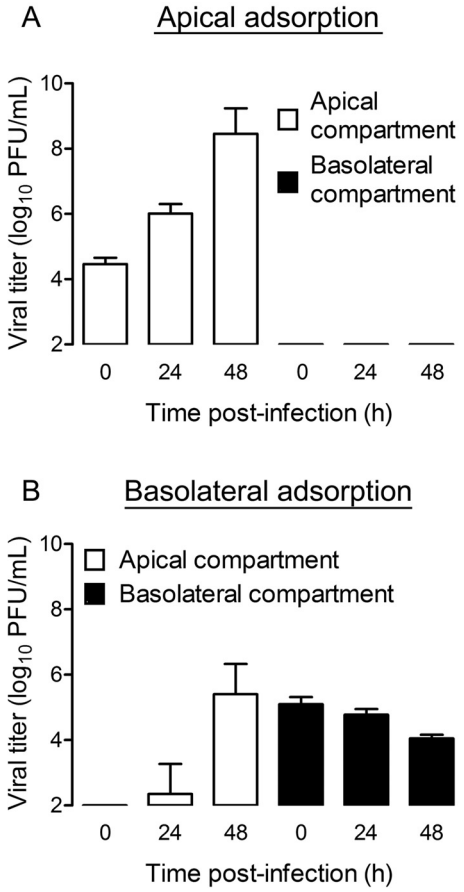

FIG 4 Reovirus release from polarized HBMECs occurs from the apical surface. Polarized HBMECs were adsorbed either apically (A) or basolaterally (B) with reovirus T3SA+ at an MOI of 10 PFU per cell. Cells were washed, fresh medium was added to the apical and basolateral compartments, and cells were incubated for the times shown. Viral titers in the medium from the apical (white bars) and basolateral (black bars) compartments were determined by plaque assay. A representative experiment of three performed, with each experiment conducted in duplicate, is shown. Error bars indicate the range of data for the duplicates.

apical adsorption, the viral titer in the apical compartment increased more than 30-fold at 24 h and more than 3,000-fold at 48 h (Fig. 4A). Interestingly, no virus was detected in the basolateral compartment at any time point tested (Fig. 4A). After basolateral adsorption, virus was detected in the basolateral compartment at all of the intervals tested (Fig. 4B). However, titers did not increase over time, suggesting that infectious virus in this compartment is most likely residual virus from the inoculum. The viral titer within the apical compartment was detected at 24 h postinfection and increased approximately 100,000-fold by 48 h postinfection (Fig. 4B). Therefore, regardless of the route of adsorption, reovirus egress from polarized endothelial cells occurs from the apical surface.

Reovirus infection does not alter endothelial cell TJ integrity. To determine whether reovirus infection alters the integrity of TJs in the polarized monolayer, we quantified the transendothelial electrical resistance (TEER) at both early and late times postadsorption. After adsorption with a multiplicity of infection (MOI) of 1,000 PFU per cell, no significant alteration in TEER was ob-

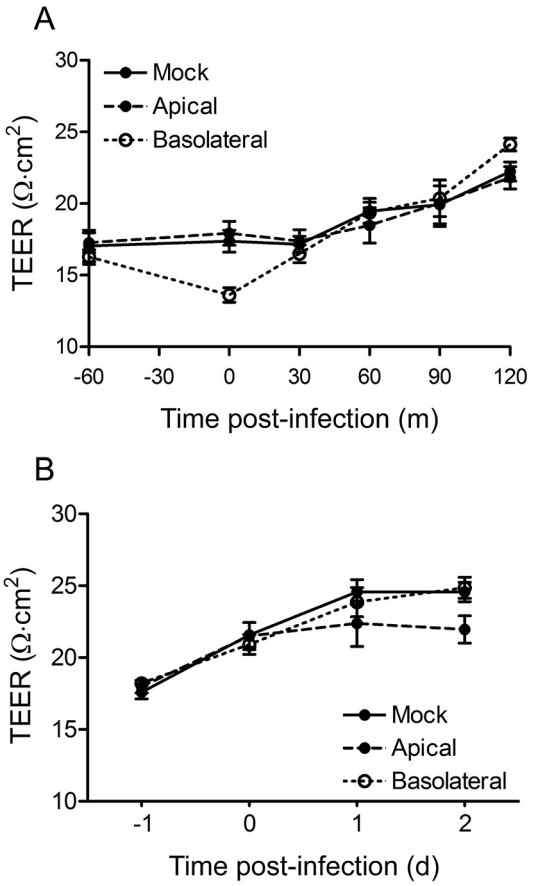

FIG 5 Reovirus infection of polarized HBMECs does not disrupt TJs. Polarized HBMECs were mock infected (closed circle, solid line) or adsorbed either apically (closed circle, dashed line) or basolaterally (open circle, dotted line) with reovirus T3SA+ at an MOI of 1,000 PFU per cell (A) or 10 PFU per cell (B). Cells were washed, fresh medium was added to the apical and basolateral compartments, and TEER was determined at the times shown. A representative experiment of two (A) or three (B) performed, with each experiment conducted in duplicate, is shown. Error bars indicate the range of data for the duplicates. TEER from the various samples was compared by one-way ANOVA. Student's *t* test was used to evaluate differences between mock-infected and apically infected (A) or mock-infected and basolaterally infected (B) samples. No differences were statistically significant.

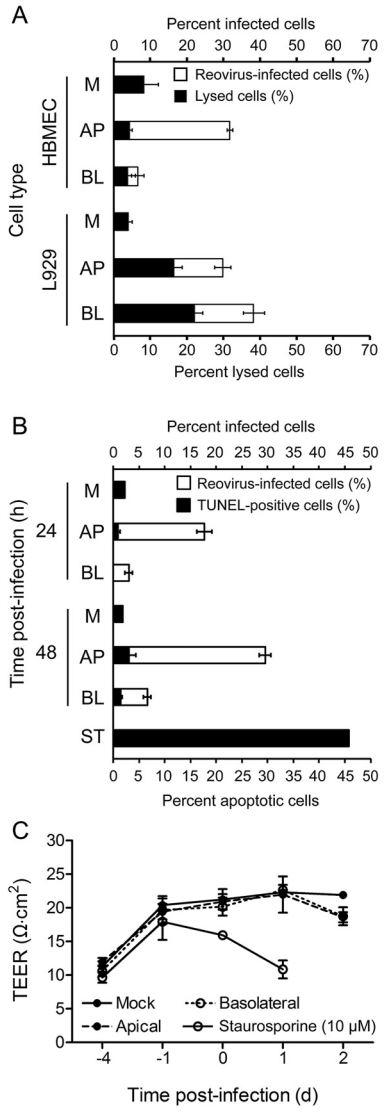

FIG 6 Reovirus infection of polarized HBMECs is noncytolytic. (A) Polarized HBMECs or confluent L929 cells cultured on Transwell inserts were mock infected (M) or adsorbed either apically (AP) or basolaterally (BL) with reovirus T3SA+ at an MOI of 10 PFU per cell. Cells were washed, fresh medium was added to the apical and basolateral compartments, and cells were incubated at 37°C for 20 to 24 h. Cells were harvested and incubated with trypan blue or permeabilized and stained for reovirus antigen with Alexa Fluor-conjugated, reovirus-specific antiserum. The percentage of infected cells (white bars) and the percentage of lysed cells (black bars) are shown in a stacked-column graph. A representative experiment of two performed, with each experiment conducted in duplicate, is shown. Error bars indicate the range of data for the duplicates. (B, C) Polarized HBMECs were mock infected (M) or adsorbed either apically (AP) or basolaterally (BL) with reovirus T3SA+ at an MOI of 100 PFU per cell. Cells were incubated at 37°C and harvested at 24 or 48 h postinfection. As a control for apoptosis, staurosporine (ST, 10 μM) was added to the medium in the apical and basolateral compartments of uninfected cells, which were incubated for 18 h. (B) Cells were stained for reovirus antigen with Alexa Fluor-conjugated, reovirus-specific antiserum and for apoptosis by the TUNEL technique. The percentage of infected cells (white bars) and the percentage of TUNEL-positive cells (black bars) within the population of infected cells are shown in a stacked-column graph. A representative experiment of three performed, with each experiment conducted in duplicate, is shown. Error bars indicate the range of data for the duplicates. (C) TEER was recorded for each sample at the time of cell harvest. A representative experiment of three performed, with each experiment conducted in duplicate, is shown. Error bars indicate the range of data for the duplicates.

served in the 2-h postinfection interval (Fig. 5A). Similarly, after adsorption with an MOI of 10 PFU per cell, no significant alteration in TEER was observed at 1 or 2 days postinfection (Fig. 5B). We conclude from these data that reovirus does not alter the function of endothelial TJs during infection.

Reovirus egress from polarized HBMECs occurs noncytolytically. To determine whether reovirus egress from infected polarized HMBECs is associated with cell lysis, we assessed cell viability with trypan blue. Polarized HBMECs or confluent L929 cells cultured on Transwell inserts were adsorbed apically or basolaterally at an MOI of 10 PFU per cell, and cell viability was quantified at 24 h postinfection. Levels of HBMEC lysis were lower than the background levels of lysis in mock-treated HBMECs after either apical or basolateral virus adsorption (Fig. 6A). In contrast, more than half of the population of infected L929 cells was lysed at 24 h postinfection. These data suggest that reovirus infection of polarized HBMECs does not compromise cell viability.

Reovirus is capable of inducing apoptosis in many types of cultured cells (25–28) and in the CNS of infected mice (1–3, 29). Although polarized HBMECs remain intact after reovirus infection, we wondered whether reovirus egress from polarized HBMEC monolayers might occur via apoptosis. To test this hypothesis, we adsorbed polarized HBMECs apically or basolaterally at an MOI of 100 PFU per cell and quantified levels of apoptosis at 24 and 48 h postinfection by using terminal deoxynucleotidyltransferase-mediated dUTP-biotin nick end labeling (TUNEL) staining. At 24 h postinfection, 17.7% of the cells were infected after apical adsorption but apoptosis was detectable in only 0.9% of those cells (Fig. 6B). At 24 h after basolateral adsorption, 3.0% of the cells were infected but apoptosis was not detected in those cells (Fig. 6B). At 48 h after apical adsorption, 29.5% of the cells were infected with reovirus, with only 3.0% showing evidence of apoptosis (Fig. 6B). After basolateral adsorption, 6.6% of the cells were infected with reovirus, yet only 1.4% of those cells were apoptotic (Fig. 6B). As a positive control, treatment of polarized HBMECs with staurosporine resulted in ~50% of the cells displaying evidence of apoptosis with a concomitant decrease in TEER (Fig. 6B and C), suggesting that the low levels of apoptosis in reovirus-infected cells are not attributable to an inherent block to apoptosis in HBMECs. These data suggest that reovirus egress from polarized HBMECs occurs without inducing apoptosis.

DISCUSSION

Many viruses cause disease in infected hosts after bloodstream spread from an initial site of infection to a distant target site. Reoviruses are neurotropic viruses that first replicate within the small intestine and disseminate systemically via the blood, nerves, and lymphatics. Reovirus penetration of the endothelium to invade the bloodstream may occur within the intestine or lymph nodes to allow the establishment of primary viremia. To investigate reovirus infection of the endothelium, we cultured HBMECs on Transwell membranes until polarization was achieved (see Fig. S1 in the supplemental material). Although reoviruses use TJ protein JAM-A as a receptor, TEER was not altered immediately following reovirus adsorption (Fig. 5), suggesting that TJ integrity remains intact after infection. Adsorption of polarized endothelial cells either apically or basolaterally with reovirus resulted in productive infection (Fig. 1; see Fig. S2 in the supplemental material). Interestingly, reovirus strain T3D replicated more efficiently than strain type 1 Lang (T1L) in polarized endothelial cells (compare Fig. 1; see Fig. S2). This discrepancy might be due to differences in the cell surface expression of the sialylated glycans used by the different reovirus serotypes or cell-intrinsic properties of endothelial cells that confer serotype-dependent differences in reovirus susceptibility. Regardless of the serotype, replication was more efficient when reovirus was adsorbed to the endothelial cell apical surface (Fig. 1; see Fig. S2), and significantly more reovirus antigen-positive cells were detected following adsorption by this route (Fig. 1B; see Fig. S2). The observed increase in infectivity and replication after apical adsorption was most likely due to increased virus binding to the apical surface (Fig. 1C). The number of cells bound by virus was actually higher than the number of cells productively infected. This finding suggests that not all viral particles bound to the cell surface complete an infectious cycle, a phenomenon observed in other cell lines (30–32). Reovirus infection of polarized endothelial cells by either the apical or the basolateral route requires the engagement of sialylated glycans and JAM-A (Fig. 2). Consistent with these findings, substantially more JAM-A is distributed to the apical than to the basolateral surface of polarized HBMECs (Fig. 3). Subconfluent, nonpolarized HBMECs are substantially more susceptible to reovirus infection than are polarized HBMECs (data not shown), presumably because of higher levels of JAM-A on the cell surface and the absence of a restriction of JAM-A expression to TJs.

Regardless of the route of adsorption, reovirus egress from infected polarized HBMECs occurs solely from the apical surface (Fig. 4; see Fig. S2 in the supplemental material). Similarly, reovirus infection of polarized human airway epithelial cells results in apical release of progeny virions (33). Although TEER did not change appreciably over a time course of reovirus infection of HBMECs (Fig. 5), we questioned whether infected cells are extruded from the monolayer in a manner analogous to epithelial cell turnover (34). If they are, we would expect TEER to be maintained despite the detection of an increased number of nonviable cells over time. To test this hypothesis, we used trypan blue staining to determine whether polarized HBMECs infected with reovirus are lysed. Compared with infected L929 cells, which display substantial cytopathic effect after reovirus infection (28) (Fig. 6A), polarized HBMECs infected with reovirus apically or basolaterally do not undergo cell lysis (Fig. 6A), despite the presence of high viral titers in cells and supernatants (Fig. 1 and 4). Sonication of supernatants harvested from the apical surface of polarized HBMECs did not lead to an increased viral titer, suggesting that released virus was not trapped within extruded cells or membrane-bound vesicles (data not shown). Apical or basolateral adsorption of polarized HBMECs with reovirus led to an increase in reovirus antigen-positive cells, but the number of apoptotic cells did not increase above that in mock-treated samples (Fig. 6B). Additionally, levels of apoptosis in reovirus-infected HBMECs were lower than in mock-infected cells by the complementary acridine orange and annexin V staining assays (see Fig. S3 in the supplemental material). We conclude from these data that regardless of the route of entry, reovirus release occurs from the apical surface in a manner that maintains cell viability. Because infection of polarized endothelial cells is noncytolytic, clearance of reovirus from an infected host may require cytotoxic T lymphocyte-mediated immunity in addition to neutralizing antibodies (35–39).

Virus infection of endothelial cells may serve as an additional mechanism to produce and maintain high levels of viremia. For example, dengue virus infection of endothelial cells leads to high-titer viremia by inducing endothelial cell apoptosis, resulting in endothelial barrier dysfunction and vascular leakage (40). Murine cytomegalovirus primarily infects hepatocytes, but virus produced from infected hepatic endothelial cells is responsible for dissemination to other organs (41, 42). Similarly, reovirus may use the endothelium as a means to amplify to high titers in the bloodstream (Fig. 7). Reovirus infection from the basolateral route is not efficient, but progeny viral particles are efficiently transported to and released from the apical surface of polarized endothelial cells. Once released, progeny virions have access to the apical surface of adjacent endothelial cells and can enter those cells efficiently. This cycle may serve as a mechanism to generate high titers of virus in the bloodstream, which are observed during reovirus infection (4, 10, 21). Sialylated glycans and JAM-A are required for the infection of endothelial cells by both the apical and

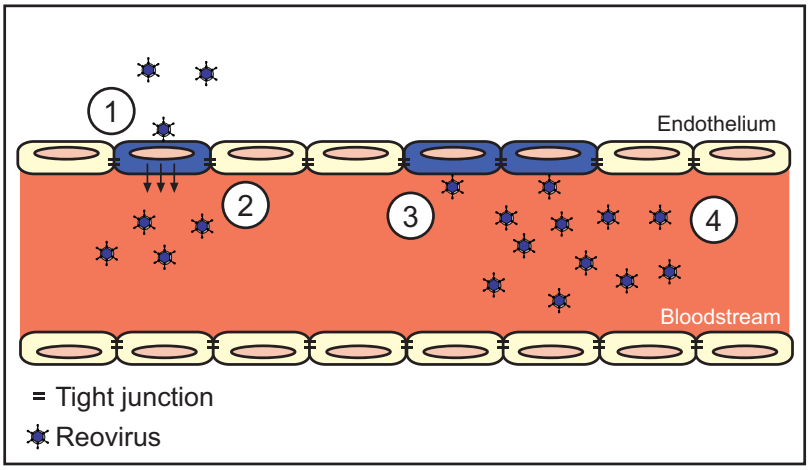

FIG 7 Model of reovirus infection of the endothelium. A cross-sectional schematic of a blood vessel is shown. The blood vessel is lined with endothelial cells that are linked via TJs (black bars). Following reovirus infection of endothelial cells from the basolateral surface (step 1), virus is routed apically (or luminally) into the bloodstream (step 2). Once within the bloodstream, virus is capable of infecting endothelial cells from the apical surface (step 3). Reovirus binding to JAM-A, found mostly within TJs, and sialic acid at the apical surface may account for the increased efficiency of infection. After reovirus infects cells from the apical surface, progeny virions are routed apically into the bloodstream. The efficiency of apical infection may allow for endothelial amplification of reovirus (step 4), resulting in higher levels of viremia within an infected host.

basolateral routes, which may account for the markedly diminished viremia in reovirus-infected JAM-A-deficient mice (4).

How reovirus exits the bloodstream is not clear from our study. Because JAM-A is present on the surface of hematopoietic cells, it is possible that reovirus-infected hematopoietic cells transport the virus from the bloodstream to sites of secondary replication, including the CNS. It also is possible that cells adjacent to blood vessels become infected as a consequence of infection of the endothelium. Epstein-Barr virus (EBV) binding to B cells leads to conjugate formation between B cells and epithelial cells, resulting in EBV entry into epithelial cells (43, 44). Blood vessels in the brain closely appose pericytes and astrocytes, and reovirus infection of endothelial cells may induce modifications of these cells, resulting in invasion of the CNS.

Bloodstream spread is an important step in the pathogenesis of many viral diseases, but the mechanisms used by viruses to gain entry into the bloodstream are not well understood. Our work describes how viral infection of endothelial cells may allow access to and amplification within the circulation. We show that reovirus productively infects polarized endothelial cells by both the apical and basolateral routes. Infection after apical adsorption is more efficient than basolateral adsorption because of increased utilization of sialic acid and JAM-A at the apical surface. Reovirus release from polarized endothelial cells occurs exclusively from the apical surface in a manner that maintains TJ integrity and cell viability. Since TJ proteins are used as receptors by a diverse array of viruses, including adenovirus (45), feline calicivirus (46), hepatitis C virus (47, 48), and several picornaviruses (45, 49), our findings may provide a more general understanding of how viruses establish viremia for bloodstream spread. Moreover, the apical release mechanism employed by reovirus may be similarly generalizable, providing a potential new target for a host-specific, broad-spectrum antiviral therapeutic.

MATERIALS AND METHODS

Cells, viruses, enzymes, and antibodies. Spinner-adapted murine L929 fibroblast cells were grown in either suspension or monolayer cultures as previously described (10, 50). HBMECs (51, 52) were grown in RPMI 1640 medium (Mediatech) supplemented to contain 10% fetal bovine serum, 10% NuSerum (BD Biosciences), nonessential amino acids (Sigma), 1 mM sodium pyruvate, MEM Vitamins (Mediatech), 2 mM L-glutamine, 100 U/ml penicillin, 100 μg/ml streptomycin, and 25 ng/ml amphotericin B. HBMECs and L929 cells were cultured on collagen-coated Transwell inserts (6.5-mm diameter, 0.4-μm pores; Costar) for 7 days prior to infection or imaging experiments.

Reovirus strain T1L is a laboratory stock. Strain T3SA+ was generated as previously described (15). Recombinant viruses rsT3D, rsT3D-σ1R202W, and rsT3D-σ1G381A were generated by plasmid-based reverse genetics (21, 24). Virus was purified as previously described (53). Viral titers were determined by plaque assay with L929 cells (37).

The immunoglobulin G (IgG) fraction of a rabbit antiserum raised against strains T1L and T3D (31) was purified by protein A-Sepharose as previously described (9, 15). Reovirus-specific IgG was conjugated to Alexa Fluor 647 with an APEX antibody labeling kit (Invitrogen). JAM-A-specific monoclonal antibody J10.4 (provided by Charles Parkos, Emory University) and claudin-1-specific antibody ab15098 (Abcam) were used in confocal microscopy imaging experiments. Alexa Fluor-conjugated antibodies (Invitrogen) were used as secondary antibodies.

TEER measurements. TEER across polarized HBMEC monolayers was quantified at 3 and 6 days postseeding, on the day of infection, and at various intervals postinfection with an EVOM voltohmmeter and an EndOhm-6 cup electrode (World Precision Instruments). TEER readings for test samples were normalized by subtracting the TEER of blank collagen-coated Transwell inserts. The data are presented as unit area resistance ($\Omega \cdot cm^2$) (54).

Virus assays. Polarized HBMECs cultivated on Transwell inserts were adsorbed with virus apically or basolaterally at an MOI of 10 PFU per cell. For apical adsorption, 30 μl of virus inoculum was added to the apical compartment. For basolateral adsorption, the Transwell insert was inverted in a sterile dish and 30 μl of virus inoculum was added to the basolateral surface. In some experiments, cells were treated with medium, anti-JAM-A antibody (20 μg/ml), or *Arthrobacter ureafaciens* neuraminidase (80 mU/ml; MP Biomedicals) prior to virus adsorption. After adsorption of virus at room temperature for 1 h, cells were washed twice with phosphate-buffered saline (PBS) and 200 μl of medium was added to the apical compartment and 1 ml of medium was added to the basolateral compartment. For viral release assays, medium from the apical or baso-

lateral compartment was collected at various intervals and viral titers in medium from each compartment were determined by plaque assay with L929 cells (37). For viral replication assays, Transwell membrane inserts were removed from Transwell inserts with a scalpel, submerged in 500 μl of medium, and subjected to two cycles of freezing and thawing. Viral titers in cell lysates were determined by plaque assay with L929 cells (37).

For infectivity studies, cells were incubated at 37°C for 20 to 24 h, harvested with 0.05% trypsin-EDTA (Invitrogen) at room temperature, and quenched with medium collected from the apical compartment of the respective sample. Cells were stained with Alexa Fluor-conjugated, reovirus-specific antiserum as previously described (50). The percentage of reovirus antigen-positive cells was determined by flow cytometry. For binding studies, cells were detached from the Transwell insert immediately after adsorption with Cellstripper (Mediatech) at 37°C for 5 min and stained with Alexa Fluor-conjugated, reovirus-specific antiserum as previously described (50). The mean fluorescence intensity (MFI) of each sample was determined by flow cytometry. All cell staining was quantified with FlowJo software (Tree Star).

Cell imaging. Polarized HBMECs were fixed in 100% methanol at −20°C for 5 min. Cells were blocked in PBS containing 5% bovine serum albumin at room temperature for 30 min. Cells were stained with antibodies specific for JAM-A (1:1,000) and claudin-1 (1:100) as previously described (50, 55). After staining, Transwell membranes containing cells were excised with a scalpel. Membranes were placed onto glass slides, and glass coverslips (#1.5; Thermo Scientific) were mounted with Aqua-Poly/Mount mounting medium (Polysciences, Inc.). Cell images were captured with a Zeiss LSM 510 Meta laser-scanning confocal microscope with a 63×/1.40 Plan-Apochromat objective lens. A standard threshold pixel intensity was used for all images, and the pinhole size used was the same for all fluorophores. Images represent a single section or a series of sections from within a *z* stack and were adjusted for brightness and contrast to the same extent. The MFI of pixels from apical and basolateral sections of cells ($n = 5$) was quantified with ImageJ software (NIH).

Trypan blue exclusion assay. HBMECs and L929 cells were cultured on Transwell inserts until polarized and confluent, respectively. Virus was adsorbed apically or basolaterally at an MOI of 10 PFU per cell, and cells were incubated at 37°C for 20 to 24 h. After incubation, cells were harvested with trypsin-EDTA, quenched with medium collected from the apical compartment, and washed once with PBS. A small aliquot (20 μl) of cells was removed for analysis of cell lysis. An equal volume of trypan blue (0.4% [wt/vol] in PBS; Mediatech) was added to cells, which were then incubated at room temperature for 3 min. Lysed and intact cells were enumerated using a hemocytometer with bright-field microscopy. The percentage of reovirus-infected cells in the remainder of each sample was quantified by flow cytometry.

TUNEL assay. Polarized HBMECs were adsorbed with virus at an MOI of 100 PFU per cell, washed twice with PBS, and incubated at 37°C for 24 or 48 h. Cells were removed from the Transwell insert with trypsin-EDTA, quenched with medium collected from the apical compartment, washed once with PBS, and assayed for the percentage of apoptotic cells by the TUNEL technique (APO-BrdU TUNEL assay kit; Invitrogen) according to the manufacturer's instructions. After TUNEL staining, cells were stained with Alexa Fluor-conjugated, reovirus-specific antiserum (1:1,000) at 4°C for 30 min, washed, and pelleted. The samples were resuspended in 0.5 ml propidium iodide-containing buffer. Stained cells were analyzed for apoptosis and the presence of reovirus antigen by flow cytometry. See Text S1 in the supplemental material for the additional methods used.

Statistical analysis. Experiments were performed in duplicate and repeated at least twice. Representative results of single experiments are shown. Mean values were compared with an unpaired Student's *t* test or one-way analysis of variance (ANOVA) (GraphPad Prism). Error bars denote the range of data or standard deviation. *P* values of <0.05 were considered statistically significant.

SUPPLEMENTAL MATERIAL

Supplemental material for this article may be found at http://mbio.asm.org/lookup/suppl/doi:10.1128/mBio.00049-13/-/DCSupplemental.

Text S1, DOCX file, 0 MB.
Figure S1, EPS file, 3.5 MB.
Figure S2, EPS file, 3.8 MB.
Figure S3, EPS file, 3.9 MB.

ACKNOWLEDGMENTS

We thank members of the Dermody laboratory for many useful discussions and Alison Ashbrook, Jennifer Konopka, and Jennifer Stencel for critical review of the manuscript.

This research was supported by Public Health Service awards T32 GM007347 (C.M.L.), F31 NS074596 (C.M.L.), T32 HL07751 (B.A.M.), F32 A1801082 (B.A.M.), and R37 AI38296 (T.S.D.) and the Elizabeth B. Lamb Center for Pediatric Research. Additional support was provided by the Vanderbilt Institute for Clinical and Translational Research (UL1 RR024975), the Vanderbilt-Ingram Cancer Center (CA68485), the Vanderbilt Flow Cytometry Shared Resource (DK058404), and the Vanderbilt Cell Imaging Shared Resource (DK20593).

REFERENCES

1. **Tyler KL, McPhee DA, Fields BN.** 1986. Distinct pathways of viral spread in the host determined by reovirus S1 gene segment. Science **233**:770–774.
2. **Weiner HL, Drayna D, Averill DR, Jr, Fields BN.** 1977. Molecular basis of reovirus virulence: role of the S1 gene. Proc. Natl. Acad. Sci. U. S. A. **74**:5744–5748.
3. **Weiner HL, Powers ML, Fields BN.** 1980. Absolute linkage of virulence and central nervous system cell tropism of reoviruses to viral hemagglutinin. J. Infect. Dis. **141**:609–616.
4. **Antar AR, Konopka JL, Campbell JA, Henry RA, Perdigoto AL, Carter BD, Pozzi A, Abel TW, Dermody TS.** 2009. Junctional adhesion molecule-A is required for hematogenous dissemination of reovirus. Cell Host Microbe **5**:59–71.
5. **Boehme KW, Frierson JM, Konopka JL, Kobayashi T, Dermody TS.** 2011. The reovirus sigma1s protein is a determinant of hematogenous but not neural virus dissemination in mice. J. Virol. **85**:11781–11790.
6. **Jacobs BL, Atwater JA, Munemitsu SM, Samuel CE.** 1985. Biosynthesis of reovirus-specified polypeptides: the s1 mRNA synthesized *in vivo* is structurally and functionally indistinguishable from *in vitro*-synthesized s1 mRNA and encodes two polypeptides, sigma 1a and sigma 1bNS. Virology **147**:9–18.
7. **Jacobs BL, Samuel CE.** 1985. Biosynthesis of reovirus-specified polypeptides: the reovirus S1 mRNA encodes two primary translation products. Virology **143**:63–74.
8. **Sarkar G, Pelletier J, Bassel-Duby R, Jayasuriya A, Fields BN, Sonenberg N.** 1985. Identification of a new polypeptide coded by reovirus gene S1. J. Virol. **54**:720–725.
9. **Barton ES, Youree BE, Ebert DH, Forrest JC, Connolly JL, Valyi-Nagy T, Washington K, Wetzel JD, Dermody TS.** 2003. Utilization of sialic acid as a coreceptor is required for reovirus-induced biliary disease. J. Clin. Invest. **111**:1823–1833.
10. **Boehme KW, Guglielmi KM, Dermody TS.** 2009. Reovirus nonstructural protein sigma1s is required for establishment of viremia and systemic dissemination. Proc. Natl. Acad. Sci. U. S. A. **106**:19986–19991.
11. **Kaye KM, Spriggs DR, Bassel-Duby R, Fields BN, Tyler KL.** 1986. Genetic basis for altered pathogenesis of an immune-selected antigenic variant of reovirus type 3 (Dearing). J. Virol. **59**:90–97.
12. **Tardieu M, Weiner HL.** 1982. Viral receptors on isolated murine and human ependymal cells. Science **215**:419–421.
13. **Dichter MA, Weiner HL.** 1984. Infection of neuronal cell cultures with reovirus mimics *in vitro* patterns of neurotropism. Ann. Neurol. **16**:603–610.
14. **Tardieu M, Powers ML, Hafler DA, Hauser SL, Weiner HL.** 1984. Autoimmunity following viral infection: demonstration of monoclonal antibodies against normal tissue following infection of mice with reovirus and demonstration of shared antigenicity between virus and lymphocytes. Eur. J. Immunol. **14**:561–565.
15. **Barton ES, Connolly JL, Forrest JC, Chappell JD, Dermody TS.** 2001. Utilization of sialic acid as a coreceptor enhances reovirus attachment by multistep adhesion strengthening. J. Biol. Chem. **276**:2200–2211.

16. **Bazzoni G.** 2003. The JAM family of junctional adhesion molecules. Curr. Opin. Cell Biol. **15**:525–530.
17. **Martìn-Padura I, Lostaglio S, Schneemann M, Williams L, Romano M, Fruscella P, Panzeri C, Stoppacciaro A, Ruco L, Villa A, Simmons D, Dejana E.** 1998. Junctional adhesion molecule, a novel member of the immunoglobulin superfamily that distributes at intercellular junctions and modulates monocyte transmigration. J. Cell Biol. **142**:117–127.
18. **Woodfin A, Reichel CA, Khandoga A, Corada M, Voisin MB, Scheiermann C, Haskard DO, Dejana E, Krombach F, Nourshargh S.** 2007. JAM-A mediates neutrophil transmigration in a stimulus-specific manner *in vivo*: evidence for sequential roles for JAM-A and PECAM-1 in neutrophil transmigration. Blood **110**:1848–1856.
19. **Sobocka MB, Sobocki T, Banerjee P, Weiss C, Rushbrook JI, Norin AJ, Hartwig J, Salifu MO, Markell MS, Babinska A, Ehrlich YH, Kornecki E.** 2000. Cloning of the human platelet F11 receptor: a cell adhesion molecule member of the immunoglobulin superfamily involved in platelet aggregation. Blood **95**:2600–2609.
20. **Ostermann G, Weber KS, Zernecke A, Schröder A, Weber C.** 2002. Jam-1 is a ligand of the beta(2) integrin LFA-1 involved in transendothelial migration of leukocytes. Nat. Immunol. **3**:151–158.
21. **Frierson JM, Pruijssers AJ, Konopka JL, Reiter DM, Abel TW, Stehle T, Dermody TS.** 2012. Utilization of sialylated glycans as coreceptors enhances the neurovirulence of serotype 3 reovirus. J. Virol. **86**: 13164–13173.
22. **Barton ES, Forrest JC, Connolly JL, Chappell JD, Liu Y, Schnell FJ, Nusrat A, Parkos CA, Dermody TS.** 2001. Junction adhesion molecule is a receptor for reovirus. Cell **104**:441–451.
23. **Reiter DM, Frierson JM, Halvorson EE, Kobayashi T, Dermody TS, Stehle T.** 2011. Crystal structure of reovirus attachment protein σ1 in complex with sialylated oligosaccharides. PLoS Pathog. **7**:e1002166. http://doi.10.1371/journal.ppat.1002166.
24. **Kirchner E, Guglielmi KM, Strauss HM, Dermody TS, Stehle T.** 2008. Structure of reovirus sigma1 in complex with its receptor junctional adhesion molecule-A. PLoS Pathog. **4**:e1000235. http://doi.10.1371/journal.ppat.1000235.
25. **Connolly JL, Rodgers SE, Clarke P, Ballard DW, Kerr LD, Tyler KL, Dermody TS.** 2000. Reovirus-induced apoptosis requires activation of transcription factor NF-kappaB. J. Virol. **74**:2981–2989.
26. **Connolly JL, Barton ES, Dermody TS.** 2001. Reovirus binding to cell surface sialic acid potentiates virus-induced apoptosis. J. Virol. **75**: 4029–4039.
27. **Rodgers SE, Barton ES, Oberhaus SM, Pike B, Gibson CA, Tyler KL, Dermody TS.** 1997. Reovirus-induced apoptosis of MDCK cells is not linked to viral yield and is blocked by Bcl-2. J. Virol. **71**:2540–2546.
28. **Tyler KL, Squier MK, Rodgers SE, Schneider BE, Oberhaus SM, Grdina TA, Cohen JJ, Dermody TS.** 1995. Differences in the capacity of reovirus strains to induce apoptosis are determined by the viral attachment protein sigma 1. J. Virol. **69**:6972–6979.
29. **Morrison LA, Sidman RL, Fields BN.** 1991. Direct spread of reovirus from the intestinal lumen to the central nervous system through vagal autonomic nerve fibers. Proc. Natl. Acad. Sci. U. S. A. **88**:3852–3856.
30. **Dermody TS, Nibert ML, Wetzel JD, Tong X, Fields BN.** 1993. Cells and viruses with mutations affecting viral entry are selected during persistent infections of L cells with mammalian reoviruses. J. Virol. **67**:2055–2063.
31. **Wetzel JD, Chappell JD, Fogo AB, Dermody TS.** 1997. Efficiency of viral entry determines the capacity of murine erythroleukemia cells to support persistent infections by mammalian reoviruses. J. Virol. **71**:299–306.
32. **Rubin DH, Wetzel JD, Williams WV, Cohen JA, Dworkin C, Dermody TS.** 1992. Binding of type 3 reovirus by a domain of the sigma 1 protein important for hemagglutination leads to infection of murine erythroleukemia cells. J. Clin. Invest. **90**:2536–2542.
33. **Excoffon KJ, Guglielmi KM, Wetzel JD, Gansemer ND, Campbell JA, Dermody TS, Zabner J.** 2008. Reovirus preferentially infects the basolateral surface and is released from the apical surface of polarized human respiratory epithelial cells. J. Infect. Dis. **197**:1189–1197.
34. **Gu Y, Rosenblatt J.** 2012. New emerging roles for epithelial cell extrusion. Curr. Opin. Cell Biol. **24**:865–870.
35. **Barkon ML, Haller BL, Virgin HW.** 1996. Circulating immunoglobulin G can play a critical role in clearance of intestinal reovirus infection. J. Virol. **70**:1109–1116.
36. **George A, Kost SI, Witzleben CL, Cebra JJ, Rubin DH.** 1990. Reovirus-induced liver disease in severe combined immunodeficient (SCID) mice. A model for the study of viral infection, pathogenesis, and clearance. J. Exp. Med. **171**:929–934.
37. **Virgin HW IV, Bassel-Duby R, Fields BN, Tyler KL.** 1988. Antibody protects against lethal infection with the neurally spreading reovirus type 3 (Dearing). J. Virol. **62**:4594–4604.
38. **Virgin HW, Tyler KL.** 1991. Role of immune cells in protection against and control of reovirus infection in neonatal mice. J. Virol. **65**:5157–5164.
39. **Tyler KL, Mann MA, Fields BN, Virgin HW IV.** 1993. Protective anti-reovirus monoclonal antibodies and their effects on viral pathogenesis. J. Virol. **67**:3446–3453.
40. **Dalrymple NA, Mackow ER.** 2012. Roles for endothelial cells in dengue virus infection. Adv. Virol. 2012:840654. PubMed.
41. **Sacher T, Podlech J, Mohr CA, Jordan S, Ruzsics Z, Reddehase MJ, Koszinowski UH.** 2008. The major virus-producing cell type during murine cytomegalovirus infection, the hepatocyte, is not the source of virus dissemination in the host. Cell Host Microbe **3**:263–272.
42. **Sacher T, Andrassy J, Kalnins A, Dölken L, Jordan S, Podlech J, Ruzsics Z, Jauch KW, Reddehase MJ, Koszinowski UH.** 2011. Shedding light on the elusive role of endothelial cells in cytomegalovirus dissemination. PLoS Pathog. **7**:e1002366. http://doi.10.1371/journal.ppat.1002366.
43. **Shannon-Lowe CD, Neuhierl B, Baldwin G, Rickinson AB, Delecluse HJ.** 2006. Resting B cells as a transfer vehicle for Epstein-Barr virus infection of epithelial cells. Proc. Natl. Acad. Sci. U. S. A. **103**:7065–7070.
44. **Shannon-Lowe C, Rowe M.** 2011. Epstein-Barr virus infection of polarized epithelial cells via the basolateral surface by memory B cell-mediated transfer infection. PLoS Pathog. **7**:e1001338. http://doi.10.1371/journal.ppat.1001338.
45. **Bergelson JM, Cunningham JA, Droguett G, Kurt-Jones EA, Krithivas A, Hong JS, Horwitz MS, Crowell RL, Finberg RW.** 1997. Isolation of a common receptor for coxsackie B viruses and adenoviruses 2 and 5. Science **275**:1320–1323.
46. **Makino A, Shimojima M, Miyazawa T, Kato K, Tohya Y, Akashi H.** 2006. Junctional adhesion molecule 1 is a functional receptor for feline calicivirus. J. Virol. **80**:4482–4490.
47. **Evans MJ, von Hahn T, Tscherne DM, Syder AJ, Panis M, Wölk B, Hatziioannou T, McKeating JA, Bieniasz PD, Rice CM.** 2007. Claudin-1 is a hepatitis C virus co-receptor required for a late step in entry. Nature **446**:801–805.
48. **Ploss A, Evans MJ, Gaysinskaya VA, Panis M, You H, de Jong YP, Rice CM.** 2009. Human occludin is a hepatitis C virus entry factor required for infection of mouse cells. Nature **457**:882–886.
49. **Bewley MC, Springer K, Zhang YB, Freimuth P, Flanagan JM.** 1999. Structural analysis of the mechanism of adenovirus binding to its human cellular receptor, CAR. Science **286**:1579–1583.
50. **Mainou BA, Dermody TS.** 2012. Transport to late endosomes is required for efficient reovirus infection. J. Virol. **86**:8346–8358.
51. **Stins MF, Badger J, Sik Kim K.** 2001. Bacterial invasion and transcytosis in transfected human brain microvascular endothelial cells. Microb. Pathog. **30**:19–28.
52. **Stins MF, Gilles F, Kim KS.** 1997. Selective expression of adhesion molecules on human brain microvascular endothelial cells. J. Neuroimmunol. **76**:81–90.
53. **Furlong DB, Nibert ML, Fields BN.** 1988. Sigma 1 protein of mammalian reoviruses extends from the surfaces of viral particles. J. Virol. **62**: 246–256.
54. **Grab DJ, Perides G, Dumler JS, Kim KJ, Park J, Kim YV, Nikolskaia O, Choi KS, Stins MF, Kim KS.** 2005. Borrelia burgdorferi, host-derived proteases, and the blood-brain barrier. Infect. Immun. **73**:1014–1022.
55. **Mainou BA, Dermody TS.** 2011. Src kinase mediates productive endocytic sorting of reovirus during cell entry. J. Virol. **85**:3203–3213.

APPENDIX B

MECHANISMS OF REOVIRUS BLOODSTREAM SPREAD

Karl W. Boehme, Caroline M. Lai, Terence S. Dermody

Advances in Virus Research 87:1-35; 2013

CHAPTER ONE

Mechanisms of Reovirus Bloodstream Dissemination

Karl W. Boehme[*,†,1], **Caroline M. Lai**[†,‡], **Terence S. Dermody**[*,†,‡,2]
[*]Department of Pediatrics, Vanderbilt University School of Medicine, Nashville, Tennessee, USA
[†]Elizabeth B. Lamb Center for Pediatric Research, Vanderbilt University School of Medicine, Nashville, Tennessee, USA
[‡]Department of Pathology, Microbiology, and Immunology, Vanderbilt University School of Medicine, Nashville, Tennessee, USA
[1]Current address: Department of Microbiology and Immunology, University of Arkansas for Medical Sciences, Little Rock, Arkansas, USA.
[2]Corresponding author: e-mail address: terry.dermody@vanderbilt.edu

Contents

Abstract

Many viruses cause disease within an infected host after spread from an initial portal of entry to sites of secondary replication. Viruses can disseminate via the bloodstream or through nerves. Mammalian orthoreoviruses (reoviruses) are neurotropic viruses that use both bloodborne and neural pathways to spread systemically within their hosts

Advances in Virus Research, Volume 87
ISSN 0065-3527
http://dx.doi.org/10.1016/B978-0-12-407698-3.00001-6

to cause disease. Using a robust mouse model and a dynamic reverse genetics system, we have identified a viral receptor and a viral nonstructural protein that are essential for hematogenous reovirus dissemination. Junctional adhesion molecule-A (JAM-A) is a member of the immunoglobulin superfamily expressed in tight junctions and on hematopoietic cells that serves as a receptor for all reovirus serotypes. Expression of JAM-A is required for infection of endothelial cells and development of viremia in mice, suggesting that release of virus into the bloodstream from infected endothelial cells requires JAM-A. Nonstructural protein σ1s is implicated in cell cycle arrest and apoptosis in reovirus-infected cells but is completely dispensable for reovirus replication in cultured cells. Surprisingly, a recombinant σ1s-null reovirus strain fails to spread hematogenously in infected mice, suggesting that σ1s facilitates apoptosis of reovirus-infected intestinal epithelial cells. It is possible that apoptotic bodies formed as a consequence of σ1s expression lead to reovirus uptake by dendritic cells for subsequent delivery to the mesenteric lymph node and the blood. Thus, both host and viral factors are required for efficient hematogenous dissemination of reovirus. Understanding mechanisms of reovirus bloodborne spread may shed light on how microbial pathogens invade the bloodstream to disseminate and cause disease in infected hosts.

1. INTRODUCTION

Many pathogenic human and animal viruses disseminate from mucosal sites to peripheral tissues where they cause organ-specific disease (Nathanson & Tyler, 1997). The capacity of a virus to spread systemically can correlate with increased virulence (de Jong et al., 2006; Gu et al., 2007; Kuiken et al., 2003; Pallansch & Roos, 2001). Systemic dissemination requires that the virus effectively navigate diverse intracellular and extracellular environments to infect, replicate, and evade immune detection in multiple cell types and tissues (Adair et al., 2012; Antar et al., 2009; Boehme, Frierson, Konopka, Kobayashi, & Dermody, 2011; Boehme, Guglielmi, & Dermody, 2009). Although some general principles of virus dissemination are understood, little is known about the precise viral and cellular determinants that govern virus spread. Defining mechanisms by which viruses disseminate within their hosts is of fundamental importance to an understanding of viral pathogenesis.

Mammalian orthoreoviruses (reoviruses) are highly tractable models for studies of viral pathogenesis. Studies of reovirus neural spread have provided important information about mechanisms by which neurotropic viruses cause disease in the central nervous system (CNS). The recent identification of new viral and host determinants that govern reovirus spread by the blood provides new insights into how hematogenous dissemination contributes to viral disease.

1.1. Reoviruses

Viruses of the *Reoviridae* family infect a wide range of host organisms, including mammals, birds, insects, and plants (Dermody, Parker, & Sherry, 2013). The *Reoviridae* includes rotaviruses, the most common diarrheal pathogen among children (Parashar, Bresee, Gentsch, & Glass, 1998), orbiviruses, which are economically important pathogens of sheep, cattle, and horses (Coetzee et al., 2012), and reoviruses. Three reovirus serotypes (T1, T2, and T3) currently circulate in humans and other mammals. The serotypes are distinguished on the basis of antibody-mediated neutralization of infectivity and inhibition of hemagglutination. Each serotype is represented by a prototype strain isolated from a human host: type 1 Lang (T1L), type 2 Jones (T2J), and type 3 Dearing (T3D). These strains differ dramatically in host cell tropism, mechanisms of cell killing, modes of dissemination, and CNS disease. In particular, studies of T1 and T3 reoviruses have generated foundational knowledge about strategies used by viruses to replicate and cause neural injury. Development of a plasmid-based reverse genetics system allows introduction of mutations into the viral genome to test specific hypotheses about the structure and function of viral proteins and RNAs (Kobayashi et al., 2007; Kobayashi, Ooms, Ikizler, Chappell, & Dermody, 2010). In concert with an experimentally facile mouse model of infection (Fields, 1992; Parashar, Tarlow, & McCrae, 1992), reovirus is an ideal experimental platform for studies of virus–host interactions.

Reoviruses are nonenveloped, icosahedral viruses that contain a genome consisting of 10 segments of double-stranded (ds) RNA (Fig. 1.1; Dermody et al., 2013). There are three large (L1, L2, L3), three medium (M1, M2, M3), and four small (S1, S2, S3, S4) dsRNA segments that are packaged in an equimolar stoichiometric relationship with one copy of each per virion. With the exception of the M3 and S1 gene segments, each of the reovirus gene segments is monocistronic. Reovirus virions are composed of two concentric protein shells, the outer capsid and core (Fig. 1.1; Dryden et al., 1993). The outer capsid consists of heterohexameric complexes of the μ1 (encoded by M2) and σ3 (encoded by S4) proteins. At each of the icosahedral fivefold symmetry axes, the attachment protein σ1 (encoded by S1) extends from turret-like structures formed by pentamers of λ2 (encoded by L2) protein. The inner core shell is formed by parallel asymmetric dimers of λ1 (encoded by L3) protein that are stabilized by σ2 (encoded by S2) protein. The λ3 (encoded by L1) and μ2 (encoded by M1) proteins are anchored to the inner surface of the core via interactions

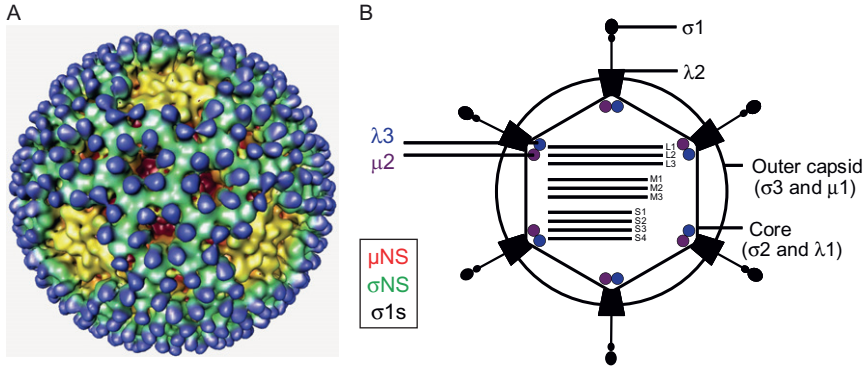

Figure 1.1 The reovirus virion. (A) Cryoelectron micrograph image reconstruction of a reovirus virion. Outer-capsid protein σ3 (blue) is the initial target for virion disassembly in infected cells. Pentameric λ2 protein (yellow) forms an insertion pedestal for σ1, which is the viral attachment protein. (B) Schematic of a reovirus virion. Reovirus particles are formed from two concentric protein shells, the outer capsid and core. The core contains the viral genome, which consists of 10 dsRNA segments. Reovirus also encodes nonstructural proteins, σNS, μNS, and σ1s. *Copyright © American Society for Microbiology, Nason et al. (2001).*

with λ1. Lastly, the M3 gene segment encodes nonstructural protein μNS, the S3 gene segment encodes nonstructural protein σNS, and the S1 gene segment encodes nonstructural protein σ1s.

Viral attachment protein σ1 is a long filamentous molecule with head-and-tail morphology (Fig. 1.2A; Chappell, Prota, Dermody, & Stehle, 2002; Fraser et al., 1990; Mercier et al., 2004; Reiter et al., 2011). The σ1 protein is comprised of three distinct structural domains: an N-terminal α-helical coiled-coil tail, a central β-spiral body, and a C-terminal globular head (Chappell et al., 2002; Reiter et al., 2011). Short regions of undefined structure partition each domain and are hypothesized to permit molecular flexibility required to engage cellular receptors during viral entry (Bokiej et al., 2012; Chappell et al., 2002; Fraser et al., 1990; Reiter et al., 2011). Attachment of the σ1 protein to cell-surface receptors initiates reovirus infection of susceptible host cells (Lee, Hayes, & Joklik, 1981; Weiner, Ault, & Fields, 1980; Weiner, Powers, & Fields, 1980). The σ1 protein of T3 reovirus targets two different receptors, α-linked sialic acid (SA) (Armstrong, Paul, & Lee, 1984; Dermody, Nibert, Bassel-Duby, & Fields, 1990a; Pacitti & Gentsch, 1987; Paul, Choi, & Lee, 1989; Paul & Lee, 1987) and junctional adhesion molecule-A (JAM-A) (Barton, Forrest, et al., 2001; Campbell et al., 2005; Prota et al., 2003). Residues in the T3 σ1 β-spiral body domain bind SA

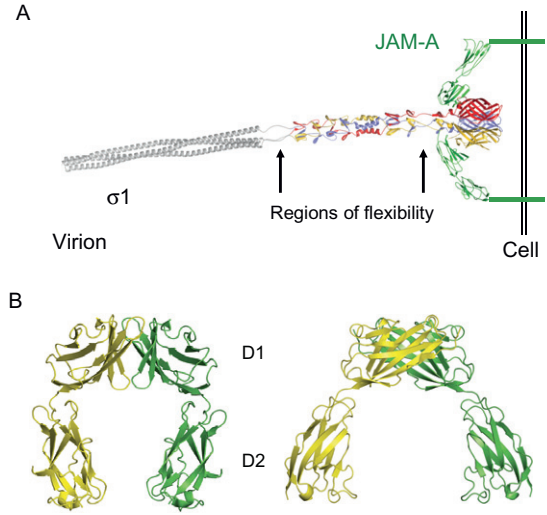

Figure 1.2 Structure of σ1 and JAM-A. (A) Full-length model of attachment protein σ1 bound to JAM-A. A model of full-length σ1 extending from the virion is shown as a ribbon drawing, with the known structure of the C-terminus (Reiter et al., 2011) in tricolor and the predicted structure of the N-terminus in gray. Arrows indicate predicted regions of flexibility. A model of full-length JAM-A is shown in green as a ribbon drawing of the known structure of the extracellular domain (Prota et al., 2003) and a schematic representation of the transmembrane and intracellular domains. For clarity, only two JAM-A monomers are shown bound to σ1. (B) Structure of human JAM-A D1 and D2 domains. Ribbon drawings of a JAM-A homodimer, with one monomer shown in yellow and the other in green. Two orthogonal views are displayed. *(A) Adapted from Kirchner, Guglielmi, Strauss, Dermody, and Stehle (2008, Fig. 1). (B) Adapted from Prota et al. (2003). Copyright (2003) National Academy of Sciences, USA.*

(Chappell, Duong, Wright, & Dermody, 2000; Reiter et al., 2011), whereas sequences in the σ1 globular head domain engage JAM-A (Barton, Forrest, et al., 2001; Kirchner et al., 2008).

After receptor binding, virions are internalized into endosomes via a process dependent on β1 integrin (Maginnis et al., 2006) and distributed to organelles marked by Rab7 and Rab9 where viral disassembly takes place (Mainou & Dermody, 2012). During viral disassembly, outer-capsid protein σ3 is degraded by cathepsin proteases, attachment protein σ1 undergoes a conformational change, and outer-capsid protein μ1 is cleaved to form infectious subvirion particles (ISVPs) (Danthi et al., 2010). The μ1 cleavage fragments undergo conformational rearrangement to facilitate endosome penetration and delivery of transcriptionally active core particles into the

cytoplasm (Nibert, Odegard, Agosto, Chandran, & Schiff, 2005; Odegard et al., 2004). Primary transcription occurs within the viral core, and nascent RNAs are translated or encapsidated into new viral cores, where they serve as templates for negative-strand synthesis. Within new viral cores, secondary rounds of transcription occur. Outer-capsid proteins are added to nascent cores, which silences viral transcription and yields progeny viral particles. Reovirus release from host cells is hypothesized to occur via a lytic mechanism, but the egress pathway is not understood (Dermody et al., 2013).

1.2. Junctional adhesion molecule-A

JAM-A is the only known proteinaceous receptor for reovirus. It mediates entry of prototype and field-isolated strains of all three reovirus serotypes (Barton, Forrest, et al., 2001; Campbell et al., 2005). JAM-A is a member of the immunoglobulin (Ig) superfamily of proteins that functions in cell–cell adhesion (Bazzoni, 2003). It is expressed on the surface of endothelial and epithelial cells as a component of tight junctions that maintain the integrity of barriers formed between polarized cells (Martin-Padura et al., 1998; Woodfin et al., 2007). JAM-A also is expressed on hematopoietic cells, where it mediates leukocyte extravasation (Corada et al., 2005; Ghislin et al., 2011), and on platelets, where it functions in platelet activation during blood clot formation (Bazzoni, 2003; Sobocka et al., 2004). JAM-A contains three distinct structural domains: an N-terminal ectodomain, a single-span transmembrane anchor, and a C-terminal cytoplasmic tail (Fig. 1.2B; Prota et al., 2003). The ectodomain consists of two Ig-like domains, a membrane-distal D1 domain and a membrane-proximal D2 domain. The cytoplasmic tail terminates in a PDZ-binding domain that interacts with intracellular tight junction components (Bazzoni et al., 2005; Nomme et al., 2011). JAM-A participates in homotypic interactions between D1 domains on opposing monomers (Prota et al., 2003). An interaction between two JAM-A monomers on adjacent cells promotes cell adhesion (Iden et al., 2012; Mandell, Babbin, Nusrat, & Parkos, 2005; Ostermann et al., 2005).

The σ1 protein interacts with the JAM-A D1 domain to adhere reovirus virions to the surface of target cells (Kirchner et al., 2008). Interestingly, the σ1–JAM-A interaction is substantially stronger (approximately 1000-fold) than the interaction between JAM-A monomers (Kirchner et al., 2008). Consequently, σ1 binding to JAM-A likely disrupts JAM-A homodimers. Studies using JAM-A-deficient mice indicate that JAM-A is required for the establishment of viremia, which is essential for dissemination and disease

in newborn mice following peroral inoculation of reovirus (Antar et al., 2009). JAM-A is not required for reovirus replication in the murine CNS or development of encephalitis (Antar et al., 2009). These findings suggest that reovirus utilizes other cell-surface receptors to mediate entry into specific cell types.

1.3. Reovirus pathogenesis

Reoviruses are highly virulent in newborn mice and cause injury to a variety of host organs, including the CNS, heart, and liver (Dermody et al., 2013). T1 and T3 reovirus strains invade the CNS but use different routes and produce distinct pathologic consequences following peroral or intramuscular inoculation. T1 reoviruses spread by hematogenous routes and infect ependymal cells, causing nonlethal hydrocephalus (Tyler, McPhee, & Fields, 1986; Weiner, Drayna, Averill, & Fields, 1977; Weiner, Powers, et al., 1980). T3 reoviruses spread to the CNS by both hematogenous and neural routes, and infect neurons (Antar et al., 2009; Boehme et al., 2011; Tyler et al., 1986). In the brain, T3 reoviruses induce neuronal apoptosis, which results in fatal encephalitis (Morrison, Sidman, & Fields, 1991; Tyler et al., 1986; Weiner et al., 1977; Weiner, Powers, et al., 1980). Studies using T1L × T3D reassortant viruses mapped the major determinant of CNS pathology to the viral S1 gene (Dichter & Weiner, 1984; Tardieu & Weiner, 1982), which encodes attachment protein σ1 and nonstructural protein σ1s (Sarkar et al., 1985; Weiner, Ault, et al., 1980). Because of its role in viral attachment and entry, these serotype-specific differences in dissemination and disease have largely been ascribed to the σ1 protein. However, σ1s plays a critical role in promoting reovirus spread by the bloodstream (Boehme et al., 2011, 2009).

1.4. Nonstructural protein σ1s

Protein σ1s is a 14 kDa nonstructural protein encoded by the viral S1 gene segment (Cashdollar, Chmelo, Wiener, & Joklik, 1985; Ernst & Shatkin, 1985; Sarkar et al., 1985). The σ1s open-reading frame (ORF) completely overlaps the σ1 coding sequence; however, σ1s lies in a different reading frame (Cashdollar et al., 1985; Cenatiempo et al., 1984; Dermody, Nibert, Bassel-Duby, & Fields, 1990b; Ernst & Shatkin, 1985; Sarkar et al., 1985). Although every reovirus strain sequenced to date contains a σ1s ORF, little amino acid sequence identity exists between the σ1s proteins from the different reovirus serotypes (Cashdollar et al., 1985;

Dermody et al., 1990b). The only conserved sequence among σ1s proteins is a cluster of basic amino acids near the amino terminus (Cashdollar et al., 1985; Dermody et al., 1990b). The basic cluster from T3 σ1s functions as an autonomous nuclear localization signal that can redirect an appended heterologous protein to the nucleus (Hoyt, Bouchard, & Tyler, 2004). While the majority of native σ1s localizes to the nucleus (Rodgers, Connolly, Chappell, & Dermody, 1998), it is not known whether the basic cluster mediates nuclear translocation in the context of reovirus infection. Functionally, the σ1s protein is implicated in reovirus-induced cell cycle arrest at the G_2/M boundary (Poggioli, Dermody, & Tyler, 2001; Poggioli, Keefer, Connolly, Dermody, & Tyler, 2000) and may influence reovirus neurovirulence by promoting reovirus-induced apoptosis in the murine CNS (Hoyt et al., 2005). Initial studies to define the function of σ1s in reovirus pathogenesis were complicated by the use of nonisogenic σ1s-null mutant and parental virus strains (Rodgers et al., 1998).

Development of a plasmid-based reverse genetics system for mammalian reovirus (Kobayashi et al., 2007, 2010) made it possible to elucidate the function of σ1s in reovirus replication and pathogenesis. Recombinant reoviruses deficient in σ1s expression were engineered by incorporating a single nucleotide change (AUG to ACG) to disrupt the σ1s translational start site into the plasmid containing the cDNA encoding the S1 gene segment. Importantly, the mutation does not affect the coding sequence of the overlapping σ1 ORF. Thus, except for σ1s expression, the resultant viruses are isogenic with the parental strain. Viruses deficient in σ1s expression have been generated in the T1 and T3 S1 gene backgrounds. In both cases, the σ1s-null viruses are viable and replicate with equivalent kinetics and produce yields of progeny virus comparable to the corresponding wild-type viruses, indicating that the σ1s protein is dispensable for reovirus replication in cultured cells (Boehme et al., 2011, 2009). These viruses were used to uncover a role for σ1s in promoting hematogenous reovirus dissemination.

2. DYNAMICS OF REOVIRUS INFECTION IN THE INTESTINE AND LUNG

Reoviruses infect their hosts by the fecal-oral and respiratory routes. Virus enters the host by ingestion of contaminated food or inhalation of virus-containing aerosols. At both portals of entry, reoviruses infect epithelial cells and disseminate to peripheral sites where they cause disease.

2.1. Infection via the gastrointestinal tract

Reoviruses have been isolated from the stools of healthy (Ramos-Alvarez & Sabin, 1954, 1956) and ill (Ramos-Alvarez & Sabin, 1958) children as well as a variety of animals (Ramos-Alvarez & Sabin, 1958). These findings suggest that reovirus is ingested into and shed from the gastrointestinal tract. The dynamics of reovirus infection *in vivo* have largely been elucidated using experimental mouse and rat model systems. Following entry into the gastrointestinal tract of rodents, intestinal proteases rapidly convert reovirus virions to ISVPs, suggesting that the form of the reovirus particle that initiates infection in the intestine is the ISVP (Bass et al., 1990; Bodkin, Nibert, & Fields, 1989; Chappell et al., 1998). In newborn mice, cells at the tips of microvilli are readily infected, whereas cells in the intestinal crypts are spared (Antar et al., 2009; Boehme et al., 2009). In contrast, intestinal crypt cells are infected in adult mice, and cells at the villus tips are uninfected (Rubin, Kornstein, & Anderson, 1985). Infectious reovirus can be recovered following peroral inoculation from the duodenum, jejunum, ileum, and colon (Rubin, Eaton, & Anderson, 1986; Rubin et al., 1985). However, the vast majority of virus is produced in the ileum. This differential production of virus may be due to the capacity of reovirus to infect Peyer patches. Reoviruses are thought to penetrate the intestinal barrier via transport across microfold (M) cells, which are specialized cells of the follicle-associated epithelium (FAE) that overlay the Peyer patches (Amerongen, Wilson, Fields, & Neutra, 1994; Wolf, Dambrauskas, Sharpe, & Trier, 1987; Wolf et al., 1983, 1981). M cells transfer antigens from the intestinal lumen to lymphoid cells of the gut-associated lymphoid tissue (van de Pavert & Mebius, 2010) and serve to monitor luminal contents by exposing Peyer patch lymphoid cells to food antigens, the intestinal microbiota, and invading pathogens. This process is essential for induction of oral tolerance and activation of immune responses to pathogenic microorganisms (van de Pavert & Mebius, 2010). The preferential targeting of crypt cells observed in adult mice is hypothesized to result from transcytosis of virus across M cells and subsequent infection of crypt cells via the basolateral surface (Rubin, 1987). However, M cells also take up reovirus in neonatal mice (Antar et al., 2009; Boehme et al., 2009; Wolf et al., 1981), suggesting that viral transcytosis across M cells is unlikely to explain the difference in intestinal cell tropism observed in adult and newborn mice. It is possible that the proliferative status of stem cells in the crypts of adult mice may recapitulate the cellular environment of neonatal intestinal cells, thereby facilitating reovirus infection of intestinal crypt cells.

2.2. Infection via the respiratory tract

Reovirus also infects the respiratory tract (Sabin, 1959). In rats, both T1 and T3 reovirus strains cause a pneumonia that is characterized by destruction of type 1 alveolar epithelial cells and infiltration of leukocytes into the alveolar spaces (Morin, Warner, & Fields, 1996). The pathology associated with reovirus infection closely mimics disease progression in bronchiolitis obliterans organizing pneumonia, which is notable for fibrous extensions into alveolar spaces in the context of an organizing pneumonia (Bellum et al., 1997). Following inoculation into the respiratory tract, lung proteases convert reovirus virions to ISVPs (Golden & Schiff, 2005; Nygaard, Golden, & Schiff, 2012). Similar to infection in the intestine, reovirus infects the lung by transcytosis through M cells that overlie the bronchus-associated lymphoid tissue (Morin, Warner, & Fields, 1994; Morin et al., 1996).

3. HEMATOGENOUS SPREAD OF REOVIRUS

3.1. Transport of reovirus from the intestine to the bloodstream

Systemic reovirus infection is thought to originate from infected lymphoid cells in the Peyer patch. From the Peyer patch, reovirus transits intestinal lymphatics to the mesenteric lymph node (MLN) and ultimately enters the bloodstream via the thoracic duct (Antar et al., 2009; Boehme et al., 2009; Wolf et al., 1981). Many pathogens that cause systemic disease, including poliovirus (Bodian, 1955; Sabin, 1956) and *Salmonella* (Carter & Collins, 1974; Galan & Curtiss, 1989; Jones, Ghori, & Falkow, 1994), initiate extraintestinal infection and access the bloodstream via this route.

Reovirus reaches the Peyer patches early after infection; viral antigen is detected in Peyer patches within 24 h after peroral inoculation (Antar et al., 2009; Bass, Trier, Dambrauskas, & Wolf, 1988; Boehme et al., 2009; Wolf et al., 1987, 1983, 1981). However, the mechanism by which reovirus infects Peyer patch cells is not known. It is possible that dendritic cells in the Peyer patches take up reovirus virions immediately following viral transcytosis across M cells. This is the most direct route from the intestinal lumen to the Peyer patch and the primary pathway used for processing of intestinal antigens for immune surveillance. A second possibility is that progeny virions released from the basolateral surface of infected FAE cells are taken up by lymphoid cells in Peyer patches. Both viral structural and nonstructural proteins are detected in FAE cells (Fleeton et al., 2004), indicating

that active viral replication occurs in these cells. However, it is not known whether FAE cells produce virus. A third possibility is that dendritic cells in Peyer patches take up apoptotic fragments from infected FAE cells, which undergo apoptosis following reovirus infection (Fleeton et al., 2004). Dendritic cells in the underlying Peyer patches immediately adjacent to apoptotic FAE cells contain both active caspase-3 and reovirus structural proteins (Fleeton et al., 2004). These observations suggest that Peyer patch dendritic cells take up apoptotic bodies from infected FAE cells. Additionally, apoptosis induction in the FAE may signal Peyer patch cells to phagocytose the apoptotic remnants, along with reovirus particles.

Regardless of the mechanism by which reovirus accesses Peyer patches, reovirus antigen is detected in the MLN 24 h after peroral inoculation. Little is known about the cell types that support reovirus replication within the intestine and dissemination to the MLN. In adult mice, $CD11c^+$ dendritic cells harbor reovirus antigen, but these cells are not thought to be actively infected (Fleeton et al., 2004). Viral nonstructural proteins are not present in these cells (Fleeton et al., 2004), suggesting that active replication does not occur. $CD11c^+$ dendritic cells are present in neonatal animals (Muthukkumar, Goldstein, & Stein, 2000), but it is not known whether these cells internalize reovirus following peroral inoculation of newborn mice. Reovirus productively infects bulk splenocytes isolated from newborn mice (Tardieu, Powers, & Weiner, 1983), suggesting that reovirus can replicate in primary lymphoid cells. Reovirus cannot productively infect splenocytes explanted after the mouse reaches 7 days of age (Tardieu et al., 1983). Thus, the lack of viral replication in Peyer patch cells in older animals may contribute to the age restriction to reovirus infection.

From Peyer patches, reovirus is hypothesized to traffic via afferent lymphatics to the MLN, then through efferent lymphatics to the blood. It is possible that infected lymphoid cells or lymphoid cells harboring virus mediate transport from the Peyer patches to the bloodstream. However, migrating dendritic cells rarely exit lymph nodes once they enter and present antigen to B and T cells (Iwasaki, 2007). Thus, the cells responsible for transport of reovirus from the Peyer patch are likely retained in the MLN. Reovirus titers in the MLN increase rapidly after peroral inoculation (Antar et al., 2009; Boehme et al., 2009), suggesting that active viral replication occurs in the MLN. However, it is also possible that the increase in viral load in the MLN represents migration of infected lymphoid cells from the Peyer patches. Dissemination from the MLN to the bloodstream may occur as free virus or within another lymphoid cell subset.

An alternative mechanism for accessing the blood is direct uptake of viral particles from the gut. $CD18^+$ phagocytes extend cellular processes between enterocytes to directly sample luminal contents. Dendritic cells also extend processes through the epithelial monolayer, while maintaining barrier integrity to sample gut pathogens (Rescigno et al., 2001). A number of pathogens, including *Salmonella* (Vazquez-Torres et al., 1999) and *Yersinia* (Isberg & Barnes, 2001), use macrophages or dendritic cells to invade the bloodstream and cause extraintestinal infection. Following uptake of luminal pathogens, $CD18^+$ phagocytes traffic across the lamina propria and directly into the blood allowing for rapid entry of the pathogen into the bloodstream.

3.2. Reovirus viremia

Although virus is detected in the blood of infected animals, it is not known whether reovirus virions within the blood are free in the plasma or associated with hematopoietic cells. Other *Reoviridae* family members, including bluetongue virus (BTV) and Colorado tick fever virus, produce cell-associated viremia during infection. BTV infects and replicates in mononuclear cells, lymphocytes, and endothelial cells (Barratt-Boyes & MacLachlan, 1994; Ellis et al., 1993; MacLachlan, Jagels, Rossitto, Moore, & Heidner, 1990; Mahrt & Osburn, 1986; Veronesi et al., 2009). Colorado tick fever virus is detected in mature erythrocytes (Oshiro, Dondero, Emmons, & Lennette, 1978). However, arthropod vectors transmit BTV and Colorado tick fever virus, making viremia a necessary part of the viral infectious cycle in nature. Mammalian reoviruses are not transmitted by arthropod vectors and may produce a distinctly different type of viremia. Studies in which oncolytic reovirus was delivered intravenously to persons with cancer revealed that virus is largely found in hematopoietic cells, specifically mononuclear cells, granulocytes, and platelets (Adair et al., 2012). Each of these cell types express JAM-A (Martin-Padura et al., 1998; Naik, Naik, Eckfeld, Martin-DeLeon, & Spychala, 2001; Sobocka et al., 2000), suggesting that reovirus associates with or infects blood cells to disseminate through the blood to target organs. However, in these studies, virus was delivered directly into the bloodstream by intravenous inoculation. It is not known how reovirus spreads systemically following infection from a natural portal, such as the intestine or lung.

3.3. Role of receptors in reovirus dissemination

Interactions between viral attachment proteins and host cell receptors play a pivotal role in viral pathogenesis. Receptor engagement is a primary

mechanism to define cells targeted by viruses. Therefore, patterns of receptor expression are a key determinant of viral disease. Reoviruses engage two types of cellular receptors: cell-surface carbohydrate (Paul et al., 1989) and JAM-A (Barton, Forrest, et al., 2001). Both T1 and T3 (Dermody et al., 1990a; Pacitti & Gentsch, 1987; Paul et al., 1989) reoviruses bind cell-surface SA (Armstrong et al., 1984; Dermody et al., 1990a; Pacitti & Gentsch, 1987; Paul et al., 1989; Paul & Lee, 1987). However, the domains of σ1 that engage glycans differ between the serotypes (Dermody et al., 1990a; Chappell et al., 2000), as do the specific glycans bound (Reiss et al., 2012).

SA engagement enhances reovirus infection through an adhesion-strengthening mechanism in which viral particles are tethered to the cell surface via a low-affinity interaction with the carbohydrate (Barton, Connolly, Forrest, Chappell, & Dermody, 2001). This interaction maintains the virus on the cell surface and increases the opportunity to engage JAM-A. SA-binding reovirus strains have an increased capacity to infect cells compared with non-SA-binding viruses; pretreatment of cells with neuraminidase to remove cell-surface SA eliminates this advantage (Barton, Connolly, et al., 2001). SA engagement also enhances reovirus tropism for bile duct epithelial cells in mice following peroral inoculation (Barton et al., 2003). The resulting disease closely mimics biliary atresia in human infants (Barton et al., 2003), an illness epidemiologically associated with reovirus (Richardson, Bishop, & Smith, 1994; Tyler et al., 1998).

Reovirus strains circulating in nature vary in the capacity to bind SA (Dermody et al., 1990a, 1990b). This finding suggests that SA binding comes with a fitness cost. Accordingly, SA binding appears to inhibit the capacity of reovirus to establish infection at mucosal portals of entry. Non-SA-binding viruses infect primary human airway epithelial cells substantially more efficiently than SA-binding strains (Excoffon et al., 2008). Moreover, infection of primary human airway epithelial cells by SA-binding viruses is enhanced by removal of cell-surface SA with neuraminidase. Mucosal surfaces are covered with a glycocalyx consisting of polysaccharides and glycoproteins that are rich in SA (Excoffon et al., 2008). SA-binding viruses may be trapped by SA within the glycocalyx and incapable of reaching the underlying epithelium (Excoffon et al., 2008). However, once infection is established, SA binding may enhance the capacity of reovirus to cause disease. In addition to the capacity to target bile duct epithelium, SA-binding strains are more neurovirulent than non-SA-binding viruses following intracranial inoculation (Barton et al., 2003; Frierson et al., 2012). This increase in virulence is likely due to more

efficient infection of neurons, which results in neuronal apoptosis and encephalitis. The function of SA binding in reovirus hematogenous spread remains to be determined.

Although all reoviruses bind JAM-A, T1, and T3 reoviruses infect distinct cells and cause serotype-specific patterns of pathologic injury within the CNS. These observations suggest that JAM-A binding does not influence serotype-specific differences in reovirus neural tropism and CNS disease. Following peroral inoculation, reovirus produces similar viral titers in the intestine of wild-type and JAM-A-deficient mice, suggesting that JAM-A is not required for reovirus replication in the mouse gastrointestinal tract (Antar et al., 2009). In sharp contrast, viral titers at all sites of secondary replication are significantly lower in JAM-A-deficient animals compared with wild-type controls (Fig. 1.3). Viral loads are comparable within the brains of wild-type and JAM-A-deficient animals after intracranial inoculation, suggesting that JAM-A is not required for viral replication at this site of secondary replication (Antar et al., 2009). These results suggest that JAM-A is required for dissemination of the virus from the intestine to replication sites in target organs.

How might JAM-A promote hematogenous dissemination? Substantially lower reovirus titers are detected in the blood of JAM-A-deficient mice compared with wild-type mice (Fig. 1.4), suggesting that JAM-A is involved in the establishment of viremia (Antar et al., 2009). Diminished viremia is detected in mice inoculated with either T1 or T3 reovirus, indicating that JAM-A functions in promoting bloodborne spread of T1 viruses that disseminate by strictly hematogenous mechanisms as well as neurotropic T3 reoviruses. Primary pulmonary endothelial cells isolated from JAM-A-deficient mice are refractory to reovirus infection compared with those harvested from wild-type mice (Fig. 1.5). These data suggest that reovirus engages JAM-A to infect endothelial cells, likely in the lymphatics or vasculature of the gastrointestinal tract. It is possible that virus released from endothelial cells invades the bloodstream to disseminate to peripheral target organs either free in the plasma or associated with hematopoietic cells.

3.4. Function of nonstructural protein σ1s in reovirus dissemination

Studies using T1 σ1s-null virus uncovered a role for σ1s in promoting bloodborne reovirus spread (Boehme et al., 2009). The σ1s protein is not required for the initial establishment of reovirus infection in the gut.

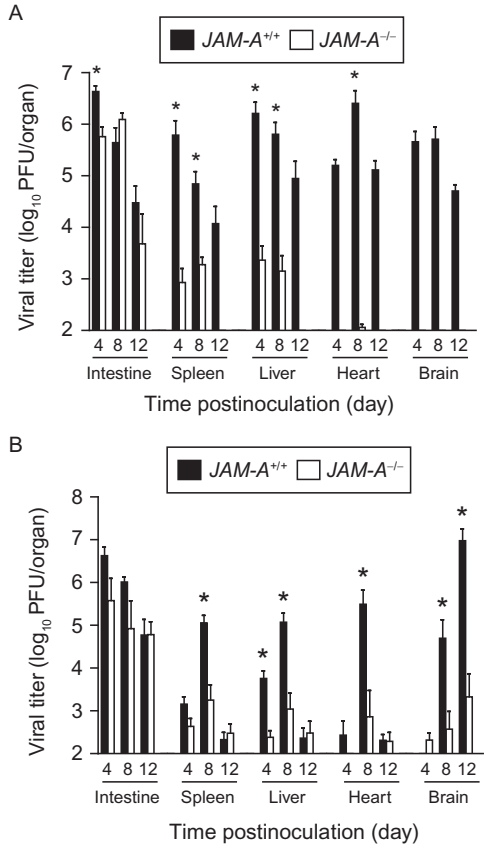

Figure 1.3 JAM-A is required for hematogenous reovirus dissemination. (A) Newborn C57/BL6 *JAM-A*$^{+/+}$ and *JAM-A*$^{-/-}$ mice were inoculated perorally with 10^6 PFU of strain T1L. At days 4, 8, and 12 after inoculation, mice were euthanized, organs were resected, and viral titers were determined by plaque assay. Results are expressed as mean viral titers for six animals for each time point. Error bars indicate SD. $^*P < 0.005$ by Student's *t*-test. When all values are less than the limit of detection (spleen, liver, heart, and brain in *JAM-A*$^{-/-}$ mice), a Student's *t*-test *P* value cannot be calculated. (B) Newborn *JAM-A*$^{+/+}$ and *JAM-A*$^{-/-}$ mice were inoculated perorally with 10^4 PFU of strain T3SA−. At days 4, 8, and 12 after inoculation, mice were euthanized, organs were resected, and viral titers were determined by plaque assay. Results are expressed as mean viral titers for 6–13 animals for each time point. Error bars indicate SD. $^*P < 0.05$ by Student's *t*-test in comparison to *JAM-A*$^{-/-}$ mice. *Reprinted from Antar et al. (2009), Copyright (2009), with permission from Elsevier.*

Wild-type and σ1s-null viruses replicate to comparable levels in the gastrointestinal tract following peroral inoculation (Fig. 1.6). Reovirus antigen is evident in the intestinal epithelium and Peyer patches of mice inoculated with wild-type or σ1s-null virus, indicating that σ1s does not influence

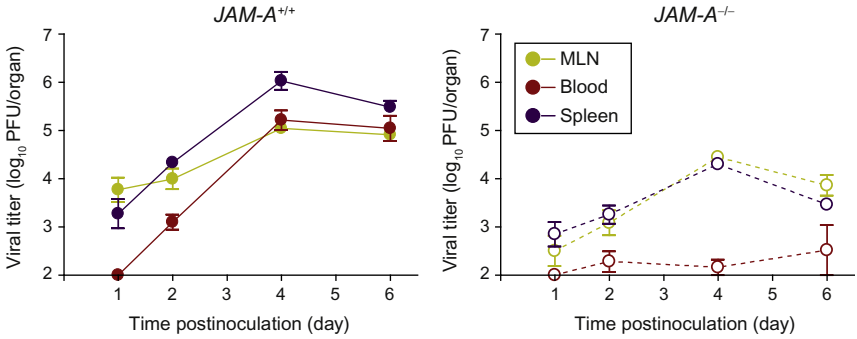

Figure 1.4 JAM-A is required for reovirus viremia. Newborn C57/BL6 *JAM-A*$^{+/+}$ and *JAM-A*$^{-/-}$ mice were inoculated perorally with 10^8 PFU of T1L. At days 1, 2, 4, and 6 after inoculation, mice were euthanized, mesenteric lymph node (MLN), blood, and spleen were collected, and viral titers were determined by plaque assay. Results are expressed as mean viral titers for three to eight animals for each time point. Error bars indicate SD. *Reprinted from Antar et al. (2009), Copyright (2009), with permission from Elsevier.*

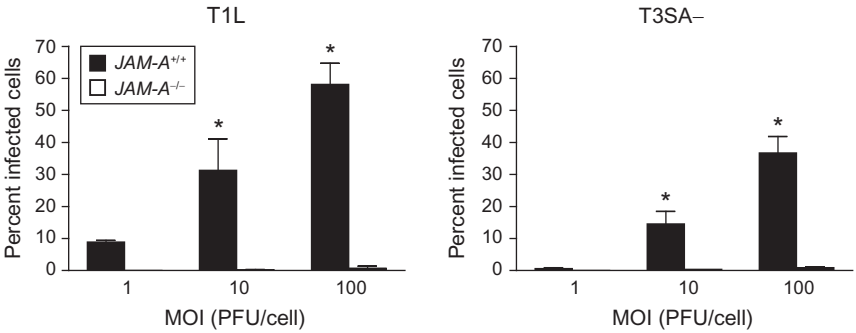

Figure 1.5 JAM-A is required for efficient reovirus infection of endothelial cells. *JAM-A*$^{+/+}$ and *JAM-A*$^{-/-}$ primary endothelial cells were adsorbed with T1L or T3SA− at MOIs of 1, 10, or 100 PFU/cell and incubated for 20 h. The percentage of infected cells was quantified by dividing the number of cells exhibiting reovirus staining by the total number of cell nuclei exhibiting DAPI staining in whole 96 wells for triplicate experiments. Wells contained between 200 and 1600 nuclei. Error bars indicate SD. $^*P < 0.05$ as determined by Student's *t*-test in comparison to *JAM-A*$^{-/-}$ endothelial cells inoculated at the same MOI. *Reprinted from Antar et al. (2009), with permission from Elsevier.*

reovirus tropism in the intestine. In contrast to wild-type virus, the σ1s-null mutant fails to produce substantial titers in the MLN. The σ1s-null virus is detected at low titer in the MLN, but viral titers do not increase over the course of infection. These findings indicate that σ1s either is essential for transit through lymphatic channels to the MLN or serves to promote

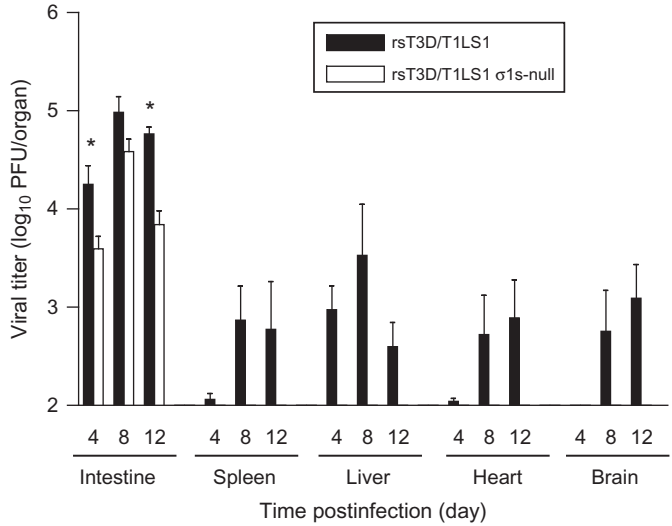

Figure 1.6 The σ1s protein is required for systemic reovirus dissemination following peroral inoculation. Newborn C57/BL6 mice were inoculated perorally with 10^4 PFU of wild-type or σ1s-null reovirus. At days 4, 8, and 12 postinoculation, viral titers in the organs shown were determined by plaque assay. Error bars indicate SEM. $^*P < 0.05$ as determined by Mann–Whitney test in comparison to wild-type virus. When all values are less than the limit of detection, a Mann–Whitney test *P* value cannot be calculated. *Adapted from Boehme et al. (2009). Copyright (2009) National Academy of Sciences, USA.*

replication in MLN cells. Wild-type virus is detected in the blood and sites of secondary viral replication, including the brain, heart, liver, and spleen (Fig. 1.6). The σ1s-null virus is not detected in the blood or any of the target organs examined. This difference is probably not due to a requirement for σ1s in mediating replication at these sites, as wild-type and σ1s-null viruses produce comparable titers in the brain following intracranial inoculation. Together, these findings suggest that the σ1s protein performs a function that is essential for reovirus to spread from the gut through intestinal lymphatics and ultimately to the blood where it gains access peripheral organs.

In contrast to T1 reoviruses that spread by strictly hematogenous mechanisms, T3 reoviruses disseminate by both hematogenous and neural pathways. The amino acid sequences of the σ1s proteins from the different reovirus serotypes differ markedly (Dermody et al., 1990b). Therefore, it is possible that the σ1s proteins perform serotype-specific functions. In nature, reovirus infects by the peroral route and spreads to the CNS in infant animals resulting in neuropathology. However, infectivity of T3 prototype

strain T3D is diminished significantly within the gastrointestinal tract (Bodkin & Fields, 1989; Bodkin et al., 1989) due to cleavage of its σ1 protein by intestinal proteases (Bodkin & Fields, 1989; Bodkin et al., 1989; Nibert, Chappell, & Dermody, 1995). Consequently, intramuscular inoculation into the hindlimb is used to assess mechanisms of T3D dissemination. Inoculation of Type 3 reoviruses intramuscularly leads to invasion of the brain by neural routes (Tyler et al., 1986). Following intramuscular inoculation, wild-type T3D produces substantially higher titers than the σ1s-null virus in peripheral organs including the heart, liver, intestine, and spleen, similar to results obtained using wild-type and σ1s-null T1 viruses (Boehme et al., 2011). Moreover, wild-type T3D but not the T3D σ1s-null mutant virus is detected in the blood. Together, these data suggest that σ1s functions to promote the establishment of reovirus viremia in a serotype-independent manner, which ultimately leads to infection of peripheral target tissues.

In contrast to its function in hematogenous spread, the σ1s protein is dispensable for reovirus spread to the CNS by neural routes. Both wild-type and σ1s-null viruses produce comparable titers in the spinal cord following inoculation into the hindlimb muscle (Boehme et al., 2011). Both viruses also produce comparable titers in the brain following direct intracranial inoculation and in cultured primary neurons. Together, these findings indicate that σ1s is not required for reovirus neural spread or replication in the murine CNS. Thus, although T3 viruses spread via neural and hematogenous mechanisms, the T3 σ1s protein only influences the efficiency of hematogenous dissemination.

4. NEURAL DISSEMINATION OF REOVIRUS

In addition to bloodborne spread, T3 reoviruses use neural circuits to disseminate to the CNS (Boehme et al., 2011; Tyler et al., 1986). Spread via neural routes is a fundamental mechanism of reovirus pathogenesis that is essential for development of reovirus-induced encephalitis (Boehme et al., 2011; Tyler et al., 1986). Direct infection of neurons at peripheral sites provides the virus with access to the CNS and serves as a conduit to the brain. Although the importance of neural spread in reovirus pathogenesis is well appreciated, the cellular and molecular mechanisms that underlie neuronal reovirus trafficking are not well understood.

In contrast to hematogenous spread, JAM-A is dispensable for neural dissemination. Although JAM-A is expressed in the brain, the cell types on which it is present have not been defined. JAM-A is found on NG2-glia

cells, which are a subset of stem cells that give rise to oligodendrocytes (Nomme et al., 2011). It is unclear whether JAM-A is expressed on peripheral or CNS neurons. Viral titers in the brains of wild-type and JAM-A-deficient mice are comparable after intracranial inoculation (Antar et al., 2009). Viral tropism in the brain for hippocampal, thalamic, and cortical regions also does not differ between wild-type and JAM-A-deficient mice. Concordantly, primary cortical neurons isolated from wild-type and JAM-A-deficient mice are equally susceptible to reovirus infection and produce equivalent yields of viral progeny (Antar et al., 2009). Together, these data indicate JAM-A is not required for reovirus infection of neural tissue and suggest that JAM-A is dispensable for reovirus spread by neural routes. These findings further suggest that a cellular receptor distinct from JAM-A mediates reovirus infection of neurons.

Some evidence exists about the means by which reovirus traverses neural pathways. Treatment of animals with colchicine to inhibit fast axonal transport impairs reovirus spread to the spinal cord following hindlimb inoculation (Sjostrand & Karlsson, 1969; Tyler et al., 1986). However, treatment with β-β′-iminodipropionitrile to inhibit slow axonal transport does not affect reovirus dissemination to the spinal cord (Hansson, Kristensson, Olsson, & Sjostrand, 1971; Mahrt & Osburn, 1986). These findings suggest that reovirus traffics in neurons by fast axonal transport. However, these inhibitors may act nonspecifically to impair other aspects of viral replication. It also is not known whether reovirus uses afferent or efferent neurons to traffic to the CNS or whether virions can travel using both retrograde and anterograde pathways within neurons. Finally, it is not known where or how progeny virions exit neurons. Much work is required to fully elucidate how reoviruses replicate and traffic in neurons.

5. FUNCTION OF HEMATOGENOUS AND NEURAL SPREAD IN REOVIRUS PATHOGENESIS

T1 reoviruses disseminate to sites of secondary viral replication solely by hematogenous pathways. Following peroral inoculation of JAM-A-deficient mice, T1 reovirus does not reach the blood or peripheral organs (Antar et al., 2009). Similarly, T1 σ1s-null virus fails to disseminate from the intestine to sites of secondary replication (Boehme et al., 2009). Because T1 reoviruses utilize a single mechanism to spread within its host, inhibiting that mode of dissemination prevents virus-induced systemic disease.

T3 reoviruses, in contrast, disseminate to peripheral organs using a combination of hematogenous and neural mechanisms. Neural spread is essential for maximal neural injury induced by T3 reovirus (Tyler et al., 1986). Following peroral inoculation or inoculation into the hindlimb muscle, T3 reovirus infects peripheral neurons and travels along nerve fibers to infect the CNS and cause disease (Morrison et al., 1991; Tyler et al., 1986). Inhibiting neural spread by sectioning the sciatic nerve prior to hindlimb inoculation prevents virus spread to the spinal cord (Tyler et al., 1986). This finding indicates that T3 reovirus spreads along neural routes to the CNS and suggests that neural dissemination is essential for reovirus neuropathogenesis.

The importance of hematogenous spread in reovirus neuropathogenesis is evident from studies that identified host and viral factors that mediate reovirus transport through the blood. JAM-A-deficient mice are completely resistant to reovirus-induced disease following peroral inoculation with T3 reovirus, whereas wild-type mice succumb to infection (Antar et al., 2009). Viral titers in the brains of JAM-A-deficient mice are substantially reduced in comparison to those in wild-type controls. Concordantly, viral loads in the blood of JAM-A-deficient mice are lower than those detected in wild-type mice (Antar et al., 2009). However, following intracranial inoculation, wild-type and JAM-A-deficient mice are equally susceptible to reovirus disease, and equivalent viral yields are produced in the brains of wild-type and JAM-A-deficient mice (Antar et al., 2009). These results indicate that reduced reovirus virulence in JAM-A-deficient mice following peroral inoculation is not the result of differences in reovirus replication in the brain.

Studies of T3 σ1s-null viruses also highlight the requirement of hematogenous dissemination for reovirus neuropathogenesis. Wild-type T3 reovirus is substantially more virulent than the T3 σ1s-null virus following hindlimb inoculation (Fig. 1.7). Approximately 75% of animals inoculated with wild-type virus succumb to infection compared with 25% of mice inoculated with the σ1s-null virus (Boehme et al., 2011). Wild-type and σ1s-null T3 reoviruses induced 100% mortality following intracranial inoculation, although animals inoculated with wild-type virus succumbed to CNS disease with slightly faster kinetics than those inoculated with the σ1s-null virus. Wild-type and σ1s-null viruses also produce equivalent titers in the brain following intracranial inoculation, indicating that σ1s is dispensable for viral replication in the murine CNS. Thus, the disparity in virulence between wild-type and σ1s-null viruses following intramuscular inoculation does not result from differences in replication in the CNS between the two viral strains.

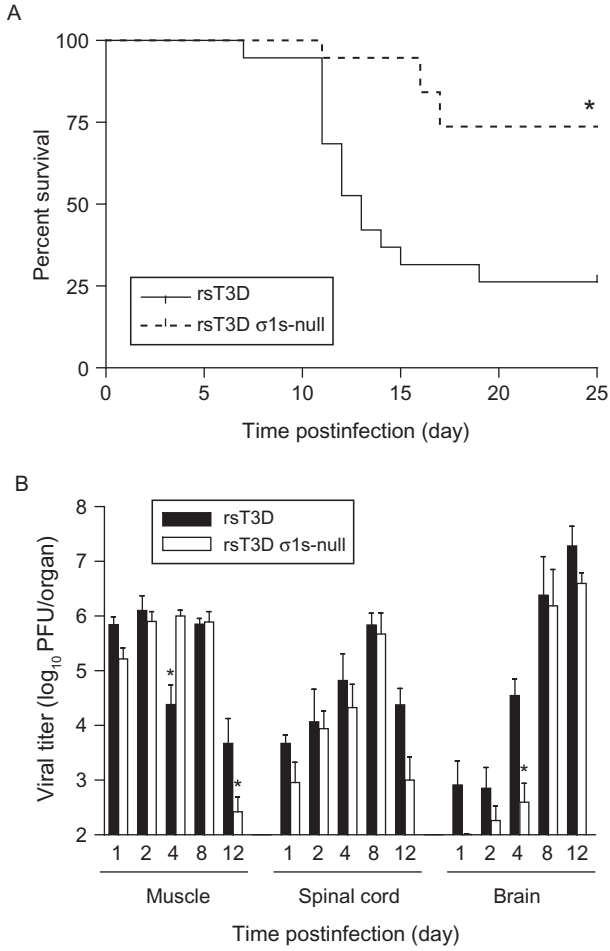

Figure 1.7 The σ1s protein enhances reovirus virulence following intramuscular inoculation. (A) Newborn C57/BL6 mice were inoculated in the left hindlimb with 10^6 PFU of wild-type or σ1s-null T3 reovirus. Mice ($n = 19$ for each virus strain) were monitored for survival for 25 days. $^*P < 0.001$ as determined by log-rank test in comparison to wild-type T3 reovirus. (B) The σ1s protein is not required for reovirus spread by neural routes. Newborn C57/BL6 mice were inoculated in the left hindlimb with 10^6 PFU of wild-type or σ1s-null T3 reovirus. At days 1, 2, 4, 8, and 12 postinoculation, mice were euthanized, hindlimb muscle, spinal cord, and brain were resected, and viral titers were determined by plaque assay. Results are expressed as mean viral titers for six to nine animals for each time point. Error bars indicate SEM. $^*P < 0.05$ as determined by Mann–Whitney test in comparison to wild-type T3 reovirus. *Copyright © American Society for Microbiology, Boehme et al. (2011).*

Following hindlimb inoculation, wild-type virus is detected in the brain 1 day after infection (Fig. 1.7). In contrast, the σ1s-null virus is not found in the brain until 2 days after inoculation. At days 2 and 4 postinoculation, viral titers in the brains of animals inoculated with wild-type virus are markedly higher than those observed in mice inoculated with the σ1s-null mutant. This finding correlates with significantly higher loads of wild-type virus in the blood of infected animals at early times postinoculation compared with the σ1s-null virus (Boehme et al., 2011). Comparable titers of wild-type and σ1s-null viruses are found in the spinal cord at days 1, 2, and 4 post-inoculation. This observation suggests that transport of the σ1s-null virus to the CNS by neural pathways is not impaired. At day 8 postinoculation, titers of wild-type and σ1s-null viruses in the brain are equivalent, possibly reflecting delivery of virus to the brain via neural routes. Collectively, these findings suggest that hematogenous spread is required for reovirus transport to the brain at early times after infection. These results also suggest that the timing of reovirus delivery to the brain is critical for neuropathogenesis. Viral transport by neural routes does not differ between wild-type and σ1s-null viruses, and both virus strains produce equivalent peak titers in the brain. However, peak titers of the σ1s-null virus appear to be achieved after the mice reach the age-imposed limit to reovirus infection, and these animals are no longer susceptible to reovirus-induced CNS disease (Mann, Knipe, Fischbach, & Fields, 2002). Thus, reovirus transport to the brain by the blood at early times after infection is critical for neuropathogenesis.

Reovirus spreads to the spinal cord via the sciatic nerve following intramuscular inoculation into the hindlimb (Tyler et al., 1986). Transection of the sciatic nerve prior to inoculation inhibits neural transmission of the virus to the spinal cord; however, viral dissemination by the blood is unaffected (Tyler et al., 1986). T3 reovirus retains the capacity to spread to the brain after sciatic nerve section (Boehme et al., 2011), suggesting that reovirus can access the brain even in the absence of neural spread, likely via the bloodstream (Fig. 1.8). In addition, almost no virus is detected in the brain following hindlimb inoculation with the σ1s-null virus when the sciatic nerve is sectioned. Thus, virus cannot access the brain when both hematogenous and neural pathways of spread are inhibited.

Together, these findings suggest that (i) spread by neural routes alone is not sufficient to cause reovirus CNS disease, (ii) bloodborne spread is required for delivery of reovirus to the brain at early times postinfection, (iii) hematogenous viral dissemination to the brain is an essential mechanism of reovirus neuropathogenesis, and (iv) virus must be delivered to the brain by the blood early after inoculation for full reovirus neurovirulence.

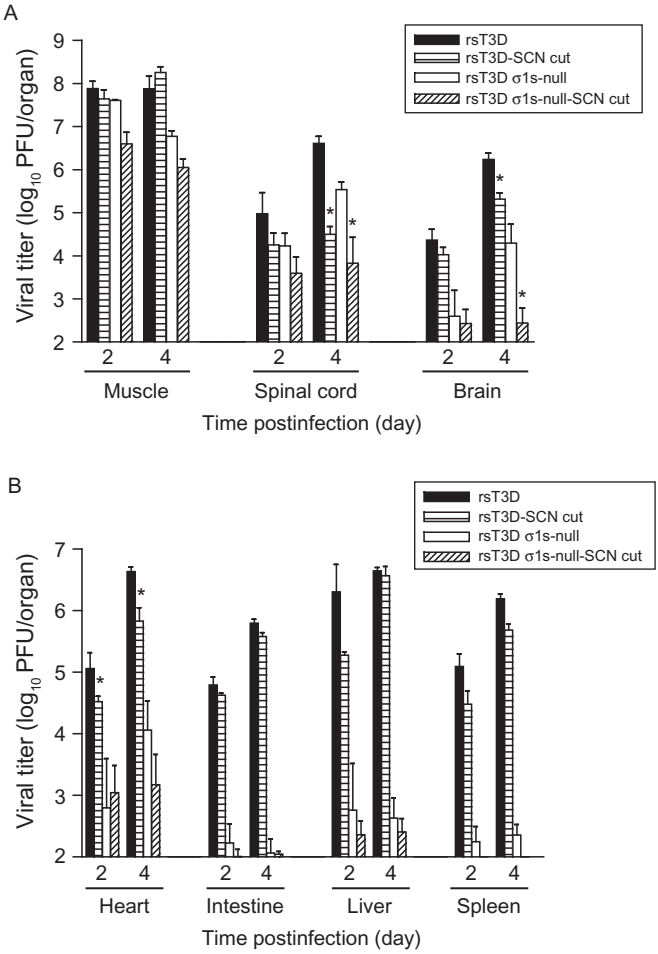

Figure 1.8 Reovirus disseminates to the CNS by hematogenous and neural routes. The left sciatic nerve of newborn C57/BL6 mice was sectioned prior to inoculation in the left hindlimb with 10^6 PFU of wild-type or σ1s-null T3 reovirus. In parallel, mice in which the left sciatic nerve was not sectioned were inoculated in the left hindlimb with 10^6 PFU of wild-type or σ1s-null T3 reovirus. At days 2 and 4 postinoculation, mice were euthanized: (A) hindlimb muscle, spinal cord, and brain and (B) heart, intestine, liver, and spleen were resected, and viral titers were determined by plaque assay. Results are expressed as mean viral titers for six animals for each time point. Error bars indicate SEM. $^*P < 0.05$ as determined by Mann–Whitney test in comparison to animals in which the sciatic nerve was not sectioned. *Copyright © American Society for Microbiology, Boehme et al. (2011).*

6. UNANSWERED QUESTIONS AND FUTURE DIRECTIONS

We have identified host and viral factors essential for the hematogenous dissemination of reovirus. However, many unanswered questions remain. Because viruses capable of bloodstream spread may share similar mechanisms of dissemination, understanding how reovirus spreads in the infected host may aid in the development of therapeutics that target this critical step in viral pathogenesis.

6.1. How does reovirus enter and exit the bloodstream?

To spread to peripheral organs by hematogenous pathways, reovirus must first enter the bloodstream. Studies of reovirus pathogenesis suggest that following peroral inoculation, reovirus infects Peyer patch lymphoid cells that transport virus to the bloodstream (Fig. 1.9). However, reovirus also

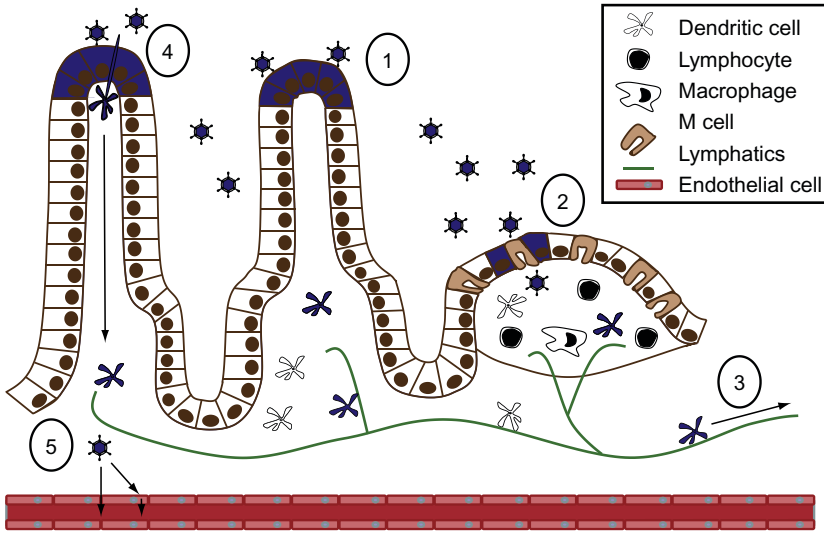

Figure 1.9 Model of reovirus hematogenous spread from the intestine. (1) Following peroral inoculation, reovirus infects intestinal epithelial cells (2) and is taken up by lymphoid cells in the Peyer patch. (3) Infected dendritic cells or lymphocytes carry reovirus from the Peyer patch through the lymphatics and finally to the blood. (4) Phagocytic cells that extend processes into the lumen of the intestine also might be infected for subsequent transport of virus through the lymphatics. (5) Reovirus may enter directly into the blood by passing between endothelial cells or via release into the bloodstream from infected cells.

disseminates hematogenously following intracranial inoculation (Boehme et al., 2011, 2009). This observation suggests that reovirus has the capacity to cross endothelial barriers to enter the blood. Little is known about how reovirus infects polarized cells, such as those that constitute the endothelium. JAM-A localizes to tight junctions linking endothelial cells and functions in maintaining the barrier between the tissue and blood compartments. JAM-A is required for hematogenous spread of reovirus and infection of primary cultures of pulmonary vascular endothelial cells (Antar et al., 2009). We envision several possible mechanisms to explain how reovirus uses JAM-A to facilitate entry into the blood. First, JAM-A may function as a gatekeeper for reovirus entry into the bloodstream (Fig. 1.9). Although reovirus infection does not change the barrier function of primary human airway epithelial cells (Excoffon et al., 2008), it is unclear whether the same phenomenon occurs during reovirus infection of the endothelium. Free reovirus virions may interact with JAM-A in endothelial cell tight junctions, transiently disrupt these structures, and cause focal breaches of the endothelial barrier to allow viral invasion of the bloodstream. Other viruses are known to disrupt polarized cell barriers during infection. Mouse adenovirus-1 infection of endothelial cells reduces tight junction protein expression and decreases barrier function in polarized endothelial cell monolayers (Gralinski et al., 2009). Coxsackieviruses engage decay-accelerating factor, an apically distributed protein of polarized epithelial cells, to disrupt tight junctions (Coyne, Shen, Turner, & Bergelson, 2007). In doing so, coxsackieviruses gain access to the basolaterally located coxsackievirus and adenovirus receptor (Coyne et al., 2007). HIV-1 gp120 diminishes expression of tight junction proteins and increases vascular permeability (Kanmogne et al., 2005).

Second, it is possible that reovirus infects endothelial cells to allow progeny virus to be released directly into the blood (Fig. 1.9). Endothelial cells function as sites of amplification for many viruses that spread via the bloodstream. Murine cytomegalovirus dissemination occurs after an episode of secondary viremia that requires viral replication in endothelial cells (Sacher et al., 2008). It is possible that reovirus productively infects endothelium from the basolateral surface on the abluminal side of the endothelium and is released from the apical surface into the blood. Many viruses that infect polarized cells egress apically (Roberts, 1995). This mechanism is common for respiratory viruses, in which release from the apical surface of infected respiratory epithelial cells ensures that the virus will be shed into the respiratory tract to facilitate transmission to susceptible hosts

(Brock et al., 2003; Gerl et al., 2012; Rodriguez & Sabatini, 1978). Studies of reovirus infection of polarized endothelial cells will shed light on mechanisms used by the virus to traverse endothelial monolayers.

Third, reovirus spread may involve infection or association with hematopoietic cells (Fig. 1.9). Hematopoietic cells express JAM-A as an adhesin to allow monocyte extravasation across endothelial barriers (Martin-Padura et al., 1998; Williams, Martin-Padura, Dejana, Hogg, & Simmons, 1999). It is not known whether hematopoietic cells are infected or whether infected blood cells transport reovirus systemically following infection by a natural route of inoculation. However, in cancer patients treated with an intravenous infusion of reovirus, virions associate with mononuclear cells, granulocytes, and platelets to allow dissemination to tumors localized in the viscera (Adair et al., 2012). If hematopoietic cells are responsible for hematogenous reovirus dissemination, age-dependent restriction of reovirus replication in these cells may be one mechanism to explain the limitation of reovirus disease to newborn animals (Tardieu et al., 1983).

Reovirus exit from the bloodstream is required for infection and replication in target tissues and development of organ-specific disease. After peroral inoculation of reovirus, high viral titers are found in virtually all organs (Antar et al., 2009; Boehme et al., 2011, 2009). Mechanisms similar to those that facilitate reovirus entry into the vasculature may mediate reovirus escape from the blood. Reovirus interactions with JAM-A may induce localized perturbations of tight junction integrity that permit virus escape into tissues. Reovirus virions in the blood may infect endothelial cells from the apical surface and progeny virions may be released basolaterally. Finally, infected hematopoietic cells may transport virus from the blood into target organs. None of these possibilities is mutually exclusive; reovirus may use multiple strategies to enter and exit the bloodstream. Studies using mice with tissue-specific expression of JAM-A may help to elucidate mechanisms by which JAM-A facilitates reovirus spread through the bloodstream.

6.2. How does σ1s promote hematogenous spread?

Mechanisms by which σ1s promotes dissemination have not been determined. The σ1s protein is required for reovirus-induced cell cycle arrest at the G_2/M boundary (Poggioli et al., 2002, 2001) and has been implicated in apoptosis *in vivo* (Hoyt et al., 2005). It not known whether inhibition of cell cycle progression is related to the induction of apoptosis following reovirus infection. Cells respond to replication stress or DNA damage by

activating checkpoints that arrest the cell cycle. For cells in which genomic damage cannot be repaired, apoptosis is induced to ensure that only faithfully replicated DNA is passed to daughter cells. The relationship between cell cycle arrest and apoptosis in the context of reovirus infection has not been examined. It is possible that σ1s-mediated cell cycle arrest contributes to reovirus-induced apoptosis. Interaction of σ1s with components of the host cell cycle machinery that inhibit normal cell cycle progression could cause the cell to undergo apoptosis.

It is not known whether σ1s-dependent cell cycle arrest and apoptosis are responsible for σ1s-mediated reovirus dissemination. It is possible that σ1s-dependent apoptosis in intestinal epithelial cells promotes reovirus uptake by phagocytic cells at the site of inoculation, and these cells in turn traffic virus to the bloodstream where the virus has access to JAM-A. Although σ1s is not required for reovirus replication in cultured cells (Boehme et al., 2011, 2009; Rodgers et al., 1998), it is possible that σ1s is necessary for efficient reovirus replication in specific cell types that are required for viral dissemination. Defining the cell types used by reovirus to spread through the blood may help uncover how σ1s promotes hematogenous spread. Finally, σ1s may mediate evasion of the host immune response, thereby allowing viral spread. Differences in viral dissemination between wild-type and σ1s are evident at early times postinoculation. This suggests that σ1s would dampen host innate immune mechanisms, as opposed to adaptive responses that develop at later times after infection. Determining how σ1s promotes hematogenous reovirus spread is essential to understand how an enteric, neurotropic virus transits from the intestine to the CNS.

6.3. Clinical implications

Defining factors that govern reovirus dissemination in the blood is essential for optimum use of reovirus in clinical applications. Reovirus efficiently replicates in and kills cancer cells (Adair et al., 2012; Karapanagiotou et al., 2012). Phase II and III clinical trials are underway to test the efficacy of reovirus as an adjunct to conventional cancer therapies (Adair et al., 2012; Karapanagiotou et al., 2012; Kottke et al., 2011). Following intravenous administration, reovirus must navigate and exit the bloodstream to infect solid organ tumors. Intratumoral injection of reovirus may allow for enhanced replication in tumor cells and subsequent spread through the blood to target metastatic tumor foci. Thus, defining viral and cellular

determinants underlying how reoviruses gain access to the blood compartment, spread within the bloodstream, and exit from the circulation may aid in oncolytic design. Use of the reverse genetics system may allow engineering of reovirus therapeutics with mutations that increase vector potency or safety by manipulating dissemination determinants (Kobayashi et al., 2007).

We have uncovered a central role for hematogenous dissemination in reovirus neuropathogenesis and elucidated molecular mechanisms that govern reovirus spread by the blood. However, we have much more to learn. Understanding mechanisms of reovirus dissemination will provide broader insight into events at the pathogen–host interface that lead to systemic disease and may aid in the development of therapeutics that target this critical step in viral pathogenesis.

ACKNOWLEDGMENTS

We thank members of our laboratories and Dr. J. Craig Forrest for many useful discussions. This research was supported by Public Health Service awards K22 AI094079 (K. W. B.), F31 NS074596 (C. M. L.), R37 AI38296 (T. S. D.), and the Elizabeth B. Lamb Center for Pediatric Research.

REFERENCES

Adair, R. A., Roulstone, V., Scott, K. J., Morgan, R., Nuovo, G. J., Fuller, M., et al. (2012). Cell carriage, delivery, and selective replication of an oncolytic virus in tumor in patients. *Science Translational Medicine*, *4*, 138ra177.

Amerongen, H. M., Wilson, G. A. R., Fields, B. N., & Neutra, M. R. (1994). Proteolytic processing of reovirus is required for adherence to intestinal M cells. *Journal of Virology*, *68*, 8428–8432.

Antar, A. A. R., Konopka, J. L., Campbell, J. A., Henry, R. A., Perdigoto, A. L., Carter, B. D., et al. (2009). Junctional adhesion molecule-A is required for hematogenous dissemination of reovirus. *Cell Host & Microbe*, *5*, 59–71.

Armstrong, G. D., Paul, R. W., & Lee, P. W. (1984). Studies on reovirus receptors of L cells: Virus binding characteristics and comparison with reovirus receptors of erythrocytes. *Virology*, *138*, 37–48.

Barratt-Boyes, S. M., & MacLachlan, N. J. (1994). Dynamics of viral spread in bluetongue virus infected calves. *Veterinary Microbiology*, *40*, 361–371.

Barton, E. S., Connolly, J. L., Forrest, J. C., Chappell, J. D., & Dermody, T. S. (2001). Utilization of sialic acid as a coreceptor enhances reovirus attachment by multistep adhesion strengthening. *The Journal of Biological Chemistry*, *276*, 2200–2211.

Barton, E. S., Forrest, J. C., Connolly, J. L., Chappell, J. D., Liu, Y., Schnell, F., et al. (2001). Junction adhesion molecule is a receptor for reovirus. *Cell*, *104*, 441–451.

Barton, E. S., Youree, B. E., Ebert, D. H., Forrest, J. C., Connolly, J. L., Valyi-Nagy, T., et al. (2003). Utilization of sialic acid as a coreceptor is required for reovirus-induced biliary disease. *The Journal of Clinical Investigation*, *111*, 1823–1833.

Bass, D. M., Bodkin, D., Dambrauskas, R., Trier, J. S., Fields, B. N., & Wolf, J. L. (1990). Intraluminal proteolytic activation plays an important role in replication of type 1 reovirus in the intestines of neonatal mice. *Journal of Virology*, *64*, 1830–1833.

Bass, D. M., Trier, J. S., Dambrauskas, R., & Wolf, J. L. (1988). Reovirus type 1 infection of small intestinal epithelium in suckling mice and its effect on M cells. *Laboratory Investigations*, *58*, 226–235.

Bazzoni, G. (2003). The JAM family of junctional adhesion molecules. *Current Opinion in Cell Biology*, *15*, 525–530.

Bazzoni, G., Tonetti, P., Manzi, L., Cera, M. R., Balconi, G., & Dejana, E. (2005). Expression of junctional adhesion molecule-A prevents spontaneous and random motility. *Journal of Cell Science*, *118*, 623–632.

Bellum, S. C., Dove, D., Harley, R. A., Greene, W. B., Judson, M. A., London, L., et al. (1997). Respiratory reovirus 1/L induction of intraluminal fibrosis. A model for the study of bronchiolitis obliterans organizing pneumonia. *The American Journal of Pathology*, *150*, 2243–2254.

Bodian, D. (1955). Emerging concept of poliomyelitis infection. *Science*, *122*, 105–108.

Bodkin, D. K., & Fields, B. N. (1989). Growth and survival of reovirus in intestinal tissue: Role of the L2 and S1 genes. *Journal of Virology*, *63*, 1188–1193.

Bodkin, D. K., Nibert, M. L., & Fields, B. N. (1989). Proteolytic digestion of reovirus in the intestinal lumens of neonatal mice. *Journal of Virology*, *63*, 4676–4681.

Boehme, K. W., Frierson, J. M., Konopka, J. L., Kobayashi, T., & Dermody, T. S. (2011). The reovirus sigma1s protein is a determinant of hematogenous but not neural virus dissemination in mice. *Journal of Virology*, *85*, 11781–11790.

Boehme, K. W., Guglielmi, K. M., & Dermody, T. S. (2009). Reovirus nonstructural protein σ1s is required for establishment of viremia and systemic dissemination. *Proceedings of the National Academy of Sciences of the United States of America*, *106*, 19986–19991.

Bokiej, M., Ogden, K. M., Ikizler, M., Reiter, D. M., Stehle, T., & Dermody, T. S. (2012). Optimum length and flexibility of reovirus attachment protein sigma1 are required for efficient viral infection. *Journal of Virology*, *86*, 10270–10280.

Brock, S. C., Goldenring, J. R., & Crowe, J. E., Jr. (2003). Apical recycling systems regulate directional budding of respiratory syncytial virus from polarized epithelial cells. *Proceedings of the National Academy of Sciences of the United States of America*, *100*, 15143–15148.

Campbell, J. A., Shelling, P., Wetzel, J. D., Johnson, E. M., Wilson, G. A. R., Forrest, J. C., et al. (2005). Junctional adhesion molecule-A serves as a receptor for prototype and field-isolate strains of mammalian reovirus. *Journal of Virology*, *79*, 7967–7978.

Carter, P. B., & Collins, F. M. (1974). The route of enteric infection in normal mice. *The Journal of Experimental Medicine*, *139*, 1189–1203.

Cashdollar, L. W., Chmelo, R. A., Wiener, J. R., & Joklik, W. K. (1985). Sequences of the S1 genes of the three serotypes of reovirus. *Proceedings of the National Academy of Sciences of the United States of America*, *82*, 24–28.

Cenatiempo, Y., Twardowski, T., Shoeman, R., Ernst, H., Brot, N., Weissbach, H., et al. (1984). Two initiation sites detected in the small s1 species of reovirus mRNA by dipeptide synthesis in vitro. *Proceedings of the National Academy of Sciences of the United States of America*, *81*, 1084–1088.

Chappell, J. D., Barton, E. S., Smith, T. H., Baer, G. S., Duong, D. T., Nibert, M. L., et al. (1998). Cleavage susceptibility of reovirus attachment protein σ1 during proteolytic disassembly of virions is determined by a sequence polymorphism in the σ1 neck. *Journal of Virology*, *72*, 8205–8213.

Chappell, J. D., Duong, J. L., Wright, B. W., & Dermody, T. S. (2000). Identification of carbohydrate-binding domains in the attachment proteins of type 1 and type 3 reoviruses. *Journal of Virology*, *74*, 8472–8479.

Chappell, J. D., Prota, A., Dermody, T. S., & Stehle, T. (2002). Crystal structure of reovirus attachment protein σ1 reveals evolutionary relationship to adenovirus fiber. *The EMBO Journal*, *21*, 1–11.

Coetzee, P., Van Vuuren, M., Stokstad, M., Myrmel, M., & Venter, E. H. (2012). Bluetongue virus genetic and phenotypic diversity: towards identifying the molecular determinants that influence virulence and transmission potential. *Veterinary Microbiology*, *161*, 1–12.

Corada, M., Chimenti, S., Cera, M. R., Vinci, M., Salio, M., Fiordaliso, F., et al. (2005). Junctional adhesion molecule-A-deficient polymorphonuclear cells show reduced diapedesis in peritonitis and heart ischemia-reperfusion injury. *Proceedings of the National Academy of Sciences of the United States of America*, *102*, 10634–10639.

Coyne, C. B., Shen, L., Turner, J. R., & Bergelson, J. M. (2007). Coxsackievirus entry across epithelial tight junctions requires occludin and the small GTPases Rab34 and Rab5. *Cell Host & Microbe*, *2*, 181–192.

Danthi, P., Guglielmi, K. M., Kirchner, E., Mainou, B., Stehle, T., & Dermody, T. S. (2010). From touchdown to transcription: The reovirus cell entry pathway. *Current Topics in Microbiology and Immunology*, *343*, 91–119.

de Jong, M. D., Simmons, C. P., Thanh, T. T., Hien, V. M., Smith, G. J., Chau, T. N., et al. (2006). Fatal outcome of human influenza A (H5N1) is associated with high viral load and hypercytokinemia. *Nature Medicine*, *12*, 1203–1207.

Dermody, T. S., Nibert, M. L., Bassel-Duby, R., & Fields, B. N. (1990a). A σ1 region important for hemagglutination by serotype 3 reovirus strains. *Journal of Virology*, *64*, 5173–5176.

Dermody, T. S., Nibert, M. L., Bassel-Duby, R., & Fields, B. N. (1990b). Sequence diversity in S1 genes and S1 translation products of 11 serotype 3 reovirus strains. *Journal of Virology*, *64*, 4842–4850.

Dermody, T. S., Parker, J. S., & Sherry, B. (2013). Orthoreoviruses. In: Knipe, D. M., and P. M. Howley (eds.): Fields Virology. Sixth Edition. Lippincott Williams & Wilkins, Philadelphia, pp. 1304–1346.

Dichter, M. A., & Weiner, H. L. (1984). Infection of neuronal cell cultures with reovirus mimics in vitro patterns of neurotropism. *Annals of Neurology*, *16*, 603–610.

Dryden, K. A., Wang, G., Yeager, M., Nibert, M. L., Coombs, K. M., Furlong, D. B., et al. (1993). Early steps in reovirus infection are associated with dramatic changes in supramolecular structure and protein conformation: Analysis of virions and subviral particles by cryoelectron microscopy and image reconstruction. *The Journal of Cell Biology*, *122*, 1023–1041.

Ellis, J. A., Coen, M. L., MacLachlan, N. J., Wilson, W. C., Williams, E. S., & Leudke, A. J. (1993). Prevalence of bluetongue virus expression in leukocytes from experimentally infected ruminants. *American Journal of Veterinary Research*, *54*, 1452–1456.

Ernst, H., & Shatkin, A. J. (1985). Reovirus hemagglutinin mRNA codes for two polypeptides in overlapping reading frames. *Proceedings of the National Academy of Sciences of the United States of America*, *82*, 48–52.

Excoffon, K. J. D. A., Guglielmi, K. M., Wetzel, J. D., Gansemer, N. D., Campbell, J. A., Dermody, T. S., et al. (2008). Reovirus preferentially infects the basolateral surface and is released from the apical surface of polarized human respiratory epithelial cells. *The Journal of Infectious Diseases*, *197*, 1189–1197.

Fields, B. N. (1992). Studies of reovirus pathogenesis reveal potential sites for antiviral intervention. *Advances in Experimental Medicine and Biology*, *312*, 1–14.

Fleeton, M., Contractor, N., Leon, F., Wetzel, J. D., Dermody, T. S., & Kelsall, B. (2004). Peyer's patch dendritic cells process viral antigen from apoptotic epithelial cells in the intestine of reovirus-infected mice. *The Journal of Experimental Medicine*, *200*, 235–245.

Fraser, R. D. B., Furlong, D. B., Trus, B. L., Nibert, M. L., Fields, B. N., & Steven, A. C. (1990). Molecular structure of the cell-attachment protein of reovirus: Correlation of computer-processed electron micrographs with sequence-based predictions. *Journal of Virology*, *64*, 2990–3000.

Frierson, J. M., Pruijssers, A. J., Konopka, J. L., Reiter, D. M., Abel, T. W., Stehle, T., et al. (2012). Utilization of sialylated glycans as coreceptors enhances the neurovirulence of serotype 3 reovirus. *Journal of Virology*, *86*, 13164–13173.

Galan, J. E., & Curtiss, R., 3rd. (1989). Cloning and molecular characterization of genes whose products allow Salmonella typhimurium to penetrate tissue culture cells. *Proceedings of the National Academy of Sciences of the United States of America*, *86*, 6383–6387.

Gerl, M. J., Sampaio, J. L., Urban, S., Kalvodova, L., Verbavatz, J. M., Binnington, B., et al. (2012). Quantitative analysis of the lipidomes of the influenza virus envelope and MDCK cell apical membrane. *Journal of Cell Biology*, *196*, 213–221.

Ghislin, S., Obino, D., Middendorp, S., Boggetto, N., Alcaide-Loridan, C., & Deshayes, F. (2011). Junctional adhesion molecules are required for melanoma cell lines transendothelial migration in vitro. *Pigment Cell & Melanoma Research*, *24*, 504–511.

Golden, J. W., & Schiff, L. A. (2005). Neutrophil elastase, an acid-independent serine protease, facilitates reovirus uncoating and infection in U937 promonocyte cells. *Virology Journal*, *2*, 48.

Gralinski, L. E., Ashley, S. L., Dixon, S. D., & Spindler, K. R. (2009). Mouse adenovirus type 1-induced breakdown of the blood-brain barrier. *Journal of Virology*, *83*, 9398–9410.

Gu, J., Xie, Z., Gao, Z., Liu, J., Korteweg, C., Ye, J., et al. (2007). H5N1 infection of the respiratory tract and beyond: A molecular pathology study. *The Lancet*, *370*, 1137–1145.

Hansson, G., Kristensson, K., Olsson, Y., & Sjostrand, J. (1971). Embryonal and postnatal development of mast cells in rat peripheral nerve. *Acta Neuropathologica*, *17*, 139–149.

Hoyt, C. C., Bouchard, R. J., & Tyler, K. L. (2004). Novel nuclear herniations induced by nuclear localization of a viral protein. *Journal of Virology*, *78*, 6360–6369.

Hoyt, C. C., Richardson-Burns, S. M., Goody, R. J., Robinson, B. A., Debiasi, R. L., & Tyler, K. L. (2005). Nonstructural protein σ1s is a determinant of reovirus virulence and influences the kinetics and severity of apoptosis induction in the heart and central nervous system. *Journal of Virology*, *79*, 2743–2753.

Iden, S., Misselwitz, S., Peddibhotla, S. S. D., Tuncay, H., Rehder, D., Gerke, V., et al. (2012). aPKC phosphorylates JAM-A at Ser285 to promote cell contact maturation and tight junction formation. *The Journal of Cell Biology*, *196*, 623–639.

Isberg, R. R., & Barnes, P. (2001). Subversion of integrins by enteropathogenic Yersinia. *Journal of Cell Science*, *114*, 21–28.

Iwasaki, A. (2007). Mucosal dendritic cells. *Annual Review of Immunology*, *25*, 381–418.

Jones, B. D., Ghori, N., & Falkow, S. (1994). Salmonella typhimurium initiates murine infection by penetrating and destroying the specialized epithelial M cells of the Peyer's patches. *The Journal of Experimental Medicine*, *180*, 15–23.

Kanmogne, G. D., Primeaux, C., & Grammas, P. (2005). HIV-1 gp120 proteins alter tight junction protein expression and brain endothelial cell permeability: implications for the pathogenesis of HIV-associated dementia. *Journal of Neuropathology and Experimental Neurology*, *64*, 498–505.

Karapanagiotou, E. M., Roulstone, V., Twigger, K., Ball, M., Tanay, M., Nutting, C., et al. (2012). Phase I/II trial of carboplatin and paclitaxel chemotherapy in combination with intravenous oncolytic reovirus in patients with advanced malignancies. *Clinical Cancer Research*, *18*, 2080–2089.

Kirchner, E., Guglielmi, K. M., Strauss, H. M., Dermody, T. S., & Stehle, T. (2008). Structure of reovirus σ1 in complex with its receptor junctional adhesion molecule-A. *PLoS Pathology*, *4*, e1000235.

Kobayashi, T., Antar, A. A. R., Boehme, K. W., Danthi, P., Eby, E. A., Guglielmi, K. M., et al. (2007). A plasmid-based reverse genetics system for animal double-stranded RNA viruses. *Cell Host & Microbe*, *1*, 147–157.

Kobayashi, T., Ooms, L. S., Ikizler, M., Chappell, J. D., & Dermody, T. S. (2010). An improved reverse genetics system for mammalian orthoreoviruses. *Virology*, *2*, 194–200.

Kottke, T., Chester, J., Ilett, E., Thompson, J., Diaz, R., Coffey, M., et al. (2011). Precise scheduling of chemotherapy primes VEGF-producing tumors for successful systemic oncolytic virotherapy. *Molecular Therapy*, *19*, 1802–1812.

Kuiken, T., Fouchier, R. A., Schutten, M., Rimmelzwaan, G. F., van Amerongen, G., van Riel, D., et al. (2003). Newly discovered coronavirus as the primary cause of severe acute respiratory syndrome. *The Lancet*, *362*, 263–270.

Lee, P. W., Hayes, E. C., & Joklik, W. K. (1981). Protein sigma 1 is the reovirus cell attachment protein. *Virology*, *108*, 156–163.

MacLachlan, N. J., Jagels, G., Rossitto, P. V., Moore, P. F., & Heidner, H. W. (1990). The pathogenesis of experimental bluetongue virus infection of calves. *Veterinary Pathology*, *27*, 223–229.

Maginnis, M. S., Forrest, J. C., Kopecky-Bromberg, S. A., Dickeson, S. K., Santoro, S. A., Zutter, M. M., et al. (2006). Beta1 integrin mediates internalization of mammalian reovirus. *Journal of Virology*, *80*, 2760–2770.

Mahrt, C. R., & Osburn, B. I. (1986). Experimental bluetongue virus infection of sheep; effect of vaccination: Pathologic, immunofluorescent, and ultrastructural studies. *American Journal of Veterinary Research*, *47*, 1198–1203.

Mainou, B. A., & Dermody, T. S. (2012). Transport to late endosomes is required for efficient reovirus infection. *Journal of Virology*, *86*, 8346–8358.

Mandell, K. J., Babbin, B. A., Nusrat, A., & Parkos, C. A. (2005). Junctional adhesion molecule-1 (JAM1) regulates epithelial cell morphology through effects on β1 integrins and Rap1 activity. *The Journal of Biological Chemistry*, *280*, 11665–11674.

Mann, M. A., Knipe, D. M., Fischbach, G. D., & Fields, B. N. (2002). Type 3 reovirus neuroinvasion after intramuscular inoculation: Direct invasion of nerve terminals and age-dependent pathogenesis. *Virology*, *303*, 222–231.

Martin-Padura, I., Lostaglio, S., Schneemann, M., Williams, L., Romano, M., Fruscella, P., et al. (1998). Junctional adhesion molecule, a novel member of the immunoglobulin superfamily that distributes at intercellular junctions and modulates monocyte transmigration. *The Journal of Cell Biology*, *142*, 117–127.

Mercier, G. T., Campbell, J. A., Chappell, J. D., Stehle, T., Dermody, T. S., & Barry, M. A. (2004). A chimeric adenovirus vector encoding reovirus attachment protein σ1 targets cells expressing junctional adhesion molecule 1. *Proceedings of the National Academy of Sciences of the United States of America*, *101*, 6188–6193.

Morin, M. J., Warner, A., & Fields, B. N. (1994). A pathway for entry of reoviruses into the host through M cells of the respiratory tract. *The Journal of Experimental Medicine*, *180*, 1523–1527.

Morin, M. J., Warner, A., & Fields, B. N. (1996). Reovirus infection in rat lungs as a model to study the pathogenesis of viral pneumonia. *Journal of Virology*, *70*, 541–548.

Morrison, L. A., Sidman, R. L., & Fields, B. N. (1991). Direct spread of reovirus from the intestinal lumen to the central nervous system through vagal autonomic nerve fibers. *Proceedings of the National Academy of Sciences of the United States of America*, *88*, 3852–3856.

Muthukkumar, S., Goldstein, J., & Stein, K. E. (2000). The ability of B cells and dendritic cells to present antigen increases during ontogeny. *The Journal of Immunology*, *165*, 4803–4813.

Naik, U. P., Naik, M. U., Eckfeld, K., Martin-DeLeon, P., & Spychala, J. (2001). Characterization and chromosomal localization of JAM-1, a platelet receptor for a stimulatory monoclonal antibody. *Journal of Cell Science*, *114*, 539–547.

Nason, E. L., Wetzel, J. D., Mukherjee, S. K., Barton, E. S., Prasad, B. V. V., & Dermody, T. S. (2001). A monoclonal antibody specific for reovirus outer-capsid protein σ3 inhibits σ1-mediated hemagglutination by steric hindrance. *Journal of Virology*, *75*, 6625–6634.

Nathanson, N., & Tyler, K. L. (1997). Entry, dissemination, shedding, and transmission of viruses. In N. Nathanson (Ed.), *Viral pathogenesis* (pp. 13–33). Philadelphia: Lippincott-Raven.

Nibert, M. L., Chappell, J. D., & Dermody, T. S. (1995). Infectious subvirion particles of reovirus type 3 Dearing exhibit a loss in infectivity and contain a cleaved σ1 protein. *Journal of Virology*, *69*, 5057–5067.

Nibert, M. L., Odegard, A. L., Agosto, M. A., Chandran, K., & Schiff, L. A. (2005). Putative autocleavage of reovirus mu1 protein in concert with outer-capsid disassembly and activation for membrane permeabilization. *Journal of Molecular Biology*, *345*, 461–474.

Nomme, J., Fanning, A. S., Caffrey, M., Lye, M. F., Anderson, J. M., & Lavie, A. (2011). The Src homology 3 domain is required for junctional adhesion molecule binding to the third PDZ domain of the scaffolding protein ZO-1. *The Journal of Biological Chemistry*, *286*, 43352–43360.

Nygaard, R., Golden, J. W., & Schiff, L. A. (2012). Impact of host proteases on reovirus infection in the respiratory tract. *Journal of Virology*, *86*, 1238–1243.

Odegard, A. L., Chandran, K., Zhang, X., Parker, J. S., Baker, T. S., & Nibert, M. L. (2004). Putative autocleavage of outer capsid protein micro1, allowing release of myristoylated peptide micro1N during particle uncoating, is critical for cell entry by reovirus. *Journal of Virology*, *78*, 8732–8745.

Oshiro, L. S., Dondero, D. V., Emmons, R. W., & Lennette, E. H. (1978). The development of Colorado tick fever virus within cells of the haemopoietic system. *The Journal of General Virology*, *39*, 73–79.

Ostermann, G., Fraemohs, L., Baltus, T., Schober, A., Lietz, M., Zernecke, A., et al. (2005). Involvement of JAM-A in mononuclear cell recruitment on inflamed or atherosclerotic endothelium: Inhibition by soluble JAM-A. *Arteriosclerosis, Thrombosis, and Vascular Biology*, *25*, 729–735.

Pacitti, A., & Gentsch, J. R. (1987). Inhibition of reovirus type 3 binding to host cells by sialylated glycoproteins is mediated through the viral attachment protein. *Journal of Virology*, *61*, 1407–1415.

Pallansch, M. A., & Roos, R. P. (2001). Enteroviruses: Polioviruses, coxsacieviruses, echoviruses. In D. M. Knipe & P. M. Howley (Eds.), *Fields virology* (pp. 723–775). Philadelphia: Lippincott-Raven Press.

Parashar, U. D., Bresee, J. S., Gentsch, J. R., & Glass, R. I. (1998). Rotavirus. *Emerging Infectious Diseases*, *4*, 561–570.

Parashar, K., Tarlow, M. J., & McCrae, M. A. (1992). Experimental reovirus type 3-induced murine biliary tract disease. *Journal of Pediatric Surgery*, *27*, 843–847.

Paul, R. W., Choi, A. H., & Lee, P. W. K. (1989). The α-anomeric form of sialic acid is the minimal receptor determinant recognized by reovirus. *Virology*, *172*, 382–385.

Paul, R. W., & Lee, P. W. K. (1987). Glycophorin is the reovirus receptor on human erythrocytes. *Virology*, *159*, 94–101.

Poggioli, G. J., DeBiasi, R. L., Bickel, R., Jotte, R., Spalding, A., Johnson, G. L., et al. (2002). Reovirus-induced alterations in gene expression related to cell cycle regulation. *Journal of Virology*, *76*, 2585–2594.

Poggioli, G. J., Dermody, T. S., & Tyler, K. L. (2001). Reovirus-induced σ1s-dependent G2/M cell cycle arrest results from inhibition of p34cdc2. *Journal of Virology*, *75*, 7429–7434.

Poggioli, G. J., Keefer, C. J., Connolly, J. L., Dermody, T. S., & Tyler, K. L. (2000). Reovirus-induced G2/M cell cycle arrest requires σ1s and occurs in the absence of apoptosis. *Journal of Virology*, *74*, 9562–9570.

Prota, A. E., Campbell, J. A., Schelling, P., Forrest, J. C., Peters, T. R., Watson, M. J., et al. (2003). Crystal structure of human junctional adhesion molecule 1: Implications for reovirus binding. *Proceedings of the National Academy of Sciences of the United States of America*, *100*, 5366–5371.

Ramos-Alvarez, M., & Sabin, A. B. (1954). Characteristics of poliomyelitis and other enteric viruses recovered in tissue culture from healthy American children. *Proceedings of the Society for Experimental Biology and Medicine*, *87*, 655–661.

Ramos-Alvarez, M., & Sabin, A. B. (1956). Intestinal flora of healthy children demonstrable by monkey kidney tissue culture. *American Journal of Public Health*, *46*, 295–299.
Ramos-Alvarez, M., & Sabin, A. B. (1958). Enteropathogenic viruses and bacteria. Role in summer diarrheal diseases of infancy and early childhood. *JAMA: The Journal of the American Medical Association*, *167*, 147–158.
Reiss, K., Stencel, J. E., Liu, Y., Blaum, B. S., Reiter, D. M., Feizi, T., et al. (2012). The GM2 glycan serves as a functional coreceptor for serotype 1 reovirus. *PLoS Pathogens*, *8*, e1003078.
Reiter, D. M., Frierson, J. M., Halvorson, E. E., Kobayashi, T., Dermody, T. S., & Stehle, T. (2011). Crystal structure of reovirus attachment protein σ1 in complex with sialylated oligosaccharides. *PLoS Pathology*, *7*, e1002166.
Rescigno, M., Rotta, G., Valzasina, B., & Ricciardi-Castagnoli, P. (2001). Dendritic cells shuttle microbes across gut epithelial monolayers. *Immunobiology*, *204*, 572–581.
Richardson, S. C., Bishop, R. F., & Smith, A. L. (1994). Reovirus serotype 3 infection in infants with extrahepatic biliary atresia or neonatal hepatitis. *Journal of Gastroenterology and Hepatology*, *9*, 264–268.
Roberts, S. R., Compans, R. W., & Wertz, G. W. (1995). Respiratory syncytial virus matures at the apical surfaces of polarized epithelial cells. *Journal of Virology*, *69*, 2667–2673.
Rodgers, S. E., Connolly, J. L., Chappell, J. D., & Dermody, T. S. (1998). Reovirus growth in cell culture does not require the full complement of viral proteins: Identification of a σ1s-null mutant. *Journal of Virology*, *72*, 8597–8604.
Rodriguez Boulan, E., & Sabatini, D. D. (1978). Asymmetric budding of viruses in epithelial monolayers: a model system for study of epithelial polarity. *Proceedings of the National Academy of Sciences of the United States of America*, *75*, 5071–5075.
Rubin, D. H. (1987). Reovirus serotype 1 binds to the basolateral membrane of intestinal epithelial cells. *Microbial Pathogenesis*, *3*, 215–220.
Rubin, D. H., Eaton, M. A., & Anderson, A. O. (1986). Reovirus infection in adult mice: The virus hemagglutinin determines the site of intestinal disease. *Microbial Pathogenesis*, *1*, 79–87.
Rubin, D. H., Kornstein, M. J., & Anderson, A. O. (1985). Reovirus serotype 1 intestinal infection: A novel replicative cycle with ileal disease. *Journal of Virology*, *53*, 391–398.
Sabin, A. B. (1956). Pathogenesis of poliomyelitis; reappraisal in the light of new data. *Science*, *123*, 1151–1157.
Sabin, A. B. (1959). Reoviruses: A new group of respiratory and enteric viruses formerly classified as ECHO type 10 is described. *Science*, *130*, 1387–1389.
Sacher, T., Podlech, J., Mohr, C. A., Jordan, S., Ruzsics, Z., Reddehase, M. J., et al. (2008). The major virus-producing cell type during murine cytomegalovirus infection, the hepatocyte, is not the source of virus dissemination in the host. *Cell Host & Microbe*, *3*, 263–272.
Sarkar, G., Pelletier, J., Bassel-Duby, R., Jayasuriya, A., Fields, B. N., & Sonenberg, N. (1985). Identification of a new polypeptide coded by reovirus gene S1. *Journal of Virology*, *54*, 720–725.
Sjostrand, J., & Karlsson, J. O. (1969). Axoplasmic transport in the optic nerve and tract of the rabbit: A biochemical and radioautographic study. *Journal of Neurochemistry*, *16*, 833–844.
Sobocka, M. B., Sobocki, T., Babinska, A., Hartwig, J., Li, M., Ehrlich, Y. H., et al. (2004). Signaling pathways of the F11 receptor (F11R; a.k.a. JAM-1, JAM-A) in human platelets: F11R dimerization, phosphorylation and complex formation with the integrin GPIIIa. *Journal of Receptors and Signal Transduction Research*, *24*, 85–105.
Sobocka, M. B., Sobocki, T., Banerjee, P., Weiss, C., Rushbrook, J. I., Norin, A. J., et al. (2000). Cloning of the human platelet F11 receptor: A cell adhesion molecule member of the immunoglobulin superfamily involved in platelet aggregation. *Blood*, *95*, 2600–2609.

Tardieu, M., Powers, M. L., & Weiner, H. L. (1983). Age-dependent susceptibility to reovirus type 3 encephalitis: Role of viral and host factors. *Annals of Neurology*, *13*, 602–607.
Tardieu, M., & Weiner, H. L. (1982). Viral receptors on isolated murine and human ependymal cells. *Science*, *215*, 419–421.
Tyler, K. L., McPhee, D. A., & Fields, B. N. (1986). Distinct pathways of viral spread in the host determined by reovirus S1 gene segment. *Science*, *233*, 770–774.
Tyler, K. L., Sokol, R. J., Oberhaus, S. M., Le, M., Karrer, F. M., Narkewicz, M. R., et al. (1998). Detection of reovirus RNA in hepatobiliary tissues from patients with extrahepatic biliary atresia and choledochal cysts. *Hepatology*, *27*, 1475–1482.
van de Pavert, S. A., & Mebius, R. E. (2010). New insights into the development of lymphoid tissues. *Nature Reviews. Immunology*, *10*, 664–674.
Vazquez-Torres, A., Jones-Carson, J., Baumler, A. J., Falkow, S., Valdivia, R., Brown, W., et al. (1999). Extraintestinal dissemination of Salmonella by CD18-expressing phagocytes. *Nature*, *401*, 804–808.
Veronesi, E., Darpel, K. E., Hamblin, C., Carpenter, S., Takamatsu, H. H., Anthony, S. J., et al. (2009). Viraemia and clinical disease in Dorset Poll sheep following vaccination with live attenuated bluetongue virus vaccines serotypes 16 and 4. *Vaccine*, *28*, 1397–1403.
Weiner, H. L., Ault, K. A., & Fields, B. N. (1980). Interaction of reovirus with cell surface receptors. I. Murine and human lymphocytes have a receptor for the hemagglutinin of reovirus type 3. *The Journal of Immunology*, *124*, 2143–2148.
Weiner, H. L., Drayna, D., Averill, D. R., Jr., & Fields, B. N. (1977). Molecular basis of reovirus virulence: Role of the S1 gene. *Proceedings of the National Academy of Sciences of the United States of America*, *74*, 5744–5748.
Weiner, H. L., Powers, M. L., & Fields, B. N. (1980). Absolute linkage of virulence and central nervous system cell tropism of reoviruses to viral hemagglutinin. *The Journal of Infectious Diseases*, *141*, 609–616.
Williams, L. A., Martin-Padura, I., Dejana, E., Hogg, N., & Simmons, D. L. (1999). Identification and characterisation of human junctional adhesion molecule (JAM). *Molecular Immunology*, *36*, 1175–1188.
Wolf, J. L., Dambrauskas, R., Sharpe, A. H., & Trier, J. S. (1987). Adherence to and penetration of the intestinal epithelium by reovirus type 1 in neonatal mice. *Gastroenterology*, *92*, 82–91.
Wolf, J. L., Kauffman, R. S., Finberg, R., Dambrauskas, R., Fields, B. N., & Trier, J. S. (1983). Determinants of reovirus interaction with the intestinal M cells and absorptive cells of murine intestine. *Gastroenterology*, *85*, 291–300.
Wolf, J. L., Rubin, D. H., Finberg, R., Kaufman, R. S., Sharpe, A. H., Trier, J. S., et al. (1981). Intestinal M cells: A pathway of entry of reovirus into the host. *Science*, *212*, 471–472.
Woodfin, A., Reichel, C. A., Khandoga, A., Corada, M., Voisin, M. B., Scheiermann, C., et al. (2007). JAM-A mediates neutrophil transmigration in a stimulus-specific manner in vivo: Evidence for sequential roles for JAM-A and PECAM-1 in neutrophil transmigration. *Blood*, *110*, 1848–1856.

REFERENCES

1. **Dermody TS, Parker JS, Sherry B.** 2013. Orthoreoviruses, p. 1304-1346. *In* Knipe DM, Howley PM (ed.), Fields Virology, Sixth ed. Lippincott Williams & Wilkins, Philadelphia.

2. **Parashar UD, Bresee JS, Gentsch JR, Glass RI.** 1998. Rotavirus. Emerging Infectious Diseases **4:**561-570.

3. **Coetzee P, Stokstad M, Venter EH, Myrmel M, Van Vuuren M.** 2012. Bluetongue: a historical and epidemiological perspective with the emphasis on South Africa. Virology Journal **9:**198.

4. **Kobayashi T, Antar AAR, Boehme KW, Danthi P, Eby EA, Guglielmi KM, Holm GH, Johnson EM, Maginnis MS, Naik S, Skelton WB, Wetzel JD, Wilson GJ, Chappell JD, Dermody TS.** 2007. A plasmid-based reverse genetics system for animal double-stranded RNA viruses. Cell Host Microbe **1:**147-157.

5. **Kobayashi T, Ooms LS, Ikizler M, Chappell JD, Dermody TS.** 2010. An improved reverse genetics system for mammalian orthoreoviruses. Virology **2:**194-200.

6. **Fields BN.** 1992. Studies of reovirus pathogenesis reveal potential sites for antiviral intervention. Advances in Experimental Medical Biology **312:**1-14.

7. **Parashar K, Tarlow MJ, McCrae MA.** 1992. Experimental reovirus type 3-induced murine biliary tract disease. Journal of Pediatric Surgery **27:**843-847.

8. **Dryden KA, Wang G, Yeager M, Nibert ML, Coombs KM, Furlong DB, Fields BN, Baker TS.** 1993. Early steps in reovirus infection are associated with dramatic changes in supramolecular structure and protein conformation: analysis of virions and subviral particles by cryoelectron microscopy and image reconstruction. Journal of Cell Biology **122:**1023-1041.

9. **Chappell JD, Prota A, Dermody TS, Stehle T.** 2002. Crystal structure of reovirus attachment protein s1 reveals evolutionary relationship to adenovirus fiber. EMBO Journal **21:**1-11.

10. **Fraser RDB, Furlong DB, Trus BL, Nibert ML, Fields BN, Steven AC.** 1990. Molecular structure of the cell-attachment protein of reovirus: correlation of computer-processed electron micrographs with sequence-based predictions. Journal of Virology **64:**2990-3000.

11. **Reiter DM, Frierson JM, Halvorson EE, Kobayashi T, Dermody TS, Stehle T.** 2011. Crystal structure of reovirus attachment protein s1 in complex with sialylated oligosaccharides. PLoS Pathogens **7:**e1002166.

12. **Mercier GT, Campbell JA, Chappell JD, Stehle T, Dermody TS, Barry MA.** 2004. A chimeric adenovirus vector encoding reovirus attachment protein s1 targets cells expressing junctional adhesion molecule 1. Proceedings of the National Academy of Sciences USA **101:**6188-6193.

13. **Bokiej M, Ogden KM, Ikizler M, Reiter DM, Stehle T, Dermody TS.** 2012. Optimum length and flexibility of reovirus attachment protein s1 are required for efficient viral infection. Journal of Virology **86:**10270-10280.

14. **Weiner HL, Ault KA, Fields BN.** 1980. Interaction of reovirus with cell surface receptors. I. Murine and human lymphocytes have a receptor for the hemagglutinin of reovirus type 3. J Immunol **124:**2143-2148.

15. **Lee PW, Hayes EC, Joklik WK.** 1981. Protein sigma 1 is the reovirus cell attachment protein. Virology **108:**156-163.

16. **Paul RW, Choi AH, Lee PWK.** 1989. The a-anomeric form of sialic acid is the minimal receptor determinant recognized by reovirus. Virology **172:**382-385.

17. **Paul RW, Lee PWK.** 1987. Glycophorin is the reovirus receptor on human erythrocytes. Virology **159:**94-101.

18. **Armstrong GD, Paul RW, Lee PW.** 1984. Studies on reovirus receptors of L cells: virus binding characteristics and comparison with reovirus receptors of erythrocytes. Virology **138:**37-48.

19. **Dermody TS, Nibert ML, Bassel-Duby R, Fields BN.** 1990. A s1 region important for hemagglutination by serotype 3 reovirus strains. Journal of Virology **64:**5173-5176.

20. **Pacitti A, Gentsch JR.** 1987. Inhibition of reovirus type 3 binding to host cells by sialylated glycoproteins is mediated through the viral attachment protein. Journal of Virology **61:**1407-1415.

21. **Reiss K, Stencel JE, Liu Y, Blaum BS, Reiter DM, Feizi T, Dermody TS, Stehle T.** 2012. The GM2 glycan serves as a functional co-receptor for serotype 1 reovirus. PLoS Pathogens **8:**e1003078.

22. **Barton ES, Forrest JC, Connolly JL, Chappell JD, Liu Y, Schnell F, Nusrat A, Parkos CA, Dermody TS.** 2001. Junction adhesion molecule is a receptor for reovirus. Cell **104:**441-451.

23. **Campbell JA, Shelling P, Wetzel JD, Johnson EM, Wilson GAR, Forrest JC, Aurrand-Lions M, Imhof B, Stehle T, Dermody TS.** 2005. Junctional adhesion molecule-A serves as a receptor for prototype and field-isolate strains of mammalian reovirus. Journal of Virology **79:**7967-7978.

24. **Prota AE, Campbell JA, Schelling P, Forrest JC, Peters TR, Watson MJ, Aurrand-Lions M, Imhof B, Dermody TS, Stehle T.** 2003. Crystal structure of human junctional adhesion molecule 1: implications for reovirus binding. Proceedings of the National Academy of Sciences USA **100:**5366-5371.

25. **Chappell JD, Duong JL, Wright BW, Dermody TS.** 2000. Identification of carbohydrate-binding domains in the attachment proteins of type 1 and type 3 reoviruses. Journal of Virology **74:**8472-8479.

26. **Kirchner E, Guglielmi KM, Strauss HM, Dermody TS, Stehle T.** 2008. Structure of reovirus s1 in complex with its receptor junctional adhesion molecule-A. PLoS Pathogens **4:**e1000235.

27. **Maginnis MS, Forrest JC, Kopecky-Bromberg SA, Dickeson SK, Santoro SA, Zutter MM, Nemerow GR, Bergelson JM, Dermody TS.** 2006. Beta1 integrin mediates internalization of mammalian reovirus. J Virol **80:**2760-2770.

28. **Mainou BA, Dermody TS.** 2012. Transport to late endosomes is required for efficient reovirus infection. Journal of Virology **86:**8346-8358.

29. **Danthi P, Guglielmi KM, Kirchner E, Mainou B, Stehle T, Dermody TS.** 2010. From touchdown to transcription: the reovirus cell entry pathway. Current Topics in Microbiology & Immunology **343:**91-119.

30. **Nibert ML, Odegard AL, Agosto MA, Chandran K, Schiff LA.** 2005. Putative autocleavage of reovirus mu1 protein in concert with outer-capsid disassembly and activation for membrane permeabilization. J Mol Biol **345:**461-474.

31. **Odegard AL, Chandran K, Zhang X, Parker JS, Baker TS, Nibert ML.** 2004. Putative autocleavage of outer capsid protein micro1, allowing release of myristoylated peptide micro1N during particle uncoating, is critical for cell entry by reovirus. J Virol **78:**8732-8745.

32. **Ooms LS, Jerome WG, Dermody TS, Chappell JD.** 2012. Reovirus replication protein M2 influences cell tropism by promoting particle assembly within viral inclusions. Journal of Virology **86:**10979-10987.

33. **Leone G, Coffey MC, Gilmore R, Duncan R, Maybaum L, Lee PWK.** 1996. C-terminal trimerization, but not N-terminal trimerization, of the reovirus cell attachment protein is a posttranslational and Hsp70/ATP- dependent process. Journal of Biological Chemistry **271:**8466-8471.

34. **Zhao Y, Gilmore R, Leone G, Coffey M, Weber B, Lee P.** 2001. Hsp90 phosphorylation is linked to its chaperoning function: Assembly of the reovirus cell attachment protein. Journal of Biological Chemistry.

35. **Connolly JL, Rodgers SE, Clarke P, Ballard DW, Kerr LD, Tyler KL, Dermody TS.** 2000. Reovirus-induced apoptosis requires activation of transcription factor NF-kB. Journal of Virology **74:**2981-2989.

36. **Connolly JL, Barton ES, Dermody TS.** 2001. Reovirus binding to cell surface sialic acid potentiates virus-induced apoptosis. Journal of Virology **75:**4029-4039.

37. **Rodgers SE, Barton ES, Oberhaus SM, Pike B, Gibson CA, Tyler KL, Dermody TS.** 1997. Reovirus-induced apoptosis of MDCK cells is not linked to viral yield and is blocked by Bcl-2. Journal of Virology **71:**2540-2546.

38. **Tyler KL, Squier MK, Rodgers SE, Schneider SE, Oberhaus SM, Grdina TA, Cohen JJ, Dermody TS.** 1995. Differences in the capacity of reovirus strains to induce apoptosis are determined by the viral attachment protein s1. Journal of Virology **69:**6972-6979.

39. **Bazzoni G.** 2003. The JAM family of junctional adhesion molecules. Current Opinion in Cell Biology **15:**525-530.

40. **Martin-Padura I, Lostaglio S, Schneemann M, Williams L, Romano M, Fruscella P, Panzeri C, Stoppacciaro A, Ruco L, Villa A, Simmons D, Dejana E.** 1998. Junctional adhesion molecule, a novel member of the immunoglobulin superfamily that distributes at intercellular junctions and modulates monocyte transmigration. Journal of Cell Biology **142:**117-127.

41. **Woodfin A, Reichel CA, Khandoga A, Corada M, Voisin MB, Scheiermann C, Haskard DO, Dejana E, Krombach F, Nourshargh S.** 2007. JAM-A mediates neutrophil transmigration in a stimulus-specific manner in vivo: evidence for sequential roles for JAM-A and PECAM-1 in neutrophil transmigration. Blood **110:**8.

42. **Corada M, Chimenti S, Cera MR, Vinci M, Salio M, Fiordaliso F, De Angelis N, Villa A, Bossi M, Staszewsky LI, Vecchi A, Parazzoli D, Motoike T, Latini R, Dejana E.** 2005. Junctional adhesion molecule-A-deficient polymorphonuclear cells show reduced diapedesis in peritonitis and heart ischemia-reperfusion injury. Proceedings of the National Academy of Sciences USA **102:**10634-10639.

43. **Ghislin S, Obino D, Middendorp S, Boggetto N, Alcaide-Loridan C, Deshayes F.** 2011. Junctional adhesion molecules are required for melanoma cell lines transendothelial migration in vitro. Pigment Cell Melanoma Research **24:**504-511.

44. **Sobocka MB, Sobocki T, Babinska A, Hartwig J, Li M, Ehrlich YH, Kornecki E.** 2004. Signaling pathways of the F11 receptor (F11R; a.k.a. JAM-1, JAM-A) in human platelets: F11R dimerization, phosphorylation and complex formation with the integrin GPIIIa. J Recept Signal Transduct Res **24:**85-105.

45. **Bazzoni G, Tonetti P, Manzi L, Cera MR, Balconi G, Dejana E.** 2005. Expression of junctional adhesion molecule-A prevents spontaneous and random motility. Journal of Cell Science **118:**623–632.

46. **Nomme J, Fanning AS, Caffrey M, Lye MF, Anderson JM, Lavie A.** 2011. The Src homology 3 domain is required for junctional adhesion molecule binding to the third PDZ domain of the scaffolding protein ZO-1. Journal of Biological Chemistry **286:**43352-43360.

47. **Mandell KJ, Babbin BA, Nusrat A, Parkos CA.** 2005. Junctional adhesion molecule-1 (JAM1) regulates epithelial cell morphology through effects on b1 integrins and Rap1 activity. Journal of Biological Chemistry **280:**11665-11674.

48. **Ostermann G, Fraemohs L, Baltus T, Schober A, Lietz M, Zernecke A, Liehn EA, Weber C.** 2005. Involvement of JAM-A in mononuclear cell recruitment on inflamed or atherosclerotic endothelium: inhibition by soluble JAM-A. Arteriosclerosis, Thrombosis, and Vascular Biology **25:**729-735.

49. **Iden S, Misselwitz S, Peddibhotla SSD, Tuncay H, Rehder D, Gerke V, Robenek H, Suzuki A, Ebnet K.** 2012. aPKC phosphorylates JAM-A at Ser285 to promote cell contact maturation and tight junction formation. Journal of Cell Biology **196:**623-639.

50. **Guglielmi KM, Kirchner E, Holm GH, Stehle T, Dermody TS.** 2007. Reovirus binding determinants in junctional adhesion molecule-A. Journal of Biological Chemistry **282:**17930-17940.

51. **Antar AAR, Konopka JL, Campbell JA, Henry RA, Perdigoto AL, Carter BD, Pozzi A, Abel TW, Dermody TS.** 2009. Junctional adhesion molecule-A is required for hematogenous dissemination of reovirus. Cell Host Microbe **5:**59-71.

52. **Dejana E.** 2004. Endothelial cell-cell junctions: happy together. Nat Rev Mol Cell Biol **5:**261-270.

53. **Coyne CB, Shen L, Turner JR, Bergelson JM.** 2007. Coxsackievirus entry across epithelial tight junctions requires occludin and the small GTPases Rab34 and Rab5. Cell Host Microbe **2:**181-192.

54. **Liu S, Yang W, Shen L, Turner JR, Coyne CB, Wang T.** 2009. Tight junction proteins claudin-1 and occludin control hepatitis C virus entry and are downregulated during infection to prevent superinfection. J Virol **83:**2011-2014.

55. **Bergelson JM, Cunningham JA, Droguett G, Kurt-Jones EA, Krithivas A, Hong JS, Horwitz MS, Crowell RL, Finberg RW.** 1997. Isolation of a common receptor for Coxsackie B viruses and adenoviruses 2 and 5. Science **275:**1320-1323.

56. **Makino A, Shimojima M, Miyazawa T, Kato K, Tohya Y, Akashi H.** 2006. Junctional adhesion molecule 1 is a functional receptor for feline calicivirus. J Virol **80:**4482-4490.

57. **Amieva MR, Vogelmann R, Covacci A, Tompkins LS, Nelson WJ, Falkow S.** 2003. Disruption of the epithelial apical-junctional complex by Helicobacter pylori CagA. Science **300:**1430-1434.

58. **Ramos-Alvarez M, Sabin AB.** 1954. Characteristics of poliomyelitis and other enteric viruses recovered in tissue culture from healthy American children. Proceedings of the Society for Experimental Biology and Medicine **87:**655-661.

59. **Ramos-Alvarez M, and Sabin, A.B.** 1956. Intestinal flora of healthy children demonstrable by monkey kidney tissue culture. American Journal of Public Health **46:**295-299.

60. **Ramos-Alvarez M, Sabin AB.** 1958. Enteropathogenic viruses and bacteria. Role in summer diarrheal diseases of infancy and early childhood. Journal of the American Medical Association **167:**147-158.

61. **Bodkin DK, Nibert ML, Fields BN.** 1989. Proteolytic digestion of reovirus in the intestinal lumens of neonatal mice. Journal of Virology **63:**4676-4681.

62. **Bass DM, Bodkin D, Dambrauskas R, Trier JS, Fields BN, Wolf JL.** 1990. Intraluminal proteolytic activation plays an important role in replication of type 1 reovirus in the intestines of neonatal mice. Journal of Virology **64:**1830-1833.

63. **Chappell JD, Barton ES, Smith TH, Baer GS, Duong DT, Nibert ML, Dermody TS.** 1998. Cleavage susceptibility of reovirus attachment protein s1 during proteolytic disassembly of virions is determined by a sequence polymorphism in the s1 neck. Journal of Virology **72:**8205-8213.

64. **Boehme KW, Guglielmi KM, Dermody TS.** 2009. Reovirus nonstructural protein s1s is required for establishment of viremia and systemic dissemination. Proceedings of the National Academy of Sciences USA **106:**19986-19991.

65. **Rubin DH, Kornstein MJ, Anderson AO.** 1985. Reovirus serotype 1 intestinal infection: a novel replicative cycle with ileal disease. Journal of Virology **53:**391-398.

66. **Rubin DH, Eaton MA, Anderson AO.** 1986. Reovirus infection in adult mice: the virus hemagglutinin determines the site of intestinal disease. Microbial Pathogenesis **1:**79-87.

67. **Wolf JL, Rubin DH, Finberg R, Kaufman RS, Sharpe AH, Trier JS, Fields BN.** 1981. Intestinal M cells: a pathway of entry of reovirus into the host. Science **212:**471-472.

68. **Amerongen HM, Wilson GAR, Fields BN, Neutra MR.** 1994. Proteolytic processing of reovirus is required for adherence to intestinal M cells. Journal of Virology **68:**8428-8432.

69. **Wolf JL, Kauffman RS, Finberg R, Dambrauskas R, Fields BN, Trier JS.** 1983. Determinants of reovirus interaction with the intestinal M cells and absorptive cells of murine intestine. Gastroenterology **85:**291-300.

70. **Wolf JL, Dambrauskas R, Sharpe AH, Trier JS.** 1987. Adherence to and penetration of the intestinal epithelium by reovirus type 1 in neonatal mice. Gastroenterology **92:**82-91.

71. **van de Pavert SA, Mebius RE.** 2010. New insights into the development of lymphoid tissues. Nature Reviews Immunology **10:**664-674.

72. **Rubin DH.** 1987. Reovirus serotype 1 binds to the basolateral membrane of intestinal epithelial cells. Microbial Pathogenesis **3:**215-220.

73. **Sabin AB.** 1956. Pathogenesis of poliomyelitis; reappraisal in the light of new data. Science **123:**1151-1157.

74. **Bodian D.** 1955. Emerging concept of poliomyelitis infection. Science **122:**105-108.

75. **Carter PB, Collins FM.** 1974. The route of enteric infection in normal mice. Journal of Experimental Medicine **139:**1189-1203.

76. **Jones BD, Ghori N, Falkow S.** 1994. Salmonella typhimurium initiates murine infection by penetrating and destroying the specialized epithelial M cells of the Peyer's patches. Journal of Experimental Medicine **180:**15-23.

77. **Galan JE, Curtiss R, 3rd.** 1989. Cloning and molecular characterization of genes whose products allow Salmonella typhimurium to penetrate tissue culture cells. Proceedings of the National Academy of Sciences USA **86:**6383-6387.

78. **Bass DM, Trier JS, Dambrauskas R, Wolf JL.** 1988. Reovirus type 1 infection of small intestinal epithelium in suckling mice and its effect on M cells. Laboratory Investigations **58:**226-235.

79. **Fleeton M, Contractor N, Leon F, Wetzel JD, Dermody TS, Kelsall B.** 2004. Peyer’s patch dendritic cells process viral antigen from apoptotic epithelial cells in the intestine of reovirus-infected mice. Journal of Experimental Medicine **200:**235-245.

80. **Muthukkumar S, Goldstein J, Stein KE.** 2000. The ability of B cells and dendritic cells to present antigen increases during ontogeny. Journal of Immunology **165:**4803-4813.

81. **Iwasaki A.** 2007. Mucosal dendritic cells. Annual Review in Immunology **25:**381-418.

82. **Rescigno M, Rotta G, Valzasina B, Ricciardi-Castagnoli P.** 2001. Dendritic cells shuttle microbes across gut epithelial monolayers. Immunobiology **204:**572-581.

83. **Vazquez-Torres A, Jones-Carson J, Baumler AJ, Falkow S, Valdivia R, Brown W, Le M, Berggren R, Parks WT, Fang FC.** 1999. Extraintestinal dissemination of Salmonella by CD18-expressing phagocytes. Nature **401:**804-808.

84. **Isberg RR, Barnes P.** 2001. Subversion of integrins by enteropathogenic Yersinia. Journal of Cell Science **114:**21-28.

85. **Weiner HL, Powers ML, Fields BN.** 1980. Absolute linkage of virulence and central nervous system cell tropism of reoviruses to viral hemagglutinin. J Infect Dis **141:**609-616.

86. **Weiner HL, Drayna D, Averill DR, Jr., Fields BN.** 1977. Molecular basis of reovirus virulence: role of the S1 gene. Proc Natl Acad Sci U S A **74:**5744-5748.

87. **Tyler KL, McPhee DA, Fields BN.** 1986. Distinct pathways of viral spread in the host determined by reovirus S1 gene segment. Science **233:**770-774.

88. **Boehme KW, Frierson JM, Konopka JL, Kobayashi T, Dermody TS.** 2011. The reovirus s1s protein is a determinant of hematogenous but not neural virus dissemination in mice. Journal of Virology **85:**11781-11790.

89. **Morrison LA, Sidman RL, Fields BN.** 1991. Direct spread of reovirus from the intestinal lumen to the central nervous system through vagal autonomic nerve fibers. Proc Natl Acad Sci U S A **88:**3852-3856.

90. **Tardieu M, Weiner HL.** 1982. Viral receptors on isolated murine and human ependymal cells. Science **215:**419-421.

91. **Dichter MA, Weiner HL.** 1984. Infection of neuronal cell cultures with reovirus mimics in vitro patterns of neurotropism. Annals of Neurology **16:**603-610.

92. **Sarkar G, Pelletier J, Bassel-Duby R, Jayasuriya A, Fields BN, Sonenberg N.** 1985. Identification of a new polypeptide coded by reovirus gene S1. Journal of Virology **54:**720-725.

93. **Mahrt CR, Osburn BI.** 1986. Experimental bluetongue virus infection of sheep; effect of vaccination: pathologic, immunofluorescent, and ultrastructural studies. American Journal of Veterinary Research **47:**1198-1203.

94. **MacLachlan NJ, Jagels G, Rossitto PV, Moore PF, Heidner HW.** 1990. The pathogenesis of experimental bluetongue virus infection of calves. Veterinary Pathology **27:**223-229.

95. **Ellis JA, Coen ML, MacLachlan NJ, Wilson WC, Williams ES, Leudke AJ.** 1993. Prevalence of bluetongue virus expression in leukocytes from experimentally infected ruminants. American Journal of Veterinary Research **54:**1452-1456.

96. **Barratt-Boyes SM, MacLachlan NJ.** 1994. Dynamics of viral spread in bluetongue virus infected calves. Veterinary Microbiology **40:**361-371.

97. **Veronesi E, Darpel KE, Hamblin C, Carpenter S, Takamatsu HH, Anthony SJ, Elliott H, Mertens PP, Mellor PS.** 2009. Viraemia and clinical disease in Dorset Poll sheep following vaccination with live attenuated bluetongue virus vaccines serotypes 16 and 4. Vaccine **28:**1397-1403.

98. **Oshiro LS, Dondero DV, Emmons RW, Lennette EH.** 1978. The development of Colorado tick fever virus within cells of the haemopoietic system. Journal of General Virology **39:**73-79.

99. **Adair RA, Roulstone V, Scott KJ, Morgan R, Nuovo GJ, Fuller M, Beirne D, West EJ, Jennings VA, Rose A, Kyula J, Fraser S, Dave R, Anthoney DA, Merrick A, Prestwich R, Aldouri A, Donnelly O, Pandha H, Coffey M, Selby P, Vile R, Toogood G, Harrington K, Melcher AA.** 2012. Cell carriage, delivery, and selective replication of an oncolytic virus in tumor in patients. Science Translational Medicine **4:**138ra177.

100. **Sobocka MB, Sobocki T, Banerjee P, Weiss C, Rushbrook JI, Norin AJ, Hartwig J, Salifu MO, Markell MS, Babinska A, Ehrlich YH, Kornecki E.** 2000. Cloning of the human platelet F11 receptor: a cell adhesion molecule member of the immunoglobulin superfamily involved in platelet aggregation. Blood **95:**2600-2609.

101. **Naik UP, Naik MU, Eckfeld K, Martin-DeLeon P, Spychala J.** 2001. Characterization and chromosomal localization of JAM-1, a platelet receptor for a stimulatory monoclonal antibody. Journal of Cell Science **114:**539-547.

102. **Barton ES, Connolly JL, Forrest JC, Chappell JD, Dermody TS.** 2001. Utilization of sialic acid as a coreceptor enhances reovirus attachment by multistep adhesion strengthening. Journal of Biological Chemistry **276:**2200-2211.

103. **Barton ES, Youree BE, Ebert DH, Forrest JC, Connolly JL, Valyi-Nagy T, Washington K, Wetzel JD, Dermody TS.** 2003. Utilization of sialic acid as a coreceptor is required for reovirus-induced biliary disease. Journal of Clinical Investigation **111:**1823-1833.

104. **Richardson SC, Bishop RF, Smith AL.** 1994. Reovirus serotype 3 infection in infants with extrahepatic biliary atresia or neonatal hepatitis. Journal of Gastroenterology & Hepatology **9:**264-268.

105. **Tyler KL, Sokol RJ, Oberhaus SM, Le M, Karrer FM, Narkewicz MR, Tyson RW, Murphy JR, Low R, Brown WR.** 1998. Detection of reovirus RNA in hepatobiliary tissues from patients with extrahepatic biliary atresia and choledochal cysts. Hepatology **27:**1475-1482.

106. **Dermody TS, Nibert ML, Bassel-Duby R, Fields BN.** 1990. Sequence diversity in S1 genes and S1 translation products of 11 serotype 3 reovirus strains. Journal of Virology **64:**4842-4850.

107. **Excoffon KJDA, Guglielmi KM, Wetzel JD, Gansemer ND, Campbell JA, Dermody TS, Zabner J.** 2008. Reovirus preferentially infects the basolateral surface and is released from the apical surface of polarized human respiratory epithelial cells. Journal of Infectious Diseases **197:**1189-1197.

108. **Stelzer S, Ebnet K, Schwamborn JC.** 2010. JAM-A is a novel surface marker for NG2-Glia in the adult mouse brain. BMC Neuroscience **11:**27.

109. **Sjostrand J, Karlsson JO.** 1969. Axoplasmic transport in the optic nerve and tract of the rabbit: a biochemical and radioautographic study. Journal of Neurochemistry **16:**833-844.

110. **Hansson G, Kristensson K, Olsson Y, Sjostrand J.** 1971. Embryonal and postnatal development of mast cells in rat peripheral nerve. Acta Neuropathology **17:**139-149.

111. **Strong JE, Coffey MC, Tang D, Sabinin P, Lee PW.** 1998. The molecular basis of viral oncolysis: usurpation of the Ras signaling pathway by reovirus. EMBO J **17:**3351-3362.

112. **Coffey MC, Strong JE, Forsyth PA, Lee PW.** 1998. Reovirus therapy of tumors with activated Ras pathway. Science **282:**1332-1334.

113. **Vidal L, Pandha HS, Yap TA, White CL, Twigger K, Vile RG, Melcher A, Coffey M, Harrington KJ, DeBono JS.** 2008. A phase I study of intravenous oncolytic reovirus type 3 Dearing in patients with advanced cancer. Clinical Cancer Research **14:**7127-7137.

114. **Lai CM, Mainou BA, Kim KS, Dermody TS.** 2013. Directional release of reovirus from the apical surface of polarized endothelial cells. MBio **4:**e00049.

115. **VW vH.** 2012. Tie2 lineage deletion of α6 integrin: endothelial and haematopoietic cells in neovascularization. Cardiovascular Research **95:**2.

116. **Cameron PU, Freudenthal PS, Barker JM, Gezelter S, Inaba K, Steinman RM.** 1992. Dendritic cells exposed to human immunodeficiency virus type-1 transmit a vigorous cytopathic infection to CD4+ T cells. Science **257:**383-387.

117. **Puryear WB, Akiyama H, Geer SD, Ramirez NP, Yu X, Reinhard BM, Gummuluru S.** 2013. Interferon-inducible mechanism of dendritic cell-mediated HIV-1 dissemination is dependent on Siglec-1/CD169. PLoS Pathogens **9:**e1003291.

118. **Dalrymple NA, Mackow ER.** Roles for endothelial cells in dengue virus infection. Advances in Virology **2012:**8.

119. **Nguyet MN, Duong TH, Trung VT, Nguyen TH, Tran CN, Long VT, Dui le T, Nguyen HL, Farrar JJ, Holmes EC, Rabaa MA, Bryant JE, Nguyen TT, Nguyen HT, Nguyen LT, Pham MP, Nguyen HT, Luong TT, Wills B, Nguyen CV, Wolbers M, Simmons CP.** 2013. Host and viral features of human dengue cases shape the population of infected and infectious Aedes aegypti mosquitoes. Proc Natl Acad Sci U S A **110:**9072-9077.

120. **Frierson JM, Pruijssers AJ, Konopka JL, Reiter DM, Abel TW, Stehle T, Dermody TS.** 2012. Utilization of sialylated glycans as coreceptors enhances the neurovirulence of serotype 3 reovirus. Journal of Virology **86:**13164-13173.

121. **Dermody TS, Nibert ML, Wetzel JD, Tong X, Fields BN.** 1993. Cells and viruses with mutations affecting viral entry are selected during persistent infections of L cells with mammalian reoviruses. Journal of Virology **67:**2055-2063.

122. **Wetzel JD, Chappell JD, Fogo AB, Dermody TS.** 1997. Efficiency of viral entry determines the capacity of murine erythroleukemia cells to support persistent infections by mammalian reoviruses. Journal of Virology **71:**299-306.

123. **Rubin DH, Wetzel JD, Williams WV, Cohen JA, Dworkin C, Dermody TS.** 1992. Binding of type 3 reovirus by a domain of the s1 protein important for hemagglutination leads to infection of murine erythroleukemia cells. Journal of Clinical Investigation **90:**2536-2542.

124. **Evans MJ, von Hahn T, Tscherne DM, Syder AJ, Panis M, Wolk B, Hatziioannou T, McKeating JA, Bieniasz PD, Rice CM.** 2007. Claudin-1 is a hepatitis C virus co-receptor required for a late step in entry. Nature **446:**801-805.

125. **Ploss A, Evans MJ, Gaysinskaya VA, Panis M, You H, de Jong YP, Rice CM.** 2009. Human occludin is a hepatitis C virus entry factor required for infection of mouse cells. Nature **457:**882-886.

126. **Bewley MC, Springer K, Zhang YB, Freimuth P, Flanagan JM.** 1999. Structural analysis of the mechanism of adenovirus binding to its human cellular receptor, CAR. Science **286:**1579-1583.

127. **Morrison LA, Sidman RL, Fields BN.** 1991. Direct spread of reovirus from the intestinal lumen to the central nervous system through vagal autonomic nerve fibers. Proceedings of the National Academy of Sciences USA **88:**3852-3856.

128. **Weiner HL, Drayna D, Averill DR, Jr, Fields BN.** 1977. Molecular basis of reovirus virulence: role of the S1 gene. Proceedings of the National Academy of Sciences USA **74:**5744-5748.

129. **Weiner HL, Powers ML, Fields BN.** 1980. Absolute linkage of virulence and central nervous system tropism of reoviruses to viral hemagglutinin. Journal of Infectious Diseases **141:**609-616.

130. **Feng Z, Hensley L, McKnight KL, Hu F, Madden V, Ping L, Jeong SH, Walker C, Lanford RE, Lemon SM.** 2013. A pathogenic picornavirus acquires an envelope by hijacking cellular membranes. Nature **496:**367-371.

131. **Gu Y, Rosenblatt J.** 2012. New emerging roles for epithelial cell extrusion. Current Opinion in Cell Biology **24:**865-870.

132. **Barkon ML, Haller BL, Virgin HW.** 1996. Circulating immunoglobulin G can play a critical role in clearance of intestinal reovirus infection. J Virol **70:**1109-1116.

133. **George A, Kost SI, Witzleben CL, al e.** 1990. Reovirus-induced liver disease in severe combined immunodeficient (SCID) mice: a model for the study of viral infection, pathogenesis, and clearance. Journal of Experimental Medicine **171:**929-934.

134. **Virgin HW, IV, Bassel-Duby R, Fields BN, Tyler KL.** 1988. Antibody protects against lethal infection with the neurally spreading reovirus type 3 (Dearing). Journal of Virology **62:**4594-4604.

135. **Virgin HW, Tyler KL.** 1991. Role of immune cells in protection against and control of reovirus infection in neonatal mice. Journal of Virology **65:**5157-5164.

136. **Tyler KL, Mann MA, Fields BN, Virgin HW, IV.** 1993. Protective anti-reovirus monoclonal antbodies and their effects on viral pathogenesis. Journal of Virology **67:**3446-3453.

137. **Sacher T, Podlech J, Mohr CA, Jordan S, Ruzsics Z, Reddehase MJ, Koszinowski UH.** 2008. The major virus-producing cell type during murine cytomegalovirus infection, the hepatocyte, is not the source of virus dissemination in the host. Cell Host Microbe **3:**263-272.

138. **Sacher T, Andrassy J, Kalnins A, Dolken L, Jordan S, Podlech J, Ruzsics Z, Jauch KW, Reddehase MJ, Koszinowski UH.** Shedding light on the elusive role of endothelial cells in cytomegalovirus dissemination. PLoS Pathogens **7:**e1002366.

139. **Shannon-Lowe CD, Neuhierl B, Baldwin G, Rickinson AB, Delecluse HJ.** 2006. Resting B cells as a transfer vehicle for Epstein-Barr virus infection of epithelial cells. Proceedings of the National Academy of Sciences USA **103:**7065-7070.

140. **Shannon-Lowe C, Rowe M.** 2011. Epstein-Barr virus infection of polarized epithelial cells via the basolateral surface by memory B cell-mediated transfer infection. PLoS Pathogens **7:**e1001338.

141. **Cereijido M CR, Shoshani L, Flores-Benitez D, Larre I.** 2008. Tight junction and polarity interaction in the transporting epithelial phenotype. Biochimica et biophysica acta **1778:**23.

142. **Monteiro AC PC.** 2012. Intracellular mediators of JAM-A-dependent epithelial barrier function. Annals of the New York Academy of Sciences **1257:**9.

143. **Severson EA, Lee WY, Capaldo CT, Nusrat A, Parkos CA.** 2009. Junctional adhesion molecule A interacts with Afadin and PDZ-GEF2 to activate Rap1A, regulate beta1 integrin levels, and enhance cell migration. Mol Biol Cell **20:**1916-1925.

144. **Maginnis MS, Forrest JC, Kopecky-Bromberg SA, Dickeson SK, Santoro SA, Zutter MM, Nemerow GR, Bergelson JM, Dermody TS.** 2006. b1 integrin mediates internalization of mammalian reovirus. Journal of Virology **80:**2760-2770.

145. **Montermini D, Winlove CP, Michel C.** 2002. Effects of perfusion rate on permeability of frog and rat mesenteric microvessels to sodium fluorescein. J Physiol **543:**959-975.

146. **Kozler P, Pokorny J.** 2003. Altered blood-brain barrier permeability and its effect on the distribution of Evans blue and sodium fluorescein in the rat brain applied by intracarotid injection. Physiology Research **52:**607-614.

147. **Oishi R, Baba M, Nishibori M, Itoh Y, Saeki K.** 1989. Involvement of central histaminergic and cholinergic systems in the morphine-induced increase in blood-brain barrier permeability to sodium fluorescein in mice. Naunyn Schmiedebergs Archives in Pharmacology **339:**159-165.

148. **Gralinski LE, Ashley SL, Dixon SD, Spindler KR.** 2009. Mouse adenovirus type 1-induced breakdown of the blood-brain barrier. J Virol **83:**9398-9410.

149. **Coyne CB, Bergelson JM.** 2006. Virus-induced Abl and Fyn kinase signals permit coxsackievirus entry through epithelial tight junctions. Cell **124:**119-131.

150. **Kanmogne GD, Schall K, Leibhart J, Knipe B, Gendelman HE, Persidsky Y.** 2007. HIV-1 gp120 compromises blood-brain barrier integrity and enhances

monocyte migration across blood-brain barrier: implication for viral neuropathogenesis. Journal of Cerebral Blood Flow and Metabolism **27:**123-134.

151. **Jackson WT, Giddings TH, Jr., Taylor MP, Mulinyawe S, Rabinovitch M, Kopito RR, Kirkegaard K.** 2005. Subversion of cellular autophagosomal machinery by RNA viruses. PLoS Biology **3:**e156.

152. **Sun MX, Huang L, Wang R, Yu YL, Li C, Li PP, Hu XC, Hao HP, Ishag HA, Mao X.** 2012. Porcine reproductive and respiratory syndrome virus induces autophagy to promote virus replication. Autophagy **8:**1434-1447.

153. **Thirukkumaran CM, Shi ZQ, Luider J, Kopciuk K, Gao H, Bahlis N, Neri P, Pho M, Stewart D, Mansoor A, Morris DG.** 2013. Reovirus modulates autophagy during oncolysis of multiple myeloma. Autophagy **9:**413-414.

154. **Tanida I, Ueno T, Kominami E.** 2008. LC3 and Autophagy. Methods Mol Biol **445:**77-88.

155. **Nchoutmboube JA, Viktorova EG, Scott AJ, Ford LA, Pei Z, Watkins PA, Ernst RK, Belov GA.** 2013. Increased long chain acyl-Coa synthetase activity and fatty acid import is linked to membrane synthesis for development of picornavirus replication organelles. PLoS Pathog **9:**e1003401.

156. **Karapanagiotou EM, Roulstone V, Twigger K, Ball M, Tanay M, Nutting C, Newbold K, Gore ME, Larkin J, Syrigos KN, Coffey M, Thompson B, Mettinger K, Vile RG, Pandha HS, Hall GD, Melcher AA, Chester J, Harrington KJ.** 2012. Phase I/II trial of carboplatin and paclitaxel chemotherapy in combination with intravenous oncolytic reovirus in patients with advanced malignancies. Clin Cancer Res **18:**2080-2089.

157. **Kottke T, Chester J, Ilett E, Thompson J, Diaz R, Coffey M, Selby P, Nuovo G, Pulido J, Mukhopadhyay D, Pandha H, Harrington K, Melcher A, Vile R.** 2011. Precise scheduling of chemotherapy primes VEGF-producing tumors for successful systemic oncolytic virotherapy. Mol Ther **19:**1802-1812.

158. **van den Wollenberg DJ, Dautzenberg IJ, van den Hengel SK, Cramer SJ, de Groot RJ, Hoeben RC.** 2012. Isolation of reovirus T3D mutants capable of infecting human tumor cells independent of junction adhesion molecule-A. PLoS One **7:**e48064.

159. **Kim M, Garant KA, zur Nieden NI, Alain T, Loken SD, Urbanski SJ, Forsyth PA, Rancourt DE, Lee PW, Johnston RN.** 2011. Attenuated reovirus displays oncolysis with reduced host toxicity. British Journal of Cancer **104:**290-299.

160. **Sloane BF, Yan S, Podgorski I, Linebaugh BE, Cher ML, Mai J, Cavallo-Medved D, Sameni M, Dosescu J, Moin K.** 2005. Cathepsin B and tumor

proteolysis: contribution of the tumor microenvironment. Seminar in Cancer Biolology **15:**149-157.

161. **Borsa J, Morash BD, Sargent MD, Copps TP, Lievaart PA, Szekely JG.** 1979. Two modes of entry of reovirus particles into L cells. Journal of General Virology **45:**161-170.

162. **Stins MF, Badger J, Sik Kim K.** 2001. Bacterial invasion and transcytosis in transfected human brain microvascular endothelial cells. Microbial Pathogenesis **30:**19-28.

163. **Stins MF, Gilles F, Kim KS.** 1997. Selective expression of adhesion molecules on human brain microvascular endothelial cells. Journal of Neuroimmunology **76:**81-90.

164. **Furlong DB, Nibert ML, Fields BN.** 1988. Sigma 1 protein of mammalian reoviruses extends from the surfaces of viral particles. Journal of Virology **62:**246-256.

165. **Kisanuki YY, Hammer RE, Miyazaki J, Williams SC, Richardson JA, Yanagisawa M.** 2001. Tie2-Cre transgenic mice: a new model for endothelial cell-lineage analysis in vivo. Developmental Biology **230:**230-242.

166. **de Boer J, Williams A, Skavdis G, Harker N, Coles M, Tolaini M, Norton T, Williams K, Roderick K, Potocnik AJ, Kioussis D.** 2003. Transgenic mice with hematopoietic and lymphoid specific expression of Cre. European Journal of Immunology **33:**314-325.

167. **Kienstra KA, Freysdottir D, Gonzales NM, Hirschi KK.** 2007. Murine neonatal intravascular injections: modeling newborn disease. Journal of the American Association of Lab Animal Sciences **46:**50-54.

168. **Pozzi A, Moberg PE, Miles LA, Wagner S, Soloway P, Gardner HA.** 2000. Elevated matrix metalloprotease and angiostatin levels in integrin alpha 1 knockout mice cause reduced tumor vascularization. Proceedings of the National Academy of Sciences USA **97:**2202-2207.

169. **Grab DJ, Perides G, Dumler JS, Kim KJ, Park J, Kim YV, Nikolskaia O, Choi KS, Stins MF, Kim KS.** 2005. Borrelia burgdorferi, host-derived proteases, and the blood-brain barrier. Infection and Immunity **73:**1014-1022.

170. **Mainou BA, Dermody TS.** 2011. Src kinase mediates productive endocytic sorting of reovirus during cell entry. Journal of Virology **85:**3203-3213.

171. **Risco C, Rodriguez JR, Lopez-Iglesias C, Carrascosa JL, Esteban M, Rodriguez D.** 2002. Endoplasmic reticulum-Golgi intermediate compartment membranes and vimentin filaments participate in vaccinia virus assembly. Journal of Virology **76:**1839-1855.